UNIVERSITY OF MODENA AND REGGIO EMILIA

Doctorate School in
INDUSTRIAL INNOVATION ENGINEERING

XXXII cycle

Life Cycle Assessment of the valorisation process of organic waste using insects to obtain bioplastics

Candidate: Dott.ssa Rosangela Spinelli

Tutor: Prof. Anna Maria Ferrari

Academic year 2018/2019

School Coordinator: Prof. Franco Zambonelli

Acknowledgements

At first all my gratitude goes to both my tutor Prof. Anna Maria Ferrari for giving me the opportunity to work in the Life Cycle Assessment (LCA) field and especially for believing and supporting me at all times and to Eng. Paolo Neri, the person that leaded me over these last three years through the LCA methodology, supporting and encouraging me to face all the difficulties which I encountered and to deepen the complex world of LCA.

Special thanks to Prof. Peter Fantke from DTU (Technical University of Denmark) for giving me the opportunity to spend five great months at DTU and for helping me to perform a very challenging project.

Many thanks go to all the people, past and present, from LCA Working Group, Department of Sciences and Methods for Engineering - University of Modena and Reggio Emilia.

I would like to thank
Prof. Monia Montorsi from the Department of Sciences and Methods for Engineering - University of Modena and Reggio Emilia (Italy) and her researcher Silvia Barbi.

Prof. Lara Maistrello from the Department of Life Sciences and Interdepartmental Center BIOGEST-SITEIA of the University of Modena and Reggio Emilia, Italy.

Prof. Augusta Caligiani from the Department of Food and Drug - University of Parma (Italy) and her researcher Angela Marseglia.

Abstract

The aim of this study is to evaluate the potential environmental impacts of bioconversion of waste from the livestock production chain using insects, to produce biomaterials that can be reintroduced in the agricultural production cycle, in order to achieve sustainability throughout the technological process. After stabilization, black soldier fly mature larvae, reared on a substrate composed of poultry manure, zeolite and water, were chemically separated in the laboratory to extract the proteic, lipidic and chitinic fractions. Proteins were then isolated and added to other components in order to produce bioplastics.

This type of bioplastic can replace the materials currently employed in agriculture, avoiding the critical issues of soil pollution, caused by conventional plastic end-life. Different plasticizing agents (glycerol and polyethylene glycol) were tested and the ability to generate a homogenous film through wet casting, was evaluated. Tensile properties as well as water absorption characteristics were evaluated to estimate the effect of the different plasticizers employed. Bioplastic formed by proteins/glycerol showed interesting properties, contributing to the formation of homogeneous and free-standing films.

The environmental impacts of laboratory scale production of bioplastics obtained from BSFs derived proteins was evaluated through the Life Cycle Assessment (LCA) methodology. Inventory analysis was conducted using primary data as well as data from the Ecoinvet database. LCA analysis was performed using SimaPro 8.5 software and the IMPACT 2002+ evaluation method. The analysis showed that energy consumption is high (contributing for the 44.20% to the overall environmental load). This can be mainly attributed to the laboratory-scale production process of bioplastic for which the energy consumption of the aspiration system represents the main contribution (93.06%). Therefore, these results will help design industrial production of innovative bioplastics in order to minimize the here highlighted environmental issues. Two other important sources of potential impact are the extraction of lipid, protein and chitin fraction as well as BSFs breeding phase.

The here presented study, concerning the application of LCA methodology to a complex system, (ranging from the BSFs breeding phase up to bioplastic production), aims also to experimentally analyze some methodological aspects that, up to date, have not yet been studied in depth. These include for example local and indoor emissions, for which, a calculation framework (for air compartment) was developed, based on EcoIndicator 99 and *Gaussian Plume Modelling* (GPM). In order to optimize the implementation, a thorough study of the USEtox model was carried out.

Abstract

Lo scopo di questo studio è di valutare i potenziali impatti ambientali della bioconversione tramite insetti dei rifiuti da allevamento, per produrre biomateriali che possono rientrare nel ciclo produttivo agricolo, al fine di raggiungere la sostenibilità durante tutto il processo tecnologico. Dopo la stabilizzazione, le prepupe di mosca soldato allevate su un substrato composto da letame di pollame, zeolite e acqua sono state separate chimicamente in laboratorio per estrarre le frazioni proteica, lipidica e chitinica. Le proteine sono state quindi isolate e aggiunte ad altri componenti al fine di ottenere bioplastiche.

Questo tipo di bioplastica può sostituire gli attuali materiali impiegati in agricoltura, evitando i problemi critici relativi all'inquinamento del suolo a causa del fine vita della plastica convenzionale. Sono stati testati diversi agenti plastificanti (glicerolo e glicole polietilenico) ed è stata valutata la capacità di generare un film omogeneo, mediante colata a umido. Sono state eseguite caratterizzazioni sulle proprietà di trazione e assorbimento d'acqua per stimare l'effetto dei diversi plastificanti impiegati. La bioplastica formata da proteine/glicerolo ha mostrato proprietà interessanti, contribuendo alla formazione di film omogenei e *free-standing*.

La valutazione di impatto ambientale della produzione su scala di laboratorio di bioplastiche ottenute dalle proteine estratte da mosche soldato è stata condotta mediante metodologia di valutazione del ciclo di vita (LCA).

L'analisi di inventario è stata condotta utilizzando prevalentemente dati primari e il database Ecoinvet. L'analisi LCA è stata condotta utilizzando il software SimaPro 8.5 e il metodo di valutazione IMPACT 2002+. L'analisi ha mostrato che il consumo di energia è elevato (44.20%). In particolare si evince che l’impatto è correlato al consumo di energia del sistema di aspirazione (93.06%). Ciò può essere attribuito principalmente a un processo di produzione su scala di laboratorio. Pertanto, questi risultati aiuteranno la progettazione a livello industriale di bioplastiche innovative al fine di ridurre al minimo questi problemi ambientali. Altre due importanti fonti di potenziale impatto sono l'estrazione della frazione lipidica, proteica e chitinica e l'allevamento di mosca soldato.

Il presente studio, applicando l'LCA a un sistema complesso, che parte dall'allevamento fino alla produzione di bioplastiche, mira ad analizzare sperimentalmente alcuni aspetti metodologici che non sono ancora stati approfonditi fino ad oggi, ad esempio le emissioni locali e indoor, per i quali, un modello di calcolo (per il compartimento aria) è stato sviluppato basandosi su EcoIndicator 99 e *Gaussian Plume Modeling* (GPM). Al fine di ottimizzare l'implementazione del metodo approssimato è stato condotto uno studio approfondito del modello USEtox.

Introduction

The disposal of livestock manure/waste from the zootechnical value chain is subjected to strict regulations in terms of traceability, thus leading to high disposal costs and contributing to prevent alternative uses. Therefore, the valorization and recovery of this kind of waste, that is ultimately used to produce poor quality compost, would in all likelihood contribute to significantly limit the related environmental pollution. From a sustainability viewpoint, it is crucial to implement systems able to reduce the content of polluting elements in waste.
The solution to these issues may partly be found in the use of selected insects that operate at the end of the food chain and contribute to transforming organic matter, so that it can be reused in the ecosystem. Their ability to degrade large amounts of organic matter in a relatively short time allows them to be used for the enhancement of organic waste and, being "macro-organisms", to obtain a series of useful by-products in the food and industrial sectors.

My doctoral thesis work fits exactly in this particular framework. During my PhD I have followed a project co-financed by Emilia-Romagna Region and carried out within a collaboration among the University of Modena and Reggio Emilia (BIOGEST SITEIA, INTERMECH.MORE and LCA WORKING GROUP) and the University of Parma (SITEIA-PARMA).

The aim of the project is to create an effective circular economy in the agricultural sector, wherein, tanks to insects, zootechnical value chain waste (manure) and other organic waste sources are transformed into innovative bioplastics with specific properties. Particularly *Hermetia Illucens* (also known as Black Soldier Fly – BSF) is the insect species selected for the study. BSF larvae are extremely voracious (they consume a quantity of food substrate equal to twice their weight on a daily base) and can grow on different types of organic waste, including waste from agri-food industry and agricultural processes, zootechnical waste, and urban wet waste, thereby reducing its mass significantly (Dienier et al. 2009, Van Huis et al. 2013). In this project, larvae of black soldier fly (prepupae) were used to process waste (manure) and then, when they reach pre-pupal stage, they are detached from residual substrate and collected. Subsequently, they are fractionated to obtain proteins, which are employed in a bioplastic with potential for biodegradability. These bioplastics, mainly employable in the agricultural sector (e.g. sheet mulching and biodegradable vases), in addition to carrying out their primary function, act as a slow-release fertilizer, releasing nitrogen during their decomposition.

The goal of this thesis is to evaluate, through the Life Cycle Assessment (LCA) methodology, the environmental profile of insect-based products and their role as a valuable alternative for waste valorization. Quantification of environmental performance, associated whit the whole life cycle of all processes, is carried out in order to identify the hot spots of the process at laboratory scale and to support their eco-design, ensuring an industrial scale-up with low environmental impact. Furthermore, applying the Life Cycle Assessment analysis to a complex system, the present study has the goal to analyse, in an experimental way, some methodological aspects of the current LCA-based environmental assessment models, including local as well as indoor emissions, that have not yet been thoroughly investigated.

A first level of innovation in this thesis is the analysis and modelling of a complex system, which starts from BSF breeding up to the production of insect-based bioplastic film, passing through the phases of waste bioconversion, isolation, characterization and extraction of targeted macromolecules. In the international scientific literature there are many studies concerning the utilization of insects for waste bioconversion, but very few articles related to the application of Life Cycle Assessment (LCA) in this sector (Salomone et al. 2017;van Zanten et al. 2015; de Boer et al. 2014; Oonincx and de Boer 2012) in which dried larvae and compost are produced from food waste bioconversion,. Morever, these studies did not analyse the potential environmental impacts associated with the isolation and extraction of macromolecules from BSF mature larvae (prepupae).

The second level of innovation is the attempt to overcome some limits of Life Cycle Assessment analysis. Among the life-cycle based methods, Life Cycle Assessment is recognised as a strategic and effective tool to evaluate the potential environmental impacts occurring in the whole product life cycle, as well as to identify possible areas for improvement. Nevertheless, when applying Life Cycle Assessment, the practitioner has to deal with some methodological problems. One of these is the absence of a spatial component. For this reason, LCA working group have developed an approximated method for the calculation of the damage factor (DF) for indoor and local air emissions. This method was created starting from the *Eco-indicator 99* method and the *Gaussian Plume Modelling* (GMP).

In the first part of the thesis, all the laboratory steps that I followed in order to collect primary data and model the system under study in a more representative manner was described. In Life Cycle Assessment Analysis, data quality is essential to obtain high quality results.
Therefore, to obtain a more representative index of environmental performance of the system considered, it resulted necessary to personally follow all the phases of the project, to develop a model as realistic as possible. The detailed description of all the macro-phases of the system also allows to make the work comparable with any other studies performed on similar systems.

I start by describing the laboratory experiments that were carried out: a) to balance substrate components (in terms of chicken manure, compost from urban pruning and water) in order to obtain the maximum number of of black soldier fly adult larvae (prepupae); b) to study adult mating and oviposition by changing important parameters such as: temperature, humidity, light spectrum, light intensity, flies density (flies/m^2). The aim of this phase of the project is to develop a rearing protocol for black soldier fly in an automated pilot plant for organic substrate processing. Using the breeding conditions identified in the laboratory, a pilot plant for the mass breeding of black soldier fly larvae for the valorisation of organic waste was designed in collaboration with Kour Energy company s.r.l..

The next phase of the model analysis concerns the extraction of macromolecules (lipids, proteins, chitin) from insect biomass. In literature, only a few extraction protocols are reported. Most of them had the aim to extract just one component from insect biomass, in particular protein extraction. However, insects, especially black soldier fly, are good sources of other valuable biomolecules like lipids and chitin. Therefore, it is necessary to develop a systematic approach able to recover all the three fractions in subsequent steps, along the same chain in a cascade bio refinery, in order to obtain the maximum benefit from the process. The thesis describes this innovative phase of the project

carried out thanks to the collaboration of University of Parma (SITEIA PARMA): several systematic procedures aimed to recover, at the highest purity level, the three main classes of biomolecules from black soldier fly with homogeneous methodologies in a bio refinery approach. Three different approaches were tested on the black soldier fly: two different chemical protocols, principally differing for the protein extraction method, and an enzymatic one.

The last phase of the model concerns the production process of protein-based bioplastic films. The optimization of the mixture for the production of protein-based bioplastic films in the laboratory and their characterization are described in detail. The use of proteins as components of bioplastics presents some problems that limit the developments of the material itself. The identification of an appropriate mixture of additives/components starting from black soldier fly proteins and the potential technological application is a key point to guarantee the real processability and obtaining of functional bioplastics. In order to rationalize the design of the process , Design of Experiments (DoE) techniques were used and particularly a mixture design approach was selected.

All the data collected were implemented in SimaPro calculation code to model the system under study and carry out environmental evaluation.

In the second part of the thesis a focus will be given to the approximated method for the calculation of the damage factor (DF) of indoor and local air emissions. This method was created starting from the Eco-indicator 99 method and the *Gaussian Plume Modeling*. Starting from the state of the art, the thesis presents a critical analysis of the work done and highlights the parts on which to focus future implementation work. It seems that the local air dispersion model is completely independent of the physico-chemical properties of the pollutant. Therefore for background concentrations, specific inputs from other sources need to be used. It is important to understand how to combine the dispersion model with a model that takes into account the physical and chemical properties of the pollutant.
This is why I have been carrying out a thorough study of the USEtox model. In particular I tried to understand and demonstrate some equations on which USEtox Environmental Fate is based.

The thesis is divided into 8 chapters:
Chapter 1 provides an introduction to the Black Soldier Fly and its life cycle.
Chapter 2 describes:

- analysis of the optimization of Black Soldier Fly larvae rearing on organic waste substrate;
- assessment of the effect of adding zeolite on the BSF rearing as well as on the quality and olfactory impact of the resulting compost;
- assessment of biological parameters and performance index for the optimization of processes and setting up of a pilot plant for the rearing of black soldier flies.

Chapter 3 describes:

- centesimal composition of black soldier fly prepupae;
- different extraction procedures tested in laboratory underlining advantages and disadvantages in order to identify the most promising ones.

Chapter 4 describes the analysis of activities which include:

- design of protein mixtures and other macromolecules through mixture design;
- optimization of the process to obtain biomaterials through Design of Experiments;

- thermal, structural and mechanical characterization of the new bioplastic materials obtained.

Chapter 5 illustrates Life Cycle Assessment methodology.
Chapter 6 presents the Life Cycle Assessment analysis of protein - based film production, with a focus on environmental assessment of the extraction process of lipid, protein, chitin fraction and BSF-Breeding.
Chapter 7 describes the approximated method used to calculate local and indoor emissions, its limits and possible implementations.
Chapter 8 describes the analysis of the USEtox method.
Finally, general conclusions for the overall research activity are included in chapter 9.

Chapter 1
Black soldier fly - BSF

1 BLACK SOLDIER FLY - BSF

Black Soldier Fly (*Hermetia illucens*), hereafter called BSF, is a diptera insect that belongs to the Stratiomyidae family. The species has a cosmopolitan spread in tropical and warm temperate regions (between about 45°N and 40°S). The BSF is native to America (McCallan, 1974; Gujarathi and Pejaver, 2013), but human activities and climate change have facilitated its diffusion also in other continents such as Europe, Asia and Australia (Olivier, 2009; Leek, 2017).

Taxonomical Classification

Kingdom	Animalia
Phylum	Arthropoda
Class	Insecta
Order	Diptera
Suborder	Brachycera
Superfamily	Stratiomyoidea
Family	Stratiomyidae
Subfamily	Hermetiinae
Genus	Hermetia
Species	*H. illucens*

Figure 1-1 Taxonomical classification of Black Soldier fly (*Hermetia illucens*)

1.1 Basic anatomy

These flies are predominantly black in color with brown-tinged wings that are folded horizontally on the abdomen and overlapped when resting. As with other dipterian species, the adult body is divided into head, thorax and abdomen. The eyes are widely separated and naked. The abdomen is composed of 5 segments with the presence of white abdominal spots. Females are generally shorter compared to males but have larger wings. The length of the body generally varies from 12 to 20 mm and the wings from 8 to 14.8 mm (Üstüner et al., 2003). The mouth has no functional parts (Sheppard et al., 2002; Tomberlin and Sheppard, 2002; Diener et al., 2011).

1.2 Life Cycle

The black soldier fly undergoes several stages to complete its metamorphosis. The life cycle is generally divided into five main phases called: egg, larva, prepupa, pupa and adult (Figure 1-2).
In optimal breeding conditions, it is estimated that the life cycle of a BSF from egg to adult lasts approximately 40-43 days, but it can stretch up to six months in unsuitable breeding conditions (Popa and Green, 2012).
The larval phase (13-18 days) and the pupal phase (10 days to months) represent the longest part of the life cycle (Popa and Green, 2012). The larval stage also influences the longevity of other stages and the productivity of the adult stage (Holmes et al., 2012).

In the presence of low temperatures or low amounts of food, they can reach a flexible life cycle through the extension of their larval stage (reportedly up to 4 months) (Furman et al., 1959). However, the quality of food determines the production of eggs and the development of larvae (Chippindale et al., 1993).
The larvae are photophobic, prefer environments within an organic material of 2-3 cm, while the adults are photophiles and attracted in the direction of origin of the light (Hall and Gerhardt, 2002). In the first phase the larvae prefer aquatic and semi-aquatic habitats, but when they mature they prefer drier conditions. During the prepupa and pupa phases dry terrestrial habitats are preferred (Hall and Gerhardt, 2002).

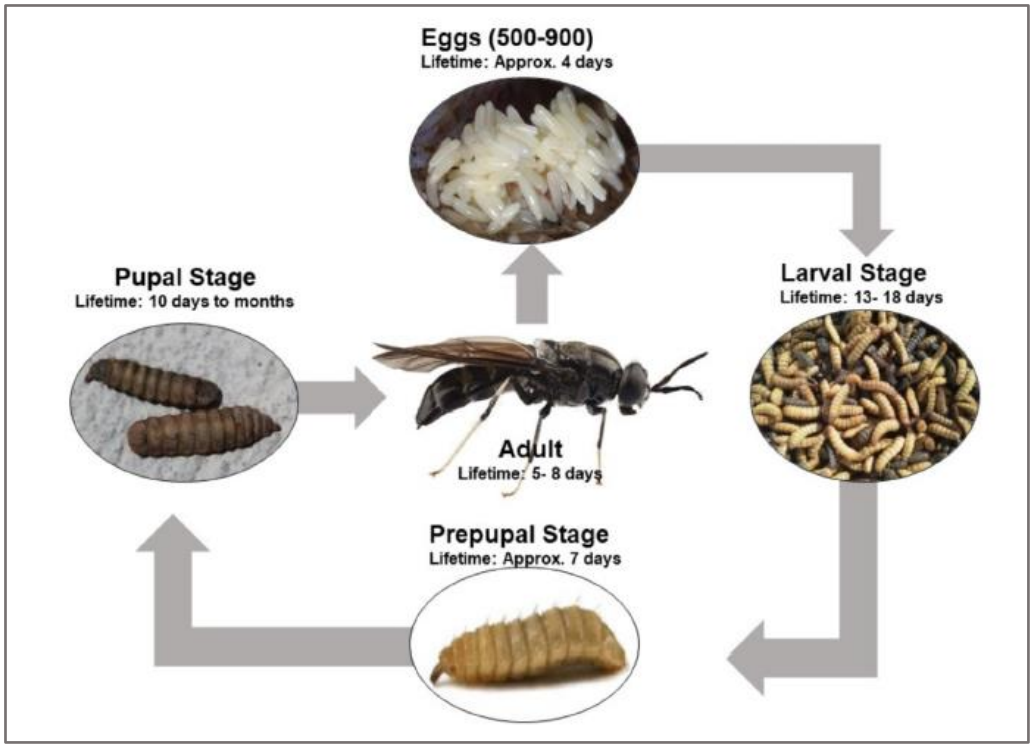

Figure 1-2 Life cycle stages of Black Soldier Fly - BSF

1.2.1 Egg stage

Adult females lay eggs two days after copulation. The eggs measure about 1 mm in length and are oval in shape. Since the life span of BSF is very short, one female produces a large number of eggs, from about 200 to 700 eggs (Helena Cickovà, 2015). Hatching takes place in about 4 days.
The eggs are deposited in cracks or fissures, in dry environments, near the larval substrate. Once born, the larvae fall into the substrate source of food where they will feed. The eggs are never laid directly on the wet decomposing material, due to the relatively long period between oviposition and eclosion.

1.2.2 Larva stage

The larva in the first stages is 1.5-2 mm long, apoda and eukephala with a cylindrical-fusiform body. The color of the larva gradually darkens during its development from creamy, opaque white, blackish gray and finally dark brown.
The larvae are detritivores, they get nutrients from the decomposition of plants, animals and faeces; they are of particular importance in the decomposition process, as they are crushers of organic particles.

BSF's ability to use such variable organic matter as food sources could be due to their intestinal microbiota. In a study (Jeon et al. 2011), the analysis of gut bacterial communities showed a direct dependence on their diet. A greater complexity of bacterial species has been noted with BSF fed on food waste compared to BSF fed on cooked rice or veal fodder. However, 36 bacterial strains were shared among the BSF fed on three different diets and were different from the intestinal micro-flora found in other insects (Jeon et al. 2011). This indicates that BSF has a unique composition of intestinal microbiota, which allows them to use a wide range of food sources.
Larvae can reach maturity in 2-4 weeks depending on temperature and food availability, but can survive up to 10 months in a quiescent state (Myers et al. 2008). The last larval stage is known as the prepupal stage.

1.2.3 Prepupal stage

The prepupal stage is indicated by a change in color and behaviour. The larvae turn from white to dark brown. Prepupae have no mouthparts (Hall and Gerhardt, 2002). Prepupae show a pronounced migratory habit linked to need to leave the food source to successfully pupate into adult flies. At this stage, the prepupae are at their maximum size, exhibiting large protein and fat contents to sustain them through metamorphosis (Hale, 1973; St-Hilaire et al., 2007b; Stamer, 2005). This final stage shows slight morphological changes compared to the feeding larva. Its labrum, for example, is bent down like the beak of an eagle. It is used as a hook to pull them to a suitable pupation site (Schremmer, 1986). Given the right condition, prepupa take two weeks to change into pupa in a process called pupation. The process is characterized by a development of the puparium (casing), body stiffness, followed by immobility.

1.2.4 Pupal stage

When they find a dry medium to burrow in, prepupae change into pupae. In the dry medium, pupae go into sleeping mode for a duration of at least two weeks, during which time the embryos further develop within their exoskeletal casing. When fully developed, the casing breaks up at the tip to release an adult fly in a process called emergence (Sheppard et al., 2002). Freshly emerged adult flies have undeveloped, folded wings which gradually unfold within 2-3 hours.

1.2.5 Adult stage

An extraordinary characteristic of the adult stage is that they have no functional mouth parts, so they do not feed but survive thanks to the fat accumulated during their first larval stage (Tomberlin, 2002; Furman, 1959), hence the importance of adequate nutrition during this stage.
Adults have a lifespan of 5-12 days, during which time they mate and lay eggs (Diclaro and Kaufman, 2009). The adult females mate only once in their lifetime and therefore one single oviposition event occurs throughout their lifetime. Mated females cannot lay eggs in the absence of organic waste (Caruso et al., 2014).

1.2.6 Feeding habits

The species feed only during the larval phase on decomposing plant material or rotting food products, manure, human and animal waste (Üstüner et al., 2003). These larvae feed on organic waste double the weight of their own. Adults do not feed and are found on tree trunks, walls and garden plants in residential areas (Rozkosny, 1983; Üstüner et al., 2003).

Since the waste with high organic matter is an absolute source of food for BSF larvae, adult flies lay their eggs in cracks near the organic waste (which serves as a breeding site).
During its adult stage, BSF does not feed and relies solely on its body fat reserve. Consequently, the fly does not come into contact with any degrading or fresh organic material including foodstuffs, and can therefore not be regarded as unsanitary or a vector of diseases.

1.3 CORS system by Black Soldier Fly Larvae

The conversion of organic waste by Saprofagi (CORS), is a process that exploits the ability of insects to convert organic waste into biomass. This kind of process is therefore able to respond to two problems: the need to treat ever-increasing quantities of waste and to find alternative and low-cost sources to produce zootechnical feeds, cosmetics, polymers and energy. In order for BSF larvae to serve effectively in these dual roles, it is necessary to establish a production system with a feeding strategy that specifies important substrate factors that affect BSF larvae feeding behaviour, growth and development (Devic and Maquart, 2015). These include aspects such as larvae feeding amounts (feed rate), feeding frequency (regime), substrate types and substrate combination ratios, substrate depth, larvae stocking densities, substrate moisture content, environmental rearing conditions (e.g. temperature and relative humidity), and substrate particle size among others (Holmes et al., 2012; Van Itterbeeck, 2014).

1.4 Other benefits of the black soldier fly

Several authors also studied how BSF has a vital role in modifying the microflora present in waste during composting, reducing harmful bacteria such as E. coli and Salmonella enterica by secreting harmful bactericidal compounds (Erickson et al., 2004; Gabler and Vinneras, 2014; Lalander et al., 2015).
It has also been reported that BSF naturally controls the population of house flies by rejecting their oviposition (Furman et al., 1959; Bradley and Sheppard, 1984; Schremmer, 1986; Leclercq, 1997). Furthermore, despite heavy metal contamination and adverse conditions with consequent reduced fertility, BSF larvae have enormous potential for composting and organic waste management (Diener et al 2015, Ortel, 1995; Maryanski et al., 2002).
Indeed, the larvae are able to feed on a large variety of organic waste. BSF larvae are effective in reducing the volume of organic waste and converting waste into biomass (Diener et al. 2009). For example, the fats produced can be used for the production of oils for cosmetics and for animal feed or biodiesel (Zheng et al., 2012, Manzano-Agugliaro et al., 2012, Li et al., 2011, Leong et al. 2015)
Another interesting feature of BSF larvae is that they break down organic waste and subsequently generate nutrient residues that can be used as fertilizers. A group of authors also reported that larval manure has similar qualities to fertilizers (Diener et al., 2011a; Choi et al., 2009; Green and Popa, 2012).

1.5 Legal situation

Another interesting aspect of black soldier fly treatment and its implementation is related to the legal issues. In the European Union, insects are not accurately considered in the feedstuff legislation, they are considered as production animals and abide under the by-product regulation EC 1069/2009. Therefore, larvae of black soldier fly can not be fed on animal by-products, such as organic waste and animal manures. Even though it is forbidden to use dead animals to produce further animals, it is allowed to feed living fly larvae to animals. Under the EU regulation EC 56/2013, proteins from

insects fed on waste and manure are allowed to be use to feed aquaculture species, while it is currently forbidden to feed them to farmed animals (Smith and Pryor 2013). The situation in low- and middle-income countries as well as China is more favourable, because there are no or only a few laws and regulations regarding the production and use of insects in the feed and food industry. Therefore, due to these less strict administrative barriers, using of BSF as waste management strategy is more likely to be developed in those countries in the near future.

Chapter 2
Breeding of black soldier fly

2 BREEDING OF BLACK SOLDIER FLY

2.1 Laboratory experiments

First laboratory experiments were carried out for two different purposes:

1. to balance substrate components (in terms of chicken manure, compost from urban pruning and water) in order to obtain the maximum number of black soldier fly mature larvae (prepupae);
2. to study adult mating and oviposition by changing important parameters such as: temperature, humidity, light spectrum, light intensity, density of flies (flies/m^3).

The aim was to develop a rearing protocol for Hermetia Illucens in an automated pilot plant for organic substrate processing.

2.1.1 Growth substrate components

Initially, experiments were carried out using Special Cubic Mixture Design (Montgomery 2012) in order to test different substrates at 27 and 33°C. Substrate components were chicken manure (C), zeolitic tuff (Ca-chabazite) (B), soil improver obtained from a mixture of pruning shears of urban green (SL) and water (A). Ca-chabazite was added in order to reduce unpleasant smells, trap ammonium excess , and contribute to the formation of a post-breeding substrate that can be used as high-quality compost.

It is important to control the moisture content in the waste (growth substrate), since it influences the growth and survival of the species (Cheng et al., 2017). Many authors reported that the presence of excessive moisture content can hinder decomposition rate and the resulting residue may be accompanied by thick and clumpy material, causing difficulty in further processing (Diener et al., 2011b). According to Fatchurochim et al. (1989), the survival efficiency of filth fly fed with poultry manure was highest in the presence of moisture content between 40 and 60%. Similarly, highest growth of pupae was recorded at 85% moisture present in faecal sludge in the study by Banks (2014). All experiments and all replicates were carried out in glass containers (21 cm width x 13 cm depth x 6 cm height) filled with 300 g of mixture and 200 one-week old larvae for replicate. The results of this first set of experiments suggested to remove the soil improver and the higher temperature (33°C), due to a high mortality of larvae. Subsequently, mixtures were designed with chicken manure, Ca-chabazite of two particle sizes (coarse-grained 0-6 mm and micronized < 20µm zeolitic tuff) and water tested at 27°C. This second set of experiments suggested the exclusion of micronized Ca-chabazite because of a 3-4 day delay in prepupae development. Results from this set of experiments allowed the definition of the optimal composition for the substrates to obtain the highest percentage of prepupae (71-74%) and the highest average prepupae weight (0.069-0.072g). They were therefore selected to plan the validation test. Particularly, for the validation test, four different mixtures were selected where chicken manure ranging between 34.5 and 45.0%, Ca-chabazite (larger particle size) between 5.0 and 7.2%, and water between 50.0 and 58.3%. These four mixtures gave a percentage of prepupae between 72-97%, mortality between 20-25%, average weight of 60-100 mg, and a

percentage of emerged adults between 94-100%. Considering percentage of prepupae (PP) as the response variable, the optimal composition corresponds to mixture A (58.3%), C (34.5%), B (7.20%); considering average weight of prepupae (AW) as response variable the optimum scenario corresponds to mixture A (50%), C (45%), B (5%). If both parameters (PP and AW) are considered, optimal mixture is A (55.5%), C (38.9%), B (5.6%) while if both parameters are considered, with an increased importance for percentage of prepupae (D), the optimal mixture is A (56.7%), C (36.9%), B (6.4%).

2.1.2 Density of flies

Tests were performed to assess the effect of population growth on larval development. Three different densities of larvae were tested. The larvae were grown on mixtures that optimized the percentage of survival of prepupae and their average weight. The results showed that optimal density is 200 larvae (59.42-74.5% prepupae), while, with an initial larvae amount of 400 and 600, prepupae percentages of 16.44-40.25% and 3.03-6% prepupae are obtained respectively.

2.1.3 Eggs laying performance in different conditions

In order to optimize adult breeding, a bioassay was conducted to evaluate the effects on fertility (as the number of eggs obtained) of a series of factors:

a) type of light sources;
b) diet;
c) population density.

The aim was to identify the best conditions to obtain the highest amounts of eggs in the shortest time. Although the information on larvae development is abundant, the necessary knowledge on adult biology to produce large amounts of eggs remains a great challenge.

Bioassay were performed considering three light sources (fluorescent tubes, white LED and the UV-green-blue combination of LEDs) and three different diets (sugar and water, just water or nothing). All the experiments were conducted in nylon mesh cages (30 cm width × 30 cm depth × 30 cm height) at 27°C ± 0.5°C and 70 ± 5% relative humidity. For each experiment 5 replicates/treatment were conducted. Each replicate consisted of 15 couples of adults (< 24 hours old). The graphs below (Figure 2-1 - Figure 2-2) show the influence of the two treatments (light and diet) on the total number of eggs collected during the entire experimental period.

For light treatment (Figure 2-1), the highest percentage of eggs obtained was registered by using the combination of LEDs (47.17% of the total amount of eggs obtained), followed by fluorescent light (31.60%) and finally the white LED (21.24%).

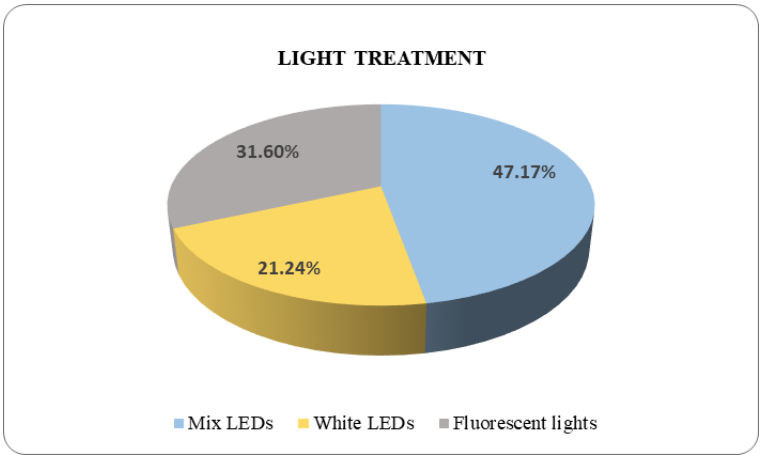

Figure 2-1 Effects of different light treatments on the percentage of eggs obtained

Regarding diet treatment (Figure 2-2), the best performance was obtained by feeding the adults on sugar and water (60.62%) followed by water (32.11%) and absence of food (7.27%).

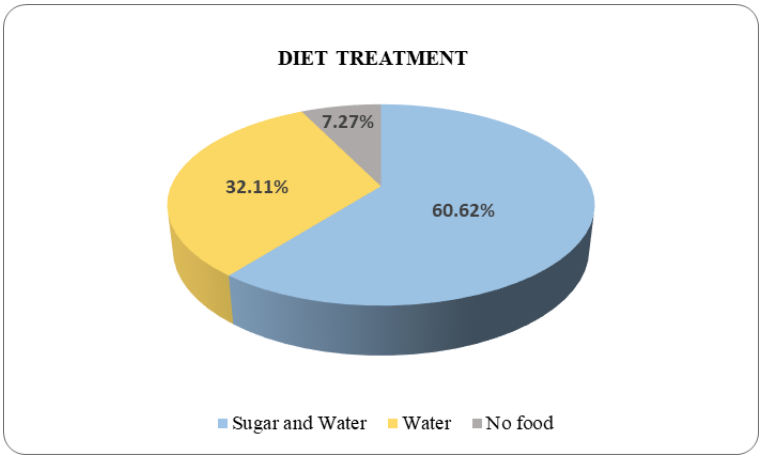

Figure 2-2 Effect of diet treatments on the percentage of eggs obtained

The number of total days for oviposition also varied with the diet: it varied from 4 days (no food) to 13 days (diet with water) and to 29 days (diet with water and sugar).
The results regarding the different tested light combinations with the different diets, allowed the identification of the optimal conditions to obtain the highest production of eggs per day, which is a crucial parameter for industrial insect rearing. The best production of eggs per day was observed by using UV-green-blue combination of LEDs combined with water and sugar diet.
For population density, tests were carried out increasing the density up to 20,000 adults per cubic meter. No negative effects were observed on the number of eggs laid, therefore the density is not a relevant parameter.

2.1.4 Evaluation of olfactory impact

The evaluation of olfactory impact on the composts obtained by breeding the larvae on the different mixtures (A/B/C) showed a significant reduction of bad smells as a consequence of the action of the larvae. In particular, for these tests four different substrates (not digested by black soldier flies) were compared with the same substrates digested by black soldier flies, showing a reduction in olfactory impact.

2.2 Design of pilot plant for breeding black soldier flies

Using the breeding conditions identified in the laboratory, a pilot plant for mass breeding of black soldier fly larvae for the valorisation of organic waste was designed by Ing. Giacomo Benassi in collaboration with Kour Energy company s.r.l. (http://www.kourenergy.com/).
The pilot plant consists of two main parts (physically separated):

1. *Nursery*.
2. *Bioconverter*.

In addition, a substrate preparation system and a sorting system were installed in the demonstration plant.

2.2.1 Nursery

Figure 2-3 Nursery unit

The purpose of nursery unit (Figure 2-3) of the plant is to produce eggs and larvae at the first life stage efficiently. These larvae are introduced in the bioconverter in order to process waste. After the adults emerge from their pupal cases, their primary focus is to mate and lay eggs. They do not feed and only drink water and sugar. The adults are kept in a nylon cage (60 cm width × 60 cm depth × 120 cm height) inside an isothermal box (80 cm width × 100 cm depth ×200 cm height) which is made up of a rigid polyethylene shell insulated with expanded polyurethane foam (thick: 80 mm). LED lamps with three specific wavelengths (515 nm, 450 nm, 365 nm), which already demonstrated the best effect on the mating and oviposition of Hermetia illucens, illuminate the cage. The temperature of the nursery is fixed at 26°C and 70% of Relative Humidity. A miniaturized single-board computer mounted directly on the box monitors the temperature and humidity. Attached to the single-board computer is an integrated camera, in order to extrapolate with dedicated algorithms the number of flies, number of matings, and number of dead flies. Just a single initial input of pupae is needed to start up the process, thereafter the production chain constantly supports itself through limited withdrawals from the larvae colony. The breeding facility includes a device to facilitate egg laying/gathering.

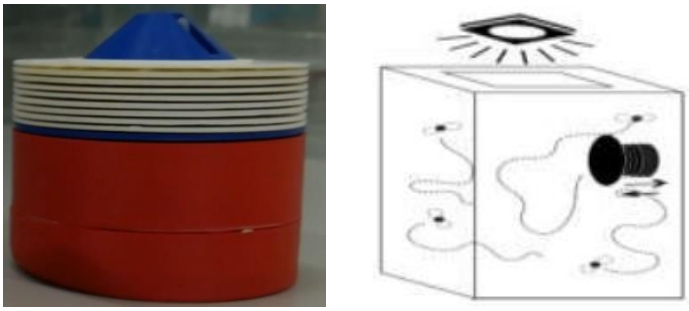

Figure 2-4 Patented device for eggs collection

This device (Figure 2-4) includes a tank that, through an opening, gives off an attractive compound for the females; it is connected to a body provided with a plurality of blades spaced apart by interspaces suitable to favor the insertion of eggs. The device has a particularly efficient, compact structure that is easy to construct. It prevents the escape of adult insects, limiting to a minimum the tampering of the eggs thanks to the peculiar extraction/insertion mechanism (Figure 2-5).

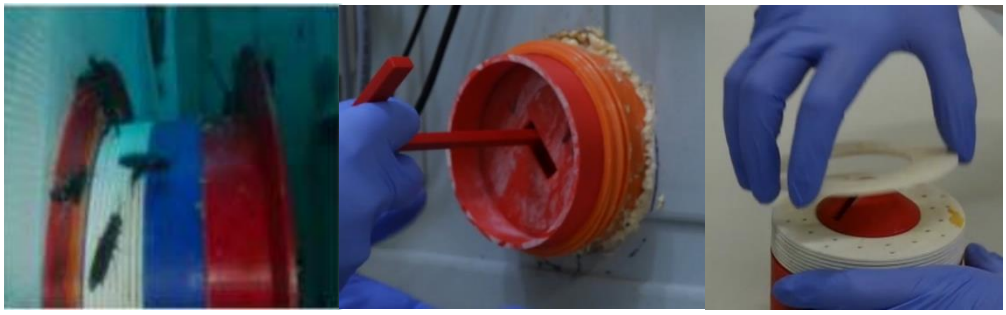

Figure 2-5 Extraction of device to remove eggs

2.2.2 Bioconversion plant

Kour Energy s.r.l. in collaboration with the University of Modena and Reggio Emilia designed the bioconverter.
The objective of the bioconverter is to produce, in semi-automatic manner, adult larvae and compost starting from the substrate and larvae newly produced by the Nursery. The bioconverter is therefore a modular structure consisting of four modules having all the same size (Figure 2-6):

1. substrate injection module.
2. Storage module 1.
3. Storage module 2.
4. Substrate tilting module.

The four modules are inserted in an isothermal container (245 cm width × 351 cm depth × 136.5 cm height).

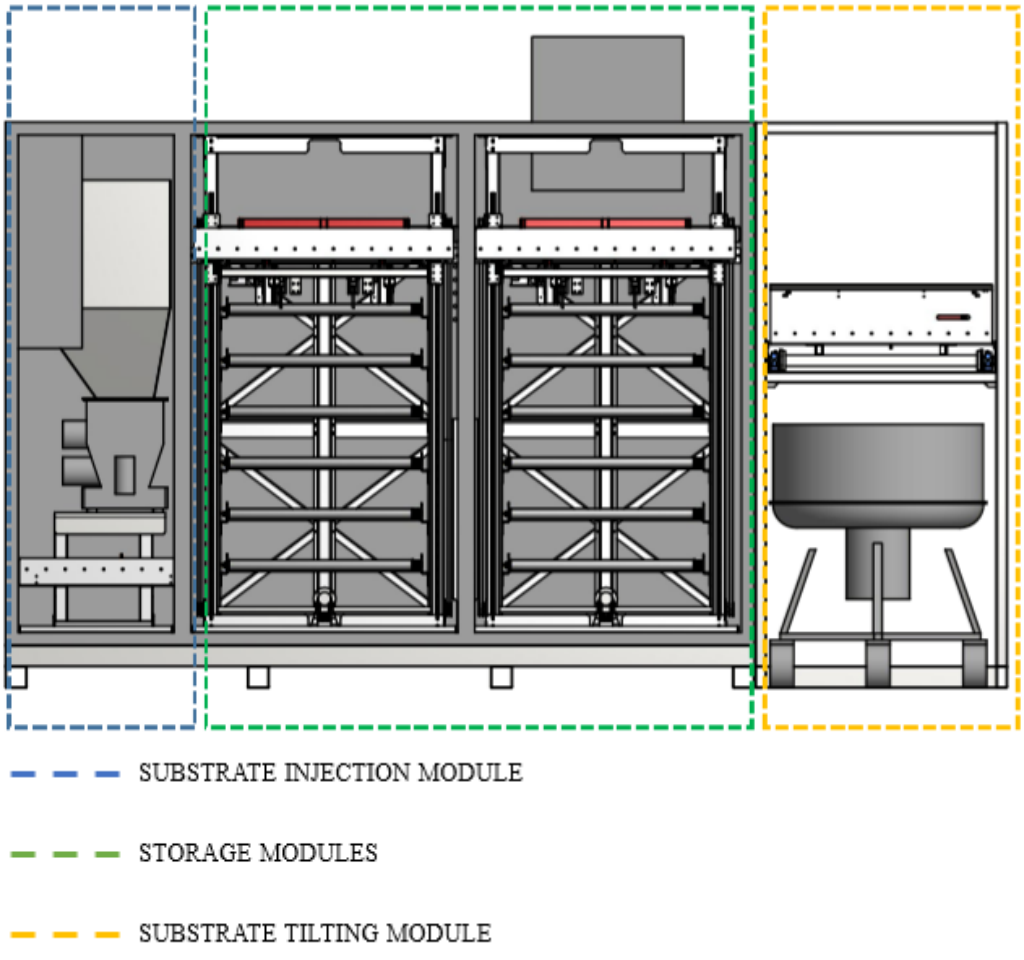

Figure 2-6 Bioconversion unit

2.2.2.1 Substrate injection module

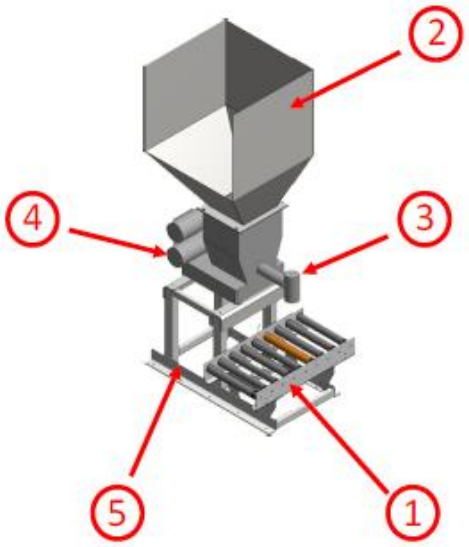

Figure 2-7 Substrate injection module

The injection substrate module (Figure 2-7) consists of the following components:

1. roller conveyor to allow the movement of the growth tray. It consists of rollers and motor-rollers.
2. Hopper.
3. Mechanical system with pusher (auger) for the introduction of the substrate in an automatic and controlled way, thanks to a load cell for measuring hopper weight loss.
4. Electric motors.
5. Support structure.

All components are in stainless steel or in S235JR non-alloy structural steel.

2.2.2.2 Storage substrate modules

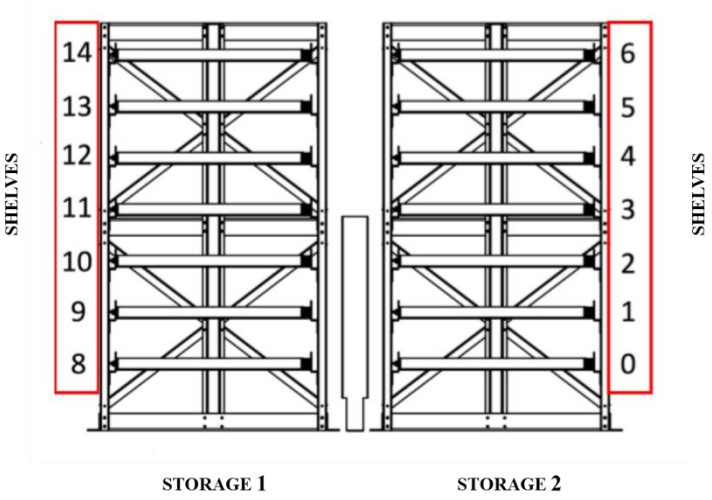

Figure 2-8 Storage substrate modules

The bioconverter consists of a high number of trays vertically arranged in order to minimize the total area of the plant. Inside the bioconverter there are two identical storage modules (Figure 2-8), each of which is identified by a number and a relative position with respect to the system. Each storage module consists of seven motorized shelves (roller conveyors) arranged vertically. Each shelf is designed to accommodate up to two growth trays simultaneously. For each type of substrate, a specific feed rate/feed quantity per day (diet) has been optimized, through lab experiments, in order to maximize larvae density and bioconversion efficiency. Despite the high-compact vertical arrangement, it must always be possible to add new substrate (feed) or water for each tray, regardless of their location inside the bioconverter. For this reason, the bioconverter is designed to move automatically all the trays (like an automated storage), to move a selected tray of interest (selected by an operator) and to eject the tray of interest "outside" the bioconverter. All these actions are performed by means of an elevator coupled with second elevator. Indeed the latter allows the tray to move vertically and horizontally. In addition to this, the elevator is able to insert and extract the trays from the shelves of the storage by means of a specific system.

2.2.2.3 Substrate tilting module

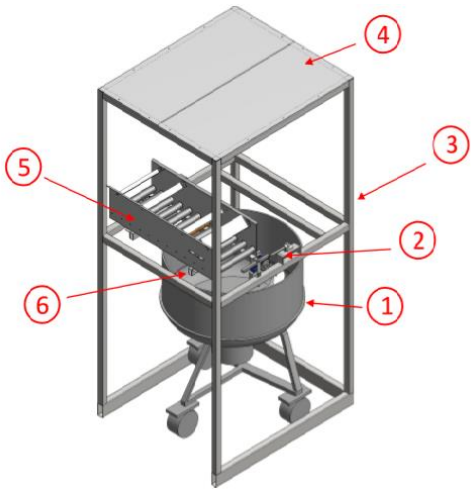

Figure 2-9 Substrate tilting module

The tilter module (Figure 2-9) is an external module to the isothermal container and mainly consists of:

1. vibrating sieve.
2. Electric motor and actuator with ring.
3. Support structure.
4. Coverage structure that prevents access by unauthorized personnel, but still allowing quick inspections.
5. Tray roller conveyor structure.
6. Translation system

Chapter 3
Extraction protocol of biomolecules: lipids, proteins, chitin

3 EXTRACTION OF BIOMOLECULES: LIPIDS, PROTEINS, CHITIN

3.1 State of the art of the extraction protocol of biomolecules from biomass of insects

In literature few extraction protocols are reported. Most of them had the aim to extract just one component from insect biomass, in particular most of these studies focused on protein extraction only.

Del Valle, Mena, and Bourges (1982) carried out protein extraction from *Anastrepha ludens* at pH 10 and successive protein precipitation at pH 5. Yi et al (2013) performed an aqueous extraction of proteins from five insect species (*Tenebrio molitor* (larvae), *Zophobas morio* (larvae), *Alphitobius diaperinus* (larvae), *Acheta domesticus* (adult) and *Blaptica dubia* (adult)). Bußler, Rumpold, Jander, Rawel, and Schlüter (2016) investigated a comparison of protein extraction methods from *Tenebrio molitor* and *Hermetia Illucens*.

However, insects, especially black soldier fly, are good sources of other valuable biomolecules like lipids and chitin. Therefore, it is necessary to develop a systematic approach to recover all the three fractions in subsequent steps, along the same chain in a cascade biorefinery, in order to obtain the maximum added value from the process. While separation of lipidic fraction is easy, the separation of proteins from chitin is more challenging.

Scarse data are available in the literature regarding the separation of proteins from chitin in the insect matrix. The available data concern separation procedures on crustaceans, currently the main source of commercial chitin/chitosan (Gortari & Hours, 2013).

In these studies it is reported that the most common method to recover chitin from crustacean shells is the chemical procedure, structured in two main steps: demineralization and deproteinization using strong acids and bases. Alternative processes to the chemical one have been investigated on crustaceans, such as fermentation and enzymatic hydrolysis (Synowiecki & Al-Khateeb, 2000).

This study, thanks to the collaboration with *SITEIA PARMA* consortium, explored, for the first time, several systematic procedures aimed to recover all the three main biomolecules of black soldier fly at the highest purity level, with homogeneous methodologies in a biorefinery approach. Particularly, three different approaches were tested on black soldier fly: two different chemical protocols, principally differing for the protein extraction method, and an enzymatic one. All the protocols were performed at laboratory scale and were repeated three times.

Data are presented as mean and standard deviation of the different trials.

3.2 Composition of Black Soldier Fly

In the first step BSF prepupae composition was calculated because it is the basis to design and evaluate fractionation procedures and to calculate their efficiency.

Results of previous studies (Sheppard, Newton, Thompson, & Savage, 1994) reported that dry matter (DM) content of BSF prepupae was found to be 34 ± 0.1%. Unlike other insect species, BSF prepupae represent a good source of energy because they have a higher lipid content (37.1± 0.1%) (DM basis) (Ramos-Bueno, González-Fernández, Sánchez-Muros-Lozano, García-Barroso, & Guil-Guerrero, 2016). Crude fat content was determined using an automatized Soxhlet extractor using diethylether. The relative fatty acid profile of the extracted fat was determined by GC-MS method after acid methylation, thus including triacylglycerol-bound fatty acids and free fatty acids. From this profile (not reported) it can be noted that the composition was dominated by lauric acid (46.7 ± 0.6%), followed by oelic acid (15.1 ± 0.9%), myristic (8.3 ± 0.1%), palmitic (8.4 ± 0.2%) and palmitoleic (7.6 ± 0.4%) acids. Minor amounts of C10:0 (1.9 ± 0.2%), C14:1 (1.3 ± 0.2%), stearic (2.5 ± 0.1%) and linoleic acid (1.8 ± 0.4%) were also found.

The strong presence of saturated fatty acids (72% of the whole lipid fraction) and the scarce presence in polyunsaturated fatty acids suggested that the addition of antioxidants in the lipid extraction media can be avoided during the development of extraction protocols because it is not essential.

Protein content is generally calculated from total nitrogen, using a standard nitrogen-to-protein conversion factor of 6.25. In the present case, the total nitrogen amount is equal to 6.61 ± 0.05%. In general, the total nitrogen content in insects consists of nitrogen originating from proteins and non proteins. In the latter case, non-protein nitrogen content is represented by chitin, a polymer of *N*-acetylglucosamine. Therefore, in order to obtain an accurate composition of black soldier fly it is necessary to separate protein and chitin contribution from total nitrogen content. For this purpose, the nitrogen conversion factor specific to BSF protein only and to chitin was calculated. The nitrogen conversion factor specific to BSF protein only was calculated from the total amino acids as reported by Thachuk (1969). To this scope, total amino acid content of BSF prepupae (expressed as (grams/100 DM) and as (mg of each amino acid/grams of crude protein)) was determined. From the amino acid distribution, a Kjeldahl conversion factor of 5.71 ± 0.2% for BSF proteins was calculated. After calculating Kjeldahl conversion factor for BSF proteins, the total amount of proteinaceous *N* was calculated from amino acid analysis. A content of 5.59 ± 0.05% on DM basis was found, indicating that in BSF prepupae, nitrogen content attributable to proteins is equal to 84%.

Using calculated Kjeldahl conversion factor for BSF proteins a global protein content of 32 ± 2% was found. From protein content, the contribution of non-protein nitrogen to total nitrogen was determined by difference:

$$N_{chitin} = N_{total} - N_{protein} = (6.61 \pm 0.05) - (5.59 \pm 0.05) = (1.02 \pm 0.04) \text{ on DM} \quad (1)$$

The nitrogen conversion factor for chitin was theoretically calculated. It can vary from 14.5, assuming a fully acetylated chitin, to 11.5 for a fully deacetylated chitin. Starting from these values and

assuming that all the non-protein nitrogen is due to chitin, a chitin content ranging from a minimum of 11.7% to a maximum of 14.6% can be calculated. The value depends on the acetylation degree.

These values are higher than those reported in literature.

To check the effective chitin content, a specific GC-MS method for the determination of glucosamine after total hydrolysis of chitin in acidic media was applied, based on the method of Flunnery et al. (2001). Using this method it was found that the chitin content is equal to 9 ± 1% on DM basis. This value corresponds to a nitrogen content of 0.62 ± 0.06%, indicating that 10% of the total nitrogen of BSF prepupae is contained in chitin. Subtracting protein and chitin content from the total nitrogen amount, a residual nitrogen (0.40% on DM) was obtained, which represented 6% of total nitrogen content.

We can therefore conclude that BSF prepupae contain a quantity of non-protein and non-chitin nitrogen that can be present as up to 3% of the dry matter weight. This amount might include melanin. Total ash was also determined after mineralization at 550°C for 5hr + 5hr. It was found that content of ashes amounts to 19% on DM basis.

It can be concluded that, on DM basis, lipids accounted for 37%, protein for 32%, chitin for 9%, ashes for 19% (Figure 3-1). Therefore the total accounted for 97%. Since we also found that nitrogen-containing compounds corresponding to non-protein and non-chitin are also present, and this content can be present in up to 3% of the dry matter weight, the mass balance of BSF prepupae seemed to be perfectly explained.

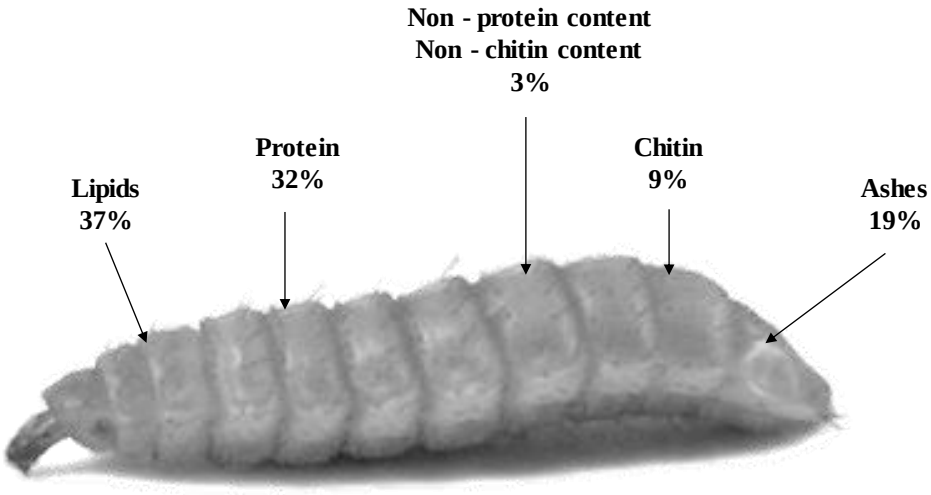

Figure 3-1 Composition of Black Soldier Fly prepupa on DM (%)

3.3 Extraction protocol 1: chemical method with one step protein extraction

The method used was adapted from the work of Sara Bußler et al.
The lab-scale extraction protocol is summarised in Figure 3-2. Extraction was performed on 375 g of finely grinded mature larvae (prepupae) of black soldier fly.

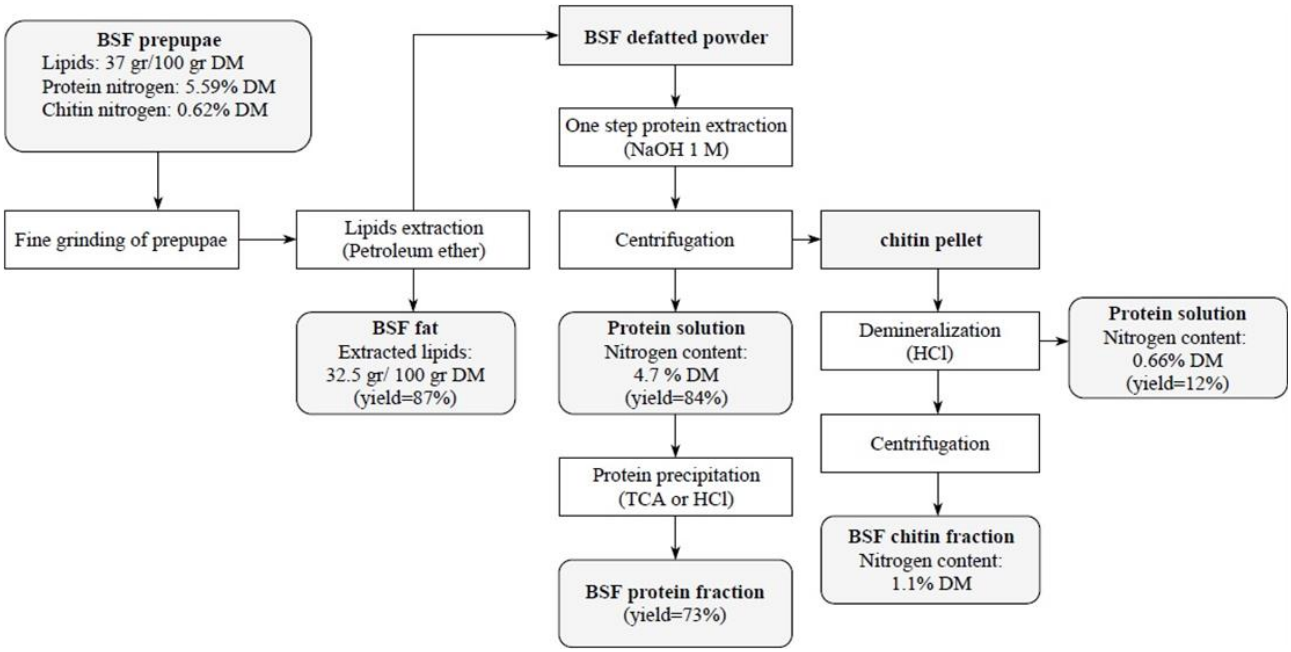

Figure 3-2 Processing and biomolecule fractionation of BSF prepupae according to protocol 1

3.3.1 Extraction lipidic fraction

As a first step, lipidic fraction was extracted. Lipids are extracted with petroleum ether (40 - 60°C boiling point fraction) by two-step manual extraction. It was decided to use petroleum ether as solvent because it showed the right compromise between extraction yield and costs, compared to other solvents tested, such as diethyl ether or CH_2Cl_2/MeOH blend.
A heated bath (60°C) of distilled water (1,540 Lt) was prepared (Figure 3-3).

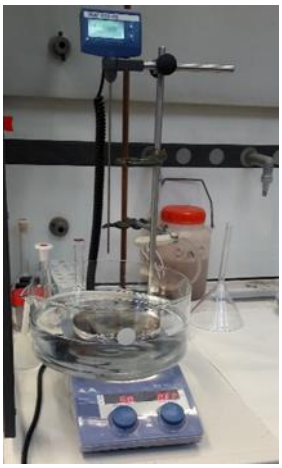

Figure 3-3 Bath of distilled water

Subsequently one part of black soldier fly biomass (375 g) and two parts of petroleum ether (1 Lt) (weight/volume) were placed in a flask and then stirred by a magnet stirrer for 1 hr, as depicted in Figure 3-4.

Figure 3-4 Flask with black soldier fly biomass and solvent

To avoid evaporation of the solvent, the flask is covered with aluminum foil. Then the solvent containing lipidic fraction is then decanted and separated from solid biomass by filtration (Figure 3-5).

Figure 3-5 Filtration

After recovering the lipids containing solvent, the lipidic fraction was isolated by petroleum ether evaporation under vacuum (Figure 3-6). The recovered solvent was used to repeat the procedure for the second time. After the second procedure, the recovered solvent was disposed of. The residual solvent was removed from the defatted insect pellet and from the lipidic fraction by overnight evaporation at room temperature (8 hr).

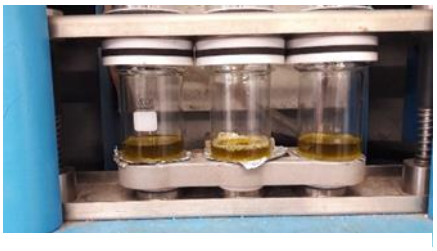

Figure 3-6 Lipidic fraction

3.3.1.1 Extraction yield determination

Extraction yield was calculated by weighting the amount of fat extracted by this process and comparing it with the total amount of fat determined previously by ethyl ether Soxhlet extraction.

The total amount of fat extracted with this method was 31.18 ± 0.5% on dry matter basis, corresponding to an extraction yield of 84% compared to the total fat obtained by Soxhlet (37.1 ± 0.1% on dry matter).

(2)

$$W_{fat} = 375 \times (1 - MC) \times yield\ (\%\ DM) \cong 39.44\ \ [\text{grams}]$$

Then

(3)

$$yield\ (\%\ WM) = \frac{W_{fat}}{375} \times 100 \cong 10.52\ [\%]$$

with

W_{fat}: $weight\ of\ \ extracted\ fat\ [grams]$

$yield\ (\%\ DM)$: $extraction\ process\ yield\ on\ dry\ matter\ basis\ [\%] = 31.18\%$

$yield\ (\%\ WM)$: $extraction\ process\ yield\ on\ wet\ matter\ basis\ [\%]$

MC: $moisture\ content\ of\ maturae\ larvae\ (prepupae)\ according\ to\ centesimal\ composition\ [\%] = 66.27\%$

3.3.2 Protein fraction extraction

Defatted BSF pellet was subjected to the deproteinization and subsequently to the demineralization steps, in order to obtain purified protein and chitin fractions. The protein fraction was separated from the chitin fraction. The separation procedure of the two fractions was based on the method developed for the isolation and purification of chitin and chitosan from shrimps (Bajaj, Winter, & Gallert, 2011; Zhang, Yuna, Songa, Zhanga, & Zhaob, 2017).

Since these methods were optimized only for the chitin extraction, it was necessary to modify them applying the mildest conditions as possible, in order to preserve both the chitinic and protein fractions and isolate them from BSF as intact as possible.

A heated bath (40°C) of distilled water (1,540 Lt) was prepared. The defatted insect pellet was treated with a 40 mL of 1 M sodium hydroxide (NaOH) solution at 40 °C under stirring for 1 hr. Subsequently, the mixture was placed into centrifuge tubes and was centrifuged for 15 minutes at 4 ° C at 4000 rpm, in order to separate the solubilized protein containing supernatant from the chitinous fraction containing pellet (Figure 3-7, Figure 3-8).

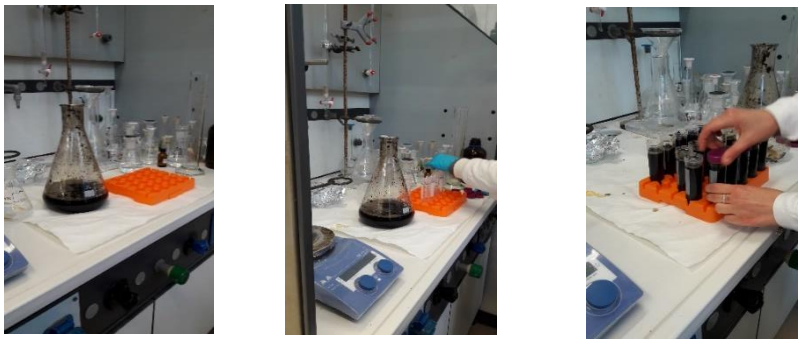

Figure 3-7 Supernatant aliquoted into centrifuge tubes

Figure 3-8 Centrifuge tubes placed into the centrifuge machine

Nitrogen content was assessed for surnatant: the percentage of nitrogen was 4.7 ± 0.5% on dry matter (Figure 3-2), corresponding to 84% recovery of protein fraction (it was found that proteinaceous N calculated from the amino acid analysis amounts to 5.59 ± 0.05% on dry matter). A residual fraction of proteins (corresponding to N % = 0.7 ± 0.2, 12% of protein content, Figure 3-2) was further solubilized during the following acidic demineralization step of chitinic pellet.

Thus, this proposed alkali extraction of defatted BSF powder allowed a final recovery of 96% of protein fraction, if the two fractions obtained are considered together. Therefore, alkali extraction was considered very efficient in terms of yield, although it can produce reactions in the protein backbone, leading to denaturation, hydrolysis, racemization, lysinoalanine and other crosslinked compounds (Schwass & Finley, 1984). These modifications might reduce both protein function and nutritional value. In order to evaluate protein modification in terms of hydrolysis, the OPA method (Spellman, McEvoy,O'Cuinn, & Fitsgerald, 2003) was used as a non-specific rapid method to evaluate protein integrity, because it can detect the number of NH_2 free groups.

The degree of hydrolysis (referring to solubilized proteins) was calculated. It amounts to 15%. Hydrolysis induced by proposed alkali extraction is therefore confirmed.

After protein separation from chitin rich residue, proteins were isolated. Three different methods were tested:

1. drying by rotary evaporator
2. freeze-drying
3. precipitation by trichloroacetic acid (TCA) or HCl.

The first two methods resulted inconvenient. Indeed proteins showed significant foaming properties in line with that reported by Hall, Jones, O'Haire, & Liceaga, 2017. An additional problem was the salt resulting from neutralization, because drying together with the sample, it leads to lowered protein purity.

Subsequently, we tested precipitation by trichloroacetic acid (TCA) or HCl. A quantity of the supernatant was treated with HCl 6N until a pH=4 (Sara Bußler BA, 2016) was achieved, the other half with 10% trichloroacetic acid (TCA) in acetone (ratio 1:1, v/v) (W.Schwert, 1956) (Figure 3-9). Precipitation with HCl was based on the principle of precipitation at the isoelectric point of proteins (pH value characterized by minimum solubility). Although positively or negatively charged, at pH=4 proteins will have a residual zero charge. This allows proteins to lose the ability to interact with other molecules and to precipitate. Conversely, the precipitation with 10% TCA in acetone, exploits the role of acetone in lowering the dielectric constant of the medium, thus, allowing protein-protein electrostatic interactions and therefore their precipitation (Sivaraman T, 1997).

Both mixtures were then incubated overnight at -20°C in order to help protein aggregation and subsequently they were centrifuged for approximately 20 minutes at 4°C at 4000 rpm. The recovered liquid phase was disposed of as hazardous special waste. The pellet precipitated with HCl was washed twice with distilled water, while the pellet precipitated with TCA was washed twice with acetone in order to eliminate the remaining acid residues.

Figure 3-9 Bottles with supernatant (supernatant with HCl 6N) & (supernatant with TCA + acetone)

The precipitation by trichloroacetic acid (TCA) allowed to avoid salt formation, thus high purity proteins were obtained. This precipitation allowed to obtain a final protein yield of 73% (calculated on the starting total protein content in BSF). A similar yield of precipitated proteins (67%) was obtained by HCl co-precipitation.
The final product corresponds to the extracted proteins which were placed into an oven to dry (2 hours at 90°C).

3.3.3 Extraction of chitinic fraction

The nitrogen content of solid residue, previously separated from the neutralized supernatant (chitin pellet) was assessed (1.1 ± 0.2%, Figure 3-2) corresponding to the chitin nitrogen, plus a small residual amount of protein and other nitrogen containing compounds, like melanin. The pellet was then demineralized with 2 N HCl solution for 24 hr at room temperature. Then, the sample was centrifuged for 15 min at 4000 rpm. The precipitate was washed twice with distilled water and the final chitin-rich residue was dried at 40°C overnight in an oven.

3.3.4 Advantages and disadvantages of extraction protocol 1

The main advantages of the above reported protocol were:

1. rapidity of execution;
2. easy scaling-up possibilities;
3. the fraction extracted can be used for technological applications (e.g. bioplastic formulations), but also as foaming/emulsifier additive.

The protocol presents a series of disadvantages including the use of solvents and acidic as well as alkali solutions, the modification of proteins and a possible depolymerization of the chitin which could affects the properties of the biopolymer.

3.4 Extraction protocol 2: total chemical extraction with stepwise protein extraction

This extraction protocol was based on the Osborne fractionation method (Osborne, 1907) with some modifications. The initial fat extraction procedure and the demineralization step remained unchanged with respect to the chemical extraction procedure previously described. As a variant of the previous method, protein fraction was extracted by a stepwise method (Figure 3-10).

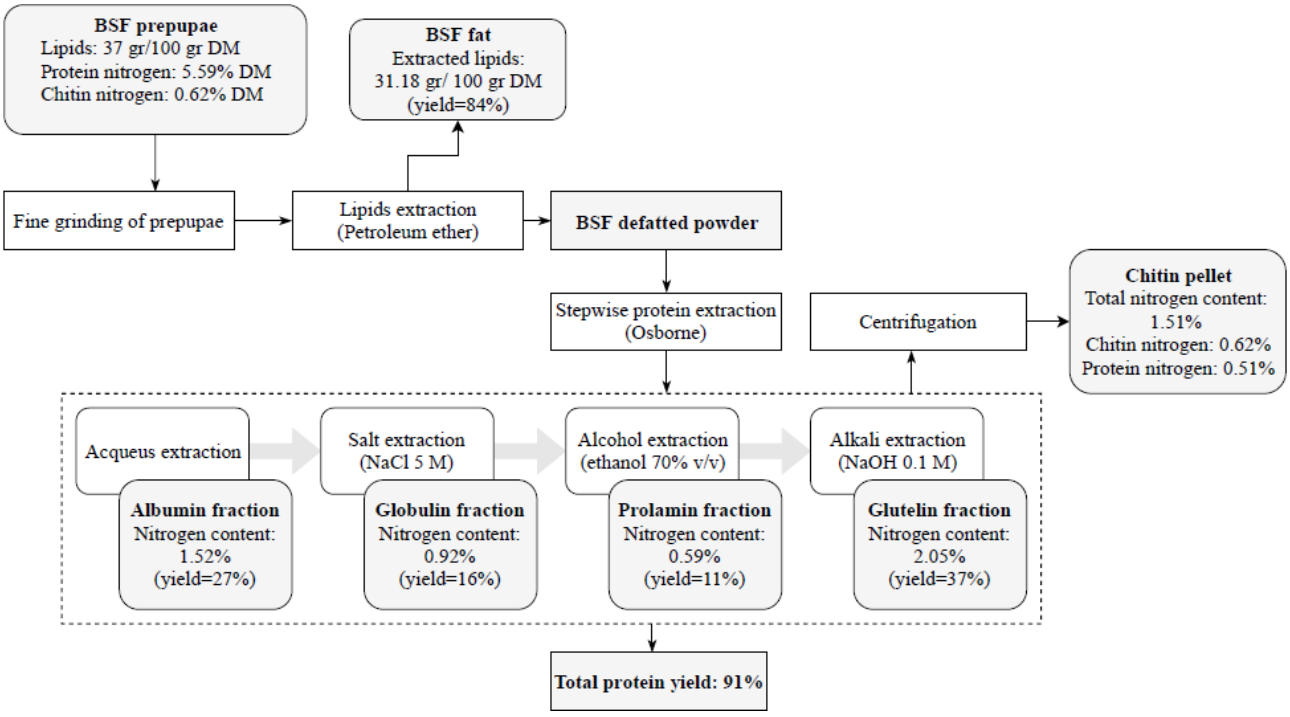

Figure 3-10 Processing and biomolecule fractionation of BSF prepupae according to protocol 2

Protein extraction was based on their different solubility in different solvents. Five fractions were obtained:

1. the first fraction consisted of proteins extractable in water, i.e. albumins. Defatted sample (2 g) was mixed with 40 mL of a solution prepared with 5 mM sodium ascorbate, 2 mM ethylenediaminetetraacetic acid (EDTA) and 10 mM tris-HCl. The suspension was mixed for 1 h at 4 °C and centrifuged for 20 min at 4000 rpm at 4 °C. The surnatant was collected as albumin fraction.
2. The second fraction was represented by the globulin fraction, soluble in saline solution. Pellet in the previous step was mixed with 40 mL of a solution prepared with 0.5 M NaCl, 5 mM sodium

ascorbate, 2 mM ethylenediaminetetraacetic acid (EDTA) and 20 mM tris-HCl. The suspension was mixed for 1 h at 4 °C and centrifuged for 20 min at 4000 rpm at 4 °C. The surnatant was collected as globulin fraction.

3. The third fraction was represented by insoluble proteins (prolamins),that were extractable in alcoholic solution. The pellet obtained in step 2 (extraction of second fraction) was mixed with 40 mL of 5 mM ascorbic acid in 70% EtOH. The suspension was mixed for 1 h at 4 °C and centrifuged for 20 min at 4000 rpm at 4 °C. The surnatant was collected as prolamin fraction.
4. The fourth fraction consisted of glutelins extractable in alkali solution. The pellet obtained in step 3 was extracted with 25 mL of 0.1 N NaOH and 5 mM ascorbic acid. The extraction was carried out under stirring at 4 °C for 1 h and then centrifuged for 20 min at 4 °C at 4000 rpm. The supernatant was collected as glutelin fraction.
5. The pellet obtained represented the chitin fraction and the eventual residual protein fraction. From this solid fraction it was possible to obtain a chitin fraction of higher purity, applying the same demineralization step described in protocol 1.

Chitin is insoluble in all the four extraction systems (Pillai, Willi, & Chandra, 2009), therefore nitrogen content in the extraction solutions can be presumed protein nitrogen. The first fraction could have contained also some non-protein nitrogen-soluble compounds, however their amount was low. This is confirmed by the OPA method (Spellman, McEvoy, O'Cuinn, & Fitsgerald 2003) used to evaluate the free amino group.

3.4.1 Advantages and disadvantages of extraction protocol 2

This extraction procedure allowed to obtain a good separation of the protein from the chitin fraction.

The total nitrogen extracted in the four fractions amounted to 90% of the theoretical protein nitrogen. As the OPA test (Spellman, McEvoy, O'Cuinn, & Fitsgerald, 2003) confirmed, protein fractions recovered by this extraction protocol were intact since all the extraction steps were performed in mild conditions Therefore, this is a good method to recover intact proteins to be used for nutritional purposes or high added-value products (e.g. for feed/food ingredients, cosmetics, pharma). It is necessary to investigate functional properties, specific amino acid profile and nutritional value of each protein fraction.

One of the major disadvantages of this extraction protocol developed at laboratory scale is represented by the high costs that would probably arise by its scaling up to an industrial level, due to the four sequential extraction phases.

3.5 Extraction protocol 3: enzymatically-assisted fractionation

In this extraction method on the grinded prepupae (Figure 3-11), without any pre-treatment, four different proteolytic enzymes were separately tested on analytical scale:

1. enzyme derived from vegetal source: *papain*.
2. enzyme derived from bacterial source: *B. licheniformis protease*.
3. enzyme derived from animal source: *pepsin and pancreatin*.

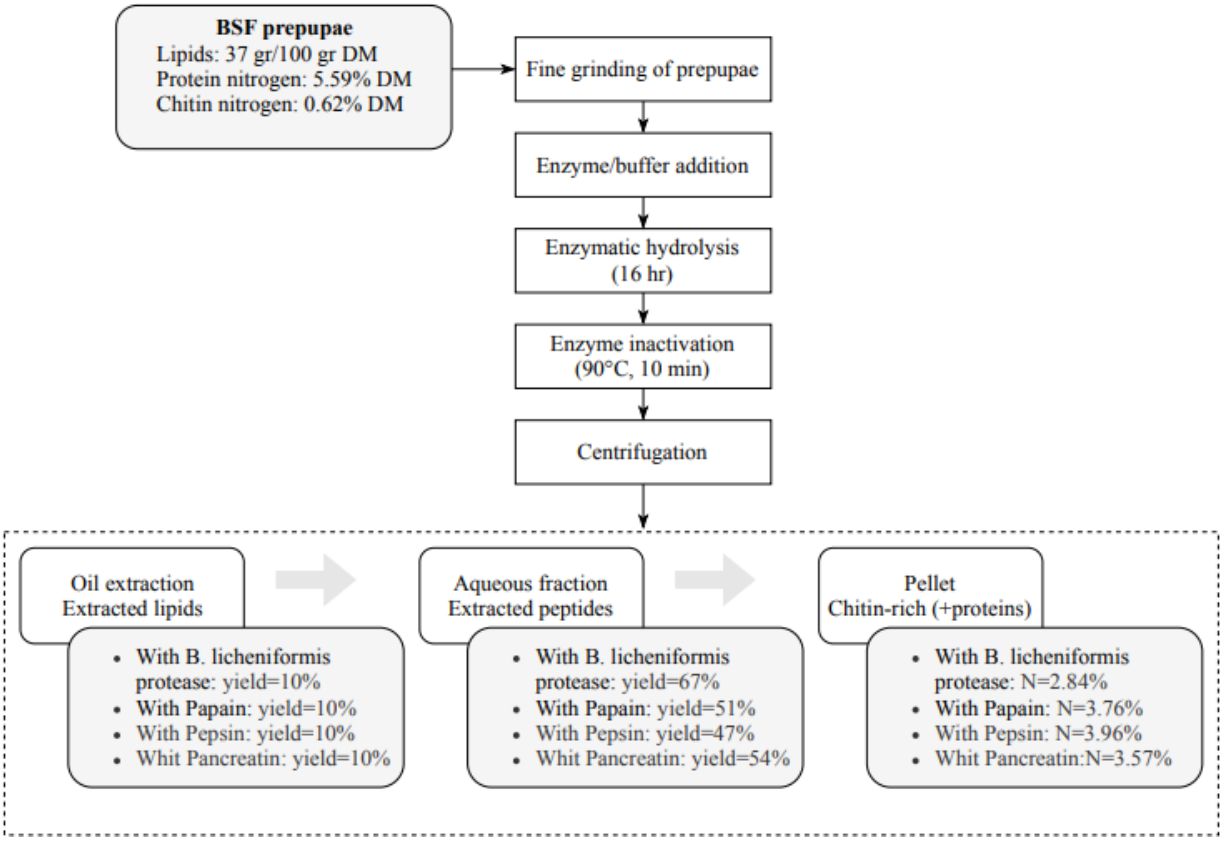

Figure 3-11 Processing and biomolecule fractionation of BSF prepupae according to protocol 3

Each enzyme requires specific reaction conditions (temperature, pH, buffer solution) (Table 3-1), chosen according to provider specifications and based on the results of a previous study (Anzani et al., 2017). Degree of hydrolysis was calculated taking into account only the proteins present in solution after enzymatic hydrolysis. Three replicates were performed and the DH% values were calculated after subtracting the absorbance of the samples without enzyme.

Enzyme	***Temp***	***pH***	***Solution buffer***	***DH% with enzyme***
B. *licheniformis* protease	60°C	6.5	10 mM Na_2HPO_4	6 ± 1
Pepsin	37°C	3.0	10 mM HCl	17 ± 5
Papain	60°C	7.5	10 mM Na_2HPO_4, 2 Mm EDTA, 10 Mm DL-cystine	25 ± 5
Pancreatin	37°C	7.8	25 mM Na_2HCO_3, 2.5 Mm $CaCl_2$	25 ± 6

Table 3-1 Degree of hydrolysis and reaction conditions of BSF prepupae treated with different enzymes

After 16 hours of hydrolysis with the four different enzymes, different fractions were separated:
a) a floating oily fraction corresponding to lipidic fraction;
b) a supernatant liquid underneath, which was mainly composed of soluble intact proteins or hydrolysed proteins;
c) pellet that consisted of insoluble proteins and chitin.

The lipid extraction obtained with the enzymatic method did not produce good results, although a higher lipolytic activity could be expected from the pancreatin enzyme compared to other enzymes, as it consists not only of trypsin and amylase but also of lipase.

For all enzymes under examination, yield amounts to 10% of the total lipids that composed the sample, thus much lower than that obtained with the solvent extraction method as confirmed in the study of Tzompa-Sosa, Yi, van Valenberg, van Boekel, and Lakemond (2014).

In order to evaluate the percentages of proteins and chitin present in the supernatant and in the pellet respectively, the Kjeldahl analysis was carried out on the different fractions, to verify the distribution of the present nitrogen. As a blank control, the determination was also done on the samples treated in the same conditions without enzymes.

Comparing the percentages of relative nitrogen of the hydrolyzate solution and of the control solution, the enzymes analyzed show a different hydrolytic capacity: B. licheniformis is the most efficient, with an extraction yield equal to 67 ± 5% of the total protein nitrogen released in the supernatants (solubilized), followed by pancreatin (54 ± 2% of the total protein nitrogen solubilized), papain (51 ± 2% of the total protein nitrogen solubilized) and pepsin, the least efficient (47 ± 3% of the total protein nitrogen solubilized).

The greater efficiency of Bacillus Licheniformis was possibly due to the greater presence of its site of action among the proteins present in the sample; being a serine protease, the active site consists of residues of Serine (Ser), Histidine (His) and Aspartate (Asp) linked by hydrogen bonds. Many studies confirmed the efficiency of proteolytic activity of this enzyme on this matrix as well as on a meat matrix (Anzani et al., 2017) and fish matrix (Kristinsson et al. 2000).

The degree of hydrolysis (DH%) was also determined with the OPA method (Spellman, McEvoy, O'Cuinn, & Fitsgerald, 2003), calculated on the proteinaceous materials released in solution (Table 3-1). Pancreatin and papain hydrolysis showed the highest DH (25%), followed by hydrolysis with pepsin (17%), and B. licheniformis protease (6%). It should be noted that this latter protease resulted in a higher degree of solubilization, but a lower degree of hydrolysis compared to pancreatin.

As for the nitrogen quantified in the pellet, again using the Kjeldahl method, the percentages were still high compared to the quantity present in the sample as is. This result was possibly due to a lack of hydrolysis of the proteins present, and therefore the quantified nitrogen was attributed both to the quantity of chitin and to non-hydrolyzed proteins as well as to other nitrogenous substances, so it would be necessary to find a method able to determine purity.

3.5.1 Advantages and disadvantages of extraction protocol 3

This extraction method was less efficient than the chemical extractions, but it allowed to avoid the use of organic solvents. Another great advantage of this extraction method is related to the possibility to tailor the hydrolysate composition obtained from BSF proteins for different purposes (such as high digestible and hypoallergenic protein supplements for feed/food, foaming agents and others).
It therefore deserves further investigation.

3.6 Which extraction protocol is more suitable for the purpose of this study?

Analyzing the results deriving by the application of the three different extraction protocols (Table 3-2), it can be concluded that the best lipid extraction is obtained with both chemical extraction protocols (extraction protocol 2 and extraction protocol 1).

With regards to the extraction of protein fraction, the yield obtained applying chemical extraction protocols was higher than the one obtained with extraction protocol 3 (enzymatically-assisted fractionation), even if chemical extraction protocol 2 presented a higher yield than chemical extraction protocol 1.

But actually, these results are not enough to discriminate one method over another, since it would also be appropriate to evaluate the quality of the extracted proteins, such as the presence of intact, degraded or hydrolyzed (totally or partially) proteins.

Finally, chitin purity is higher if chemical extraction protocol 1 was applied, probably because the different washes requested in the procedure solubilized further non-chitinous substances, making the chitin fraction purer. However, since for the application of this study it was not necessary to have intact proteins, it was agreed to choose chemical extraction protocol 1, which, despite guaranteeing a lower protein yield than chemical extraction protocol 2, allows to obtain a better degree of chitin purity and to avoid the use of another organic solvent (ethanol) in addition to petroleum ether.

	Chemical extraction protocol 1	***Chemical extraction protocol 2***	***Enzymatically-assisted extraction protocol 3***
Lipids (yield)	87%	87%	10%
Protein (yield)	84%	91%	67%
Protein fraction quality	degraded	intact	partially hydrolyzed
Chitin (purity)	92%	67%	35%
Organic solvents	Petroleum ether	Petroleum ether, Ethanol	No

Table 3-2 Comparison of extraction protocols

Chapter 4
Production process of protein-based bioplastic film

4 PRODUCTION PROCESS OF PROTEIN - BASED BIOPLASTIC FILM

This part of the work carried out in collaboration with the research group of Interdepartmental Center for Applied Research and Services in Advanced Mechanics and Motoring of University of Modena and Reggio Emilia.

4.1 Razional design of bioplastics from Hermetia illucens prepupae

4.1.1 Screening design mixing proteins, lipids, chitin

In order to maximize the recovery of the components extracted from black soldier fly prepupae, a screening design, mixing lipids and chitin derived from *Hermetia Illucens* with tannic acid and caprolactam in addition to proteins was set-up. Rational approach, codified by DoE, was employed to obtain the highest amount of information using the minimum number of experiments, saving time and costs.

DoE analysis allowed to exclude lipids and chitin because of strong chemical incompatibility between lipids and proteins, and because of the poor ability of chitosan to form an elastic and homogeneous material with proteins (Figure 4-1, Figure 4-2). The addition of tannic acid and caprolactam were also ineffective.

Figure 4-1 Bioplastic made with a mixture of lipids and chitin

Figure 4-2 Bioplastic made with chitin or lipids (down)

4.1.2 Screening design mixing proteins - plasticizer - cross-linking agents - solvent

The aim of this phase was to identify the most suitable combination of protein derived from *Hermetia Illucens*, plasticizer (glycerol, GL), cross-linking agent (citric acid, CA), and distilled water (DI) as solvent. Ranges of variability (Table 4-1) of the three factors considered (distilled water (DI), glycerol (GL), Citric Acid (CA)) were chosen in consideration of preliminary tests. Tests were performed on protein/GL and protein/CA samples using different amounts of DI. In the case of protein/GL mixture, a very positive result was obtained, in terms of the ability to form a freestanding and flexible film, for samples containing at least 50wt% of glycerol. Conversely, protein/CA samples showed a good capacity to form a cohesive material, but with loss of flexibility as CA was increased. Therefore, it was necessary to consider all three factors during set-up of the experimental plan. The reference used was a constant amount of proteins from Black Soldier Fly equal to 1 g, therefore GL and CA were considered in weight percentages, based on the fixed protein content.

Factor	Low level	High level	Unit
Distilled Water (DI)	7.00	13.00	g
Glycerol (GL)	50	100	wt%
Citric Acid (AC)	0	40	wt%

Table 4-1 Factors and their levels of variability

The experimental plan and analyses of results were performed using the Design Expert 8.0 (Stat-Ease, Minneapolis, Minnesota) code. For this study a full factorial analysis was selected, due to the limited number of factors. The number of experiments required for this experimental plan was equal to 2^3 (2 levels for 3 variables). For each experiment, 2 replicates were performed for error estimation purposes. In order to investigate the presence of curvature in the data analysis, central points, considered as the arithmetic average of the levels of factors, were added in quadruplicate. Finally, 6 more points were added in order to give a more detailed description of the behavior of the mixture without a cross-linking agent (0% of CA).

Therefore, the experimental plan consisted of 26 experiments detailed in Table 4-2. All the experiments (runs) were carried out in a random way in order to avoid the presence of systematic errors.

Run	DI [g]	GL [wt%]	CA [wt%]
1	7.00	50	10
2	13.00	100	40
3	7.00	100	40
4	10.00	75	25
5	10.00	75	25
6	13.00	50	10
7	7.00	50	40
8	7.00	100	10
9	13.00	50	10
10	13.00	50	40
11	7.00	100	40
12	13.00	100	40

Run	DI [g]	GL [wt%]	CA [wt%]
13	10.00	75	25
14	7.00	50	40
15	7.00	50	10
16	13.00	100	10
17	7.00	100	10
18	13.00	100	10
19	10.00	75	25
20	13.00	50	40
21	7.00	50	0
22	13.00	50	0
23	10.00	50	0
24	7.00	100	0
25	13.00	200	0
26	10.00	100	0

Table 4-2 Experimental plan

4.1.3 Bioplastic film preparation

After identifying the components of the mixture, films were prepared by mixing proteins, GL and CA in DI, adjusted to pH 10 with NaOH (1 M). The cross-linker, CA, and the catalyst sodium hypophosphite (50% of CA weight) were mixed in DI along with GL.

For each experiment (Table 4-2), a constant quantity equal to 1 g of proteins from BSF was employed. Solutions of protein and additives were heated at 70°C for 30 minutes and stirred at 200 rpm. The mixture was subsequently poured in aluminum dishes and allowed to cool and desiccate under a fume hood for 24 hours at room temperature. After drying, the CA containing samples were treated in an oven at 175°C for 5 minutes, in order to obtain a cross-linking reaction. All films were conditioned in a controlled environment chamber at 25°C and 50% relative humidity before characterization.

4.1.4 Materials evaluation

The capability to constitute a freestanding plastic film was evaluated firstly from a qualitative point of view through a consensual panel, based on the blind judgment of five people.
The output of each experiment was evaluated taking into account the homogeneity of the sample after drying and, therefore, its compactness and detachability from the aluminum support.

The panel test grouped all experiments in 6 categories and a score from 1 to 6 was attributed to each category (Figure 4-3,Table 4-4). Specifically, a classification number equal to 1 corresponded to the weakest quality (completely not homogeneous), whereas a score equal to 6 corresponded to the highest quality sample (homogeneous, completely compact and with good detachability).
Collected score were summarized in Table 4-4.

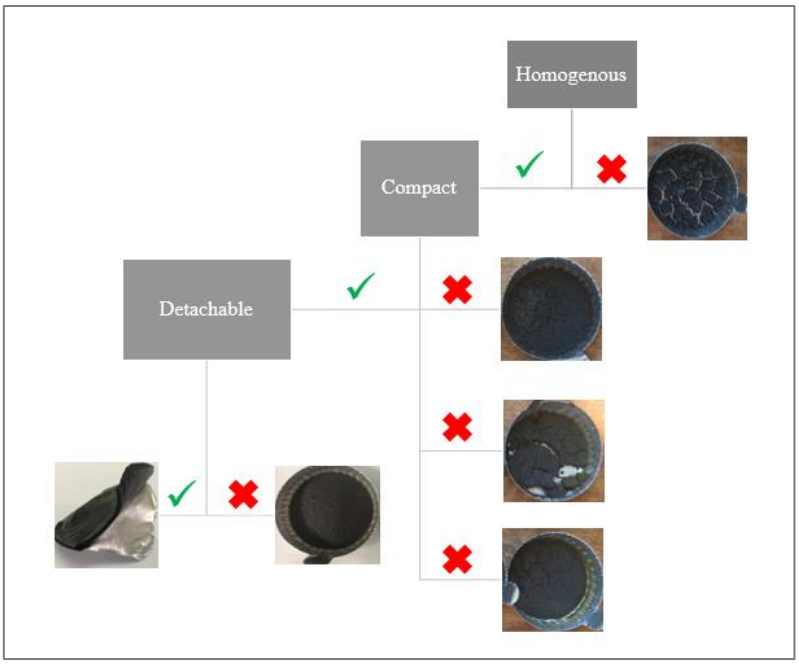

Figure 4-3 Panel test evaluation

(Reproduced from paper *Barbi. S.* https://doi.org/10.1002/bip.23250)

JUDGEMENT	SCORE
Completely not homogeneous	1
Homogenous but not compact	2
Homogenous and partially compact	3
Homogenous and almost completely compact	4
Homogenous, completely compact with poor detachability	5
Homogenous, completely compact and with good detachability	6

Table 4-3 Panel test categories and scores

RUN	1	2	3	4	5	6	7	8	9	10	11	12	13
Evaluation	2	4	2	3	3	2	1	5	2	1	2	4	3
RUN	14	15	16	17	18	19	20	21	22	23	24	25	26
Evaluation	1	2	5	5	5	3	1	1	6	6	6	6	6

Table 4-4 Collected score - panel test evaluation

A logarithmic transformation of data was required to normalize and codify the hierarchy of factors. Analysis of variance (ANOVA) was employed to evaluate the model significance and its predictive power to describe cause-effect relationship between components ratio and the capability to form freestanding materials.

The main assumptions of this statistical analysis were:

1. each input factor is independent and normally distributed;
2. response variation can be separated into different components to evaluate the effect of each factor, their interactions, and experimental error (or unexplained residual).

Through F-test, variation among all samples, usually due to process difference or factor changes, was estimated as large enough or not large enough with respect to the variation within samples obtained in same experimental conditions.
The P-value is the statistical parameter used to evaluate the significance of the model and of each factor, and represents the probability that the considered model or factor is significant (P-value<0.05) or not.

The quality of the fit in terms of regression analysis and the predictive power of the model were evaluated using the R^2 and Pred-R^2 respectively. R^2 is the proportion of the variance in the dependent variables that is predictable from the independent variables and Pred-R^2 is analogous but associated with the predicted value.

The ANOVA results are presented in Table 4-5.

Source	F Value	P-value Prob > F	
Model	13.62	< 0.0001	*Significant*
DI	4.18	0.0557	*Not significant*
GL	45.33	< 0.0001	*Significant*
CA	3.01	< 0.0001	*Significant*
DI-GL	0.15	0.7002	*Not significant*
DI-CA	0.040	0.842	*Not significant*
GL-CA	2.40	0.1387	*Not significant*
DI-GL-CA	12.73	0.0022	*Significant*
Curvature	2.34	0.1443	*Not significant*

Table 4-5 ANOVA analysis

The model correlating factors (single or with interaction) to panel data was significant, as confirmed by the F-value equal to 13.62 and by the p-value <0.0001, which means that probability of data variation due to unknown factors is statistically irrelevant.

The analysis of results showed that only GL, AC and the ternary interaction DI-GL-CA are significant factors for the quality of the obtained samples.

Although the other factors were not significant, they were considered as part of the model to respect model hierarchy. Moreover, it was relevant that the curvature was not significant and therefore the central points could be treated as additional data in the regression model, augmenting the accuracy of the design plan.

R^2 and Pred-R^2 (Table 4-6) confirmed the good fit of the data and a quite fair predictive power of the model, which was coherent with the screening design approach employed.

R^2	0.8416
Pred R^2	0.6721

Table 4-6 Model fitting parameters

In Figure 4-4 model coefficients were reported in order to describe the influence of factors (single or with interaction) on sample quality, evaluated in terms of homogeneity, compactness and freestanding ability.

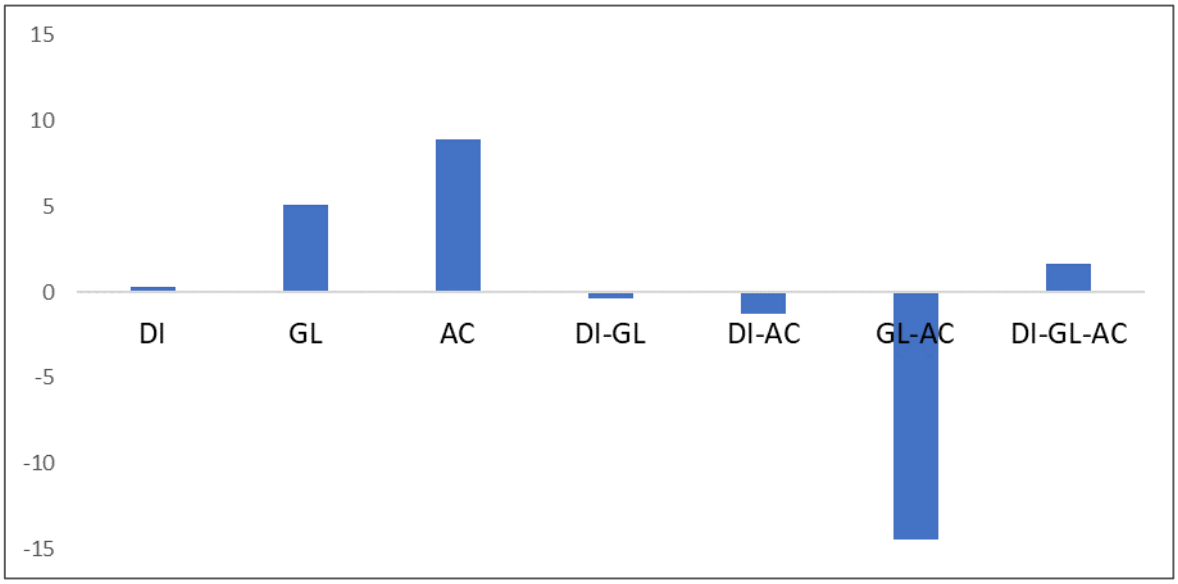

Figure 4-4 Model coefficients

The numerical description of the model was defined in terms of real factors and the relative calculated coefficients (reported in Figure 4-4) may be obtained from the equation:

(4)

$$\text{Ln (Overall film quality)} = -2.93248 + 0.33956 * DI + 5.09163 * GL + 8.91549 * CA - 0.37849 * DI * GL + 1.27052 * DI * CA - 14.44104 * GL * CA + 1.65685 * DI * GL * CA$$

From the analysis of **Errore. L'origine riferimento non è stata trovata.**, it can be stated that GL and CA play the main role on bioplastic film quality, but in opposite way depending on whether they are combined or not.
In particular, if GL and CA were used together in the mixture, their interaction impacted negatively on the quality of the final material, whereas if they were used as single factors in the mixture, their influence on the final material was positive. This can be explained considering that for BSF protein-based films, the role of CA as cross-linking can be overlapped and partially substituted by the chain linking action played by glycerol in the material polymerization. CA is an aliphatic polyfunctional bio-based raw material that contains 2 reactive primary carboxylic groups (Hazarika et al. 2016).

In this study film preparation occurred at pH=10, thus the carboxylic group in CA were most probably in the form of carboxylates, which react with functional group N-terminal amine and forms an amide

linkage, leading to a cross-link with protein after heating treatment (Xu H. et al. 2015, Woods K. et al. 2008).

Thus, when GL is added to the mixture 2 different situations can occur:

a) GL reacts with CA because of its 3-hydroxyl groups. Thus, it can engage in the reaction competing with CA during crosslinking and reducing proteins crosslinking with CA;
b) GL diffuses itself into proteins because of its low molecular weight, reducing internal hydrogen bonding within the protein due to its hydrophilic characteristics. Thereby it decreases internal forces and increases inter-molecular spacing, working as a plasticizer and inhibiting the possible crosslink with CA (A. Awadhiya et al. 2016, Martelli M. et al. 2006).

About DI, even if this factor does not have a great impact on the response, its effect increases changing from single factor to cubic interaction (DI-GL-CA) and this behavior is consistent with the role of solvent played by DI: an increase of this factor becomes relevant when the quantity of additives that have to be solubilized increases.

Figure 4-5 and Figure 4-6 help to explain final bioplastic material quality as a function of the amount of each components in the mixture. DI amount was kept constant and equal to 7 g (Figure 4-5) and 13 g (Figure 4-6).

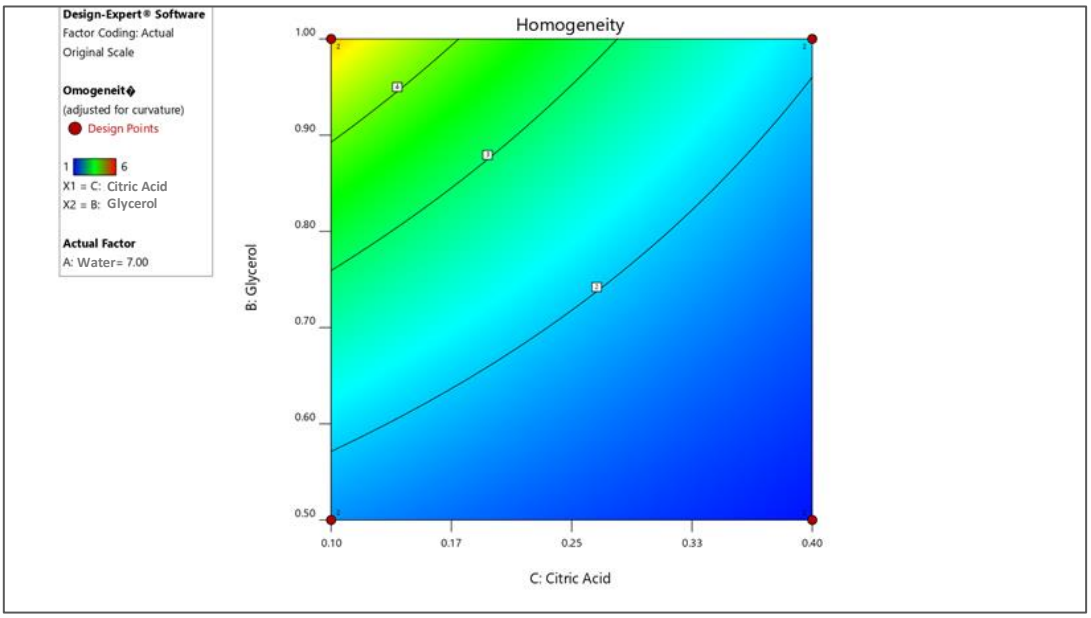

Figure 4-5 Contour plot of the mixture with DI=7 g

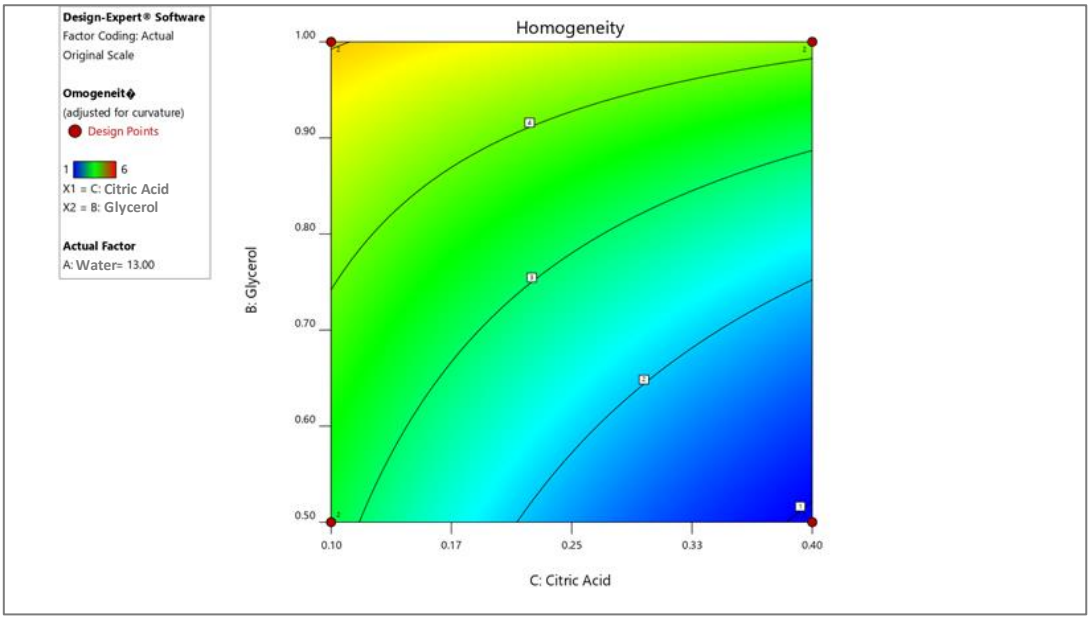

Figure 4-6 Contour plot of the mixture with DI=13 g

It can be stated that the highest quality of final bioplastic material could be achieved using a higher amount of plasticizer and avoiding the use of CA.

It can be noted that a higher DI amount promoted a wider response surface, fitting our purposes to obtain a high-quality material (red area in contour plots). This result suggests that DI does not act only as solvent but it also supports the polymerization process together with GL, therefore limiting the need for plasticizer in the mixture in order to obtain a good quality final material.

According to other studies, the addition of water in combination with GL, increases polymer-water interactions to the detriment of polymer-polymer interactions (Chen P. et al. 2005, Robertson N. L. M et al. 2013). To activate the CA, a heat treatment at 175 ° C is necessary, which could cause protein degradation, making it impossible to reach the highest score of 6. Therefore it was necessary to perform tests, heating the samples with the highest score as above, to verify that no modifications occurred, and the lower score had to be attributed to the combination of GL and CA only.

DoE analysis suggested the optimal ratio of solvent and additives to be: DI: 13 grams, GL: 85%, CA: 0%.

4.1.5 Characterization of bioplastic films

4.1.5.1 Geometry evaluation

The geometry of bioplastic films was evaluated through measurements of thickness and diameter with a digital micrometer (Mitutoyo, YY-T1BD-2GYE) in fifteen different points. The final thickness of each sample was considered the average value with its calculated standard deviation (SD). The sensitivity of the instrument was 0.02 mm.

4.1.5.2 Moisture content evaluation

The terms moisture content (MC) and water content are often used interchangeably and represent a measure of the quantity of water in a product. Moisture content was measured using any one of the different methods listed in the Official Methods of the AOAC (AOAC, 1995). Films were weighed and then dried in an oven at 105 °C for 24 hr.
Samples were then weighed again to determine their MC (Jiang L. et al.2016):

(5)

$$\mathrm{MC}\ (\%) = \frac{(w_1) - (w_0)}{(w_0)} \times 100$$

where
w_0 = initial sample mass [g]
w_1 = sample mass after drying [g]

An analytical balance with sensitivity of 0.00001 g was used to measure all the weights.

4.1.5.3 Water solubility evaluation

Solubility was determined as proposed by (Gontard et al. 1992). Dried samples were initially immersed in 200 mL of distilled water for 24 hr. Samples were then dried again in the oven at 105°C for 24 hr and reweighed. The solubility in water was expressed as a percentage of solubilized material, calculated by the following equation (Bharti et al 2016):

(6)

$$\mathrm{WS}\ (\%) = \frac{(w_1) - (w_2)}{(w_1)} \times 100$$

where
w_1 = dried sample mass [g]
w_2 = final sample mass [g]

As for the evaluation of moisture content, an analytical balance with sensitivity of 0.00001 g was used to measure all weights.

4.1.5.4 Degradation against time evaluation

The degradation profile against time was evaluated on samples according to "EN 17033:2018 and EN ISO 4892-2:2013, Method A cycle 1" for the measurement of degradation due to artificial weathering. Rectangular specimens $(50 \times 15\ \mathrm{mm}^2)$ were exposed in a closed chamber at irradiance of $0.51\ \mathrm{W/(m^2 \times nm)}$, with fixed temperature equal to 38 °C and relative humidity equal to 65% continuously for 500 hours (https://www.plasticseurope.org/en). Deionized water was sprayed during the exposure, with cycles of 18 minutes every 102 minutes. Mechanical properties were measured after the exposure.

4.1.5.5 Tensile properties

Tensile properties were measured on a dynamic mechanical analyzer (DMA, TA Q800) using a film tension set-up. Measurements were performed on rectangular specimens $(20 \times 5\ \mathrm{mm}^2)$. The

specimens were conditioned at standard conditions (25 °C; 50% Relative Humidity) for 24 hr before testing and the measures were run in duplicates. The samples were then aligned and mounted on film clamps for the DMA, using a structure designed for that purpose. Sample lengths were measured in the film holding structure under an applied force of 0.05 N. Tensile properties of plastic films were monitored as the films were elongated with an applied force that was ramped to 18 N at a rate of $0.05\ \mathrm{N} \cdot \mathrm{min}^{-1}$ from 0.05 N. All samples were tested at room temperature.

4.1.5.6 Thermogravimetric analysis (TGA)

Thermogravimetric analysis (TGA) is a method of thermal analysis in which the mass of a sample is measured over time as temperature changes. In this study TGA was conducted on 15 ± 2 mg of sample using a heating rate of $10℃ \cdot \mathrm{min}^{-1}$ from $0℃$ to $1200℃$ in inert atmosphere (nitrogen, $50\ \mathrm{ml} \cdot \mathrm{min}^{-1}$).

4.1.5.7 Differential scanning calorimetry (DSC) measurements

Differential scanning calorimetry (DSC) is a thermal analysis technique that can be used to measure the temperature and heat flow associated with the transitions that occur in a sample, the fusion enthalpies, the glass transitions and the kinetics of crystallization of materials. The basic principle of this technique consists in obtaining information on the material by heating it or cooling it in a controlled manner. In particular, the DSC is based on the measurement of the difference in thermal flows between the sample under examination and one of reference, while the two are constrained to a variable temperature defined by a pre-established program. In this study DSC measurements were performed from $-40℃$ to $200℃$ under nitrogen (flow rate $50\ \mathrm{ml} \cdot \mathrm{min}^{-1}$) with a heating rate of $10℃ \cdot \mathrm{min}^{-1}$ by a DSC TA 2010. A total of 5 ± 1 mg of each sample was loaded into a hermetic aluminum pan and an empty pan of the same material was used as reference during the same heat treatment. The obtained curves were normalized to the respective sample weights before comparison. The glass transition temperature $(\mathrm{T_g})$ was calculated as midpoint of the temperature range, bounded by the tangents to the 2 flat regions of the heat flow curve.

4.1.6 Characterization of samples with different thickness

For the study of films with different thickness, a variable quantity of proteins (0.25 - 0.5 - 1 - 2 - 4 g) was employed with a constant ratio of additives (Table 4-7), derived from the model obtained from the experimental plan (Table 4-2).

Protein (g)	DI (g)	GL (g)	CA (g)
0.25	3.25	0.21	0
0.50	6.50	0.42	0
1.00	13.00	0.85	0
2.00	26.00	1.70	0
4.00	52.00	3.40	0

Table 4-7 Composition of bioplastic films based on different amounts of proteins

4.1.6.1 Thickness and density

The effect of increasing the amount of protein on the resulting thickness and apparent density was analyzed. As shown in Figure 4-7, rising the amount of protein employed, an increase in thickness could be observed following an almost linear trend. Below 1 g of protein, the thickness seems to approach an asymptote standing around 0.2 mm. Density had a parabolic trend, reaching a sort of plateau when the amount of protein was increased over 1 g. So, for both thickness and density, a change in the respective trends could be observed at about 1 g of content of protein: below this limit, an important increase in apparent density could be noted, whereas the increase in thickness was limited, while an opposite trend could be observed over the limit of 1 g of black soldier fly (BSF) protein.

It can be supposed that most of the proteins employed to produce the specimens above 1 g contributed to increase sample volume, whereas below the same limit the added proteins filled the interchain empty spaces, increasing the apparent density of the final material.

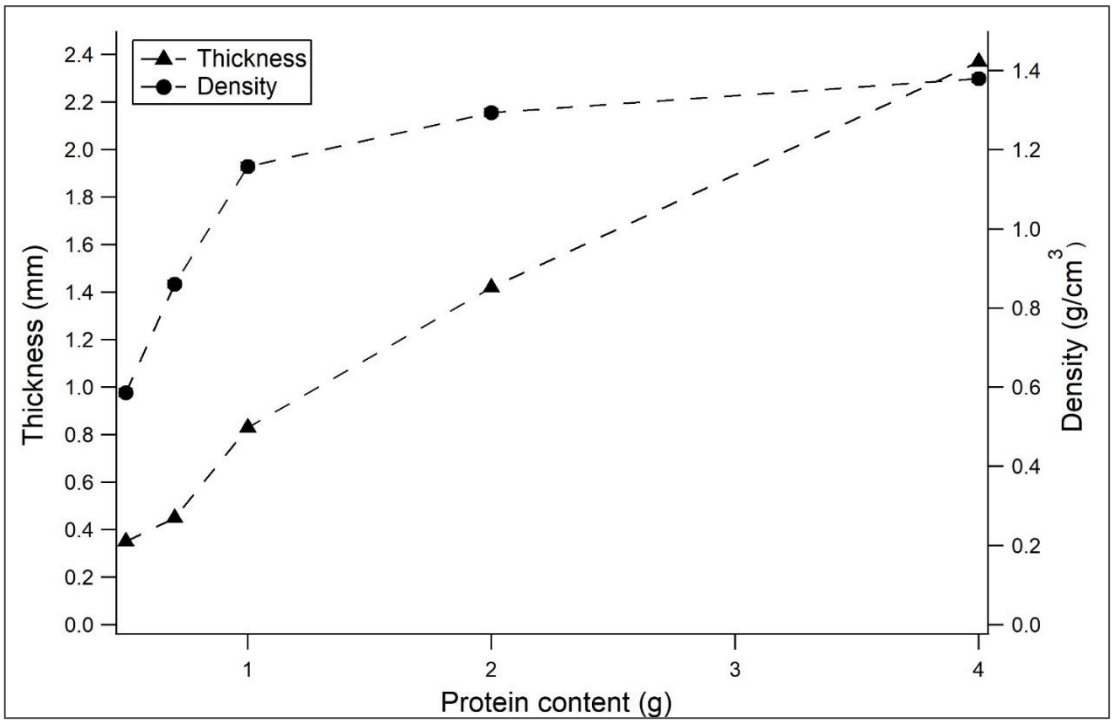

Figure 4-7 Measured thickness and calculated density in function of the amount of proteins

4.1.6.2 Moisture content (MC) and water solubility (WS)

Moisture content strongly depends on the quantity of protein employed to produce specimens, according to the high hydrophilic behavior of proteins. In particular, the average value of MC increased with the increase of quantity of protein employed from 1 g and above (Figure 4-8), and this trend was consistent with the marked hygroscopic behavior of protein chains, so an increase of this property was expected with the increase of the amount of proteins employed. Below 1 g of protein, taking into account experimental error, the samples had the same moisture content. Therefore, the quantity equal to 1 g could be considered as a threshold for moisture content increment due to increasing thickness, as packing of the protein chain became less close (due to the low quantity of plasticizer between them) letting moisture to be adsorbed more easily by the material. The water

solubility, also known as total soluble matter (TSM), was therefore strongly favored for the specimens with lower thickness and the opposite when the thickness was increased. As demonstrated in similar studies, the water solubility parameter is related to the content of highly hydrophilic components or to moisture content as well as to proteins that are not strongly associated to the network structure (Felix at al., 2014).

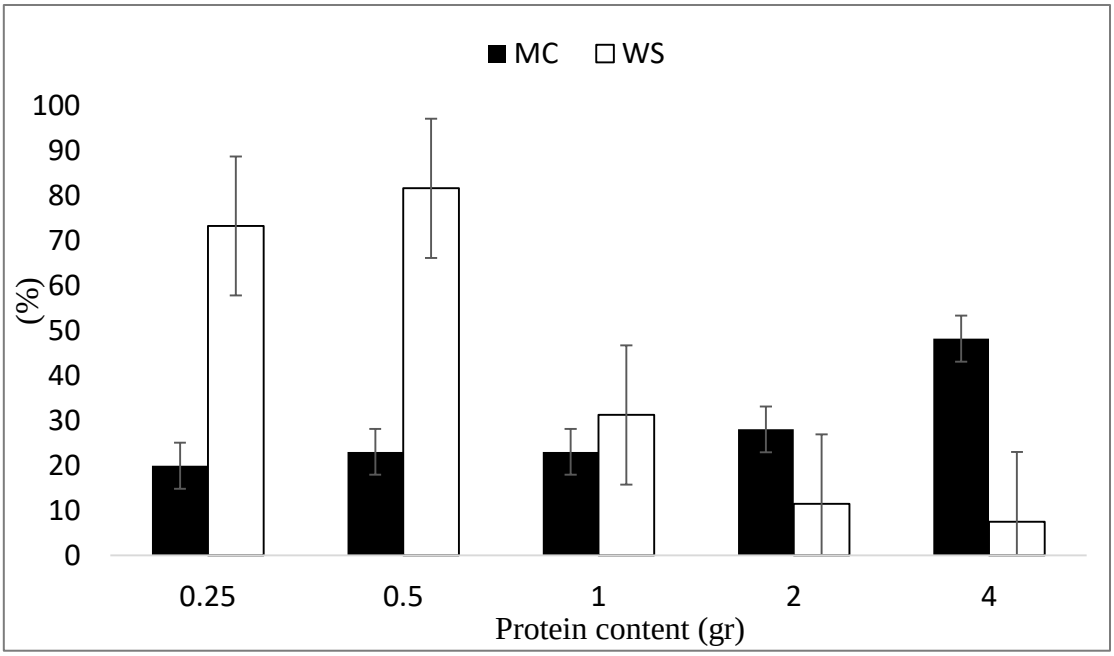

Figure 4-8 Moisture content (MC) and Water solubility (WS) of bioplastics based on different amounts of protein

4.1.6.3 Degradation against time

The degradation profile against time of 3 selected samples was measured as shown in Figure 4-9. A decrease in tensile stress at break was measured for all the samples investigated as the time of exposure to accelerated weathering was increased, with very similar rate of degradation.

Nevertheless, a decreasing in the rate of degradation could be observed moving from the sample containing 0.25 g of protein to the one containing 1 g of protein. Therefore, it can be supposed that an increasing sample thickness helped to reduce degradation rate, leading to more stable materials during exposure to the weathering agent. It must be noted that the exposure to weathering agents is not the only factor of degradation for this type of materials, in fact a burial in soil test should also be performed to achieve a complete break up, therefore this is in agreement with an only partial degradation as described in Figure 4-9.

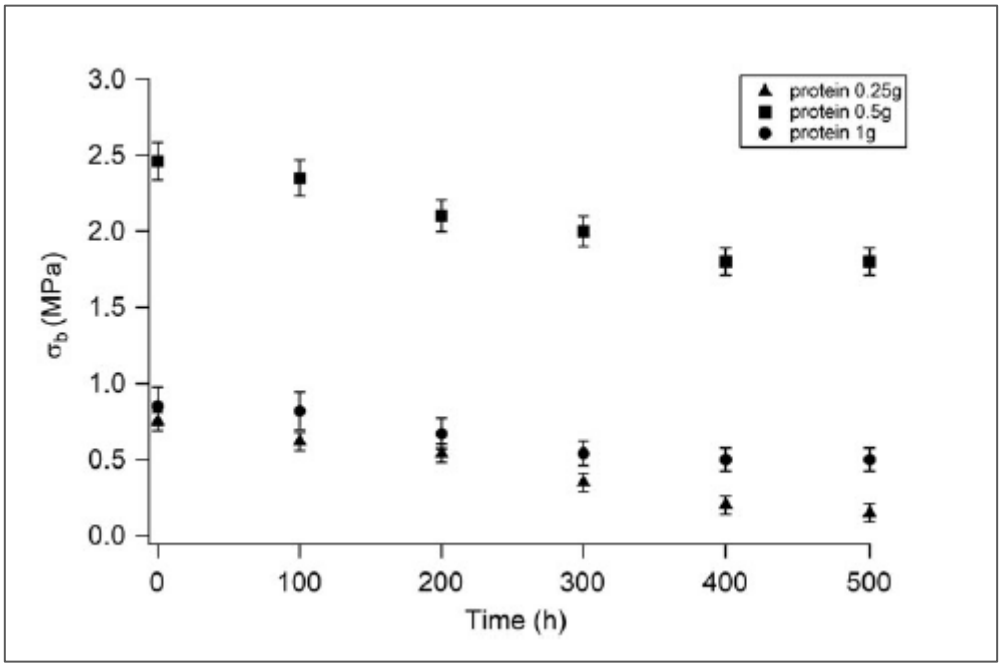

Figure 4-9 Degradation profile of tensile stress at break versus time

4.1.6.4 Mechanical properties

Mechanical properties of plastic material provide an indication of expected polymer integrity under load conditions that would occur during processing, handling, usage and storage. In the present work, tensile behavior of the produced samples was measured following the conditions in section 4.1.5.5. The higher strain at break (σ_b) was reached by the sample produced with 0.5 g of protein and a thickness of 0.4 mm as reported in Figure 4-7. Increasing or decreasing the content of proteins from 0.5 g caused a strong fall in tensile stress at break. This result confirmed that at least 85 wt% of plasticizer (protein-based content) (Table 4-7) is necessary to achieve the highest results in terms of tensile resistance at break. This suggests that, in other conditions, the microstructure configuration due to the additive content would not be suitable to perform a strong binding between proteins, due to poor chain linking density of the resulting polymer (Ganglani et al., 2002). Over 0.5 g the increment in thickness generated a higher probability to find voids, microstructural defects and local thickness differences, acting as stress concentrators and leading to restrained mechanical properties of the overall material. Concerning the tensile stress at yield (σ_y), it can be observed (Figure 4-10) that the average value was below the average value of tensile stress at break for each analyzed specimen, even if the standard deviations suggested a partial overlap of confidence ranges. This is true in particular for the sample employing the lower amount of proteins, equal to 0.25 g, indicating that, for this particular sample, the elastic component of the strain is strongly higher than the plastic one, leading to a less ductile material.

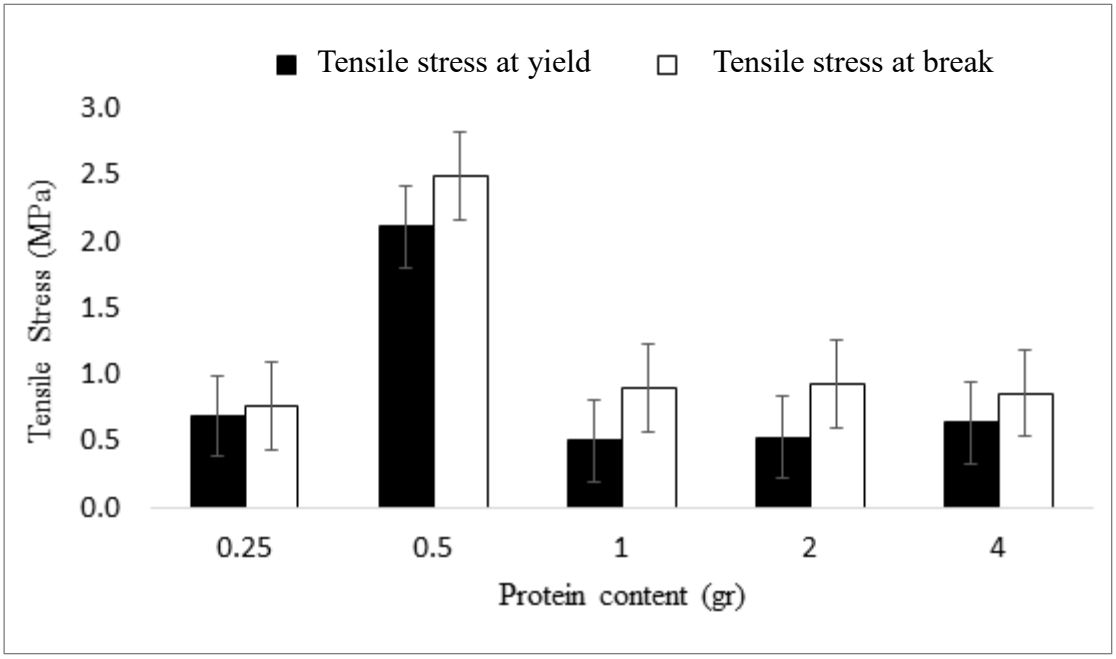

Figure 4-10 Tensile stress at yield (σ_y) and tensile stress at break (σ_b) of bioplastics based on different amounts of proteins

It can be observed that, increasing the amount of proteins, both the strain at yield (ε_y) and the strain at break (ε_b) increase (Figure 4-11).

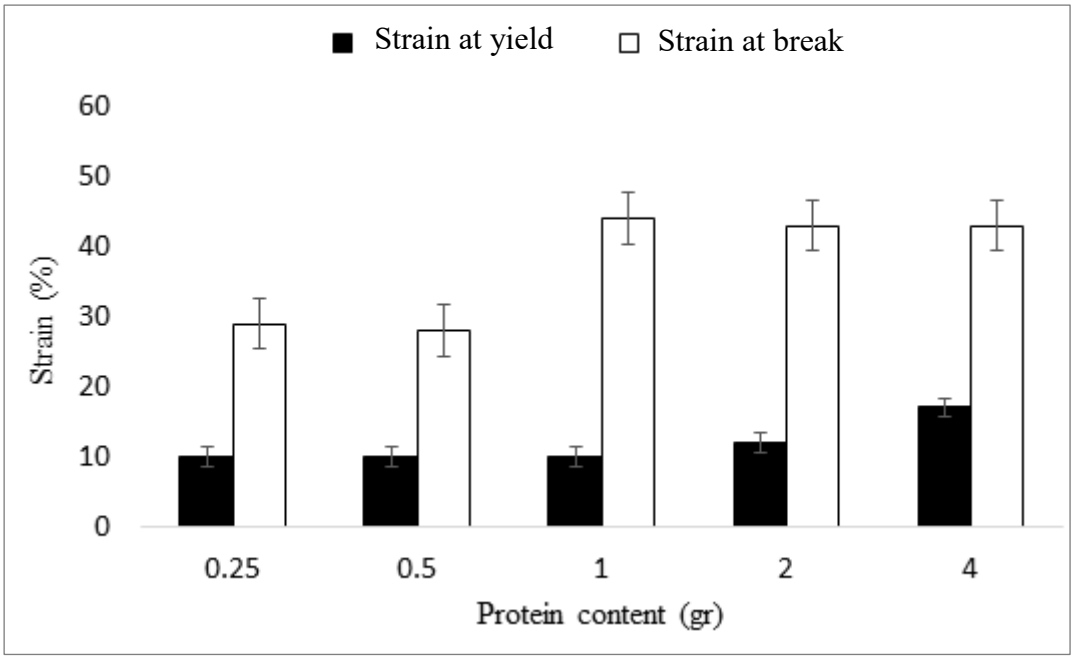

Figure 4-11 Strain at yield (ε_y) and strain at break (ε_b) of bioplastics based on different amount of proteins

4.1.6.5 Differential scanning calorimetry (DSC) analysis

The recorded curves of samples obtained employing from 0.25 to 2 g of proteins were similar in shape and peak areas from -25°C to 10°C. Since the same quantity of plasticizer (glycerol), based on protein amount, was employed, only insignificant differences could be detected from sample to sample. The significant increase of the flat region after glass transition temperature (T_g), due to the increasing amount of protein, and therefore thickness, indicated tougher water evaporation. This result suggests a stronger water-protein linkage going from lower to higher thickness, since in all samples the proportion of water and other constituents was the same.

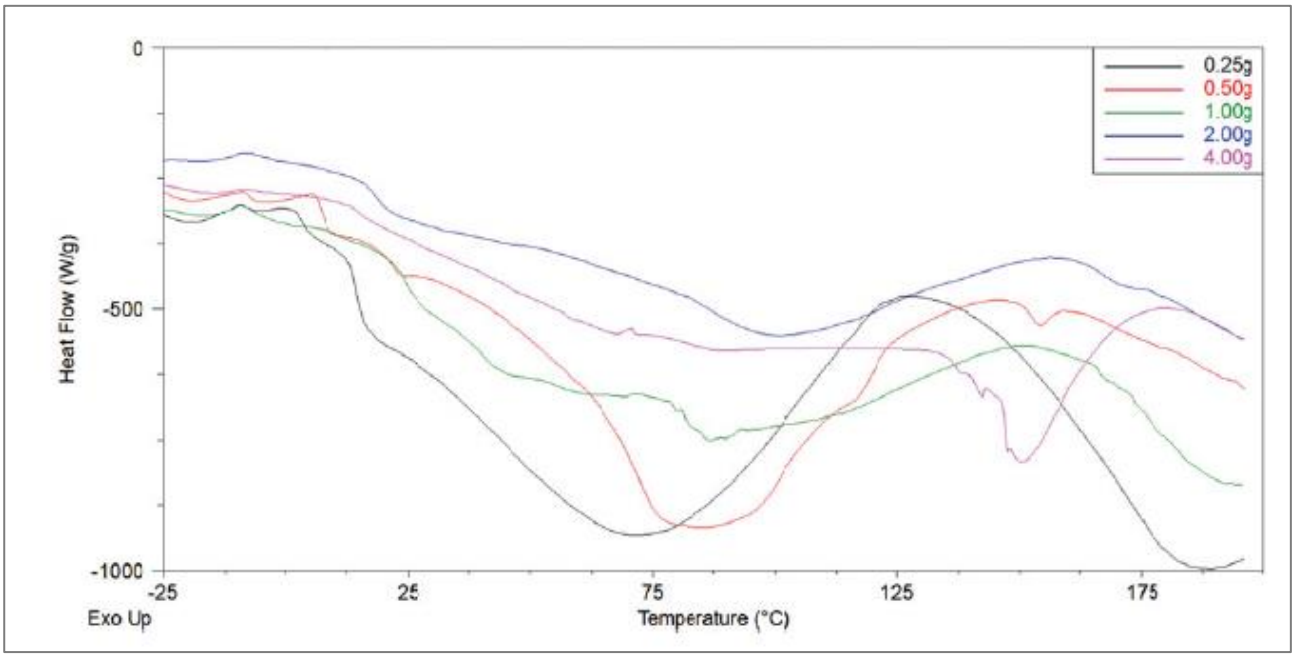

Figure 4-12 DSC thermograms of bioplastic films based on different amounts of proteins

4.1.6.6 BSF protein-based films vs other animal protein-based films

A comparison with other films obtained from animal proteins, such as albumen, crayfish and keratin was performed.

All compared samples were made mixing animal protein with 10-60 wt% glycerol only, in strong similarity with the present study. The most reliable comparison should be done only with the BSF protein-based specimen containing <1 grams of protein, because the thickness of the compared specimens was <1 mm, for all the studies considered.

In particular, Ramakrishnan et al. (2018) considered a combination of keratin and glycerol to produce bioplastic through a casting technique, obtaining lower tensile strength at break compared to the results of the present study. A similar consideration can be drawn taking into account what reported by International Biodegradable Polymer Association & working groups (www.ibaw.org) that considered crayfish as bases for bioplastic production, employing glycerol as plasticizer through injection molding. Also, albumen-based bioplastic has a lower tensile strength at break. Then if 0.5 g of protein are employed, a relatively higher tensile strength at break (not only in the average value considered, but also taking into account the SD) can be obtained if proteins from BSF are employed

compared to proteins deriving from other animal sources. However, it was not possible to reach the values of materials already available on the market and derived from vegetable sources, such as starch, that show a tensile stress at break around 20MPa and strain at break over 200% (Niaounakis, 2015).

Nevertheless, taking in account tensile resistance and elongation, among biopolymers from animal source, BSF protein-based biopolymer are the most promising animal-based alternative to vegetable-based biopolymer. As demonstrated in similar studies, for specimens with the same thickness, the water solubility parameter was related to the content of highly hydrophilic components or to moisture content as well as to proteins that were not strongly associated to the network structure (www.ibaw.org).

Compared to albumen-based bioplastic, BSF protein-based bioplastic has relatively higher water solubility (WS) and lower moisture content (MC), not only in the average values considered, but also taking into account the standard deviations on the measurements. From these results, it can be noted that BSF-protein bioplastic had a higher content of protein not strongly associated to the network, and therefore more free to be released in soil, as potential soil fertilizer during plastic degradation for agricultural purposes. Water solubility is therefore one of the key properties to evaluate compostable material, and high values of this parameter suggest a marked inclination to waste disposal as beneficial compost material in soil (www.plasticulture.com , Bharti et al. 2016).

Chapter 5
Life Cycle Assessment methodology

5 LIFE CYCLE ASSESSMENT METHODOLOGY

The increased awareness of the importance of environmental protection, and the possible impacts associated with products and services has worldwide increased the interest towards the development of methods to better understand and address these impacts. One of the techniques being developed for this purpose is Life Cycle Assessment (LCA).

"LCA addresses the environmental aspects and potential environmental impacts throughout a product's life cycle from raw material acquisition through production, use, end-of-life treatment, recycling and final disposal (i.e. cradle-to-grave)" (ISO 14040, 2006)

The International Organization for Standardization (ISO) provides guidelines for conducting a Life Cycle Assessment within the ISO 14040 and ISO 14044.

The standards have also been adopted at European and Italian level, UNI EN ISO 14040:2006 and UNI EN ISO 14044:2018.

According to the ISO 14040 and 14044 standards, the LCA is an iterative process that includes four methodological phases:

1. Goal and Scope definition
2. Life Cycle Inventory Analysis (LCI)
3. Life Cycle Impact Assessment (LCIA)
4. Life Cycle Interpretation

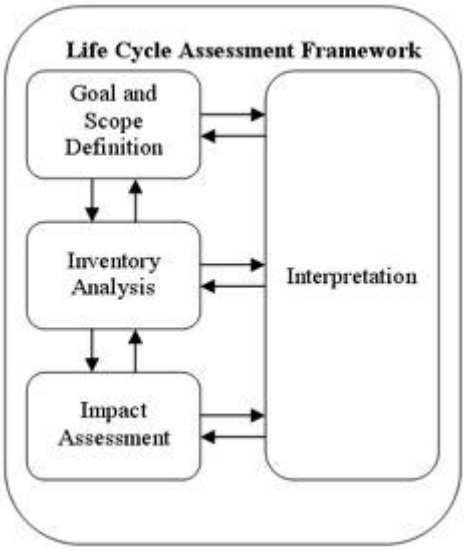

Figure 5-1 Life Cycle Assessment Framework (ISO 14044, 2006)

LCA is an iterative technique, thus as data and information are collected, various aspects of the scope may require modifications in order to meet the original goal of the study.

5.1 Goal and scope definition

The Goal and Scope of the study should be determined in the first step of an LCA. This includes an exact formulation of what is to be investigated, and how this investigation is to be carried out.
Goal and scope phase contains the following main issues:

- Goal
- Scope
- Functional Unit
- System boundaries
- Data quality

The definition of the **goal** and **scope** is the critical parts of an LCA study due to the strong influence on the LCA results.
The goal definition of an LCA needs to define the purpose of the life cycle assessment and the intended use of the results (i.e. the intended application, the reasons for carrying out the study, the intended audience, whether the results are intended to be used in comparative assertions and/or intended to be disclosed to the public). The goal can be subsequently redefined as a result of the findings obtained throughout the study.
The definition of the scope of the LCA sets the borders of the assessment (what is included in the system and which assessment methods will be used).
The scope includes the following items:

- the product system to be studied;
- the functions of the product system or, in the case of comparative studies, the systems;
- the functional unit;
- the system boundaries;
- allocation procedures;
- impact categories selected and methodology of impact assessment, and subsequent interpretation to be used;
- data requirements;
- assumptions;
- limitations;
- initial data quality requirements;
- type of critical review, if any;
- type and format of the report required for the study.

The **functional unit** sets the scale for comparison of more products. The primary purpose of a functional unit is to provide a reference to which the inputs and outputs data are normalised. This reference is necessary to ensure comparability of LCA results.

The **system boundaries** define the processes or operations, and the inputs and outputs to be taken into account in the LCA. The definition of system boundaries is a quite subjective operation.

The **data quality** reflects the quality of the finale LCA. It has to be described and assessed in a systematic way that allows others to understand and control for actual data quality. It has to satisfy stated requirements, such as time-related coverage, geographical coverage, technology coverage,

measure of the variability of the data, completeness, representativeness, consistency, reproducibility, sources of the data as well as uncertainty of the information.

5.2 Life Cycle Inventory – LCI

Life Cycle Inventory Analysis (LCI) specifies the processes occurring during the life cycle of a product. An inventory is made of all the inputs and outputs with regard to the system being studied. The LCI represents the core of LCA. The tasks are to specify all the processes involved in the product life cycle in the form of a process flow chart and collect data on each process, by consulting scientific literature or published data. Collecting the data is the most difficult part of an LCA. Once data has been collected on all processes, the critical phases can be selected for further analysis. In the last stage of an inventory analysis, the data will be processed. An inventory table will be created, in which all inputs and outputs have been translated into environmental inputs and outputs.

5.3 Life Cycle Impact Assessment – LCIA

The inventory table is used in the third step, the life cycle impact assessment (LCIA). In the impact assessment, the results (the quantified inputs and outputs) of the inventory analysis are interpreted in terms of the impacts they have on the environment. These stressors (inputs and outputs) are classified according to the kind of environmental problem to which they contribute (i.e. acidification, global warming and human toxicity). In the characterisation step, the contributions to each environmental problem are quantified. At this purpose, equivalency factors are used, which indicate how much a substance contributes to a problem, compared to a reference substance. LCIA is a relative approach based on the functional unit.

Traditionally, as in many other environmental assessments strategies, LCIA uses linear modeling and takes the effects of the substances into account, but not their background concentrations and the geographical dependency on fate. The method aggregates the environmental consequences over release points in time, release locations and substances (chemicals). This allows calculating potential impact scores.

The LCIA phase includes mandatory elements and optional elements (ISO 14044, 2006).

5.3.1 Mandatory elements of LCIA

The LCIA phase includes the following mandatory elements:

- Classification (assignment of LCI results to impact categories) should consider the assignment of LCI results that are exclusive to one impact category and the identification of LCI results related to more than one impact category (including distinction between parallel mechanisms and assignment to serial mechanisms);
- Characterization (the calculation of indicator results) involves the conversion of LCI results to common units and the aggregation of the converted results within the same impact category. This conversion uses characterization factors. The outcome of the calculation is a numerical indicator result. The method of calculating indicator results shall be identified and documented, including the values selected and assumptions used.

5.3.2 Optional elements of LCIA

In addition to the mandatory elements of LCIA, there could be optional elements and information as listed below which can be used depending on the goal and scope of LCA (ISO 14044, 2006):

- **Normalization** is the calculation of the magnitude of the category indicator results relative to some reference information. The aim of the normalization is to understand better the relative

magnitude for each indicator on the overall impact of the product system under study. Normalization transforms an indicator result by dividing it by a selected reference value.

- **Grouping** is the assignment of impact categories into one or more sets as predefined in the goal and scope definition, and it may involve sorting and/or ranking. Ranking is based on value-choices. Different individuals, organizations and societies may have different preferences, therefore, it is possible that different parties will reach different ranking results based on the same indicator results or normalized indicator results.
- **Weighting** is the process of converting indicator results of different impact categories by using numerical factors based on value-choices. It may include aggregation of the weighted indicator results. Weighting steps are based on value-choices and are not scientifically based. Different individuals, organizations and societies may have different preferences; therefore it is possible that different parties will reach different weighting results based on the same indicator results or normalized indicator results. In an LCA it may be desirable to use several different weighting factors and weighting methods, and to conduct sensitivity analysis to assess the consequences of different value-choices and weighting methods on the LCIA results.

The optional LCIA elements may use information from outside the LCIA framework. The use of such information should be explained and the explanation should be reported.

5.4 Interpretation of results

The life cycle interpretation phase comprises the following elements as follows (ISO 14044, 2006):

- identification of the significant issues based on the results of the LCI and LCIA phases of the study;
- an evaluation that considers completeness, sensitivity and consistency checks;
- conclusions, limitations, and recommendations.

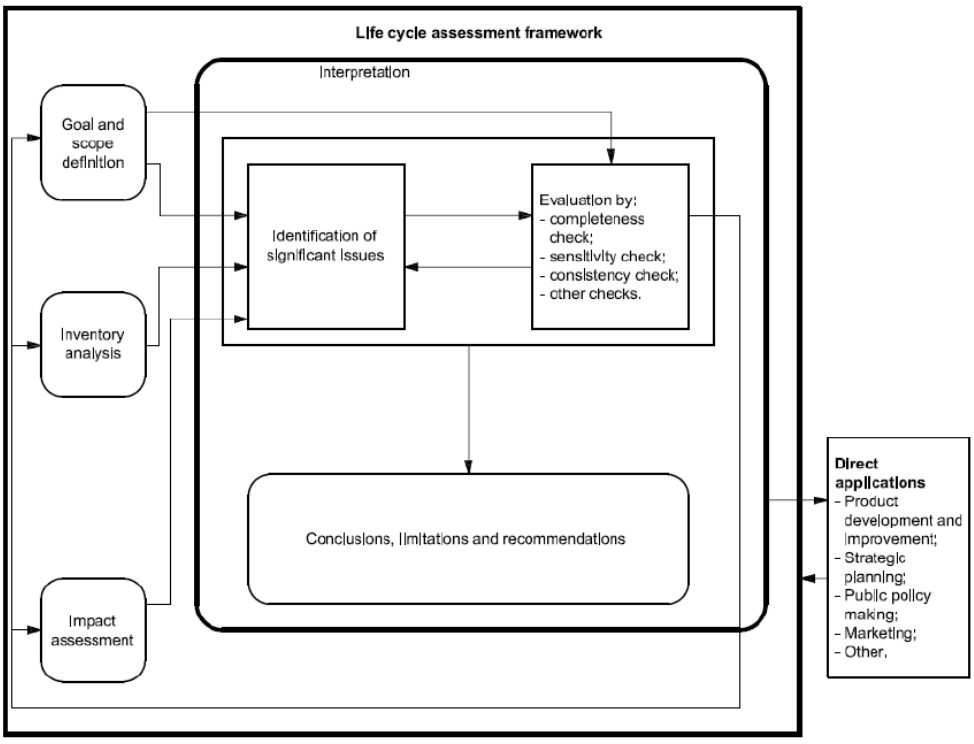

Figure 5-2 Relationship between elements within interpretation phase with the other phases of LCA (ISO 14044, 2006)

The interpretation should reflect the fact that LCIA results are based on a relative approach, they indicate potential environmental effects, and they do not predict actual impacts on category endpoints, the exceeding of thresholds or safety margins or risks.
The findings of this interpretation may take the form of conclusions and recommendations to decision-makers, consistent with the goal and scope of the study (ISO 14040, 2006).

Chapter 6
Life Cycle Assessment of protein-based bioplastic film production

6 LIFE CYCLE ASSESSMENT OF PROTEIN - BASED BIOPLASTIC FILM PRODUCTION

6.1 Goal and scope definition

6.1.1 Goal definition

The goal of the study was to assess the potential environmental impacts attributed to the production of protein-based bioplastic film, in order to identify the hot spots of the production process at laboratory scale. The LCA analysis will be used as a support for bioplastics eco-design processes, in order to pursue a low environmental impact scale-up.

6.1.2 System, functional unit and system function

The system studied was the bioplastic manufacturing process at laboratory scale, using proteins extracted from *Hermetia Illucens* prepupae grown on substrate composed mostly of poultry manure. The function of this system was the production of a new type of bioplastics for agricultural purposes. To the aim of the present study, the functional unit was the weight of the bioplastic sample produced in the laboratory (i.e. 0.403 g).

6.1.3 System boundaries

System boundaries were defined following a "from cradle to gate" approach. They ranged from rearing of black soldier flies on organic substrate to bioplastic production, through the phase of extraction of the biomolecules (lipids, proteins and chitin). The initial input of pupae (to start the process), energy, materials, water, main equipment with their end-of-life, transport, waste and relative treatment, emissions into the air, aspiration system and purification plant as well as recovery and reuse of certain solvents were also considered. Methane emissions from organic waste during the substrate production phase and methane emissions during biodigestion activity of *Hermetia Illucens* were excluded from system boundaries.
The following assumptions were also made:

- When no information about transport distance was available, standard transport distance of 100 km was assumed as estimated by the ecoinvent database (Hischier et al. 2005).

6.2 Data quality

Regarding the quality of data used for the life cycle inventory (LCI), primary data were directly collected in the laboratory during the experimental activities. In particular, laboratory data on *Hermetia Illucens* breeding, biomolecule extraction and bioplastic film production were the primary data collected during experimental tests. Where the data were not available, the study was completed on the basis of secondary data obtained from the Ecoinvent database vers.3.4 (Ecoinvent Database) which were used to model background processes (land use, production of materials, fuel and electricity production, together with transport). The sources of the data considered as well as those for background processes were indicated as follows: LAB (data experimentally collected in the

laboratory); EID (data obtained from the Ecoinvent database); LIT (data obtained by creating new processes starting from literature data); EST (estimated data).

6.3 Life Cycle Inventory

6.3.1 Life Cycle Inventory of BSFs breeding

Data collection was carried out using specific ad-hoc checklists.
As temporal reference, one cycle of production was chosen, because it represents the basic unit for the implementation of production at industrial scale.
The main process was named "Production of mature larvae (prepupae) – BSF Breeding".
Having chosen one cycle of production as a temporal reference, production of prepupae used for so-called "buffer" breeding was considered as a co-product. Therefore, the sub-processes "Production of mature larvae (prepupae) – BSF Breeding" were considered multi-output processes, which produced three different products:

1) production of mature larvae (prepupae) (primary product);
2) production of "buffer" breeding (co-product);
3) compost from residual substrate (co-product).

An economic allocation was used.
The process "Production of mature larvae (prepupae) – BSF Breeding" consisted of four sub-processes (Figure 6-1):

1. substrate preparation.
2. Nursery unit.
3. Bioconversion unit.
4. Electrical vibrating sieve to sieve prepupae and residual substrate.

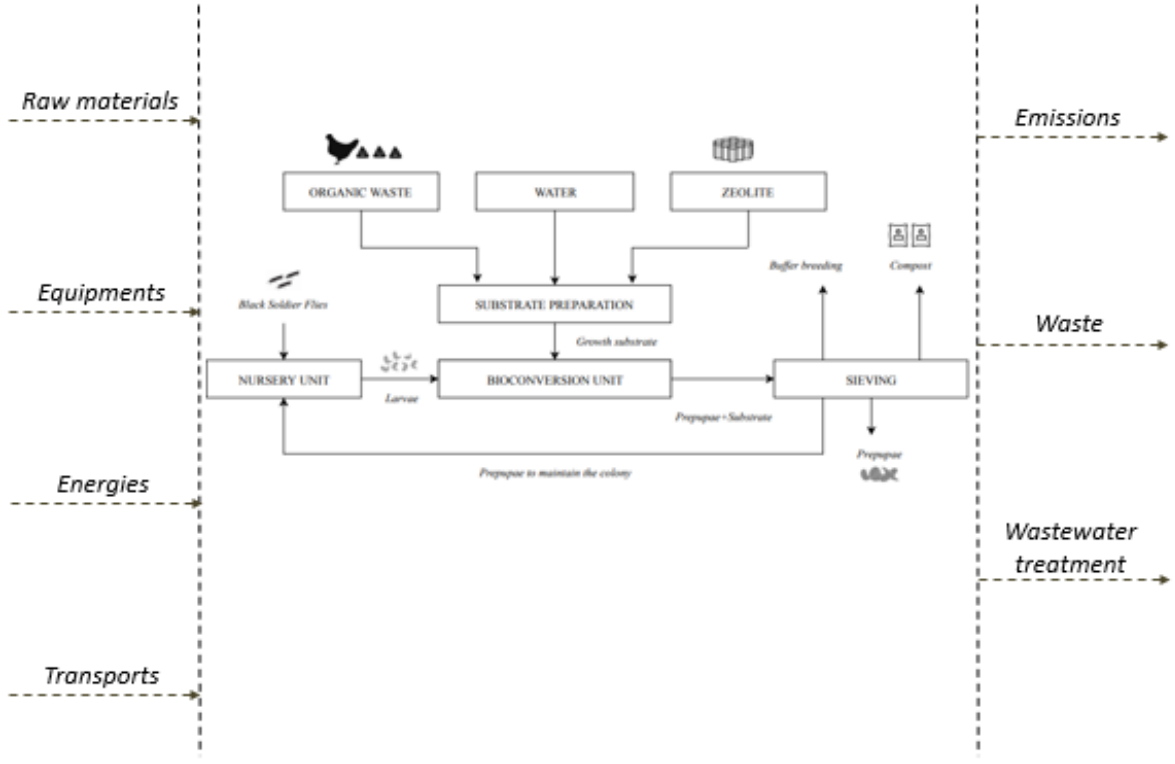

Figure 6-1 Mature larvae (prepupae) production – BSF Breeding

The following tables (Table 6-1, Table 6-2) show the details of the inventory for each sub-process.

Substrate preparation

Process "Substrate preparation" consisted of the following sub-processes:

1) substrate production;
2) energy demand for substrate preparation.

The functional unit was the amount of substrate used to produce 3.633E4 g of mature larvae (prepupae).

The duration of substrate preparation and the frequency with which the substrate preparation system was turned on was estimated based on the preliminary design of the pilot plant.

Substrate production

Substrate production was modeled for 1 kg of substrate.

The substrate consisted of: poultry manure (34.5%), zeolite (7.2%) and water (58.30%).

For the process "Poultry manure" it was used the Ecoinvent process "*Chicken for slaughtering, live weight {GLO}| chicken production | Alloc Def, U*". A renamed copy as "*Chicken for slaughtering, live weight {GLO}| chicken production | Alloc Def, U (poultry manure*" was created and subsequently some modifications were added, i.e. two coproducts derived from the chicken breeding:

1. Eggs
2. Poultry manure

Economic allocation for the environmental damage allocation was applied.

Then the coproduct "Poultry manure" was applied in the "Substrate preparation" process.

1	SUBSTRATE PREPARATION			
Functional Unit of the process: 18.38 kg				
PROCESS	BACKGROUND PROCESS	AMOUNT	BACKGROUND PROCESS DATA SOURCES	COMMENT
Substrate production	*Substrate production*	18.38 kg	EID	Amount: weight of growth substrate related to the amount of larvae produced into the nursery Amount source: LAB
Energy demand	*Electricity, low voltage {IT}| electricity voltage transformation from medium to low voltage | APOS, U*	12 kWh	EID	Amount: energy demand to prepare growth substrate Amount source: EST

Table 6-1 Inventory of substrate preparation

2	SUBSTRATE PRODUCTION			
Functional Unit of the process: 1kg				
PROCESS	BACKGROUND PROCESS	AMOUNT	BACKGROUND PROCESS DATA SOURCES	COMMENT
Zeolite	*Zeolite, powder {RER}| production | APOS, U*	0.072 kg	EID	Amount: weight of zeolite Amount source: LAB
Poultry manure	*Poultry manure*	0.345 kg	EID	Amount: weight of poultry manure Amount source: LAB
Water	*Tap water {Europe without Switzerland}| tap water production, underground water without treatment | APOS, U*	0.583 kg	EID	Amount: water weight Amount source: LAB

2	SUBSTRATE PRODUCTION			
Transport	*Transport, freight, lorry 16-32 metric ton, EURO6 {RoW}| transport, freight, lorry 16-32 metric ton, EURO6 | APOS, U*	41.7 kgkm	EID	Transport of the substrate components (zeolite and poultry manure) Transported weight: a) weight of zeolite b) weight of poultry manure Distance: 100 km Amount source: EST

Table 6-2 Inventory of substrate production

Nursery unit

The functional unit of this process is the weight (wet weight [g]) of the newly larvae of black soldier fly that are introduced into the bioconversion plant.
For the calculation of functional unit, firstly a unit of reference was fixed: this unit is 26 trays in the bioconversion plant of dimension $76.420\ cm\ width \times 26.120\ cm\ depth \times 10\ cm\ height$.
If we consider a density of 0.7 larvae/cm^2 (experimental value), the total number of larvae that is possible to produce in 26 trays and that will become prepupae is:

(7)

$$0.7 \times 26 \times (76.420 \times 26.120) \cong 3.633E4 \ \ [\text{LARVAE}]$$

Considering a 12.95% (experimental) of mortality in the growth phase of the larvae (inside the bioconversion plant), it is possible to calculate the quantity of larvae that the nursery unit must be able to produce (output of Nursery unit):

(8)

$$3.633E4 + (0.1295 \times 3.633E4) \cong 4.103E4 \ \ [\text{LARVAE}]$$

A larva (maximum 7 days of growth) weights 0.0075 g (experimental value), so the amount (wet weight) of larvae that nursery unit must be able to produce is equal to:

(9)

$$4.1033 \times 0.0075 \cong 307.75 \ \ [\text{g of LARVAE}]$$

In nursery unit modeling, the initial input of adult individuals (pupae) needed to start the process and ensure a production of mature larvae was calculated to be equal to 307.75 g.
Egg hatching efficiency is 90%, therefore the amount of eggs needed to produce 41033 of larvae may be obtained from:

(10)

$$4.103E4 + 0.10 \times (4.103E4) \cong 4.514E4 \ [\text{EGGS}]$$

Considering that every female of black soldier fly can deposit around 500 eggs (experimental value confirmed by literature), and considering an adult mortality rate equal to 10% (experimental value), it is necessary to have in the nursery unit an amount of females equal to:

(11)

$$\left(\frac{4.514E4}{500}\right) + 0.10 \times \left(\frac{4.514E4}{500}\right) \cong 99 \ [\text{FEMALES}]$$

Taking into account a percentage of females equal to 50% (experimental value confirmed by literature) and flicker efficiency equal to 93.06% (experimental value), it is possible to calculate the total population of adult black soldier flies that must be present in the nursery unit in order to produce 307.75 g of mature larvae (prepupae) into the bioconversion plant.

(12)

$$(99 \times 2) + 0.07 \times (99 \times 2) \cong 211 \ [\text{ADULT BLACK SOLDIER FLIES}]$$

Due to the lack of data, it was hypothesized that the initial input of adult individuals (pupae) needed to start the process were reared into a system equal to the one analyzed.
It is assumed that dead pupae of black soldier flies in the nursery unit are disposed of as waste.
The inventory table of Nursery unit and the inventory tables of the sub-processes that composed it showed below (Table 6-3, Table 6-4, Table 6-5, Table 6-6).

3	NURSERY UNIT			
Functional Unit of the process: 307.7 g (wet weight)				
PROCESS	BACKGROUND PROCESS	AMOUNT	BACKGROUND PROCESS DATA SOURCES	COMMENT
Pupae	*BSF Prepupae*	10.13 g	EID	Amount: weight of pupae that must be present in the Nursery to guarantee 307.7 g of prepupae. Amount source: LAB
Box	*Box Nursery*	0.0029 p	EID	Amount: unit (1 "p")[1] allocated based on time of use (16 days). Lifespan:15 years Amount source: EST
Transport	*Transport, freight, lorry 16-32 metric ton, EURO6 {RoW}| transport, freight, lorry 16-32 metric ton, EURO6 | APOS, U*	111.7 kgkm	EID	Transport of box Nursery from supplier to laboratory Transported weight: weight of box allocated based on time of use (16 days) Distance: 279 km Amount source: LAB
Pipe	*Pipes in PVC*	0.01753 p	EID	Amount: number of pipes on the wall of the nursery box allocated based on time of use (16 days) Amount source: EST

[1] "p" is a way to define the functional unit in the SimaPro software and represents the number of units (p,pieces) produced for the reference process.

3	NURSERY UNIT			
Transport	*Transport, freight, lorry 16-32 metric ton, EURO6 {RoW}| transport, freight, lorry 16-32 metric ton, EURO6 | APOS, U*	0.7298 kgkm	EID	Transport of pipes from supplier to laboratory Transported weight: weight of six pipes allocated based on time of use (16 days) Distance: 100 km Amount source: EST
Electrical box	*Electrical Box in PVC*	0.0029 p	EID	Amount: unit (1 "p") allocated based on time of use (16 days). Lifespan: 15 years Amount source: EST
Transport	*Transport, freight, lorry 16-32 metric ton, EURO6 {RoW}| transport, freight, lorry 16-32 metric ton, EURO6 | APOS, U*	0.2734 kgkm	EID	Transport of electrical box from supplier to laboratory. Transported weight: weight of electrical box allocated based on time of use (16 days) Distance: 100 km Amount source: EST

3	NURSERY UNIT			
Energy demand	*Electricity, low voltage {IT}| electricity voltage transformation from medium to low voltage | APOS, U*	1.536E4 Wh	EID	Amount: energy demand to maintain constant temperature (26 -27°C) in the nursery unit. Power of system that is used to maintain constant temperature: 40 Watt System that is used to maintain constant temperature works 24 hours a day for 16 days. Then, operating time of system that is used to maintain temperature constant is equal to 384 hours. Amount source: LAB
Energy demand	*Electricity, low voltage {IT}| electricity voltage transformation from medium to low voltage | APOS, U*	960 Wh	EID	Amount: energy demand to maintain constant the relative humidity (60% HR) in the nursery unit. Power of system that is used to maintain constant relative humidity: 5 Watt System that is used to maintain constant temperature works 12 hours a day for 16 days. Then, operating time of system that is used to maintain constant relative humidity is equal to 192 hours. Amount source: LAB

3	NURSERY UNIT			
Energy demand	*Electricity, low voltage {IT}| electricity voltage transformation from medium to low voltage | APOS, U*	2.016E4 Wh	EID	Amount: energy demand of the LED lighting system in the nursery unit. Power of the LED lighting system: 90 Watt. The LED lights stay on 14 hours a day for 16 days, then operating time of the LED lighting system is equal to 224 hours. Amount source: LAB
Energy demand	*Electricity, low voltage {IT}| electricity voltage transformation from medium to low voltage | APOS, U*	5760 Wh	EID	Amount: energy demand of control and management system of the nursery unit. Power of control and management system of the nursery unit: 15 Watt System that is used to control and manage nursery unit works 24 hours a day for 16 days. Then, operating time of system that is used to control and manage nursery unit is equal to 384 hours. Amount source: LAB
Water	*Tap water {Europe without Switzerland}| tap water production, conventional treatment | APOS, U*	0.0228 kg	EID	Amount: water weight used to feed pupae Amount source: LAB

3	NURSERY UNIT			
End of life of black soldier fly pupae that dead into the nursery unit	*Municipal solid waste {IT}| treatment of, incineration | APOS, U*	1.013 g	EID	Amount: weight of black soldier fly pupae that die into the nursery unit Amount source: LAB

Table 6-3 Inventory of nursery unit

4	BOX NURSERY			
Functional Unit of the process: 1p				
PROCESS	BACKGROUND PROCESS	AMOUNT	BACKGROUND PROCESS DATA SOURCES	COMMENT
Polyethylene (PE)	*Polyethylene, high density, granulate {RER}| production | APOS, U*	43.64 kg	EID	Amount: weight of polyethylene used to manufacture the walls of the nursery box. This quantity includes scraps generated during the processing of polyethylene. Indeed, from database process: [*1 kg of this process equals 0.976 kg of extruded plastic film*]. Total weight of walls manufactured in polyethylene: 55.86 kg Then the total quantity of material may be obtained from: 1[kg]:0,976 [kg]=X:42,59 [kg] Amount source: LAB

4	BOX NURSERY			
Processing of polyethylene	*Extrusion, plastic film {RER}| production | APOS, U*	43.64 kg	EID	Amount: total weight of polyethylene used to manufacture the walls of nursery box. Amount source: LAB
Polyurethane (PU)	*Polyurethane, rigid foam {RER}| production | APOS, U*	19.85 kg	EID	Amount: weight of polyurethane used for the insulation of the nursery isothermal box. Amount source: LAB
Nylon 6	*Nylon 6 {RER}| production | APOS, U*	2.096 kg	EID	Amount: weight of Nylon 6 used to manufacture the tires of the nursery box. Amount source: EST
Silicone	*Silicone product {RER}| production | APOS, U*	0,8391 kg	EID	Amount: weight of silicone used to manufacture the gasket on the door of the Nursery box. Amount source: EST
Steel	*Steel, chromium steel 18/8 {RER}| steel production, electric, chromium steel 18/8 | APOS, U*	71.62 kg	EID	Amount: weight of steel used to manufacture: - handles used to move, to open and to close the box; - internal door shaft; - hinges; - wheels support. Amount source: EST
Processing of steel	*Sheet rolling, chromium steel {RER}| processing | APOS, U*	71.62 kg	EID	Amount: weight of steel Amount source: EST

4	BOX NURSERY			
Transport	*Transport, freight, lorry 16-32 metric ton, EURO6 {RER}| transport, freight, lorry 16-32 metric ton, EURO6 | APOS, U*	1.38E4 kgkm	EID	Transport of materials used to manufacture nursery box. Transported weight: weight of all materials Distance: 100 km Amount source: EST
End of life of polyethylene	*Plastic recycling, multi-output process (Allocation 50%)*	42.59 kg	EID	Amount: weight of polyethylene. The end-of-life of the scraps was not considered because it has been included in the process related to the processing of polyethylene. Amount source:
End of life of polyurethane	*Polyurethane recycling*	19.85 kg	EID	Amount: weight of polyurethane. Amount source: LAB
End of life of nylon 6	*Municipal solid waste {IT}| treatment of, incineration | APOS, U*	2.096 kg	EID	Amount: weight of Nylon 6 Amount source: EST
End of life of silicone	*Municipal solid waste {IT}| treatment of, incineration | APOS, U*	0,8391 kg	EID	Amount: weight of silicone. Amount source: EST
End of life of steel	*Steel recycling, multi-output process (Allocation 50%)*	71.62 kg	EID	Amount: weight of steel Amount source: EST

Table 6-4 Inventory of nursery isothermal box

5	PIPE			
Functional Unit of process: 1p				
PROCESS	BACKGROUND PROCESS	AMOUNT	BACKGROUND PROCESS DATA SOURCES	COMMENT
Polyvinylidenchloride	*Polyvinylidenchloride, granulate {RER}| production | APOS, U*	0.418 kg	EID	Amount: weight of polyvinylidenchloride used to manufacture pipe. This quantity includes scraps generated during the processing of polyvinylidenchloride. Indeed, from database process: [*1 kg of this process equals 0.996 kg of extruded plastic pipes*]. Total weight of pipe manufactured in polyvinylidenchloride:0.4162 kg Then the total quantity of material may be obtained from: 1[kg]:0,996 [kg]=X:0.4162 [kg] Amount source: EST
Processing of polyvinylidenchloride	*Extrusion, plastic pipes {RER}| production | APOS, U*	0.418 kg	EID	Amount: weight of polyvinylidenchloride Amount source: EST
Transport	*Transport, freight, lorry 16-32 metric ton, EURO6 {RER}| transport, freight, lorry 16-32 metric ton, EURO6 | APOS, U*	41.79 kg	EID	Transport of materials used to manufacture pipe. Transported weight: pipe weight Distance: 100 km Amount: EST

5	PIPE			
End of life of polyvinylidenchloride	*Municipal solid waste {IT}| treatment of, incineration | APOS, U*	0.4162 kg	EID	Amount: weight of polyvinylidenchloride. The end-of-life of the scraps was not considered because it has been included in the process related to the processing of polyvinylidenchloride. Amount source: LAB

Table 6-5 Inventory of pipe used for patented system of eggs collection

6	ELECTRICAL BOX			
Functional Unit of the process: 1p				
PROCESS	BACKGROUND PROCESS	AMOUNT	BACKGROUND PROCESS DATA SOURCES	COMMENT
Polyvinylidenchloride	*Polyvinylidenchloride, granulate {RER}| production | APOS, U*	0.9586 kg	EID	Amount: weight of polyvinylidenchloride used to manufacture electrical box. This quantity includes scraps generated during the processing of polyvinylidenchloride. From database process: [*1 kg of this process equals 0.976 kg of extruded plastic film*]. Total weight of polyvinylidenchloride used to manufacture electrical box:0.9356 kg Then the total quantity of material may be obtained from: 1[kg]:0,976 [kg]=X:0.9356 [kg] Amount source: LAB
Processing of polyvinylidenchloride	*Blow moulding {RER}| production | APOS, U*	0.9586 kg	EID	Amount of polyvinylidenchloride Amount source: EST
Transport	*Transport, freight, lorry 16-32 metric ton, EURO6 {RER}| transport, freight, lorry 16-32 metric ton, EURO6 | APOS, U*	95.86 kgkm	EID	Transport of materials used to manufacture electrical box. Transported weight: pipe weight Distance: 100 km Amount: EST

6	ELECTRICAL BOX			
End of life of polyvinylidenchloride	*Municipal solid waste {IT}| treatment of, incineration | APOS, U*	0.9356 kg	EID	Amount: weight of polyvinylidenchloride. The end-of-life of the scraps was not considered because it has been included in the process related to the processing of polyvinylidenchloride. Amount source: LAB

Table 6-6 Inventory of electrical box

Bioconversion unit

The functional unit of the bioconversion plant was the sum of:

1. weight of residual substrate (75% of substrate weight);
2. weight of mature larvae (prepupae);
3. weight of larvae that died during the growth phase (10% of larvae produced in the nursery unit).

Since the stage of development of dead larva during the growth phase was unknown, it was considered that the weight of dead larva is equal to that of the larva leaving the Nursery unit increased by 1%.

Some components of bioconversion plant were manufactured in polyoxymethylene. Since in Ecoinvent database an updated process for polyoxymethylene was missing, it was decided to replace it with the process of production of formaldehyde (production process by oxidation of methanol) since formaldehyde is the monomer of a polyoxymethylene. Other components of the bioconversion plant were manufactured using both iron and plastic. For these components, an aggregate data was provided as the weight of the component, therefore it was assumed that the total weight of the material was equally distributed (50%) between the component materials.

Due to the lack in literature of specific data of methane emissions for *Hermetia Illucens*, it was assumed that they do not emit methane during biodigestion activity. According to Hackstein and Stumm 1994, Diptera does not seem to be a methane-emitting species of insects.

To calculate the energy demand of the handling of one tray in the bioconverter, it was assumed a temporal sequence in which the bioconverter took a tray, inserted new substrate into the tray and subsequently repositioned the tray in the storage module of the bioconversion plant (Table 6-7).

TEMPORAL SEQUENCE	DURATION [min]
1.Elevator movement in order to reach level of the tray	1
2.Movement of the tray by means of the drive roller of shelf of the storage module in the bioconversion plant	0.5
3.Movement of drive roller of elevator	0.5
4.Elevator movement in order to reach rest position	1
5.Movement of drive roller of elevator in order to bring the tray into position for placing the growth substrate	0.5
6.Turning on the substrate dosing system	immediate
7.Substrate dosage	2
8.Movement backwards and forwards of the drive roller in order to homogenize growth substrate in the tray	120
9.Turning off the substrate dosing system	immediate
10.Movement of roller drive in order to bring the tray on the elevator	0.5
11.Movement of drive roller of elevator	0.5
12.Elevator movement in order to reach level of the tray	1
13.Movement of the tray by means of the drive roller of shelf of the storage module in the bioconversion plant	0.5

Table 6-7 Temporal sequence of movement of a single tray to dosage substrate

Considering that in the bioconversion plant there were 26 trays and the growth substrate must be added every 2 days, it was possible to calculate the energy demand to move trays. To this energy it must be added:

1. energy demand of the refrigeration unit used to maintain constant the temperature and the relative humidity in the bioconversion plant;
2. energy demand of the tipping machine used to tipp trays over vibrating sieve. To calculate the energy of the tipping process it was assumed that the trays followed the same temporal sequence for the substrate dosing phase. Dosage and homogenization of substrate in the temporal sequence (step 7-8 in Table 6-7) were replaced by the tipping of substrate.

TEMPORAL SEQUENCE	DURATION [min]
1.Elevator movement in order to reach level of the tray	1
2.Movement of the tray by means of the drive roller of shelf of the storage module in the bioconversion plant	0.5
3.Movement of drive roller of elevator	0.5
4.Elevator movement in order to reach rest position	1
5.Movement of drive roller of elevator in order to bring the tray into position for placing the growth substrate	0.5
6.Turning on tipping machine	immediate
7.Substrate tipping	2
9.Turning off tipping machine	immediate
10.Movement of roller drive in order to bring the tray on the elevator	0.5
11.Movement of drive roller of elevator	0.5
12.Elevator movement in order to reach level of the tray	1
13.Movement of the tray by means of the drive roller of shelf of the storage module in the bioconversion plant	0.5

Table 6-8 Temporal sequence of movement of a single tray to tip residual substrate and prepupae into vibrating sieve

The duration of each single step of the temporal sequences, the frequency of the movement of the trays, as well as the duration and frequency of use of the tipping machine were estimated based on the preliminary design of pilot plant.

7	BIOCONVERSION UNIT			
Functional Unit of the process:1.8E4 kg				
PROCESS	BACKGROUND PROCESS	AMOUNT	BACKGROUND PROCESS DATA SOURCES	COMMENT
Water	*Tap water {Europe without Switzerland}| tap water production, conventional treatment | APOS, U*	500 g	EID	Amount: weight of water for substrate Amount source: LAB
Bioconversion plant	*Plant*	0.0022 p	EID	Amount: unit (1 "p") allocated based on time of use (16 days). Lifespan: 15 years Amount source: EST
Transport	*Transport, freight, lorry 16-32 metric ton, EURO6 {RoW}| transport, freight, lorry 16-32 metric ton, EURO6 | APOS, U*	1,855E5 kgkm	EID	Transport of plant from supplier to laboratory Transported weight: weight of plant allocated based on time of use (16 days) Distance: 100 km Amount source: EST
Energy demand	*Electricity, low voltage {IT}| electricity voltage transformation from medium to low voltage | APOS, U*	11.05 kWh	EID	Amount: energy demand to move 26 trays in order to dosage substrate. Amount source: LAB
Energy demand	*Electricity, low voltage {IT}| electricity voltage transformation from medium to low voltage | APOS, U*	864 kWh	EID	Amount: energy demand of the of the refrigeration unit used to maintain constant temperature and relative humidity. Amount source: LAB

7	BIOCONVERSION UNIT			
Energy demand	*Electricity, low voltage {IT}| electricity voltage transformation from medium to low voltage | APOS, U*	0.8882 kWh	EID	Amount: energy demand to tip 26 trays Amount source: LAB

Table 6-9 Inventory of bioconversion unit

8	BIOCONVERSION PLANT (BIOCONVERTER)			
Functional Unit of the process:1p				
PROCESS	BACKGROUND PROCESS	AMOUNT	BACKGROUND PROCESS DATA SOURCES	COMMENT
Steel	*Steel, chromium steel 18/8 {RER}| steel production, converter, chromium steel 18/8 | APOS, U*	670.7 kg	EID	Amount: weight of steel used to manufacture steel components of the bioconversion plant (bioconverter) Amount source: LAB
Processing of steel	*Sheet rolling, chromium steel {RER}| processing | APOS, U*	670.7 kg	EID	Amount of steel used to manufacture steel components of the bioconversion plant (bioconverter) Amount source: LAB

8	BIOCONVERSION PLANT (BIOCONVERTER)			
Polyethylene	*Polyethylene, high density, granulate {RER}| production | APOS, U*	93.69 kg	EID	Amount: weight of polyethylene used to manufacture polyethylene components of the bioconversion plant (bioconverter) This quantity includes scraps generated during the processing of polyethylene. From database process: [*1 kg of this process equals 0.997 kg of blow moulded plastics (e.g. bottles)*]. Total weight of polyethylene used to manufacture polyethylene components of bioconversion plant: 93,41 kg Then the total quantity of material may be obtained from: 1[kg]:0,997 [kg]=X:93,41 [kg] Amount source: LAB
Processing of polyethylene	*Blow moulding {RER}| production | APOS, U*	93.69 kg	EID	Amount of polyethylene used to manufacture polyethylene components of the bioconversion plant (bioconverter). Amount source: LAB
Iron	*Steel, low-alloyed {RER}| steel production, converter, low-alloyed | APOS, U*	92.89 kg	EID	Amount: weight of iron used to manufacture iron components of the bioconversion plant (bioconverter). Amount source: LAB

8	BIOCONVERSION PLANT (BIOCONVERTER)			
Processing of iron	*Sheet rolling, chromium steel {RER}| processing | APOS, U*	92.89 kg	EID	Amount of iron used to manufacture steel components of the bioconversion plant (bioconverter) Amount source: LAB
Reinforcing steel	*Reinforcing steel {RER}| production | APOS, U*	8.28 kg	EID	Amount: weight of reinforcing steel used to manufacture reinforcing steel components of the bioconversion plant (bioconverter). Amount source: LAB
Processing of reinforcing steel	*Sheet rolling, chromium steel {RER}| processing | APOS, U*	8.28 kg	EID	Amount of reinforcing steel used to manufacture reinforcing steel components of the bioconversion plant (bioconverter). Amount source: LAB
Aluminium	*Aluminium, cast alloy {RER}| treatment of aluminium scrap, new, at refiner | APOS, U*	2.72 kg	EID	Amount: weight of aluminium used to manufacture aluminium components of the bioconversion plant (bioconverter). Amount source: LAB
Processing of aluminium	*Sheet rolling, chromium steel {RER}| processing | APOS, U*	2.72 kg	EID	Amount of aluminium used to manufacture aluminium components of the bioconversion plant (bioconverter). Amount source: LAB

8	BIOCONVERSION PLANT (BIOCONVERTER)			
Polyoxymethylene	*Formaldehyde {RER}| oxidation of methanol | APOS, U*	0.12 kg	EID	Amount: weight of polyoxymethylene used to manufacture polyoxymethylene components of the bioconversion plant (bioconverter). Amount source: LAB
Isothermal box of bioconverter	*Isothermal Box of Bioconverter*	1 p	EID	Amount: unit (1 "p") Amount source: LAB
Trays for substrate	*Tray*	26 p	EID	Amount: unit (26 "p") Number of trays: 26 Amount source: LAB
Transport	*Transport, freight, lorry 16-32 metric ton, EURO6 {RoW}| transport, freight, lorry 16-32 metric ton, EURO6 | APOS, U*	8.684E4	EID	Transport of materials used to manufacture bioconversion plant (bioconverter). Transported weight: weight of materials Distance: 100 km Amount: EST
End of life of steel	*Steel recycling, multi-output process (Allocation 50%)*	670.7 kg	EID	Amount: weight of steel Amount source: LAB
End of life of polyethylene	*Plastic recycling, multi-output process (Allocation 50%)*	93.41 kg	EID	Amount: weight of polyethylene. The end-of-life of the scraps was not considered because it has been included in the process related to the processing of polyethylene. Amount source: LAB
End of life of iron	*Steel recycling, multi-output process (Allocation 50%)*	92.89 kg	EID	Amount: weight of iron Amount source: LAB

8	BIOCONVERSION PLANT (BIOCONVERTER)			
End of life of reinforcing steel	*Steel recycling, multi-output process (Allocation 50%)*	8.28 kg	EID	Amount: weight of reinforcing steel Amount source: LAB
End of life of aluminium	*Aluminium recycling, multi-output process (Allocation 50%)*	2.72 kg	EID	Amount: weight of aluminium Amount source: LAB
End of life of polyoxymethylene	*Municipal solid waste {IT}| treatment of, incineration | APOS, U*	0.12 kg	EID	Amount: weight of polyoxymethylene Amount source: LAB

Table 6-10 Inventory of bioconversion plant

9	TRAY			
Functional Unit of the process: 1p				
PROCESS	BACKGROUND PROCESS	AMOUNT	BACKGROUND PROCESS DATA SOURCES	COMMENT
Polypropylene	*Polypropylene, granulate {RER}| production | APOS, U*	1.153 kg	EID	Amount: weight of polypropylene used to manufacture the tray. This quantity includes scraps generated during the processing of polypropylene. From database process: [*1 kg of this process equals 0.997 kg of blow moulded plastics (e.g. bottles)*]. Total weight of polypropylene used to manufacture the tray:1,15 kg Then the total quantity of material may be obtained from: 1[kg]:0,997 [kg]=X:1.15 [kg] Amount source: LAB
Processing of polypropylene	*Blow moulding {RER}| production | APOS, U*	1.153 kg	EID	Amount: weight of polypropylene used to manufacture the tray. Amount source: LAB
Transport	*Transport, freight, lorry 16-32 metric ton, EURO6 {RER}| transport, freight, lorry 16-32 metric ton, EURO6 | APOS, U*	115,3 kgkm	EID	Transport of materials used to manufacture the tray. Transported weight: tray weight Distance: 100 km Amount: EST

9	TRAY			
End of life of polypropylene	*Municipal solid waste {IT}| treatment of, incineration | APOS, U*	1.15 kg	EID	Amount: weight of polypropylene. The end-of-life of the scraps was not considered because it has been included in the process related to the processing of polyethylene. Amount source: LAB

Table 6-11 Inventory of growth substrate tray

10	ISOTHERMAL BOX OF BIOCONVERTER			
Functional Unit of the process: 1p				
PROCESS	BACKGROUND PROCESS	AMOUNT	BACKGROUND PROCESS DATA SOURCES	COMMENT
Steel	*Steel, chromium steel 18/8 {RER}| steel production, electric, chromium steel 18/8 | APOS, U*	743.1 kg	EID	Amount: weight of steel used to manufacture the isothermal box of bioconverter. Amount source: EST
Processing of steel	*Sheet rolling, chromium steel {RER}| processing | APOS, U*	743.1 kg	EID	Amount of steel used to manufacture the isothermal box of bioconverter. Amount source: EST
Polyurethane (PU)	*Polyurethane, rigid foam {RER}| production | APOS, U*	66.16 kg	EID	Amount: weight of polyurethane used for the insulation of the bioconverter isothermal box. Amount source: LAB
Transport	*Transport, freight, lorry 16-32 metric ton, EURO6 {RER}| transport, freight, lorry 16-32 metric ton, EURO6 | APOS, U*	8.092E4 kgkm	EID	Transport of materials used to manufacture bioconverter box. Transported weight: weight of all materials Distance: 100 km Amount source: EST
End of life of steel	*Steel recycling, multi-output process (Allocation 50%)*	743.1 kg	EID	Amount: weight of steel. Amount source: EST
End of life of polyurethane	*PUR recycling*	66.16 kg	EID	Amount: weight of polyurethane. Amount source: EST

Table 6-12 Inventory of isothermal box of bioconverter

Mature larvae (prepupae) production – BSF Breeding

Substrate preparation, nursery and bioconverter were applied in this process together with vibrating sieving machine and the required energy.

The duration of sieving and the frequency with which the vibrating sieve is turning on was estimated based on the preliminary design of pilot plant.

The total weight of the vibrating sieving machine was a primary data.

It was hypothesized that the machine consisted of:

1. Steel: 20%
2. Cast iron: 50%
3. Copper: 10%
4. Aluminum: 10%
5. High-density polyethylene: 10%

11	MATURE LARVAE (PREPUPAE) PRODUCTION			
Functional Unit of the primary process: 3270 g (economic allocation 63.31%) Functional Unit of the co-product (residual substrate compost): 1.379E4 g (economic allocation 29.66%) Functional Unit of the co-product ("Buffer breeding"): 363.3 g (economic allocation 7.034%)				
PROCESS	BACKGROUND PROCESS	AMOUNT	BACKGROUND PROCESS DATA SOURCES	COMMENT
Preparation of growth substrate	*Preparation of substrate*	1.838E4 g	EID	Amount: weight of growth substrate related to the amount of larvae produced into the nursery Amount source: LAB
Production of larvae	*Nursery*	307.7 g	EID	Amount: weight of larvae produced into the nursery. The amount of larvae is related to the amount of mature larvae produced into the bioconverter. Amount source: LAB
Bioconversion unit	*Bioconversion unit*	1.8E4 g	EID	Amount: weight of mature larvae (prepupae produced in the bioconverter), residual substrate and dead mature larvae during the bioconversion process . Amount source: LAB
Vibrating sieving	*Vibrating sieving*	0,00073 p	EID	Amount: unit (1 "p") allocated based on time of use (16 days). Lifespan: 15 years Amount source: EST

11	MATURE LARVAE (PREPUPAE) PRODUCTION			
Energy demand	*Electricity, low voltage {IT}| electricity voltage transformation from medium to low voltage | APOS, U*	1.5 kWh	EID	Amount: energy demand for sieving process that is done in order to separate mature larvae (prepupae) from residual growth substrate.

Table 6-13 Inventory of prepupae production

12	VIBRATING SIEVE			
Functional Unit of the process:1p				
PROCESS	BACKGROUND PROCESS	AMOUNT	BACKGROUND PROCESS DATA SOURCES	COMMENT
Cast iron	*Cast iron {RER}| production | APOS, U*	40 kg	EID	Amount: weight of cast iron used to manufacture cast iron components of the vibrating sieve Amount source: EST
Steel	*Steel, chromium steel 18/8 {RER}| steel production, converter, chromium steel 18/8 | APOS, U*	16 kg	EID	Amount: weight of steel used to manufacture steel components of the vibrating sieve Amount source: EST
Processing of steel	*Sheet rolling, chromium steel {RER}| processing | APOS, U*	16 kg	EID	Amount of steel used to manufacture steel components of the vibrating sieve Amount source: EST

12	VIBRATING SIEVE			
Functional Unit of the process:1p				
Copper	*Copper {RER}| treatment of scrap by electrolytic refining | APOS, U*	8 kg	EID	Amount: weight of copper used to manufacture copper components of the vibrating sieve Amount source: EST
Processing of copper	*Wire drawing, copper {RER}| processing | APOS, U*	8 kg	EID	Amount of copper used to manufacture steel components of the vibrating sieve Amount source: EST
Aluminium	*Aluminium, cast alloy {RER}| treatment of aluminium scrap, new, at refiner | APOS, U*	8 kg	EID	Amount: weight of aluminium used to manufacture aluminium components of the vibrating sieve Amount source: EST
Processing of aluminium	*Sheet rolling, aluminium {RER}| processing | APOS, U*	8 kg	EID	Amount of aluminium used to manufacture steel components of the vibrating sieve Amount source: EST

12	VIBRATING SIEVE			
Functional Unit of the process:1p				
Polyethylene	*Polyethylene, high density, granulate {RER}| production | APOS, U*	8.024 kg	EID	Amount: weight of polyethylene used to manufacture polyethylene components of vibrating sieve This quantity includes scraps generated during the processing of polyethylene. From database process: [*1 kg of this process equals 0.997 kg of blow moulded plastics (e.g. bottles)*]. Total weight of polyethylene used to manufacture polyethylene components of vibrating sieve :8 kg Then the total quantity of material may be obtained from: 1[kg]:0,997 [kg]=X:8 [kg] Amount source: EST
Processing of polyethylene	*Blow moulding {RER}| production | APOS, U*	8.024 kg	EID	Amount of polyethylene used to manufacture polyethylene components of the vibrating sieve. Amount source: EST
Transport	*Transport, freight, lorry 16-32 metric ton, EURO6 {RoW}| transport, freight, lorry 16-32 metric ton, EURO6 | APOS, U*	8002 kgkm	EID	Transport of materials used to manufacture components of vibrating sieve. Transported weight: weight of materials Distance: 100 km Amount: EST

12	VIBRATING SIEVE			
Functional Unit of the process:1p				
End of life of cast iron	*Cast iron recycling, multi-output process (Allocation 50%)*	40 kg	EID	Amount: weight of cast iron Amount source: EST
End of life of steel	*Steel recycling, multi-output process (Allocation 50%)*	16 kg	EID	Amount: weight of steel Amount source: EST
End of life of copper	*Copper recycling, multi-output process (Allocation 50%)*	8 kg	EID	Amount: weight of copper Amount source: EST
End of life of aluminium	*Aluminium recycling, multi-output process (Allocation 50%)*	8 kg	EID	Amount: weight of aluminium Amount source: EST
End of life of polyethylene	*Plastic recycling, multi-output process (Allocation 50%)*	8 kg	EID	Amount: weight of polyethylene. The end-of-life of the scraps was not considered because it has been included in the process related to the processing of polyethylene. Amount source: LAB

Table 6-14 Inventory of vibrating sieve

6.3.2 Life Cycle Inventory of extraction protocol 1

Process "Extraction of lipid, protein, chitin fraction" consisted of five sub-processes:

1. Prodution of mature larvae (prepupae) - BSF Breeding (F.U. 382.7 g - wet weight)
2. preparation of BSF prepupae (F.U. 375 g - wet weight).
3. Extraction on lipid fraction (F.U. amount of lipid fraction - Dry matter (40.47 g))
4. Extraction of protein fraction (F.U. amount of protein fraction - Dry matter (34 g)).
5. Extraction of chitin fraction (F.U. amount of chitin fraction - Dry matter (10.47 g)).
6. Disposal of residual prepupae biomass (F.U. amount of residual prepupae biomass - Dry matter (41.54 g)).

The amount of water that evaporeted during the extraction process of lipid, protein, chitinic fraction was introduced as water emission.

Atmospheric and indoor emissions fractions were hypothesized. It was assumed that these fractions were both equal to 1% of the total emission. It was assumed that the efficiency of the filter of the aspiration system is equal to 99% while that of the mask worn by the worker was equal to 95%.

For laboratory equipment, processes were created "ad hoc".
"p" was chosen as functional unit.

For more details on the extraction procedure, refer to the Chapter 3 - section 3.3
In the following pages, only, Life Cycle Inventory of process "Extraction of lipid, protein, chitin fraction" (Table 6-19) and the five sub-processes that were applied in it were reported (Table 6-15, Table 6-16, Table 6-17, Table 6-18).

Preparation of prepupae

13	PREPARATION OF PREPUPAE			
Functional Unit of the process: 375 g				
PROCESS	BACKGROUND PROCESS	AMOUNT	BACKGROUND PROCESS DATA SOURCES	COMMENT
Energy demand	*Electricity, low voltage {IT}| electricity voltage transformation from medium to low voltage | APOS, U*	900 Wh	EID	Amount: energy demand to freeze BSF prepupae Amount source: EST
Analytical mill	*Analytical mill*	1.852E-5 p	EID	Analytical mill (IKA, A10 basic) Amount: unit ("p") allocated based on the time of use Amount source: EST
Mill energy demand	*Electricity, low voltage {IT}| electricity voltage transformation from medium to low voltage | APOS, U*	67.5 Wh	EID	Amount: energy demand for use of mill Amount source: LAB
Transport	*Transport, freight, lorry 3.5-7.5 metric ton, EURO6 {RER}| transport, freight, lorry 3.5-7.5 metric ton, EURO6 | Alloc Def, U*	0,00165 kgkm	EID	Transport of analytical mill from supplier to laboratory Transported weight: weight of analytical mill allocated based on time of use Distance: 100 km Amount source: EST
Flask	*Flask*	3.704E-5 p	EID	Flask Amount: unit ("p") allocated based on the time of use. Amount source: EST

13	PREPARATION OF PREPUPAE			
Transport	*Transport, freight, lorry 3.5-7.5 metric ton, EURO6 {RER}| transport, freight, lorry 3.5-7.5 metric ton, EURO6 | APOS, U*	2.571 kgkm	EID	Transport of flask used Transported weight: weight of flask allocated based on the time of use. Distance: 100 km Amount source: EST
Aspiration plant	*Aspiration plant*	4.702E-6 p	EID	Aspiration plant Amount: unit ("p") allocated based on the time of use of aspiration plant Amount source: EST
Aspiration plant energy demand	*Electricity, low voltage {IT}| electricity voltage transformation from medium to low voltage | APOS, U*	0.068 kWh	EID	Amount: energy demand for use of aspiration plant Amount source: EST
Active carbon filter	*Active carbon filter*	1.875E-5 p	EID	Active carbon Amount: unit ("p") allocated based on the time of use of aspiration plant Amount source: EST
Transport	*Transport, freight, lorry 3.5-7.5 metric ton, EURO6 {RER}| transport, freight, lorry 3.5-7.5 metric ton, EURO6 | APOS, U*	0.0006 tkm	EID	Transport of aspiration plant and active carbon from supplier to laboratory Transported weight: weight of aspiration plant and weight of active carbon allocated based on the time of use of aspiration plant Distance: 100 km Amount source: EST

13	PREPARATION OF PREPUPAE			
Protection devices	*Protection devices*	0.0091 p	EID	Protection device Amount: unit ("p") allocated based on the time of use Amount source: EST
Emission of Particulates <2.5 µm during grinding of BSF prepupae	*Particulates <2.5 µm*	0.03788 g	EID	Amount: emission [g] Amount source: EST
Emissions of Particulates <2.5 µm (amount of Particulates <2.5 µm emitted into the atmosphere through the exchange of air in the laboratory) during grinding of BSF prepupae	*Particulates <2.5 µm*	0.3826 g	EID	Amount: emission [g] Amount source: EST
Emissions of Particulates <2.5 µm (amount of Particulates <2.5 µm inhaled by the worker) during grinding of BSF prepupae	*Particulates <2.5 µm _indoor*	6.726E-7 g	EID	Amount: emission [g] Amount source: EST
Disposal of Particulates <2.5 µm (amount of Particulates <2.5 µm captured by the mask of the worker and by the filter of the aspiration system) during grinding of BSF prepupae	*Filter dust from Al electrolysis {RoW}| treatment of filter dust from Al electrolysis, residual material landfill | APOS, U*	3.75 g	EID	Amount: emission [g] Amount source: EST
Disposal of waste during grinding of BSF prepupae	*Spent solvent mixture {RoW}| treatment of, hazardous waste incineration | APOS, U*	3.827 g	EID	Amount: waste [g] Amount source: EST

Table 6-15 Inventory of preparation of prepupae

Extraction of lipidic fraction

14	EXTRACTION OF LIPIDIC FRACTION			
Functional Unit of process: 40.47 g				
PROCESS	BACKGROUND PROCESS	AMOUNT	BACKGROUND PROCESS DATA SOURCES	COMMENT
Crystallizer used to prepare distilled water bath	*Crystallizer*	0.00023 p	EID	Crystalizzer Amount: unit ("p") allocated based on the time of use. This equipment is used for both cycles, so a double allocation was considered. Amount source: EST
Transport	*Transport, freight, lorry 3.5-7.5 metric ton, EURO6 {RER}| transport, freight, lorry 3.5-7.5 metric ton, EURO6 | APOS, U*	0.0168 kgkm	EID	Transport of crystallizer used to prepare distilled water bath Transported weight: weight of crystallizer allocated based on the time of use. Distance: 100 km Amount source: EST
Distilled water	*Water, ultrapure {RoW}| production | APOS, U*	1540 g	EID	Distilled water used to prepare heated water bath Amount: distilled water Amount source: LAB
Pentane	*Pentane {RER}| production | APOS, U*	243.8 g	EID	Solvent used to extract lipids Amount: Pentane Amount source: LAB

14	EXTRACTION OF LIPIDIC FRACTION			
Hexane	*Hexane {RER}| molecular sieve separation of naphtha | APOS, U*	243.8 g	EID	Solvent used to extract lipids Amount: Hexane Amount source: LAB
Transport	*Transport, freight, lorry 3.5-7.5 metric ton, EURO6 {RER}| transport, freight, lorry 3.5-7.5 metric ton, EURO6 | APOS, U*	48.75 kgkm	EID	Transport of solvent used to extract lipids Transported weight: weight of solvent (petroleum ether) Distance: 100 km Amount source: EST
Graduated cylinder	*Graduated cylinder*	1.646-6 p	EID	Graduated cylinder used to prepare solvent Amount: unit ("p") allocated based on the time of use. Amount source: EST
Transport	*Transport, freight, lorry 3.5-7.5 metric ton, EURO6 {RER}| transport, freight, lorry 3.5-7.5 metric ton, EURO6 | APOS, U*	7.234E-5 kgkm	EID	Transport of graduated cylinder used to prepare solvent Transported weight: weight of graduated cylinder allocated based on the time of use. Distance: 100 km Amount source: EST
Flask	*Flask*	0.0011 p	EID	Flask Amount: unit ("p") allocated based on the time of use. This equipment is used for both cycles, so a double allocation was considered. Amount source: EST

14	EXTRACTION OF LIPIDIC FRACTION			
Transport	*Transport, freight, lorry 3.5-7.5 metric ton, EURO6 {RER}| transport, freight, lorry 3.5-7.5 metric ton, EURO6 | APOS, U*	0.078 kgkm	EID	Transport of flask used Transported weight: weight of flask allocated based on the time of use. Distance: 100 km Amount source: EST
Heating magnetic stirrer	*Heating Magnetic Stirrer*	0.00011 p	EID	Heating magnetic stirrer Amount: unit ("p") allocated based on the time of use This equipment is used for both cycles, so a double allocation was considered. Amount source: EST
Heating magnetic stirrer energy demand	*Electricity, low voltage {IT}| electricity voltage transformation from medium to low voltage | APOS, U*	2.73 kWh	EID	Amount: energy demand for use of heating stirrer Amount source: LAB
Transport	*Transport, freight, lorry 3.5-7.5 metric ton, EURO6 {RER}| transport, freight, lorry 3.5-7.5 metric ton, EURO6 | Alloc Def, U*	0.0288 kgkm	EID	Transport of heating magnetic stirrer from supplier to laboratory. Transported weight: weight of heating magnetic stirrer allocated based on the time of use. Distance: 100 km Amount source: EST

14	EXTRACTION OF LIPIDIC FRACTION			
Magnetic stirring rod	*Magnetic stirring rod*	9.877E-5 p	EID	Magnetic stirring rod Amount: unit ("p") allocated based on the time of use This equipment is used for both cycles, so a double allocation was considered. Amount source: EST
Transport	*Transport, freight, lorry 3.5-7.5 metric ton, EURO6 {RER}| transport, freight, lorry 3.5-7.5 metric ton, EURO6 | Alloc Def, U*	7.635E-5 kgkm	EID	Transport of magnetic stirring rod from supplier to laboratory Transported weight: weight of magnetic stirring rod allocated based on time of use Distance: 100 km Amount source: EST
Flask used to contain the liquid phase during filtering	*Flask*	8.231E-7 p	EID	Flask used to contain the liquid phase during filtering Amount: unit ("p") allocated based on the time of use. This equipment is used for both cycles, so a double allocation was considered. Amount source: EST
Transport	*Transport, freight, lorry 3.5-7.5 metric ton, EURO6 {RER}| transport, freight, lorry 3.5-7.5 metric ton, EURO6 | APOS, U*	2.468E-5 kgkm	EID	Transport of flask used to contain the liquid phase during filtering Transported weight: weight of flask allocated based on the time of use. Distance: 100 km Amount source: EST

14	EXTRACTION OF LIPIDIC FRACTION			
Funnel	*Funnel*	8.231E-7 p	EID	Funnel used to contain the liquid phase during filtering Amount: unit ("p") allocated based on the time of use. This equipment is used for both cycles, so a double allocation was considered. Amount source: EST
Transport	*Transport, freight, lorry 3.5-7.5 metric ton, EURO6 {RER}| transport, freight, lorry 3.5-7.5 metric ton, EURO6 | APOS, U*	1.68E-6 kgkm	EID	Transport of funnel used to contain the liquid phase during filtering Transported weight: weight of funnel allocated based on the time of use. Distance: 100 km Amount source: EST
Automated laboratory extractor of total fat	*Automated laboratory extractor of total fat*	4.938E-5 p	EID	Automated laboratory extractor of total fat Amount: unit ("p") allocated based on the time of use. This equipment is used for both cycles, so a double allocation was considered. Amount source: EST

14	EXTRACTION OF LIPIDIC FRACTION			
Cups of extractor	*Cup of extractor*	0.00267 p	EID	Cups of extractor Amount: unit ("p") allocated based on the time of use. This equipment is used for both cycles, so a double allocation was considered. Amount source: EST
Transport	*Transport, freight, lorry 3.5-7.5 metric ton, EURO6 {RER}| transport, freight, lorry 3.5-7.5 metric ton, EURO6 | APOS, U*	0.3146 kgkm	EID	Transport of automated laboratory extractor of total fat and cups Transported weight: weight of of automated laboratory extractor of total fat and cups allocated based on the time of use. Distance: 100 km Amount source: EST
Energy demand of automated laboratory extractor of total fat	*Electricity, low voltage {IT}| electricity voltage transformation from medium to low voltage | APOS, U*	0.5 kWh	EID	Amount: energy demand of automated laboratory extractor of total fat This is the energy demand of the two extraction cycles Amount source: LAB
Falcon 50 mL conical tube	*Falcon 50 mL conical tube*	1 p	EID	Falcon 50 mL conical tube used to storage extracted fat Amount source: EST

14	EXTRACTION OF LIPIDIC FRACTION			
Transport	*Transport, freight, lorry 3.5-7.5 metric ton, EURO6 {RER}| transport, freight, lorry 3.5-7.5 metric ton, EURO6 | APOS, U*	1.424 kgkm	EID	Transport of Falcon 50 mL conical tube Transported weight: weight of Falcon 50 mL conical tube used to storage extracted fat Distance: 100 km Amount source: EST
Energy demand to freeze extracted fat	*Electricity, low voltage {IT}| electricity voltage transformation from medium to low voltage | APOS, U*	600 Wh	EID	Amount: energy demand to freeze extracted fat Amount source: EST
Aspiration plant	*Aspiration plant*	0.00014 p	EID	Aspiration plant Amount: unit ("p") allocated based on the time of use of aspiration plant Amount source: EST
Aspiration plant energy demand	*Electricity, low voltage {IT}| electricity voltage transformation from medium to low voltage | APOS, U*	2.015 kWh	EID	Amount: energy demand for use of aspiration plant Amount source: EST
Active carbon filter	*Active carbon filter*	0.00055 p	EID	Active carbon Amount: unit ("p") allocated based on the time of use of aspiration plant Amount source: EST

14	EXTRACTION OF LIPIDIC FRACTION			
Transport	*Transport, freight, lorry 3.5-7.5 metric ton, EURO6 {RER}| transport, freight, lorry 3.5-7.5 metric ton, EURO6 | APOS, U*	0.0190 tkm	EID	Transport of aspiration plant and active carbon from supplier to laboratory Transported weight: weight of aspiration plant and weight of active carbon allocated based on the time of use of aspiration plant Distance: 100 km Amount source: EST
Protection devices	*Protection devices*	0.0675 p	EID	Protection device Amount: unit ("p") allocated based on the time of use Amount source: EST
Emission of solvent (amount emitted into atmosphere)	*Hydrocarbons, aromatic*	0.6473 g	EID	Amount: emission [g] Amount source: EST
Emission of solvent (amount emitted into the atmosphere through the exchange of air in the laboratory)	*Hydrocarbons, aromatic*	0.6538 g	EID	Amount: emission [g] Amount source: EST
Emission of solvent (amount inhaled by the worker)	*Hydrocarbons, aromatic_indoor*	0.00011 g	EID	Amount: emission [g] Amount source: EST
Disposal of solvent (amount captured by the mask of the worker and by the filter of the aspiration system)	*Filter dust from Al electrolysis {RoW}| treatment of filter dust from Al electrolysis, residual material landfill | APOS, U*	64.09 g	EID	Amount: emission [g] Amount source: EST
End of life of solvent used to extract lipids	*Spent solvent mixture {RoW}| treatment of, hazardous waste incineration | APOS, U*	422.1 g	EID	Amount: weight of residual solvent [g] Amount source: EST

Table 6-16 Inventory of extraction protocol of lipidic fraction

Extraction of protein fraction

15	EXTRACTION OF PROTEIN FRACTION			
Functional Unit of the process: 34 g				
PROCESS	BACKGROUND PROCESS	AMOUNT	BACKGROUND PROCESS DATA SOURCES	COMMENT
Crystallizer used to prepare distilled water bath	*Crystallizer*	0.00011 p	EID	Crystalizzer Amount: unit ("p") allocated based on the time of use. Amount source: EST
Transport	*Transport, freight, lorry 3.5-7.5 metric ton, EURO6 {RER}| transport, freight, lorry 3.5-7.5 metric ton, EURO6 | APOS, U*	0.0084 kgkm	EID	Transport of crystallizer used to prepare distilled water bath Transported weight: weight of crystallizer allocated based on the time of use. Distance: 100 km Amount source: EST
Distilled water	*Water, ultrapure {RoW}| production | APOS, U*	1540 g	EID	Distilled water used to prepare heated water bath Amount: distilled water Amount source: LAB
Sodium hydroxide	*Sodium hydroxide, without water, in 50% solution state {RoW}| chlor-alkali electrolysis, diaphragm cell | APOS, U*	20 g	EID	Solvent Amount: sodium hydroxide Amount source: LAB

15	EXTRACTION OF PROTEIN FRACTION			
Distilled water	*Water, ultrapure {RoW}| production | APOS, U*	500 g	EID	Distilled water used to prepare solution (1M) Amount: distilled water Amount source: LAB
Transport	*Transport, freight, lorry 3.5-7.5 metric ton, EURO6 {RER}| transport, freight, lorry 3.5-7.5 metric ton, EURO6 | APOS, U*	52 kgkm	EID	Transport of solution used to extract protein fraction Transported weight: weight of solution (NaOH 1M) Distance: 100 km Amount source: EST
Graduated cylinder	*Graduated cylinder*	1.646E-6 p	EID	Graduated cylinder used to prepare solvent (sodium hydroxide) Amount: unit ("p") allocated based on the time of use. Amount source: EST
Transport	*Transport, freight, lorry 3.5-7.5 metric ton, EURO6 {RER}| transport, freight, lorry 3.5-7.5 metric ton, EURO6 | APOS, U*	7.234E-5 kgkm	EID	Transport of graduated cylinder used to prepare solvent (sodium hydroxide) Transported weight: weight of graduated cylinder allocated based on the time of use. Distance: 100 km Amount source: EST
Flask (2Lt)	*Flask(2Lt)*	0.0010 p	EID	Flask Amount: unit ("p") allocated based on the time of use. Amount source: EST

15	EXTRACTION OF PROTEIN FRACTION			
Transport	*Transport, freight, lorry 3.5-7.5 metric ton, EURO6 {RER}| transport, freight, lorry 3.5-7.5 metric ton, EURO6 | APOS, U*	0.0699 kgkm	EID	Transport of flask used Transported weight: weight of flask allocated based on the time of use. Distance: 100 km Amount source: EST
Magnetic stirrer/heater	*Magnetic Stirrer/Heater*	5.761E-5 p	EID	Magnetic stirrer/heater Amount: unit ("p") allocated based on the time of use Amount source: EST
Magnetic stirrer/heater energy demand	*Electricity, low voltage {IT}| electricity voltage transformation from medium to low voltage | APOS, U*	0.735 kWh	EID	Amount: energy demand for use of heating stirrer Amount source: LAB
Transport	*Transport, freight, lorry 3.5-7.5 metric ton, EURO6 {RER}| transport, freight, lorry 3.5-7.5 metric ton, EURO6 | Alloc Def, U*	0.0144 kgkm	EID	Transport of heating magnetic stirrer from supplier to laboratory. Transported weight: weight of magnetic stirrer/heater allocated based on the time of use. Distance: 100 km Amount source: EST
Magnetic stirring rod	*Magnetic stirring rod*	4.938E-5 p	EID	Magnetic stirring rod Amount: unit ("p") allocated based on the time of use Amount source: EST

15	EXTRACTION OF PROTEIN FRACTION			
Transport	*Transport, freight, lorry 3.5-7.5 metric ton, EURO6 {RER}| transport, freight, lorry 3.5-7.5 metric ton, EURO6 | Alloc Def, U*	3.817E-5 kgkm	EID	Transport of magnetic stirring rod from supplier to laboratory Transported weight: weight of magnetic stirring rod allocated based on time of use Distance: 100 km Amount source: EST
Falcon 50 mL conical tube	*Falcon 50 mL conical tube*	16 p	EID	Falcon 50 mL conical tube used to storage extracted fat Amount source: EST
Transport	*Transport, freight, lorry 3.5-7.5 metric ton, EURO6 {RER}| transport, freight, lorry 3.5-7.5 metric ton, EURO6 | APOS, U*	22.78 kgkm	EID	Transport of Falcon 50 mL conical tube Transported weight: weight of 16 Falcon 50 mL conical tubes Distance: 100 km Amount source: EST
Centrifuge	*Centrifuge*	1.235E-5 p	EID	Centrifuge Amount: unit ("p") allocated based on the time of use Amount source: EST
Centrifuge energy demand	*Electricity, low voltage {IT}| electricity voltage transformation from medium to low voltage | APOS, U*	225 Wh	EID	Amount: energy demand for use of centrifuge Amount source: LAB
Transport	*Transport, freight, lorry 3.5-7.5 metric ton, EURO6 {RER}| transport, freight, lorry 3.5-7.5 metric ton, EURO6 | APOS, U*	0.1222 kgkm	EID	Transport of centrifuge Transported weight: weight of centrifuge allocated based on the time of use Distance: 100 km Amount source: EST

15	EXTRACTION OF PROTEIN FRACTION			
Flask (2.5Lt)	*Flask(2.5Lt)*	4.833E-5 p	EID	Flask Amount: unit ("p") allocated based on the time of use. Amount source: EST
Transport	*Transport, freight, lorry 3.5-7.5 metric ton, EURO6 {RER}| transport, freight, lorry 3.5-7.5 metric ton, EURO6 | APOS, U*	0.00055 kgkm	EID	Transport of flask Transported weight: weight of flask allocated based on the time of use. Distance: 100 km Amount source: EST
Graduated cylinder	*Graduated cylinder*	1.646E-6 p	EID	Graduated cylinder used to prepare solvent Amount: unit ("p") allocated based on the time of use. Amount source: EST
Transport	*Transport, freight, lorry 3.5-7.5 metric ton, EURO6 {RER}| transport, freight, lorry 3.5-7.5 metric ton, EURO6 | APOS, U*	4.323E-6 kgkm	EID	Transport of graduated cylinder used to prepare solvent Transported weight: weight of graduated cylinder allocated based on the time of use. Distance: 100 km Amount source: EST
Hydrochloric acid	*Hydrochloric acid, without water, in 30% solution state {RER}| allyl chloride production, reaction of propylene and chlorine | APOS, U*	8.75 g	EID	Amount: hydrochloric acid 6N Amount source: LAB
Water	*Tap water {Europe without Switzerland}| tap water production, conventional treatment | APOS, U*	35.25 g	EID	Amount: water for solution hydrochloric acid 6N Amount source: LAB

15	EXTRACTION OF PROTEIN FRACTION			
Transport	*Transport, freight, lorry 3.5-7.5 metric ton, EURO6 {RER}| transport, freight, lorry 3.5-7.5 metric ton, EURO6 | APOS, U*	4.4 kgkm	EID	Transport of solution Transported weight: weight of solution (HCl 6N) Distance: 100 km Amount source: EST
Pipet	*Pipet*	3.292E-6 p	EID	Pipet Amount: unit ("p") allocated based on the time of use. Amount source: EST
Transport	*Transport, freight, lorry 3.5-7.5 metric ton, EURO6 {RER}| transport, freight, lorry 3.5-7.5 metric ton, EURO6 | Alloc Def, U*	8.068E-6 kgkm	EID	Transport of disposable volumetric pipet from supplier to laboratory Transported weight: weight of pipet allocated based on the time of use. Distance: 100 km Amount source: EST
Bottle	*Bottle*	0.0012 p	EID	Bottle Amount: unit ("p") allocated based on the time of use. Amount source: EST
Transport	*Transport, freight, lorry 3.5-7.5 metric ton, EURO6 {RER}| transport, freight, lorry 3.5-7.5 metric ton, EURO6 | Alloc Def, U*	0.0324 kgkm	EID	Transport of bottle used to freeze solution Transported weight: weight of bottle allocated based on the time of use. Distance: 100 km Amount source: EST

15	EXTRACTION OF PROTEIN FRACTION			
Freezer energy demand	*Electricity, low voltage {IT}| electricity voltage transformation from medium to low voltage | APOS, U*	900 Wh	EID	Amount: energy demand for use of freezer Amount source: LAB
Falcon 50 mL conical tube	*Falcon 50 mL conical tube*	6 p	EID	Falcon 50 mL conical tube used to storage extracted fat Amount source: EST
Transport	*Transport, freight, lorry 3.5-7.5 metric ton, EURO6 {RER}| transport, freight, lorry 3.5-7.5 metric ton, EURO6 | Alloc Def, U*	8.544 kgkm	EID	Transport of Falcon 50 mL conical tube Transported weight: weight of 6 Falcon 50 mL conical tubes Distance: 100 km Amount source: EST
Centrifuge	*Centrifuge*	1.235E-5 p	EID	Centrifuge Amount: unit ("p") allocated based on the time of use Amount source: EST
Centrifuge energy demand	*Electricity, low voltage {IT}| electricity voltage transformation from medium to low voltage | APOS, U*	225 Wh	EID	Amount: energy demand for use of centrifuge Amount source: LAB
Transport	*Transport, freight, lorry 3.5-7.5 metric ton, EURO6 {RER}| transport, freight, lorry 3.5-7.5 metric ton, EURO6 | APOS, U*	0.1222 kgkm	EID	Transport of centrifuge Transported weight: weight of centrifuge allocated based on the time of use Distance: 100 km Amount source: EST

15	EXTRACTION OF PROTEIN FRACTION			
Flask (2.5Lt)	*Flask(2.5Lt)*	1.645E-6 p	EID	Flask Amount: unit ("p") allocated based on the time of use. Amount source: EST
Transport	*Transport, freight, lorry 3.5-7.5 metric ton, EURO6 {RER}| transport, freight, lorry 3.5-7.5 metric ton, EURO6 | APOS, U*	1.843E-5 kgkm	EID	Transport of flask Transported weight: weight of flask allocated based on the time of use. Distance: 100 km Amount source: EST
Energy demand to dry protein fraction	*Electricity, low voltage {IT}| electricity voltage transformation from medium to low voltage | APOS, U*	8 kWh	EID	Amount: energy demand to dry protein fraction Amount source: EST
Aspiration plant	*Aspiration plant*	0.00012 p	EID	Aspiration plant Amount: unit ("p") allocated based on the time of use of aspiration plant Amount source: EST
Aspiration plant energy demand	*Electricity, low voltage {IT}| electricity voltage transformation from medium to low voltage | APOS, U*	1.769 kWh	EID	Amount: energy demand for use of aspiration plant Amount source: EST
Active carbon filter	*Active carbon filter*	0.00048 p	EID	Active carbon Amount: unit ("p") allocated based on the time of use of aspiration plant Amount source: EST

15	EXTRACTION OF PROTEIN FRACTION			
Transport	*Transport, freight, lorry 3.5-7.5 metric ton, EURO6 {RER}| transport, freight, lorry 3.5-7.5 metric ton, EURO6 | APOS, U*	0.0167 tkm	EID	Transport of aspiration plant and active carbon from supplier to laboratory Transported weight: weight of aspiration plant and weight of active carbon allocated based on the time of use of aspiration plant Distance: 100 km Amount source: EST
Protection devices	*Protection devices*	0.0439 p	EID	Protection device Amount: unit ("p") allocated based on the time of use Amount source: EST
Emission of sodium hydroxide (amount of sodium hydroxide of solution 1M emitted into atmosphere) during agitation of defatted pellet and solution	*Sodium hydroxide*	0.0020 g	EID	Amount: emission [g] Amount source: EST
Emissions of sodium hydroxide (amount of sodium hydroxide of solution 1M emitted into the atmosphere through the exchange of air in the laboratory) during agitation of defatted pellet and solution	*Sodium hydroxide*	0.02 g	EID	Amount: emission [g] Amount source: EST
Emissions of sodium hydroxide (amount of sodium hydroxide of solution 1M inhaled by the worker) during agitation of defatted pellet and solution	*Sodium hydroxide_indoor*	1.5E-7 g	EID	Amount: emission [g] Amount source: EST

15	EXTRACTION OF PROTEIN FRACTION			
Disposal of sodium hydroxide (amount of sodium hydroxide of solution 1M captured by the mask of the worker and by the filter of the aspiration system) during agitation of defatted pellet and solution	*Filter dust from Al electrolysis {RoW}| treatment of filter dust from Al electrolysis, residual material landfill | APOS, U*	0.196 g	EID	Amount: emission [g] Amount source: EST
Water of sodium hydroxide of solution 1M that evaporated during agitation of defatted pellet and solution	*Water*	5 g	EID	Amount: weight of evaporated water [g] Amount source: EST
Emission of sodium hydroxide (amount of sodium hydroxide of solution 1M emitted into atmosphere) during drying in oven of protein fraction	*Sodium hydroxide*	0.0088 g	EID	Amount: emission [g] Amount source: EST
Emissions of sodium hydroxide (amount of sodium hydroxide of solution 1M emitted into the atmosphere through the exchange of air in the laboratory) during drying in oven of protein fraction	*Sodium hydroxide*	0.0089 g	EID	Amount: emission [g] Amount source: EST
Emissions of sodium hydroxide (amount of sodium hydroxide of solution 1M inhaled by the worker) during drying in oven of protein fraction	*Sodium hydroxide_indoor*	5.346E-6 g	EID	Amount: emission [g] Amount source: EST

15	EXTRACTION OF PROTEIN FRACTION			
Disposal of sodium hydroxide (amount of sodium hydroxide of solution 1M captured by the mask of the worker and by the filter of the aspiration system) during drying in oven of protein fraction	*Filter dust from Al electrolysis {RoW}| treatment of filter dust from Al electrolysis, residual material landfill | APOS, U*	0.8732 g	EID	Amount: emission [g] Amount source: EST
Water of sodium hydroxide of solution 1M that evaporated during drying in oven of protein fraction	*Water*	22.28 g	EID	Amount: weight of evaporated water [g] Amount source: EST
Emission of hydrochloric acid (amount of Hydrochloric acid of solution 6N emitted into atmosphere) during drying in oven of protein fraction	*Hydrochloric acid*	0.0043 g	EID	Amount: emission [g] Amount source: EST
Emissions of hydrochloric acid (amount of hydrochloric acid of solution 6N emitted into the atmosphere through the exchange of air in the laboratory) during drying in oven of protein fraction	*Hydrochloric acid*	0.0044 g	EID	Amount: emission [g] Amount source: EST
Emissions of hydrochloric acid (amount of hydrochloric acid of solution 6N inhaled by the worker) during drying in oven of protein fraction	*Hydrochloric acid_indoor*	2.625E-6 g	EID	Amount: emission [g] Amount source: EST

15	EXTRACTION OF PROTEIN FRACTION			
Disposal of hydrochloric acid (amount of hydrochloric acid of solution 6N captured by the mask of the worker and by the filter of the aspiration system) during drying in oven of protein fraction	*Filter dust from Al electrolysis {RoW}| treatment of filter dust from Al electrolysis, residual material landfill | APOS, U*	0.4288 g	EID	Amount: emission [g] Amount source: EST
Water of hydrochloric acid of solution 6N that evaporated during drying in oven of protein fraction	*Water*	1.762 g	EID	Amount: weight of evaporated water [g] Amount source: EST
End of life of solvent (sodium hydroxide and hydrochloric acid) used to extract proteins	*Spent solvent mixture {RoW}| treatment of, hazardous waste incineration | APOS, U*	482 g	EID	Amount: weight of residual solvent (sodium hydroxide and hydrochloric acid) [g] Amount source: EST

Table 6-17 Inventory of extraction protocol of protein fraction

Extraction of chitinic fraction

16	EXTRACTION OF CHITINIC FRACTION			
Functional Unit of the process: 10.47 g				
PROCESS	BACKGROUND PROCESS	AMOUNT	BACKGROUND PROCESS DATA SOURCES	COMMENT
Flask (2Lt)	*Flask(2Lt)*	0.0024 p	EID	Flask Amount: unit ("p") allocated based on the time of use. Amount source: EST

16	EXTRACTION OF CHITINIC FRACTION			
Transport	*Transport, freight, lorry 3.5-7.5 metric ton, EURO6 {RER}| transport, freight, lorry 3.5-7.5 metric ton, EURO6 | APOS, U*	0.0165 kgkm	EID	Transport of flask used Transported weight: weight of flask allocated based on the time of use. Distance: 100 km Amount source: EST
Graduated cylinder	*Graduated cylinder*	1.646E-6 p	EID	Graduated cylinder used to prepare solvent (sodium hydroxide) Amount: unit ("p") allocated based on the time of use. Amount source: EST
Transport	*Transport, freight, lorry 3.5-7.5 metric ton, EURO6 {RER}| transport, freight, lorry 3.5-7.5 metric ton, EURO6 | APOS, U*	4.323E-6 kgkm	EID	Transport of graduated cylinder used to prepare solvent (hydrochloric acid) Transported weight: weight of graduated cylinder allocated based on the time of use. Distance: 100 km Amount source: EST
Hydrochloric acid	*Hydrochloric acid, without water, in 30% solution state {RER}| allyl chloride production, reaction of propylene and chlorine | APOS, U*	72.92 g	EID	Amount: hydrochloric acid 2N Amount source: LAB
Water	*Tap water {Europe without Switzerland}| tap water production, conventional treatment | APOS, U*	442.1 g	EID	Amount: water for solution hydrochloric acid 6N Amount source: LAB

16	EXTRACTION OF CHITINIC FRACTION			
Transport	*Transport, freight, lorry 3.5-7.5 metric ton, EURO6 {RER}| transport, freight, lorry 3.5-7.5 metric ton, EURO6 | APOS, U*	51.5 kgkm	EID	Transport of solution Transported weight: weight of solution (HCl 2N) Distance: 100 km Amount source: EST
Falcon 50 mL conical tube	*Falcon 50 mL conical tube*	16 p	EID	Falcon 50 mL conical tube used to storage extracted fat Amount source: EST
Transport	*Transport, freight, lorry 3.5-7.5 metric ton, EURO6 {RER}| transport, freight, lorry 3.5-7.5 metric ton, EURO6 | APOS, U*	22.78 kgkm	EID	Transport of Falcon 50 mL conical tube Transported weight: weight of 16 Falcon 50 mL conical tubes Distance: 100 km Amount source: EST
Centrifuge	*Centrifuge*	2.469E-5 p	EID	Centrifuge Amount: unit ("p") allocated based on the time of use Amount source: EST
Centrifuge energy demand	*Electricity, low voltage {IT}| electricity voltage transformation from medium to low voltage | APOS, U*	450 Wh	EID	Amount: energy demand for use of centrifuge Amount source: LAB
Transport	*Transport, freight, lorry 3.5-7.5 metric ton, EURO6 {RER}| transport, freight, lorry 3.5-7.5 metric ton, EURO6 | APOS, U*	0.2444 kgkm	EID	Transport of centrifuge Transported weight: weight of centrifuge allocated based on the time of use Distance: 100 km Amount source: EST

16	EXTRACTION OF CHITINIC FRACTION			
Flask (2.5Lt) used to contain the supernatant	*Flask(2.5Lt)*	4.39E-5 p	EID	Flask used to contain the supernatant after centrifugation Amount: unit ("p") allocated based on the time of use. Amount source: EST
Transport	*Transport, freight, lorry 3.5-7.5 metric ton, EURO6 {RER}| transport, freight, lorry 3.5-7.5 metric ton, EURO6 | APOS, U*	0.0005 kgkm	EID	Transport of flask used to contain the supernatant after centrifugation Transported weight: weight of flask allocated based on the time of use. Distance: 100 km Amount source: EST
Flask (2.5Lt) used to contain the supernatant	*Flask(2.5Lt)*	4.554E-5 p	EID	Flask used to contain pellet after centrifugation Amount: unit ("p") allocated based on the time of use. Amount source: EST
Transport	*Transport, freight, lorry 3.5-7.5 metric ton, EURO6 {RER}| transport, freight, lorry 3.5-7.5 metric ton, EURO6 | APOS, U*	0.0005 kgkm	EID	Transport of flask used to contain pellet after centrifugation Transported weight: weight of flask allocated based on the time of use. Distance: 100 km Amount source: EST
Distilled water	*Water, ultrapure {RoW}| production | APOS, U*	0.5 g	EID	Distilled water Amount: water used to do washes of pellet after centrifugation Amount source: LAB

16	EXTRACTION OF CHITINIC FRACTION			
Falcon 50 mL conical tube	*Falcon 50 mL conical tube*	16 p	EID	Falcon 50 mL conical tube used to storage extracted fat Amount source: EST
Transport	*Transport, freight, lorry 3.5-7.5 metric ton, EURO6 {RER}| transport, freight, lorry 3.5-7.5 metric ton, EURO6 | APOS, U*	22.78 kgkm	EID	Transport of Falcon 50 mL conical tube Transported weight: weight of 16 Falcon 50 mL conical tubes Distance: 100 km Amount source: EST
Centrifuge	*Centrifuge*	2.469E-5 p	EID	Centrifuge Amount: unit ("p") allocated based on the time of use Amount source: EST
Centrifuge energy demand	*Electricity, low voltage {IT}| electricity voltage transformation from medium to low voltage | APOS, U*	450 Wh	EID	Amount: energy demand for use of centrifuge Amount source: LAB
Transport	*Transport, freight, lorry 3.5-7.5 metric ton, EURO6 {RER}| transport, freight, lorry 3.5-7.5 metric ton, EURO6 | APOS, U*	0.2444 kgkm	EID	Transport of centrifuge Transported weight: weight of centrifuge allocated based on the time of use Distance: 100 km Amount source: EST
Flask (2.5Lt) used to contain the supernatant	*Flask(2.5Lt)*	4.39E-5 p	EID	Flask used to contain the supernatant after centrifugation Amount: unit ("p") allocated based on the time of use. Amount source: EST

16	EXTRACTION OF CHITINIC FRACTION			
Transport	*Transport, freight, lorry 3.5-7.5 metric ton, EURO6 {RER}| transport, freight, lorry 3.5-7.5 metric ton, EURO6 | APOS, U*	0.0005 kgkm	EID	Transport of flask used to contain the supernatant after centrifugation Transported weight: weight of flask allocated based on the time of use. Distance: 100 km Amount source: EST
Energy demand to dry chitinic fraction	*Electricity, low voltage {IT}| electricity voltage transformation from medium to low voltage | APOS, U*	8 kWh	EID	Amount: energy demand to dry chitinic fraction Amount source: EST
Aspiration plant	*Aspiration plant*	0.00012 p	EID	Aspiration plant Amount: unit ("p") allocated based on the time of use of aspiration plant Amount source: EST
Aspiration plant energy demand	*Electricity, low voltage {IT}| electricity voltage transformation from medium to low voltage | APOS, U*	1.805 kWh	EID	Amount: energy demand for use of aspiration plant Amount source: EST
Active carbon filter	*Active carbon filter*	0.00049 p	EID	Active carbon Amount: unit ("p") allocated based on the time of use of aspiration plant Amount source: EST

16	EXTRACTION OF CHITINIC FRACTION			
Transport	*Transport, freight, lorry 3.5-7.5 metric ton, EURO6 {RER}| transport, freight, lorry 3.5-7.5 metric ton, EURO6 | APOS, U*	0.0169 tkm	EID	Transport of aspiration plant and active carbon from supplier to laboratory Transported weight: weight of aspiration plant and weight of active carbon allocated based on the time of use of aspiration plant Distance: 100 km Amount source: EST
Protection devices	*Protection devices*	0.03778 p	EID	Protection device Amount: unit ("p") allocated based on the time of use Amount source: EST
Emission of sodium hydroxide (amount of sodium hydroxide of solution 1M emitted into atmosphere) during the phase of demineralization and chitin separation	*Sodium hydroxide*	0.0196 g	EID	Amount: emission [g] Amount source: EST
Emissions of sodium hydroxide (amount of sodium hydroxide of solution 1M emitted into the atmosphere through the exchange of air in the laboratory) during the phase of demineralization and chitin separation	*Sodium hydroxide*	0.0197 g	EID	Amount: emission [g] Amount source: EST

16	EXTRACTION OF CHITINIC FRACTION			
Emissions of sodium hydroxide (amount of sodium hydroxide of solution 1M inhaled by the worker) during the phase of demineralization and chitin separation	*Sodium hydroxide_indoor*	8.909E-5 g	EID	Amount: emission [g] Amount source: EST
Emission of sodium hydroxide (amount of sodium hydroxide of solution 1M captured by the mask of the worker and by the filter of the aspiration system) during the phase of demineralization and chitin separation	*Filter dust from Al electrolysis {RoW}| treatment of filter dust from Al electrolysis, residual material landfill | APOS, U*	1.942 g	EID	Amount: emission [g] Amount source: EST
Water of sodium hydroxide of solution 1M that evaporated during the phase of demineralization and chitin separation	*Water*	49.5 g	EID	Amount: weight of evaporated water [g] Amount source: EST
Emission of hydrochloric acid (amount of Hydrochloric acid of solution 2N emitted into atmosphere) during the phase of demineralization and chitin separation	*Hydrochloric acid*	0.0072 g	EID	Amount: emission [g] Amount source: EST
Emissions of hydrochloric acid (amount of hydrochloric acid of solution 2N emitted into the atmosphere through the exchange of air in the laboratory) during the phase of demineralization and chitin separation	*Hydrochloric acid*	0.0073 g	EID	Amount: emission [g] Amount source: EST

16	EXTRACTION OF CHITINIC FRACTION			
Emissions of hydrochloric acid (amount of hydrochloric acid of solution 2N inhaled by the worker) during the phase of demineralization and chitin separation	*Hydrochloric acid_indoor*	3.281E-5 g	EID	Amount: emission [g] Amount source: EST
Disposal of hydrochloric acid (amount of hydrochloric acid of solution 2N captured by the mask of the worker and by the filter of the aspiration system) during the phase of demineralization and chitin separation	*Filter dust from Al electrolysis {RoW}| treatment of filter dust from Al electrolysis, residual material landfill | APOS, U*	0.7153 g	EID	Amount: emission [g] Amount source: EST
Water of hydrochloric acid of solution 2N that evaporated during the phase of demineralization and chitin separation	*Water*	4.421 g	EID	Amount: weight of evaporated water [g] Amount source: EST
Emission of hydrochloric acid (amount of Hydrochloric acid of solution 2N emitted into atmosphere) during drying in oven of chitin fraction	*Hydrochloric acid*	0.0018 g	EID	Amount: emission [g] Amount source: EST
Emissions of hydrochloric acid (amount of hydrochloric acid of solution 2N emitted into the atmosphere through the exchange of air in the laboratory) during drying in oven of chitin fraction	*Hydrochloric acid*	0.0018 g	EID	Amount: emission [g] Amount source: EST

16	EXTRACTION OF CHITINIC FRACTION			
Emissions of hydrochloric acid (amount of hydrochloric acid of solution 6N inhaled by the worker) during drying in oven of chitin fraction	*Hydrochloric acid_indoor*	2.707E-6 g	EID	Amount: emission [g] Amount source: EST
Disposal of hydrochloric acid (amount of hydrochloric acid of solution 2N captured by the mask of the worker and by the filter of the aspiration system) during drying in oven of chitin fraction	*Filter dust from Al electrolysis {RoW}| treatment of filter dust from Al electrolysis, residual material landfill | APOS, U*	0.1769 g	EID	Amount: emission [g] Amount source: EST
Water of hydrochloric acid of solution 2N that evaporated during drying in oven of chitin fraction	*Water*	1.094 g	EID	Amount: weight of evaporated water [g] Amount source: EST
Distilled water that evaporated during drying in oven of chitin fraction	*Water*	0.005 g	EID	Amount: weight of evaporated water [g] Amount source: EST
End of life of solvent (hydrochloric acid) used to extract chitin	*Spent solvent mixture {RoW}| treatment of, hazardous waste incineration | APOS, U*	508.6 g	EID	Amount: weight of residual solvent (hydrochloric acid) [g] Amount source: EST

Table 6-18 Inventory of extraction of chitin fraction

Extraction of lipid, protein, chitinic fraction

17	EXTRACTION OF LIPID, PROTEIN, CHITINIC FRACTION			
Functional Unit of the process: 84.95 g				
PROCESS	BACKGROUND PROCESS	AMOUNT	BACKGROUND PROCESS DATA SOURCES	COMMENT
BSF prepupae	*Production of mature larve (prepupae) – BSF Breeding*	382.7 g	EID	Amount: BSF prepupae Amount source: EST
Preparation of BSF prepupae	*Preparation of BSF prepupae*	375 g	EID	Amount: BSF prepupae Amount source: LAB
Extraction of lipid fraction	*Extraction of lipid fraction*	40.47 g	EID	Amount: lipid fraction (Dry matter) Amount source: LAB
Extraction of protein fraction	*Extraction of protein fraction*	34 g	EID	Amount: protein fraction (Dry matter) Amount source: LAB
Extraction of chitin fraction	*Extraction of chitin fraction*	10.47 g	EID	Amount: chitin fraction (Dry matter) Amount source: LAB
Water	*Tap water {Europe without Switzerland}| tap water production, conventional treatment | APOS, U*	248.5 g	EID	Amount: water that evaporated during extraction process of lipid, protein, chitin fraction Amount source: LAB
End of life of residual BSF biomass	*Spent solvent mixture {RoW}| treatment of, hazardous waste incineration | APOS, U*	41.54 g	EID	Amount: weight of residual BSF biomass Amount source: EST

Table 6-19 Extraction of lipid, protein, chitin fraction

6.3.3 Life Cycle Inventory of laboratory scale production of protein - based bioplastic film

Independently of the extraction procedure followed, the protein fraction recovered was ground and sieved. Typically, 0.5 g of sieved protein fraction was mixed with distilled water (more or less 6.5 g), glycerol (more or less 0.42 g) and NaOH solution 1 M (more or less 30 g). The mixture was then heated at 60 °C for 30 min while stirring at 200 rpm. It was subsequently poured in an aluminum wrapper and incubated under a fume hood for 24 h at room temperature (Figure 6-2).

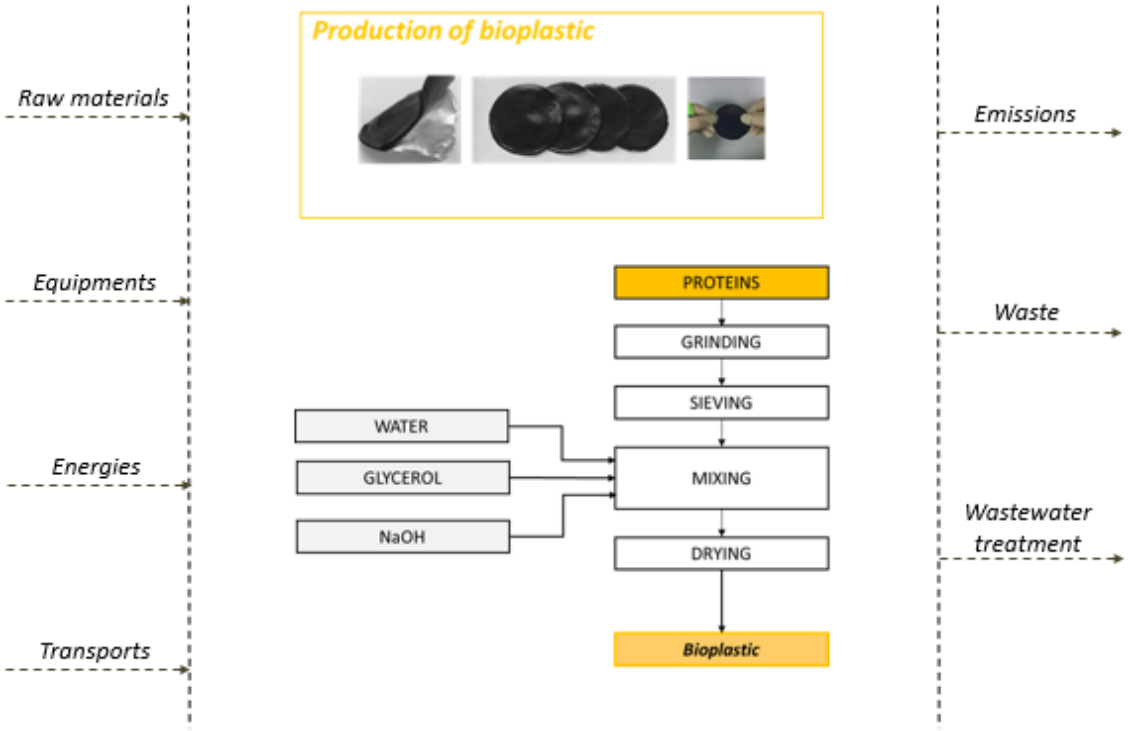

Figure 6-2 Bioplastic film production

The functional unit of the process was weight of protein-based bioplastic plastic sample (0.403 g)
The amount of proteins was increased by 1% to account for the over screening flow during the protein sieving phase.

For laboratory equipment, "ad hoc" processes were created.
"p" was chosen as the functional unit.

Also in this case, atmospheric and indoor emissions fractions was hypothesized. It was assumed that these fractions were both equal to 1% of the total emission. Again, it was assumed that the efficiency of the filter of the aspiration system is equal to 99%, while that of the mask worn by the worker is equal to 95%.
Indoor emissions were not considered for glycerol.

Production process of protein-based bioplastic film

18	LABORATORY SCALE PRODUCTION PROCESS OF FILM			
Functional Unit of the process: 0,403 g				
PROCESS	BACKGROUND PROCESS	AMOUNT	BACKGROUND PROCESS DATA SOURCES	COMMENT
Proteins	*Protein fraction*	0.5005 g	EID	Amount: protein weight The amount of proteins has been increased by 1% to consider the over screening flow during the protein sieving phase. Amount source: EST
Sodium hydroxide	*Sodium hydroxide, without water, in 50% solution state {RoW}| chlor-alkali electrolysis, membrane cell | APOS, U*	0.0015 g	EID	Amount: pure sodium hydroxide weight Amount source: LAB
Water solution sodium hydroxide	*Water, ultrapure {RoW}| production | APOS, U*	30 g	EID	Amount: water weight used to prepare sodium hydroxide solution Amount source: LAB
Water	*Water, ultrapure {RoW}| production | APOS, U*	6.5 g	EID	Amount: water weight Amount source: LAB
Glycerol	*Glycerine {RoW}| esterification of soybean oil | APOS, U*	0.42 g	EID	Amount: glycerol weight Amount source: LAB

18	LABORATORY SCALE PRODUCTION PROCESS OF FILM			
Sodium hydroxide packaging	*Sodium hydroxide packaging*	7.962E-5 p	EID	Amount: weight of plastic bottle allocated to the amount of sodium hydroxide used to produce the bioplastic sample Capacity of bottle: 0,5 Lt Sodium hydroxide 1N density: 1,04 g/mL Amount source: LAB
Glycerol packaging	*Glycerol packaging*	0.00067 p	EID	Amount: weight of plastic bottle allocated to the amount of glycerol used to produce the bioplastic sample Capacity of bottle: 0,5 Lt Density of glycerol: 1,26 kg/dm^3 Amount source: LAB
Transport	*Transport, freight, lorry 3.5-7.5 metric ton, EURO6 {RER}| transport, freight, lorry 3.5-7.5 metric ton, EURO6 | Alloc Def, U*	0.050 kgkm	EID	Transport of material used to produce bioplastic sample from supplier to laboratory Transported weight: weight of materials and their packaging Distance: 100 km Amount source: EST
Balance	*Balance*	1.646E-6 p	EID	Laboratory balance Amount: unit ("p") allocated based on the time of use Amount source: EST

18	LABORATORY SCALE PRODUCTION PROCESS OF FILM			
Transport	*Transport, freight, lorry 3.5-7.5 metric ton, EURO6 {RER}| transport, freight, lorry 3.5-7.5 metric ton, EURO6 | Alloc Def, U*	0.00089 kgkm	EID	Transport of laboratory balance from supplier to laboratory Transported weight: weight of laboratory scale allocated based on time of use Distance: 100 km Amount source: EST
Analytical mill	*Analytical mill*	1.646E-6 p	EID	Analytical mill (IKA, A10 basic) Amount: unit ("p") allocated based on the time of use Amount source: EST
Mill energy demand	*Electricity, low voltage {IT}| electricity voltage transformation from medium to low voltage | APOS, U*	0.0060 kWh	EID	Amount: energy demand for use of mill Amount source: LAB
Transport	*Transport, freight, lorry 3.5-7.5 metric ton, EURO6 {RER}| transport, freight, lorry 3.5-7.5 metric ton, EURO6 | Alloc Def, U*	0,0006 kgkm	EID	Transport of analytical mill from supplier to laboratory Transported weight: weight of analytical mill allocated based on time of use Distance: 100 km Amount source: EST
Sieve	*Sieve*	4.114E-6 p	EID	Amount: unit ("p") allocated based on the time of use Amount source: EST
Transport	*Transport, freight, lorry 3.5-7.5 metric ton, EURO6 {RER}| transport, freight, lorry 3.5-7.5 metric ton, EURO6 | Alloc Def, U*	0,00038 kgkm	EID	Transport of analytical mill from supplier to laboratory Transported weight: weight of analytical mill allocated based on time of use Distance: 100 km Amount source: EST

18	LABORATORY SCALE PRODUCTION PROCESS OF FILM			
Disposable volumetric pipet	*Disposable pipet*	2 p	EID	Amount: unit ("p") Amount source: LAB
Transport	*Transport, freight, lorry 3.5-7.5 metric ton, EURO6 {RER}| transport, freight, lorry 3.5-7.5 metric ton, EURO6 | Alloc Def, U*	0.315 kgkm	EID	Transport of disposable volumetric pipet from supplier to laboratory Transported weight: weight of used disposable volumetric pipettes Distance: 100 km Amount source: EST
pH indicator paper	*pH indicator paper*	2 p	EID	pH indicator paper Amount: unit ("p") Amount source: LAB
Transport	*Transport, freight, lorry 3.5-7.5 metric ton, EURO6 {RER}| transport, freight, lorry 3.5-7.5 metric ton, EURO6 | Alloc Def, U*	0.0026 kgkm	EID	Transport of pH indicator paper from supplier to laboratory Transported weight: weight of used pH indicator paper Distance: 100 km Amount source: EST
Magnetic stirring rod	*Magnetic stirring rod*	2.469E-5 p	EID	Magnetic stirring rod Amount: unit ("p") allocated based on the time of use Amount source: EST
Transport	*Transport, freight, lorry 3.5-7.5 metric ton, EURO6 {RER}| transport, freight, lorry 3.5-7.5 metric ton, EURO6 | Alloc Def, U*	5.901E-6 kgkm	EID	Transport of magnetic stirring rod from supplier to laboratory Transported weight: weight of magnetic stirring rod Distance: 100 km Amount source: EST

18	LABORATORY SCALE PRODUCTION PROCESS OF FILM			
Laboratory spoon	*Laboratory spoon*	4.099E-8 p	EID	Laboratory spoon Amount: unit ("p") allocated based on the time of use Amount source: EST
Transport	*Transport, freight, lorry 3.5-7.5 metric ton, EURO6 {RER}| transport, freight, lorry 3.5-7.5 metric ton, EURO6 | Alloc Def, U*	6.185E-8 kgkm	EID	Transport of laboratory spoon from supplier to laboratory Transported weight: weight of magnetic stirring rod Distance: 100 km Amount source: EST
Disposable volumetric pipet	*Disposable pipet*	1 p	EID	Volumetric pipet Amount: unit ("p") Amount source: LAB
Transport	*Transport, freight, lorry 3.5-7.5 metric ton, EURO6 {RER}| transport, freight, lorry 3.5-7.5 metric ton, EURO6 | Alloc Def, U*	0,1575 kgkm	EID	Transport of disposable volumetric pipet from supplier to laboratory Transported weight: weight of used disposable volumetric pipet Distance: 100 km Amount source: EST
Shrink-wrap film	*Shrink-wrap film*	1 p	EID	Shrink-wrap film Amount: unit ("p") Amount source: LAB
Transport	*Transport, freight, lorry 3.5-7.5 metric ton, EURO6 {RER}| transport, freight, lorry 3.5-7.5 metric ton, EURO6 | Alloc Def, U*	0.0944 kgkm	EID	Transport of shrink-wrap film from supplier to laboratory Transported weight: weight of used shrink-wrap film Distance: 100 km Amount source: EST

18	LABORATORY SCALE PRODUCTION PROCESS OF FILM			
Magnetic stirrer/heater	*Heating Magnetic Stirrer*	2.469E-5 p	EID	Heating magnetic stirrer Amount: unit ("p") allocated based on the time of use Amount source: EST
Transport	*Transport, freight, lorry 3.5-7.5 metric ton, EURO6 {RER}| transport, freight, lorry 3.5-7.5 metric ton, EURO6 | Alloc Def, U*	0,0062 kgkm	EID	Transport of heating magnetic stirrer from supplier to laboratory. Transported weight: weight of used magnetic stirrer/heater. Distance: 100 km Amount source: EST
Heating magnetic stirrer energy demand	*Electricity, low voltage {IT}| electricity voltage transformation from medium to low voltage | APOS, U*	0.315 kWh	EID	Amount: energy demand for use of magnetic stirrer/heater Amount source: LAB
Becher	*Becher*	2.598E-5 p	EID	Becher Amount: unit ("p") allocated based on the time of use Amount source: EST
Transport	*Transport, freight, lorry 3.5-7.5 metric ton, EURO6 {RER}| transport, freight, lorry 3.5-7.5 metric ton, EURO6 | Alloc Def, U*	0.00072 kgkm	EID	Transport of becher from supplier to laboratory Transported weight: weight of becher Distance: 100 km Amount source: EST
Tweezers	*Tweezers*	6.42E-8 p	EID	Tweezers Amount: unit ("p") allocated based on the time of use Amount source: EST

18	LABORATORY SCALE PRODUCTION PROCESS OF FILM			
Transport	*Transport, freight, lorry 3.5-7.5 metric ton, EURO6 {RER}| transport, freight, lorry 3.5-7.5 metric ton, EURO6 | Alloc Def, U*	1.233E-7 kgkm	EID	Transport of tweezers from supplier to laboratory Transported weight: weight of tweezers Distance: 100 km Amount source: EST
Aluminium dish	*Evaporating aluminum dish*	1 p	EID	Evaporating aluminum dish Amount: unit ("p") Amount source: LAB
Transport	*Transport, freight, lorry 3.5-7.5 metric ton, EURO6 {RER}| transport, freight, lorry 3.5-7.5 metric ton, EURO6 | Alloc Def, U*	0.1306 kgkm	EID	Transport of evaporating aluminum dish from supplier to laboratory Transported weight: weight of aluminium dish Distance: 100 km Amount source: EST
Active carbon filter	*Active carbon filter*	0.0012 p	EID	Active carbon Amount: unit ("p") allocated based on the time of use of aspiration plant Amount source: EST
Aspiration plant	*Aspiration plant*	0.0003 p	EID	Aspiration plant Amount: unit ("p") allocated based on the time of use of aspiration plant Amount source: EST
Aspiration plant energy demand	*Electricity, low voltage {IT}| electricity voltage transformation from medium to low voltage | APOS, U*	4.471 kWh	EID	Amount: energy demand for use of aspiration plant Amount source: EST

18	LABORATORY SCALE PRODUCTION PROCESS OF FILM			
Transport	*Transport, freight, lorry 3.5-7.5 metric ton, EURO6 {RER}| transport, freight, lorry 3.5-7.5 metric ton, EURO6 | Alloc Def, U*	0.04308 tkm	EID	Transport of aspiration plant and active carbon from supplier to laboratory Transported weight: weight of aspiration plant weight of active carbon Distance: 100 km Amount source: EST
Protection devices	*Protection devices*	0.0006892 p	EID	Protection device Amount: unit ("p") allocated based on the time of use Amount source: EST
Emissions of sodium hydroxide (amount of sodium hydroxide emitted into atmosphere)	*Sodium hydroxide*	0.0002 g	EID	Amount: emissions [g] Amount source: EST
Emissions of sodium hydroxide (amount of sodium hydroxide emitted into atmosphere through the exchange of air in the laboratory)	*Sodium hydroxide*	0.0002 g	EID	Amount: emissions [g] Amount source: EST
Emissions of sodium hydroxide inhaled by the worker (amount of sodium hydroxide inhaled by the worker)	*Sodium hydroxide_indoor*	1.875E-9 g	EID	Amount: emissions [g] Amount source: EST
Emission of sodium hydroxide captured by the mask of the worker and by the filter of the aspiration system	*Filter dust from Al electrolysis {RoW}| treatment of filter dust from Al electrolysis, residual material landfill | APOS, U*	0.196 g	EID	Amount: emissions [g] Amount source: EST
Emissions of glycerol (amount of glycerol emitted into atmosphere)	*Glycerol*	0.0004 g	EID	Amount: emissions [g] Amount source: EST

18	LABORATORY SCALE PRODUCTION PROCESS OF FILM			
Emission of glycerol captured by the mask of the worker and by the filter of the aspiration system	*Filter dust from Al electrolysis {RoW}| treatment of filter dust from Al electrolysis, residual material landfill | APOS, U*	0.0041g	EID	Amount: emissions [g] Amount source: EST
Emissions of Particulates <2.5 µm (amount of Particulates <2.5 µm emitted into atmosphere)	*Particulates, < 2.5 µm*	0.0005 g	EID	Amount: emissions [g] Amount source: EST
Emissions of Particulates <2.5 µm (amount of Particulates <2.5 µm emitted into atmosphere through the exchange of air in the laboratory)	*Particulates, < 2.5 µm*	0.0005 g	EID	Amount: emissions [g] Amount source: EST
Emissions of Particulates <2.5 µm (amount of Particulates <2.5 µm inhaled by the worker)	*Particulates, < 2.5 µm indoor*	7.966E-10 g	EID	Amount: emissions [g] Amount source: EST
Disposal of Particulates <2.5 µm captured by the mask of the worker and by the filter of the aspiration system	*Filter dust from Al electrolysis {RoW}| treatment of filter dust from Al electrolysis, residual material landfill | APOS, U*	0.0491 g	EID	Amount: emissions [g] Amount source: EST
Distilled water that evaporated during drying in oven of chitin fraction	*Water*	6.5 g	EID	Amount: weight of evaporated water [g] Amount source: EST

Table 6-20 Inventory of protein-based bioplastic film production

6.4 Life Cycle Impact Assessment - LCIA

After modelling the aforementioned sub-processes, by means of Simapro v. 8.5.2.2, the life cycle impact assessment (LCIA) results was carried out using the IMPACT 2002+ evaluation method. This method takes into account continental emissions diffusion (Europe), covering more impact categories than other methods and including more substances. Moreover, IMPACT 2002+ environmental assessment method, on the other hand, makes it possible to quantify environmental impacts according to midpoint-oriented (based on impact categories) and damage-oriented (based on assessment by damage categories) approaches (Bare et al. 2000). The results of the inventory analysis can be expressed in 14 midpoint categories (*human toxicity (Carcinogens, Non-carcinogens), respiratory inorganics*, *ionizing radiation*, *ozone layer depletion*, *respiratory organics*, *acquatic ecotoxicity*, *terrestrial ecotoxicity*, *terrestrial acidification/nutrification*, *land occupation*, *acquatic acidification*, *acquatic eutrophication*, *global warming*, *non-renewable energy*, *mineral extraction*) expressed in a midpoint unit (kg_{eq} C_2H_3Cl, kg_{eq} PM2.5, $BqC\text{-}14_{eq}$, $CFC\text{-}11_{eq}$, kg C_2H_{4eq}, kg TEG water, kg TEG soil, kg SO_{2eq}, m^2org.arable, kg SO_{2eq}, kg PO_4 P-lim, kg CO_{2eq}, MJ primary, MJ surplus). Then, through the damage assessment step, impacts are quantified on the basis of four damage categories: *Human Health*, *Ecosystem quality*, *Climate change*, and *Resources* expressed in an endpoint unit (DALY, PDF*m^2*yr, kg CO_{2eq}, MJ surplus).

The evaluation of environmental impacts by category of damage is expressed in eco-points (Pt) for individual impact categories. The value of 1 Pt is representative for one thousandth of the yearly environmental load of one average European inhabitant. It is calculated by dividing the total environmental load in Europe by the number of inhabitants and multiplying it with 1,000.

In order to describe the system considered in a more representative manner, the following additions and modifications were implemented:

- Land use was estimated by considering basic indicators of both land occupation and transformation. In the present study "*Transformation, to forest intensive, normal*", "*Transformation, to forest intensive*" *and* "*Transformation, to arable*" were introduced.
- Mineral extraction was characterized in consideration of some additional resources such as *silver*, *gravel*, *sand*, *lithium*, *bromine* and *water in ground*, derived from the category Minerals of Eco-indicator 99 with the same characterisation factors (Goedkoop & Spriensma, 2001)
- Radioactive waste category was added; particularly, both this kind of waste and its occupied volume was evaluated, considering the same characterization and normalization factors of EPID 2003 method (Potting and Hauschild, 2003). This category allows to take into account the possible damage of the electric energy mix, which also includes the electricity generated by nuclear plants. This latter kind of energy produces radioactive waste, which has to be safely managed and disposed of.
- *Human health indoor* and *Human health local categories* were introduced in order to evaluate, with an approximated method (Chapter 7), the impacts arising from air emissions, on both workers (indoor scale) and people living in the area surrounding the area where the analyzed process takes place (local scale).

The analysis of results (Table 6-21,Figure 6-3) showed that the total damage associated to the production process of 1 g of bioplastic was equal to 4.157E-3 Pt. Furthermore, the main environmental impact was mainly due to energy consumption (44.20%), in particular, due to the

energy consumption of the aspiration system (93.06%), because of the incubation phases under aspiration hoods. Indeed, bioplastic production required long incubation step under an aspiration hood. Table 6-21 reported the environmental performance at end-point level (damage categories). *Resources*, *Climate change* and *Human health* damage contribute to total damage by 32.32%, 27.73% and 26.22% respectively.

In particular, in **Resources** damage category, the most significant contributions to the total damage were due to:

- *Gas, natural* m^3 (for the 35.46%). It was mainly due to Electricity, medium voltage {IT}| electricity voltage transformation from high to medium voltage | APOS, U (for 44.17%), and in particular, it was due to Natural gas, high pressure {RU}| natural gas production | APOS, U (for 52.05%). This latter process considered the production of the natural gas component of the Italian electricity mix considered for the aspiration system.
- *Water, turbine use, unspecified natural origin, IT* (for 25.99%). It was mainly due to Electricity, medium voltage {IT}| electricity voltage transformation from high to medium voltage | APOS, U (for 76.78%), that in its turn was due to Electricity, high voltage {IT}| electricity production, hydro, run-of-river | APOS, U (for 96.7%). This latter process represented the production of the hydropower component of the Italian electricity mix used for the aspiration system.
- *Coal,* hard (for 14.15%). It was mainly due to Electricity, medium voltage {IT}| electricity voltage transformation from high to medium voltage | APOS, U (for 63.59%), and in particular, it was due to Hard coal {RoW}| hard coal mine operation and hard coal preparation | APOS, U (for 92.26%). This latter process was related to the mine operation and preparation of hard coal component of the Italian electricity mix used for the aspiration system.
- *Uranium* (for 10.64%). It was mainly due to Electricity, medium voltage {IT}| electricity voltage transformation from high to medium voltage | APOS, U (for 69.11%), that in its turn was due to Uranium, in yellowcake {GLO}| uranium production, in yellowcake, in-situ leaching | APOS, U (for 39.88%). This latter process represented the uranium used to produce nuclear component of the Italian electricity mix used for aspiration system.
- *Oil, Crude* (for 9.88%). It was mainly due to Electricity, medium voltage {IT}| electricity voltage transformation from high to medium voltage | APOS, U (for 35.32%), and in particular, it was due to Petroleum {RoW}| petroleum and gas production, on-shore | APOS, U (for 31.02%). This latter process considered the extraction of the petroleum used to produce component by petroleum of the Italian electricity mix.

In **Global warming** damage category the most significant contribution to the total damage was due to:

- *Carbon dioxide fossil* in air (for 91.46%). It was mainly due to Electricity, medium voltage {IT}| electricity voltage transformation from high to medium voltage | APOS, U (for 40.42%), that in its turn was due to Electricity, high voltage {IT}| electricity production, hard coal | APOS, U (for 36.79%). This latter process considers the production of the coal component of the Italian electricity mix used for the aspiration system.

In **Human health** damage category the most significant contribution to the total damage was due to:

- *Particulates* $< 2.5\ \mu m$ in air (for 27.63%). It was mainly due to Electricity, medium voltage {IT}| electricity voltage transformation from high to medium voltage | APOS, U (for 37.75%), and in particular, it was due to Electricity, high voltage {IT}| electricity production, hard coal | APOS, U (for 35.6%).

- *Nitrogen oxides* in air (for 16.74%). It was mainly due to Electricity, medium voltage {IT}| electricity voltage transformation from high to medium voltage | APOS, U (for 53.86%), and in particular, it was due to Electricity, high voltage {IT}| electricity production, hard coal | APOS, U (for 41.38%).
- *Sulfur dioxide* in air (for 16.06%). It was mainly due to Electricity, medium voltage {IT}| electricity voltage transformation from high to medium voltage | APOS, U (for 62.07%), that in its turn was due to Electricity, medium voltage {IT}| electricity voltage transformation from high to medium voltage | APOS, U (for 45.84%).
- *Hydrocarbons, aromatic* in air (for 13.03%). It was mainly due to protein fraction (for 72.25%), and in particular, it was due to the extraction of the lipidic fraction that was necessary in order to extract the protein fraction (for 88.67%).

Occupation, forest, intensive affected **Ecosystem quality** category (79.46% on the total damage) and was generated by wood used for the activated carbon filter production (i.e. the filter installed in the aspiration system).

The analysis of results showed that two other important sources of potential environmental impact were work equipment and the materials (proteins). These results have therefore led us to carry out a deep analysis of the environmental impact related to the production of proteins (BSF Breeding and Extraction process of lipid, protein and chitin fraction). The main results are reported hereafter.

LCIA results at end-point level of process "Production of bioplastic" (F.U.1 g)

DAMAGE CATEGORY	UNIT	ENERGY	WORK EQUIPMENT	MATERIALS	TRANSPORTS	WASTE TO TREATMENT
Human health	Pt	4.569E-04	3.622E-04	2.688E-04	1.972E-06	7.822E-08
Ecosystem quality	Pt	7.569E-05	4.495E-04	4.456E-05	8.959E-07	6.669E-09
Climate change	Pt	4.797E-04	4.615E-04	2.093E-04	1.737E-06	2.312E-07
Renewable energy	Pt	-	-	-	-	-
Resources	Pt	8.251E-04	2.688E-04	2.476E-04	1.892E-06	2.527E-08
Human health, local	Pt	-	5.592E-10	1.677E-11	-	-
Human health, indoor	Pt	-	5.839E-13	4.840E-07	-	-
Total	Pt	1.837E-03	1.542E-03	7.707E-04	6.497E-06	3.414E-07

Table 6-21 LCIA results at at end point level (damage category) of process "Production of bioplastic" (F.U. 1 g)

DAMAGE CATEGORY	UNIT	PROTEINS	GLYCEROL	SODIUM HYDROXYDE	DISTILLED WATER
Human health	Pt	2.680E-04	7.060E-07	1.125E-09	2.037E-08
Ecosystem quality	Pt	4.394E-05	6.191E-07	6.306E-11	9.188E-10
Climate change	Pt	2.088E-04	5.407E-07	4.726E-10	9.335E-09
Renewable energy	Pt	-	-	-	-
Resources	Pt	2.475E-04	9.152E-08	4.746E-10	9.164E-09
Human health, local	Pt	1.677E-11	-	-	-
Human health, indoor	Pt	4.840E-07	-	-	-
Total	Pt	7.687E-04	1.957E-06	2.135E-09	3.979E-08

Table 6-22 LCIA results at end-point level (damage category) related to "Materials"

DAMAGE CATEGORY	UNIT	MILL	MAGNETIC STIRRER/HEATER	ASPIRATION SYSTEM
Human health	Pt	5.938E-07	3.118E-05	4.251E-04
Ecosystem quality	Pt	1.052E-07	5.526E-06	7.006E-05
Climate change	Pt	6.219E-07	3.265E-05	4.464E-04
Renewable energy	Pt	-	-	-
Resources	Pt	1.060E-06	5.566E-05	7.684E-04
Human health, local	Pt	-	-	-
Human health, indoor	Pt	-	-	-
Total	Pt	2.381E-06	1.250E-04	1.710E-03

Table 6-23 LCIA results at end-point level (damage category) related to "Energy"

LCIA results at end-point level of process "Extraction of lipid, protein, chitin fraction" (U.F. 1 g)

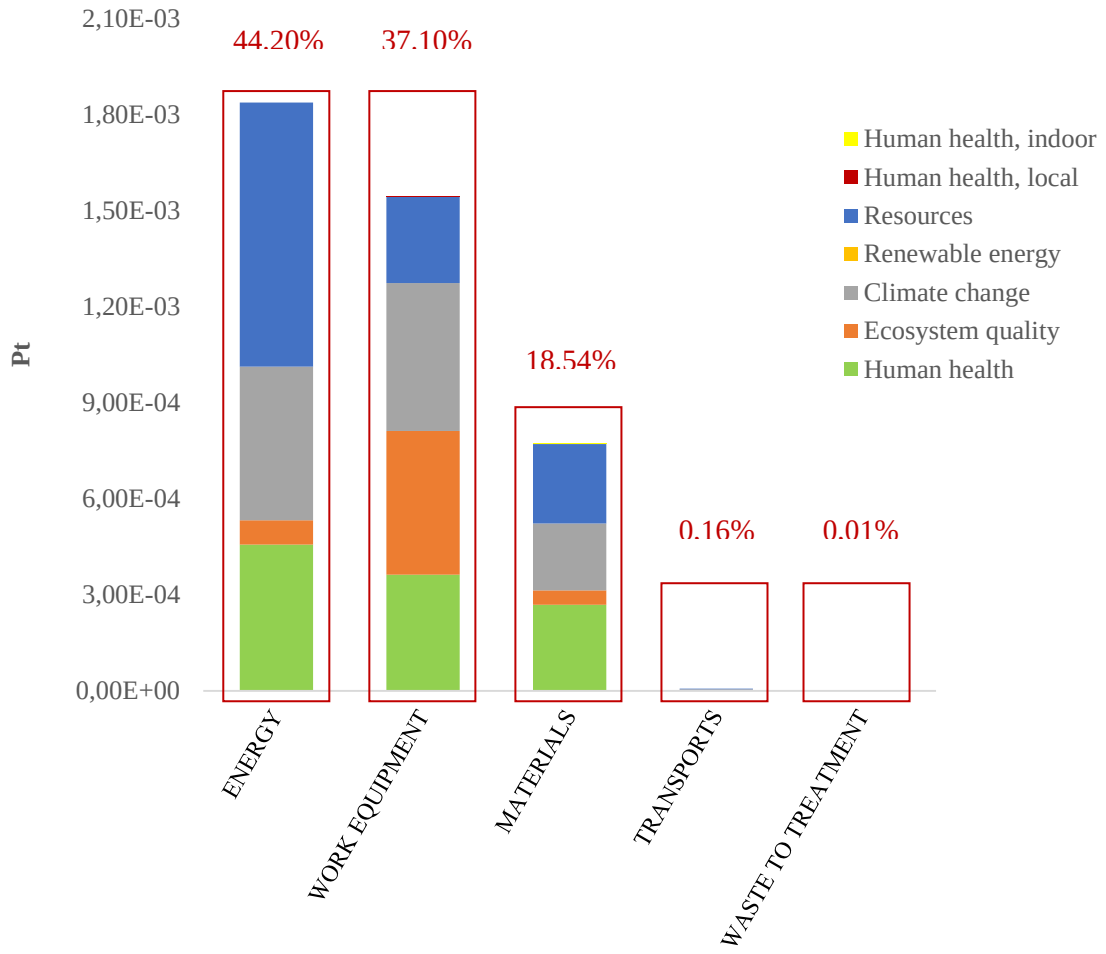

Figure 6-3 LCIA results at end point level (damage category) of process "Production of bioplastic" (F.U. 1 g)

Characterized LCIA results of process "Extraction of lipid, protein, chitin fraction" (F.U. 1 g)

IMPACT CATEGORY	UNIT	TOTAL	BSF BREEDING	PREPARATION OF PREPUPAE	EXTRACTION OF LIPID FRACTION	EXTRACTION OF PROTEIN FRACTION	EXTRACTION OF CHITIN FRACTION	DISPOSAL OF RESIDUAL PREPUPAE BIOMASS
Carcinogens	kg C_2H_3Cl eq	7.055E-02	8.841E-03	1.169E-04	5.545E-02	2.510E-03	3.620E-03	8.836E-06
Non-carcinogens	kg C_2H_3Cl eq	7.560E-03	4.077E-03	4.632E-05	8.562E-04	1.064E-03	1.500E-03	1.694E-05
Respiratory inorganics	kg PM2.5 eq	6.195E-04	4.381E-04	5.857E-06	4.381E-05	5.159E-05	8.000E-05	2.116E-07
Ionizing radiation	Bq C-14 eq	1.003E+01	7.136E+00	1.008E-01	6.424E-01	7.968E-01	1.354E+00	5.764E-04
Ozone layer depletion	kg CFC-11 eq	7.243E-08	4.993E-08	6.676E-10	5.651E-09	6.269E-09	9.891E-09	2.052E-11
Respiratory organics	kg C_2H_4 eq	1.861E-04	7.964E-05	1.291E-06	4.205E-05	2.699E-05	3.608E-05	3.068E-08
Aquatic ecotoxicity	kg TEG water	5.835E+01	4.020E+01	3.648E-01	3.635E+00	5.629E+00	8.493E+00	2.213E-02
Terrestrial ecotoxicity	kg TEG soil	1.225E+01	9.238E+00	8.985E-02	7.090E-01	8.487E-01	1.361E+00	2.870E-03
Terrestrial acid/nutri	kg SO_2 eq	1.198E-02	8.913E-03	9.475E-05	7.415E-04	8.469E-04	1.381E-03	2.886E-06
Land occupation	m^2org.arable	1.147E-01	6.798E-02	7.801E-04	1.410E-02	1.443E-02	1.737E-02	6.497E-06
Aquatic acidification	kg SO_2 eq	3.103E-03	2.235E-03	2.726E-05	2.090E-04	2.394E-04	3.919E-04	7.734E-07
Aquatic eutrophication	kg PO_4 P-lim	9.560E-05	6.146E-05	7.307E-07	8.363E-06	1.097E-05	1.403E-05	4.639E-08
Global warming	kg CO_2 eq	7.029E-01	4.021E-01	6.079E-03	7.488E-02	8.830E-02	1.305E-01	9.898E-04
Non-renewable energy	MJ primary	1.026E+01	6.554E+00	9.130E-02	9.643E-01	1.025E+00	1.623E+00	1.400E-03
Mineral extraction	MJ surplus	4.618E+00	3.503E+00	4.732E-02	2.741E-01	2.833E-01	5.103E-01	1.008E-04
Renewable energy	MJ	2.879E+00	1.889E+00	2.724E-02	2.700E-01	2.844E-01	4.086E-01	9.054E-05
Non-carcinogens, indoor	kg C_2H_3Cl eq	5.197E-11	-	1.072E-13	4.626E-11	2.772E-12	2.828E-12	-
Respiratory organics, indoor	kg C_2H_4 eq	8.033E-08	-	3.587E-18	8.033E-08	9.273E-17	9.459E-17	-
Respiratory inorganics, indoor	kg PM2.5 eq	7.596E-11	-	7.596E-11	3.492E-17	3.066E-17	3.127E-17	-
Carcinogens, indoor	kg C_2H_3Cl eq	2.882E-04	-	2.653E-10	2.882E-04	2.035E-16	2.076E-16	-
Non-carcinogens, local	kg C_2H_3Cl eq	-	-	-	-	-	-	-
Carcinogens, local	kg C_2H_3Cl eq	1.974E-11	-	2.388E-13	7.032E-12	6.174E-12	6.298E-12	-
Respiratory organics, local	kg C_2H_4 eq	-	-	-	-	-	-	-
Respiratory inorganics, local	kg PM2.5 eq	3.397E-11	-	4.110E-13	1.210E-11	1.062E-11	1.084E-11	-

Table 6-24 Characterized LCIA results of process "Extraction of lipid, protein, chitin fraction" (F.U. 1 g)

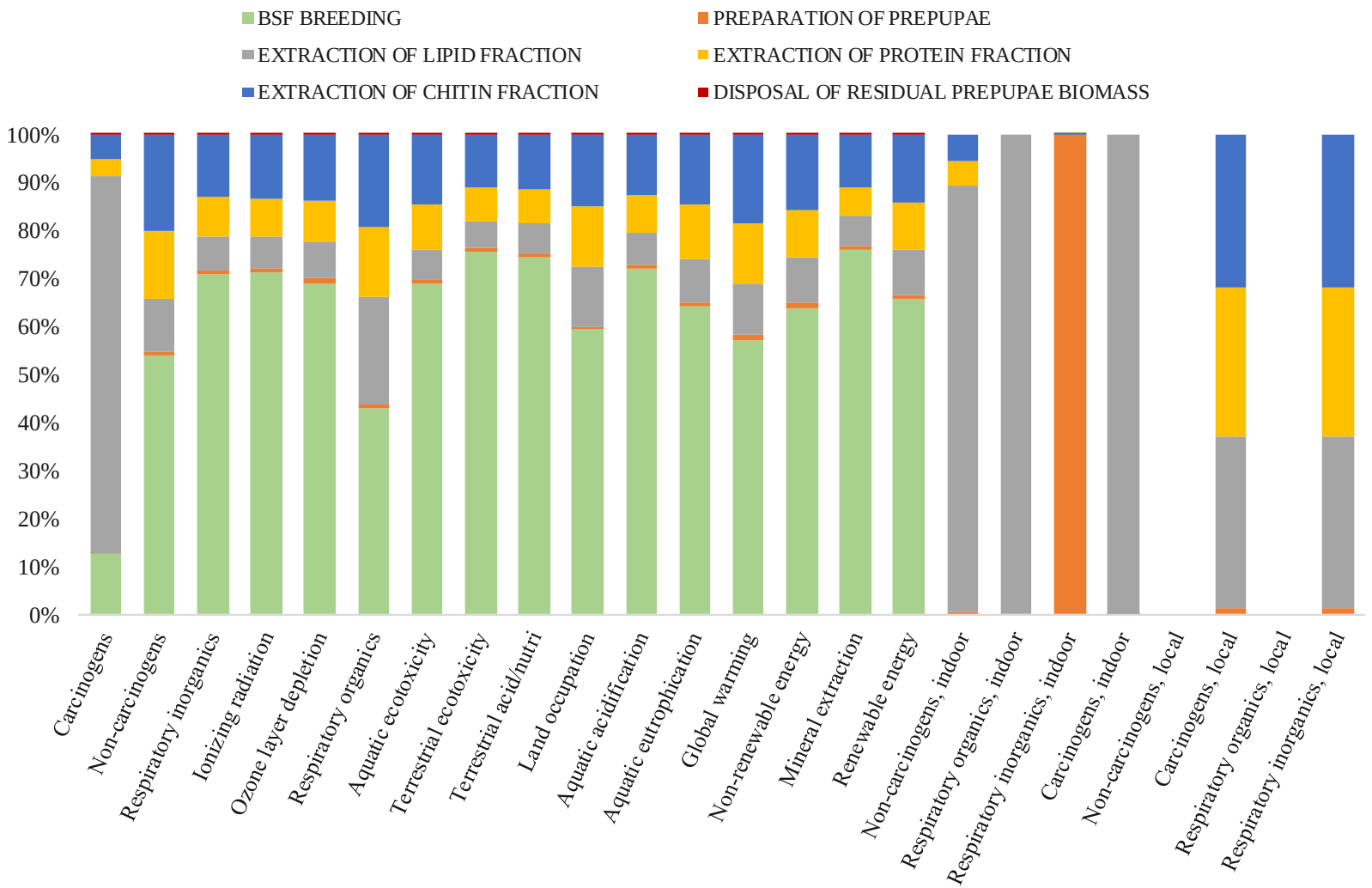

Figure 6-4 Characterized LCIA results of process "Extraction of lipid, protein, chitin fraction" (F.U 1 g)

The characterised LCIA results for the process "Extraction of lipid, protein, chitin fraction" (Table 6-24, Figure 6-4) indicated that:

- in **Carcinogens** impact category the damage was equal to 0.0706 kg C_2H_3Cl eq and it is due to:
  - *Hydrocarbons, aromatic* in air (for 87.49%). It was mainly due to Extraction of lipid fraction without grinding (for 88.71%), in particular, it was due to Extraction of lipid fraction without grinding as a direct emission (for 98.96%).
  - *Aluminium* in air (for 6.356%). It was mainly due to BSF Breeding process (for 69.25%), in particular, it was due to Blasting {RoW}| processing | APOS, U (for 54.39%). This latter process represented the extraction of the coal used to produce the electric component due to coal of the Italian electricity mix necessary into the bioconversion unit.
- in **Non Carcinogens** impact category the damage was equal to 0.0076 kg C_2H_3Cl eq and it is due to:
  - *Dioxin, 2, 3, 7, 8 Tetrachlorodibenzo-p-* in air (for 37.05%). It was mainly due to Separation of chitin fraction (for 29.74%), that in its turn was due to Process-specific burdens, hazardous waste incineration plant {RoW}| processing | APOS, U (for 63.12%). This latter process represented disposal of flask washing liquids used during chitin extraction.
  - *Arsenic* in water (for 24.02%). It was mainly due to BSF Breeding process (for 63.16%), and in particular it was due to Hard coal ash {RoW}| treatment of, residual material landfill | APOS, U (for 37.34%). This latter process represented disposal of residual ash during the electricity mix production process.
  - *Arsenic* in air (for 13.04%). It was mainly due to BSF Breeding process (for 73.48%), that in its turn was due to Ferronickel, 25% Ni {GLO}| production | APOS, U (for 25.7%). This latter process is related to the production of Steel, chromium used to manufacture the Bioconversion box.
  - *Zinc* in soil (for 6.24%). It was mainly due to BSF Breeding process (for 64.99%), and in particular, it was due to Wood ash mixture, pure {Europe without Switzerland}| treatment of wood ash mixture, pure, landfarming | APOS, U (for 72.37%). This latter process represented disposal of wood ash mixture during the electricity mix production process.
- in **Respiratory inorganics** impact category the damage was equal to 0.0006 kg PM2.5 eq and it was due to:
  - *Particulates, <2.5µm* in air (for 34.15%). It was mainly due to BSF Breeding process (for 71.27%), and in particular, it was due to Electricity, high voltage {IT}| electricity production, hard coal| APOS, U (for 20.22%). This process is related to the coal component of the electricity used in the bioconversion unit.
  - *Sulfur dioxide* in air (for 22.11%). It was mainly due to BSF Breeding process (for 69.84%), and in particular, it was due to Electricity, high voltage {IT}| electricity production, hard coal| APOS, U (for 39.76%). This latter process is related to the coal component of the electricity used into the bioconversion unit.
  - *Nitrogen oxides* in air (for 21.85%). It was mainly due to BSF Breeding process (for 67.52%), and in particular, it was due to Electricity, high voltage {IT}| electricity production, hard coal| APOS, U (for 33.96%).
  - *Particulates, > 10 µm* in air (for 8.093%). It was mainly due to BSF Breeding process (for 70.88%), that in its turn was due to Hard coal {RoW}| market for | APOS, U (for 50.13 %).

This latter process was related to the coal component of the electricity used in the bioconversion unit.

- in **Ionizing radiation** impact category the damage was equal to 10.03 Bq C-14 eq and it was due to:
  - *Radon 222* in air (for 66.55%). It was mainly due to BSF Breeding process (for 71.13%), that in its turn was due to Tailing, from uranium milling {GLO}| treatment of | APOS, U (for 96.72%). This latter process was related to the treatment of waste due to the extraction of uranium used to produce the electricity used into the bioconversion unit.
  - *Carbon-14* in air (for 31.28%). It was mainly due to BSF Breeding process (for 71.17%), and in particular, it was due to Spent nuclear fuel {RoW}| treatment of, reprocessing | APOS, U (for 37.11%). This latter process represented the treatment of spent nuclear fuel due to nuclear component of electricity used in the bioconversion unit.
- in **Ozone layer depletion** impact category the damage was equal to 7.243E-8 kg CFC-11 eq and it is due to:
  - *Methane, bromochlorodifluoro-, Halon 1211* in air (for 48.82%). It was mainly due to BSF Breeding process (for 72.21%), and in particular, it was due to Transport, pipeline, long distance, natural gas {RU}| processing | APOS, U (for 55.36%). This process represented the transport of natural gas used to produce electricity needed in the bioconversion unit.
  - *Methane, bromotrifluoro-, Halon 1301* in air (for 25.31%). It was mainly due to BSF Breeding process (for 71.03%), that in its turn was due to Petroleum {RoW}| petroleum and gas production, on-shore | APOS, U (for 71.3%). This latter process considered the extraction of the petroleum used to produce component by petroleum of the Italian electricity mix.
  - *Ethane, 1,2-dichloro-1,1,2,2-tetrafluoro-, CFC-114* in air (for 17.1%). It was mainly due to BSF Breeding process (for 71.13%), and in particular, it was due to Uranium, enriched 3.8%, per separative work unit {US}| uranium production, diffusion, enriched 3.8% | APOS, U (for 70.6%). This latter process was related to enriched uranium used to produce the Italian electricity mix.
- in **Respiratory organics** impact category the damage was equal to 0.00019 kg C_2H_4 eq and it is due to:
  - *NMVOC, non-methane volatile organic compounds, unspecified origin* in air (for 57.37%). It was mainly due to BSF Breeding process (for 52.16%), and in particular, it was due to Sweetening, natural gas {RoW}| processing | APOS, U (for 31.48%). This latter process was related to the treatment (sweetening) of the natural gas used to produce the Italian electricity mix.
  - *Ethene* in air (for 10.6%). It was mainly due to Extraction of lipid fraction without grinding (for 33.02%), that in its turn was due to Charcoal {GLO}| production | APOS, U (for 96.52%). This latter process was related to the production of activated carbon of the aspiration plant filter.
  - *Hydrocarbons aromatic* in air (for 9.244%). It was mainly due to Extraction of lipid fraction without grinding (for 88.71%), and in particular, it was due to Extraction of lipid fraction without grinding as a direct emission (for 98.96%).
- in **Aquatic ecotoxicity** impact category the damage was equal to 58.35 kg TEG water and it is due to:

- *Aluminium* in water (for 32.49%). It was mainly due to BSF Breeding process (for 88.85%), and in particular, it was due to Zeolite, powder {RER}| production | APOS, U (for 85.96%). This process was related to the production of zeolite used in the growth substrate.
- *Aluminium* in soil (for 23.09%). It was mainly due to BSF Breeding process (for 70.25%), and in particular, it was due to Drilling waste {CH}| treatment of, landfarming | APOS, U (for 62.99%). This latter process represented the disposal of waste of drilling process to extract geothermal energy, component of the Italian electricity mix.
- *Aluminium* in air (for 15.23%). It was mainly due to BSF Breeding process (for 69.25%), and in particular, it was due to Blasting {RoW}| processing | APOS, U (for 54.39%). This latter process represented the extraction of the coal used to produce the electric component due to coal of the Italian electricity mix necessary in the bioconversion unit plant.

- in **Terrestrial ecotoxicity** impact category the damage was equal to 12.25 kg TEG soil and it was due to:
  - *Aluminium* in soil (for 23.86%).
  - *Aluminium* in air (for 18.6%).
  - *Zinc* in soil (for 18.24%). It was mainly due to BSF Breeding process (for 78.78%) that in its turn was due for 55.44% to Tyre wear emissions, lorry {RoW}| treatment of | APOS, U. This latter process represented emissions during transport of the bioconversion unit plant.
  - *Copper* in soil (for 10.14%). It was mainly due to BSF Breeding process (for 68.42%), that in its turn was due to Transmission network, electricity, medium voltage {RoW}| construction | APOS, U (for 34.26%). This latter process is related to the plant of transmission of electricity necessary in the bioconversion unit.
  - *Chromium* in air (for 9.03%). It was mainly due to BSF Breeding process (for 93.98%), and in particular, it was due to Ferrochromium, high-carbon, 68% Cr {GLO}| production | APOS, U (for 98.79%). This latter process is related to the production of chromium steel 18/8 used to manufacture the bioconversion unit plant.
- in **Terrestrial acid/nutri** impact category the damage was equal to 0.0121 kg SO_2 eq and it was due to:
  - *Nitrogen oxides* in air (for 48.72%).
  - *Ammonia* in air (for 36.62%). It was mainly due to BSF Breeding process (for 85.37%), and in particular, it was due to Poultry manure (for 41.52%). This process was related to the production of poultry manure used in the growth substrate.
  - *Sulfur dioxide* in air (for 14.66%).
- in **Land occupation** impact category the damage was equal to 0.1147 m^2org.arable and it was due to:
  - *Occupation, forest*, intensive (for 54.78%). It was mainly due to BSF Breeding process (for 33.06%), and in particular, it was due to Wood chips, wet, measured as dry mass {SE}| hardwood forestry, birch, sustainable forest management | APOS, U (for 25.25%). This process is related to the wood component production of electricity mix necessary in the bioconversion unit.
  - *Trasformation to annual* crop (for 11.5%). It was mainly due to BSF Breeding process (for 98.78%), and in particular, it was due to Maize grain {RoW}| production | APOS, U (for 47.32%). This process was related to maize grain used as feed for the chicken that produced the poultry manure that is used in the growth substrate.

  - *Occupation, annual crop* (for 9.095%). It was mainly due to BSF Breeding process, and in particular, for 35.05% in Maize grain {RoW}| production | APOS, U (for 98.38%).
- in **Acquatic acidification** impact category the damage was equal to 0.0031 kg SO_2 eq and it was due to:
  - *Sulfur dioxide* in air (for 56.59%).
  - *Nitrogen oxides* in air (for 23.99%).
  - *Ammonia* in air (for 17.77%).
- in **Acquatic eutrophication** impact category the damage was equal to 9.56E-5 kg PO_4 P-lim and it is due to:
  - *Phosphate* in water (for 79.57%). It was mainly due to BSF Breeding process (for 63.07%), and in particular, it was due to Spoil from hard coal mining {GLO}| treatment of, in surface landfill | APOS, U (for 46.61%). This latter process represented the treatment of residual material generated by the extraction of the coal used to produce coal component of the Italian electricity mix used in the bioconversion unit.
  - *COD, Chemical Oxygen Demand* in water (for 9.672%). It was mainly due to BSF Breeding process (for 66.78%), and in particular it was due to Petroleum {RoW}| petroleum and gas production, on-shore | APOS, U (for 59.6%). This process considered the extraction of the petroleum used to produce component by petroleum of the Italian electricity mix.
- in **Global Warming** impact category the damage was equal to 0.7029 kg CO_2 eq and it is due to:
  - *Carbon dioxide fossil* in air (for 93.96%). It was mainly due to BSF Breeding process (for 56.68%), and in particular it was due to Electricity, high voltage {IT}| electricity production, hard coal | APOS, U (for 31.24%). This process considered the production of the coal component of the Italian electricity mix used into the bioconversion unit.
- in **Non - renewable energy** impact category the damage was equal to 10.26 MJ primary and it is due to:
  - *Gas, natural* m^3 (for 37.67%). It was mainly due to BSF Breeding process (for 65.92%) and in particular, it was due to Natural gas, high pressure {RU}| natural gas production | APOS, U (for 50.12%). This process represented the extraction of natural gas component of the Italian electricity mix used in the bioconversion unit.
  - *Coal, hard* (for 22.04%). It was mainly due to BSF Breeding process (for 70.63%), and in particular, it was due to Hard coal {RoW}| hard coal mine operation and hard coal preparation | APOS, U (for 84.56%). This latter process was related to the production of the coal component of the Italian electricity mix used in the bioconversion unit.
  - *Oil, crude* (for 20.55%). It was mainly due to BSF Breeding process (for 48.21%), and in particular, it was due to Petroleum {RoW}| petroleum and gas production, on-shore | APOS, U (for 29.84%). This process considered the extraction of the petroleum used to produce the component by petroleum of the Italian electricity mix.
  - *Uranium* (for 16.74%). It was mainly due to BSF Breeding process (for 69.27%), and in particular, it was due to Uranium, in yellowcake {GLO}| uranium production, in yellowcake, in-situ leaching | APOS, U (for 39.56%). This process represented the uranium used to produce the nuclear component of the Italian electricity mix used in the bioconversion unit.
- in **Mineral extraction** impact category the damage was equal to 4.618 MJ surplus and it was due to:

  - *Water, turbine use, unspecified natural origin, IT* (for 89.14%). It was mainly due to BSF Breeding process (for 74.57%), and in particular, it was due to Electricity, high voltage {IT}| electricity production, hydro, run-of-river | APOS, U (for 96.7%). This process represented the production of the hydropower component of the Italian electricity mix used into the bioconversion unit.
  - *Water, turbine use, unspecified natural origin, RoW* (for 9.542%). It was mainly due to BSF Breeding process (for 87.55%), and in particular, it was due to Electricity, high voltage {RoW}| electricity production, hydro, run-of-river | APOS, U (for 99.77%).
- in **Renewable energy** impact category the damage was equal to 2.879 MJ and it was due to:
  - *Energy, potential (in hydropower reservoir), converted* (for 44.39%). It was mainly due to BSF Breeding process (for 73.89%), that in its turn was due to Electricity, high voltage {IT}| electricity production, hydro, reservoir, alpine region | APOS, U (for 46.94%). This process represented the production of the hydropower component of the Italian electricity mix used in the bioconversion unit.
  - *Energy, gross calorific value, in biomass* (for 38.51%). It was mainly due to BSF Breeding process (for 52.14%), that in its turn was due to Maize grain {RoW}| production | APOS, U (for 15.68%). This process was related to the maize grain used as feed for the chicken that produces poultry manure that is used in the growth substrate.
  - *Energy, kinetic (in wind), converted* (for 9.934%). It was mainly due to BSF Breeding process (for 73.24%), that in its turn was due to Electricity, high voltage {IT}| electricity production, wind, 1-3MW turbine, onshore | APOS, U (for 56.19%). This process was related to the production of wind component of the Italian electricity mix used in the bioconversion unit.
- in **Non Carcinogens indoor** impact category the damage was equal to 5.197E-11 kg C_2H_3Cl eq and it is due to:
  - *Hydrocarbons, aromatic, indoor* in air (for 82.94%). It was mainly due to Extraction of lipid fraction without grinding (for 100%), and in particular, it was due to Extraction of lipid fraction without grinding as a direct emission (for 100%).
  - *Ammonia indoor* in air (for 17.05%). It was mainly due to Extraction of lipid fraction without grinding (for 35.62%), that in its turn was due to Sludge line (for 55.59%). This process was related to the treatment of sludge during the regeneration process of the activated carbon of the aspiration plant filter.
- in **Respiratory organic indoor** impact category the damage was equal to 8.033E-8 kg C_2H_4 eq and it was due to:
  - *Hydrocarbons, aromatic, indoor* in air (for 100%). It was mainly due to Extraction of lipid fraction without grinding (for 100%), that in its turn was due to Extraction of lipid fraction without grinding as a direct emission (for 100%).
- in **Respiratory inorganic indoor** impact category the damage was equal to 7.596E-11 kg PM2.5 eq and it was due to:
  - *Particulates, <2.5µm, indoor* in air (for 100%). It was mainly due to Preparation for extraction of lipid, protein and chitin fraction (for 100%), and in particular, it was due to Preparation for extraction of lipid, protein and chitin fraction (for 100%) as direct emission.
- in **Carcinogens indoor** impact category the damage was equal to 0.00029 kg C_2H_3Cl eq and it was due to:

  - *Hydrocarbons, aromatic, indoor* in air (for 100%). It was mainly due to Extraction of lipid fraction without grinding (for 100%), that in its turn was due to Extraction of lipid fraction without grinding as a direct emission (for 100%).
- in **Carcinogens local** impact category the damage was equal to 1.974E-11 kg C_2H_3Cl eq and it was due to:
  - *Particulates, <2.5µm* local in air (for 100%). It was mainly due to Extraction of lipid fraction without grinding (for 35.62%), that in its turn was due to Sieving line (for 100%). This process was related to the treatment of residual material during the regeneration process of the activated carbon of the aspiration plant filter.
- in **Respiratory inorganic local** impact category the damage was equal to 3.397E-11 kg PM2.5 eq and it was due to:
  - *Particulates, >10 µm, local* in air (for 59.47%). It was mainly due to Extraction of lipid fraction without grinding (for 35.62%), and in particular, it was due to Sieving line (for 100%). This process is related to the treatment of residual material during the regeneration process of the activated carbon of the aspiration plant filter.
  - *Particulates, >2.5 µm, and < 10 µm local* in air (for 23.89%). It was mainly due to Extraction of lipid fraction without grinding (for 35.62%), and in particular, it was due to Sieving line (for100%). This process is related to the treatment of residual material during the regeneration process of the activated carbon of the aspiration plant filter.
  - *Particulates, <2.5 µm, local* in air (for 16.64%). It was mainly due to Extraction of lipid fraction without grinding (for 35.62%), and in particular, it was due to Sieving line (for 100%). This process was related to the treatment of residual material during the regeneration process of the activated carbon of the aspiration plant filter.

Damage assessment results (damage category) of process "Extraction of lipid, protein, chitin fraction" (F.U. 1 g)

DAMAGE CATEGORY	UNIT	TOTAL	BSF BREEDING	PREPARATION OF PREPUPAE	EXTRACTION OF LIPID FRACTION	EXTRACTION OF PROTEIN FRACTION	EXTRACTION OF CHITIN FRACTION	DISPOSAL OF RESIDUAL PREPUPAE BIOMASS
Human health	DALY	6.550E-07	3.445E-07	4.582E-09	1.886E-07	4.635E-08	7.071E-08	2.205E-10
Ecosystem quality	PDF*m^2*yr	2.373E-01	1.585E-01	1.678E-03	2.193E-02	2.361E-02	3.157E-02	3.390E-05
Climate change	kg CO_2 eq	7.029E-01	4.021E-01	6.079E-03	7.488E-02	8.830E-02	1.305E-01	9.898E-04
Renewable energy	MJ	2.879E+00	1.889E+00	2.724E-02	2.700E-01	2.844E-01	4.086E-01	9.054E-05
Resources	MJ primary	1.488E+01	1.006E+01	1.386E-01	1.238E+00	1.308E+00	2.133E+00	1.501E-03
Human health, local	DALY	2.384E-14	-	2.883E-16	8.490E-15	7.454E-15	7.604E-15	-
Human health, indoor	DALY	8.072E-10	-	5.391E-14	8.072E-10	7.784E-18	7.940E-18	-

Table 6-25 Damage assessment results (damage category) of process "Extraction of lipid, protein, chitin fraction" (F.U. 1 g)

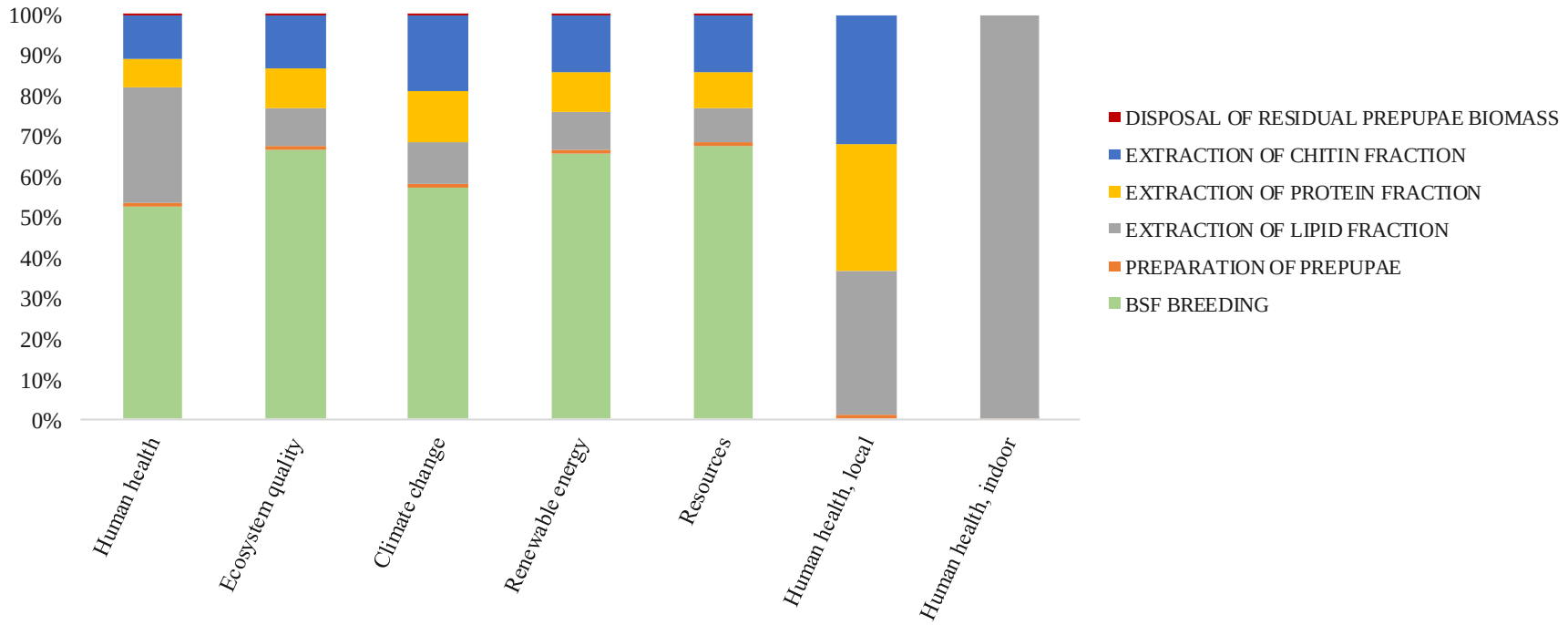

Figure 6-5 Damage assessment results (damage category) of process "Extraction of lipid, protein, chitin fraction" (F.U. 1 g)

The Damage Assessment analysis (Table 6-25, Figure 6-5) highlighted that:

- in **Human Health** the damage was worth 6.55E-7 DALY and it was due to:
  - *Hydrocarbons, aromatic* in air (for 26.39%);
  - *Particulates, <2.5µm* in air (for 22.93%);
  - *Sulfur dioxide* (for 14.64%);
  - *Nitrogen oxides* (for 14.47%).

The process with the highest environmental burden was BSF Breeding (52.6%), followed by Extraction of lipid fraction without grinding process (28.79%) and Extraction of chitinic fraction process (10.8%). Respiratory inorganics was the impact category of **Human Health** damage category that produced the highest impact (4.337E-7 DALY, i.e. 66.21%).

- In **Ecosystem Quality** the damage was worth 0.2373 PDF*m^2*yr and it was due to:
  - *Occupation, forest, intensive* (for 28.86%);
  - *Aluminium in soil* (for 10.03%);

The process with the highest environmental burden was BSF Breeding process (66.78%), followed by Extraction of chitinic fraction process (13.31%), Extraction of protein fraction without chitin demineralization process (9.949%) and Extraction of lipid fraction without grinding process (9.241%). Land occupation was the impact category of **Ecosystem Quality** damage category that produced the highest impact (0.13 PDF*m^2*yr , i.e. 54.78%).

- In **Climate change** the damage was worth 0.7029 kg CO_2 eq. and it was due to *Carbon dioxide, fossil* in air (for 93.96%). The process with the highest environmental burden was BSF Breeding process (57.21%).

- In **Resources** the damage was worth 14.88 MJ primary and it was due to:
  - *Water, turbine use, unspecified natural origin, IT* (for 27.67%);
  - *Gas, natural/m^3* (for 25.98%);
  - *Coal, hard* (for 15.2%);
  - *Oil, crude* (14.17%);
  - *Uranium* (for 11.54%).

The process with the highest environmental burden was BSF Breeding process (67.6%). Non renewable-energy was the impact category of **Resources** damage category that produced the highest impact (10.26 MJ primary, i.e. 68.95%).

- In **Human Health, indoor** the damage was worth 8.072E-10 and it was due to:
  - *Hydrocarbons, aromatic indoor* in air (for 99.99%).

The process with the highest environmental burden was Extraction of lipidic fraction without grinding process (99.99%). The impact category with the highest contribution was Carcinogens, indoor (8.07E-10 DALY, i.e. 99.98%).

- In **Human Health, local** the damage was worth 2.384E-14 DALY and it was due to:
  - *Particulates, >10 µm, local* in air (for 59.33%);
  - *Particulates, >2.5 µm,* and *< 10 µm local* in air (for 23.84%);
  - *Particulates, >2.5 µm, local* in air (for 16.83%).

The process with the highest environmental burden was Extraction of lipidic fraction without grinding process (35.62%) followed by Extraction of chitinic fraction (31.9%) and Extraction of protein fraction without demineralization process (31.27%). The impact category with the highest contribution was Respiratory inorganics local (2.378E-14 DALY, i.e. 99.75%).

- In **Renewable energy** the damage was worth 2.879 MJ and it was due for:
  - *Energy, potential (in hydropower reservoir), converted* (for 44.39%);
  - *Energy, gross calorific value, in biomass* (for 38.51%);
  - *Energy, kinetic (in wind), converted* (for 9.934%).

The process with the highest environmental burden was BSF Breeding process (65.6%) followed by Extraction of chitin fraction (14.19%).

Normalization results (damage category) of process "Extraction of lipid, protein, chitin fraction" (F.U. 1 g)

DAMAGE CATEGORY	UNIT	TOTAL	BSF BREEDING	PREPARATION OF PREPUPAE	EXTRACTION OF LIPID FRACTION	EXTRACTION OF PROTEIN FRACTION	EXTRACTION OF CHITIN FRACTION	DISPOSAL OF RESIDUAL PREPUPAE BIOMASS
Resources	dimensionless	9.788E-05	6.617E-05	9.121E-07	8.149E-06	8.607E-06	1.404E-05	9.877E-09
Human health	dimensionless	9.235E-05	4.858E-05	6.460E-07	2.659E-05	6.535E-06	9.970E-06	3.109E-08
Climate change	dimensionless	7.099E-05	4.061E-05	6.140E-07	7.563E-06	8.918E-06	1.318E-05	9.997E-08
Renewable energy	dimensionless	2.547E-05	1.671E-05	2.410E-07	2.389E-06	2.516E-06	3.614E-06	8.009E-10
Ecosystem quality	dimensionless	1.732E-05	1.157E-05	1.225E-07	1.601E-06	1.723E-06	2.305E-06	2.474E-09
Human health, indoor	dimensionless	1.138E-07	-	7.602E-12	1.138E-07	1.098E-15	1.120E-15	-
Human health, local	dimensionless	3.361E-12	-	4.066E-14	1.197E-12	1.051E-12	1.072E-12	-

Table 6-26 Normalization results (damage category) of process "Extraction of lipid, protein, chitin fraction" (F.U. 1 g)

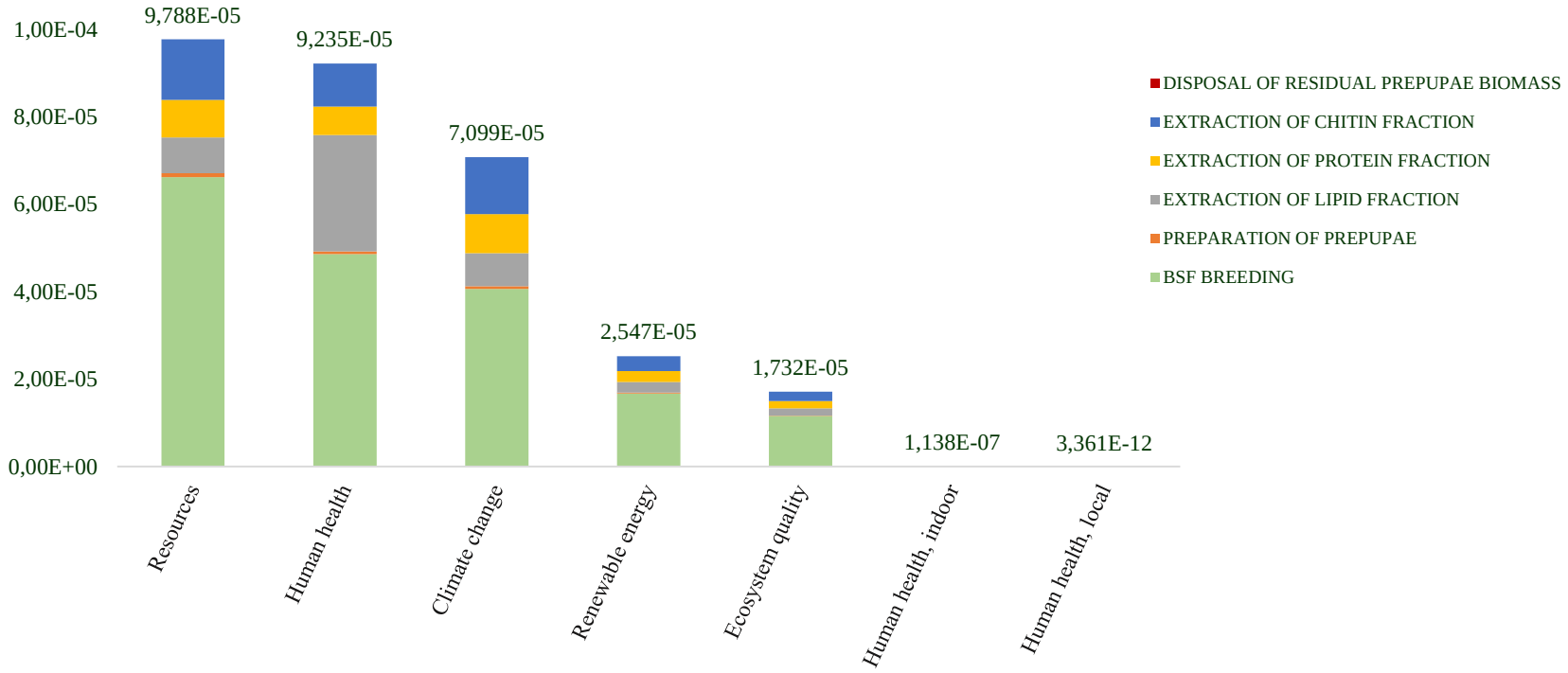

Figure 6-6 Normalization results (damage category) of process "Extraction of lipid, protein, chitin fraction" (F.U. 1 g)

The following conclusions can be drawn from the results of normalization (summarized inTable 6-26, Figure 6-6):

- in **Human Health** damage category, the damage on the European population was equal to 9.235E-5 times the one produced on the same category by anthropic activities in Europe in 1 year referred to an individual European citizen.
- In **Ecosystem quality** damage category the damage on animal and vegetable species was 1.732E-5 times the one produced on the same species by the anthropic activities in 1 year referred to an individual European citizen.
- In **Climate change** the damage on climate change was 7.099E-5 times the one produced in the same category by human activities in Europe in 1 year referred to an individual European citizen.
- In **Resources** the damage on the depletion of resources in the world was 9.788E-5 times the one produced in the same category by human activities in Europe in 1 year referred to an individual European citizen.
- In **Human Health, indoor** damage to all workers in laboratory during extraction of lipidic, protein and chitin fraction was 1.138E-7 times the one produced on the same by human activities in Europe in 1 year referred to an individual European citizen.
- In **Human health, local** damage to all citizens residing in an area of 4E8 m^2 around the laboratory was 3.361E-12 times the one produced on it by human activities in Europe in 1 year referred to an individual European citizen.
- The **Renewable energy** used was 2.547E-5 times the energy that is consumed in 1 year by the individual European citizen.

LCIA results at end-point level of process "Extraction of lipid, protein, chitin fraction" (F.U. 1 g)

From the analysis of the single score results of process "Extraction of lipid, protein, chitin fraction" (Table 6-27, Figure 6-7), it can be seen that the total damage was worth to 0.00028 Pt and is due to:

- "BSF Breeding" process (for ≅59.91%).
- "Separation of lipid fraction without grinding" process (for ≅15.79%).
- "Separation of chitin fraction" process (for ≅14.17%).
- "Separation of protein fraction without demineralization process" (for ≅9.25%).
- "Preparation of prepupae" process (for ≅0.82%).
- "Residual fraction of prepupae" process (for ≅0.05%).

Furthermore the damage was due to:

- Resources (for 35.13%)
- Human Health (for 33.14%)
- Climate Change (for 25.48%)
- Ecosystem Quality (for 6.22%)
- Human Health, indoor (for 0.04%)
- Human Health, local (for 1.206E-6%)

DAMAGE CATEGORY	UNIT	BSF BREEDING	PREPARATION OF PREPUPAE	EXTRACTION OF LIPID FRACTION	EXTRACTION OF PROTEIN FRACTION	EXTRACTION OF CHITIN FRACTION	DISPOSAL OF RESIDUAL PREPUPAE BIOMASS
Human health	Pt	4.858E-05	6.460E-07	2.659E-05	6.535E-06	9.970E-06	3.109E-08
Ecosystem quality	Pt	1.157E-05	1.225E-07	1.601E-06	1.723E-06	2.305E-06	2.474E-09
Climate change	Pt	4.061E-05	6.140E-07	7.563E-06	8.918E-06	1.318E-05	9.997E-08
Renewable energy	Pt	-	-	-	-	-	-
Resources	Pt	6.617E-05	9.121E-07	8.149E-06	8.607E-06	1.404E-05	9.877E-09
Human health, local	Pt	-	4.066E-14	1.197E-12	1.051E-12	1.072E-12	-
Human health, indoor	Pt	-	7.602E-12	1.138E-07	1.098E-15	1.120E-15	-
Total	Pt	1.669E-04	2.295E-06	4.401E-05	2.578E-05	3.949E-05	1.434E-07

Table 6-27 LCIA results at end-point level (damage category) of process "Extraction of lipid, protein, chitin fraction" (F.U. 1 g)

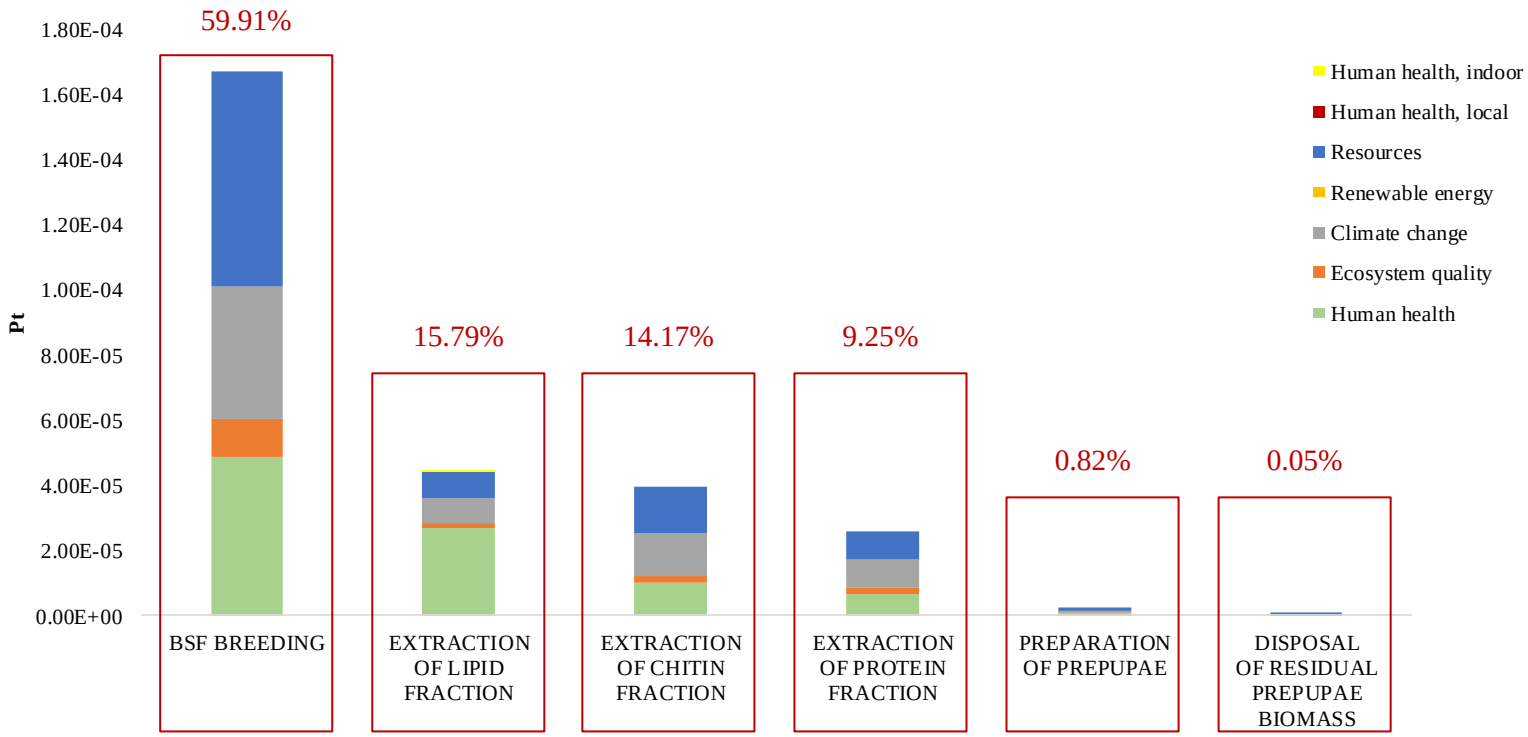

Figure 6-7 LCIA results at end-point level (damage category) of process "Extraction of lipid, protein, chitin fraction" (F.U. 1 g)

It can be concluded that the highest damage of the process "Extraction of lipid, protein and chitin fraction" is attributable to the production of BSF prepupae –BSF Breeding.
In (Figure 6-8) the environmental loads at the damage category level of process "BSF Breeding" which represents the production of prepupae is reported. From the analysis of the single score results of process "BSF Breeding" (Figure 6-8,Table 6-28), it can be seen that the total damage was worth to 3.706E-5 Pt and it was due to:

- "Bioconversion unit" process (for ≅87.08%).
- "Substrate preparation" (for ≅8.5%).
- "Nursery unit" (for ≅4.197%).
- "Vibrating sieve" (for ≅0.1013%).
- "Electricity to sieve prepupae" process (for ≅0.1255%).

Figure 6-9 shows that the most significant contribution to the total damage was due to:

- **Respiratory inorganics** impact category (25.9%) which was affected by:
  - *Particulates,<2.5 µm* in air (for 34.42%). It was mainly due to Bioconversion unit process (for 83.32%), and in particular, it was due to Electricity, high voltage {IT}| electricity production, hard coal | APOS, U (for 22.8%). This latter process considered the production of the coal component of the Italian electricity mix used in the bioconversion unit.
  - *Sulfur dioxide* in air (for 21.84%). It was mainly due to Bioconversion unit process (for 89.82%), and in particular, it was due to Electricity, high voltage {IT}| electricity production, hard coal | APOS, U (for 41.6%).
  - *Nitrogen oxides* in air (for 20.87%). It was mainly due to Bioconversion unit process (for 87.91%), and in particular, it was due to Electricity, high voltage {IT}| electricity production, hard coal | APOS, U (for 36.3%).
- **Non-renewable energy** (25.83%) which was affected by:
  - *Gas, natural/m^3* (for 38.87%). It was mainly due to Bioconversion unit process (for 91.82%), and in particular, it was due to Natural gas, high pressure {RU}| natural gas production | APOS, U (for 51.06%). This latter process represented the extraction of the natural gas component of the Italian electricity mix used in the bioconversion unit.
  - *Coal, hard* (for 24.37%). It was mainly due to Bioconversion unit process (for 89.88%), and in particular, it was due to Hard coal {RoW}| hard coal mine operation and hard coal preparation | APOS, U (for 87.48%). This latter process was related to the production of the coal component of the Italian electricity mix used into the bioconversion unit.
  - *Uranium* (for 18.15%). It was mainly due to Bioconversion unit process (for 92.09%), and in particular, it was due to Uranium, in yellowcake {GLO}| uranium production, in yellowcake, in-situ leaching | APOS, U (for 39.81%). This latter process represented the uranium used to produce nuclear component of the Italian electricity mix used in the bioconversion unit.
  - *Oil, crude* (for 15.51%). It was mainly due to Bioconversion unit process (for 90.4%), and in particular, it was due to Petroleum {RoW}| petroleum and gas production, on-shore | APOS, U (for 30.59%). This latter process considered the extraction of the petroleum used to produce the component by petroleum of the Italian electricity mix.
  - **Global warming** (24.33%) which was affected by:
  - *Carbon dioxide fossil* in air (93.08%). It was mainly due to Bioconversion unit process (for 90.64%), and in particular, it was due to Electricity, high voltage {IT}| electricity production,

hard coal | APOS, U (for 32.39%). This latter process considered the production of the coal component of the Italian electricity mix used in the bioconversion unit.

- **Mineral extraction** (13.81%) which was affected by:
  - *Water, turbine use, unspecified natural origin, IT* (for 87.63%). It was mainly due to Bioconversion unit process (for 96.7%), and in particular, it was due to Electricity, high voltage {IT}| electricity production, hydro, run-of-river | APOS, U (for 87.97%). This latter process represented the production of the hydropower component of the Italian electricity mix used in the bioconversion unit.
  - *Water, turbine use, unspecified natural origin, RoW* (for 11.01%). It was mainly due to Bioconversion unit process (for 91.42%), and in particular, it was due to Electricity, high voltage {RoW}| electricity production, hydro, run-of-river | APOS, U (for 99.86%).

LCIA results at end-point level (damage category) of process "BSF Breeding" (U.F. 1 g)

DAMAGE CATEGORY	UNIT	SUBSTRATE PREPARATION	NURSERY UNIT	BIOCONVERSION UNIT	VIBRATING SIEVE	ELECTRICITY TO SIEVE PREPUPAE
Human health	Pt	1.308E-06	4.511E-07	8.997E-06	1.696E-08	1.160E-08
Ecosystem quality	Pt	7.419E-07	7.594E-08	1.744E-06	3.970E-09	2.056E-09
Climate change	Pt	6.043E-07	3.730E-07	8.021E-06	5.696E-09	1.215E-08
Renewable energy	Pt	-	-	-	-	-
Resources	Pt	4.957E-07	6.552E-07	1.351E-05	1.093E-08	2.071E-08
Human health, local	Pt	-	-	-	-	-
Human health, indoor	Pt	-	-	-	-	-
Total	Pt	3.150E-06	1.555E-06	3.227E-05	3.755E-08	4.651E-08

Table 6-28 LCIA results at end-point level (damage category) of process "BSF Breeding" (F.U. 1 g)

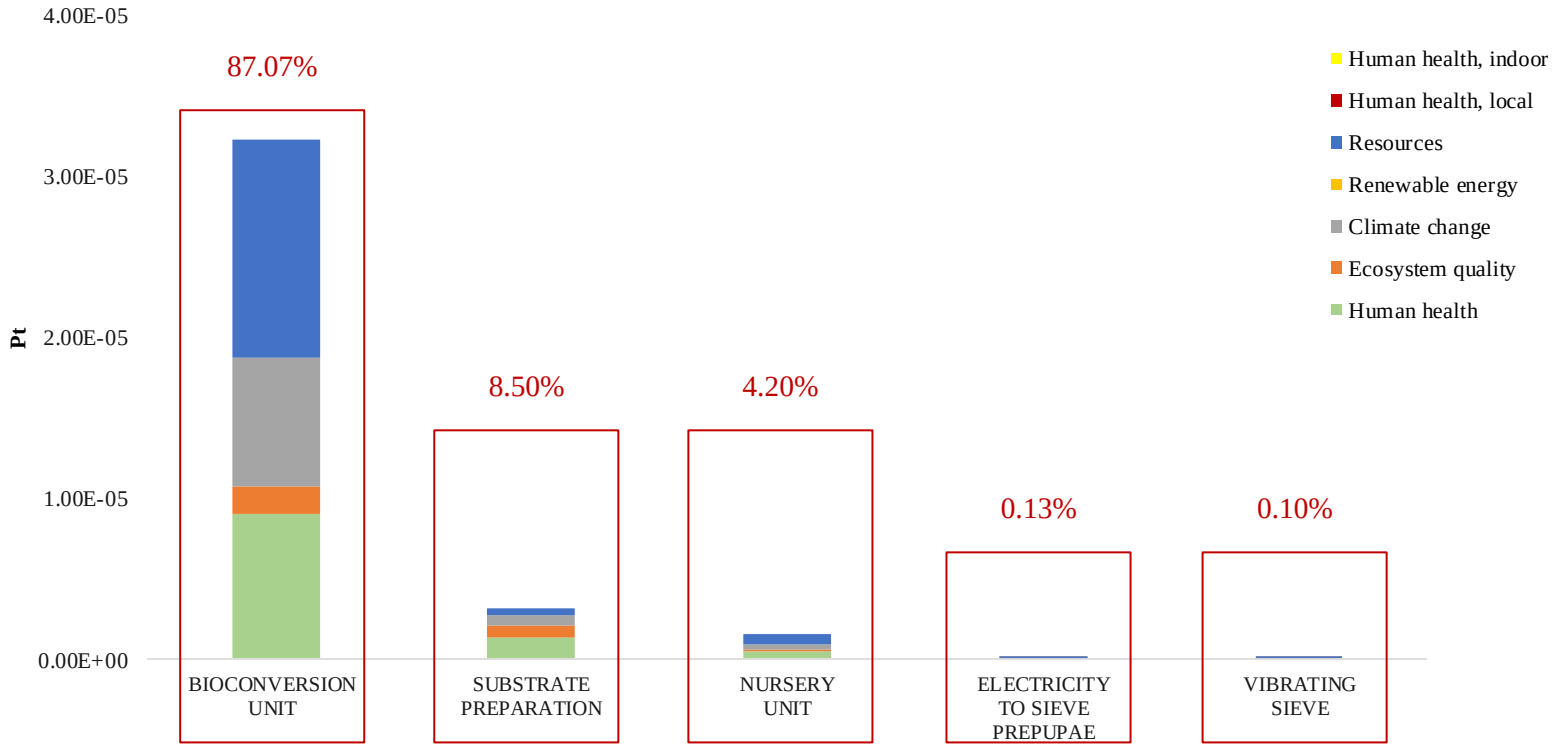

Figure 6-8 LCIA results at end-point level (damage category) of the process "BSF Breeding" (F.U. 1 g)

LCIA results at end-point level (impact category) of process "BSF Breeding" (F.U. 1 g)

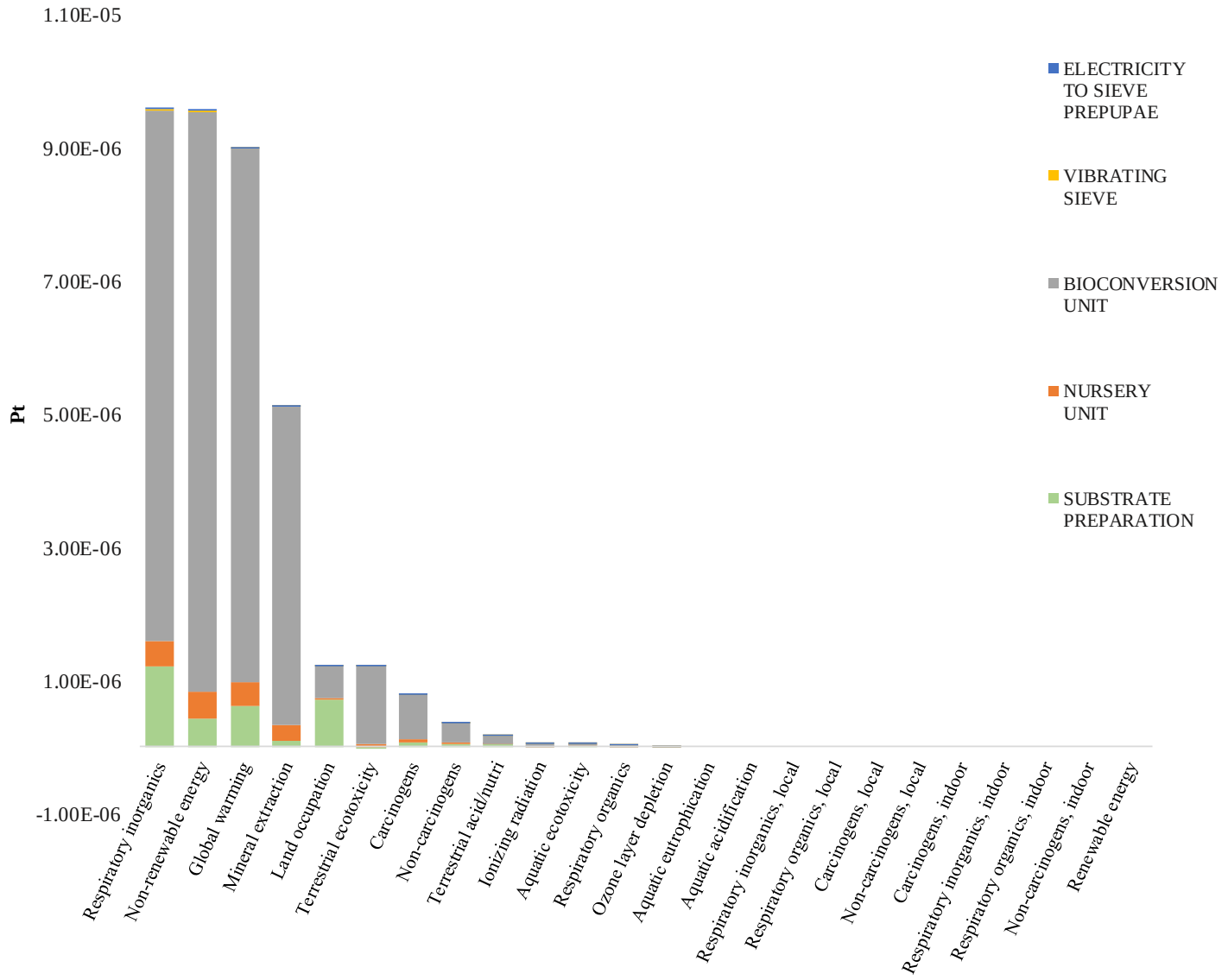

Figure 6-9 LCIA results at end-point level (impact category) of the process "BSF Breeding" (F.U. 1 g)

Chapter 7
Approximated method to calculate local and indoor emissions

7 APPROXIMATED METHOD TO CALCULATE LOCAL AND INDOOR EMISSIONS

An approximated method for the calculation of the *damage factor (DF)* for *indoor* and *local* air emissions was developed.
This method was created starting from the *Eco-indicator 99* evaluation method and *Gaussian Plume Modelling (GMP)* and taking into account the same equations adopted for assessing continental diffusion reported on "The Eco-Indicator 99 - A damage oriented method for Life Cycle Impact Assessment", Methodology Annex, 22 June 2001. The calculated *indoor* and *local damage factor (DF)* are implemented in IMPACT 2002+ evaluation method. IMPACT 2002+ method was selected since it considers a much higher number of substances than *Eco-indicator 99* method. Moreover, IMPACT 2002+ takes into account the *Non-carcinogen* impact category.
The impact categories that currently being studied are:

- *Carcinogens*.
- *Non-carcinogens*.
- *Respiratory Inorganics*.
- *Respiratory Organics*.

7.1 Eco-indicator 99 method

The calculation of damage factor to the **Human Health** damage category in *Eco-indicator99* method includes three separate steps:

1. ***Fate analysis:*** consists in passing from the emission to the concentration.
2. ***Effect analysis:*** consists in passing from concentration to cancer disease cases related to amount of emission [kg] (the risk unit).
3. ***Damage analysis:*** consists in passing from cancer disease cases related to amount of emission [kg] to DALYs related to amount of emission [kg], which measure the total amount of health problems due to disability and premature death attributable to specific diseases and injuries.

7.1.1 Fate analysis

Fate analysis for emissions to air, water, soil (urban soil and industrial soil) considers the three exposure pathways: air (inhalation), drinking water (oral uptake), food (oral uptake).
The factor that is defined in this phase is the *Fate Factor (FF)*, used to pass from the emission to the concentration. This factor represents the concentration (C) related to the emission (E) of a chemical during a reference period (T) from an emission area (A_{emit}) that in *Eco-indicator 99* is referred to as the European one.

Approximated method to calculate local and indoor emissions

The following formulas were used to calculate the *Fate Factor (FF)* related to the three exposure pathways:

- F, air→air

(13)

$$FF_{air}\ [(m^2 \cdot anno) \cdot m^{-3}] = \frac{C_{air}}{\frac{E_{air} \times T}{A_{emit}}}$$

C_{air}: $concentration\ in\ air\ [mg \cdot m^{-3}]$
E_{air}: $emission\ in\ air\ [mg \cdot d^{-1}]$
T: $reference\ period\ [d \cdot yr^{-1}]$
$Aemit$: $emission\ area\ [m^2]$

- F, air→drinking water

(14)

$$FF_{drinking\ water}\ [(m^2 \cdot anno) \cdot Lt^{-1}] = \frac{C_{drinking\ water}}{\frac{E_{air} \times T}{A_{emit}}}$$

$C_{drinking\ water}$: $concentration\ in\ drinking\ water\ [mg \cdot Lt^{-1}]$
E_{air}: $emission\ in\ air\ [mg \cdot d^{-1}]$
T: $reference\ period\ [d \cdot yr^{-1}]$
$Aemit$: $emission\ area\ [m^2]$

- F, air→food

(15)

$$FF_{food}\ [(m^2 \cdot anno) \cdot (kg \cdot d)^{-1}] = \frac{C_{food}}{\frac{E_{air} \times T}{A_{emit}}}$$

C_{food}: $dose\ by\ food\ [(mg \cdot kg^{-1}) \cdot d^{-1}]$
E_{air}: $emission\ in\ air\ [mg \cdot d^{-1}]$
T: $reference\ period\ [d \cdot yr^{-1}]$
$Aemit$: $emission\ area\ [m^2]$

To calculate Fate Factors, the concentration values in air were used, as well as the concentration values in drinking water and the dose by food resulting from the EUSES output were used, based on an emission of 10000 $[kg \cdot d^{-1}]$ and an emission area (A_{emit}) of $3{,}6 \times 10^{12} m^2$.
With the same *Fate Factor (FF)*, reference period (T) and emission area (A_{emit}), the amount of emitted chemical increases with a greater concentration.

7.1.2 Effect analysis

For the effect analysis the list of unit risk (UR) factors was used (Hofstetter 1998).
The definition of the unit risk factor is:
"*The unit risk factor for inhalation is an estimate of the probability that an average individual will develop cancer when exposed to a pollution at an ambient concentration of one microgram for cubic meter for the individual's (70 years)* $[UR\ in\ cases\ \cdot \mu gr^{-1} \cdot m^3]$".
In other words, this factor represents the number of cases of disease that can occur in the presence of a certain concentration of a particular chemical $[cases\ \cdot \mu gr^{-1} \cdot m^3]$.
In this step the *Effect Factor (EF)* was defined.
The formula used by *Eco-indicator99* to calculate the *Effect Factor (EF)* for exposure through air was:

(16)

$$Effect\ Factor\left[\frac{cases \cdot \mu gr^{-1} \cdot m^3}{yr \cdot m^2}\right] = \frac{UR}{LT} \times PD$$

where
$UR: risk\ unit\ [cases \cdot \mu gr^{-1} \cdot m^3]$
$LT: time\ of\ average\ life\ of\ an\ individual\ [70\ yr] (correction\ factor\ for\ UR\ according\ to\ EcoIndicator\ 99)$
$PD: population\ density\ [person \cdot m^2]$

Multiplying the *Effect Factor (EF)* by the *Fate Factor (FF)*, the *Incidence Factor (IF)* in cancer cases for kg emission in Europe can be calculated:

$$IF\left[\frac{cases}{kg_{emission}}\right] = EF \times 10^9 \times FF$$

where
$EF: Effect\ Factor\ [cases \cdot \mu gr^{-1} \cdot m^3 \cdot yr^{-1} \cdot m^{-2}]$
$FF: Fate\ Factor\ [(m^2 \cdot anno) \cdot m^{-3}]$
$10^9: conversion\ factor\ [\mu gr \cdot kg^{-1}]$

7.1.3 Damage-level characterization factor

The total DALYs for kg of emission to a specific compartment were calculated adding the different exposure pathways according to the following equation:

(17)

$$Damage - level\ characterization\ factor\left[\frac{DALYs}{kg_{emission}}\right]:$$

$$IF_{air-air}\left[\frac{cases}{kg_{emission}}\right] \times DALYs_{inhalation}\left[\frac{DALYs}{cases}\right]$$

$$+IF_{air-drinking\ water}\left[\frac{cases}{kg_{emission}}\right] \times DALYs_{oral\ uptake}\left[\frac{DALYs}{cases}\right]$$

$$+IF_{air-food}\left[\frac{cases}{kg_{emission}}\right] \times DALYs_{oral\ uptake}\left[\frac{DALYs}{cases}\right]$$

Approximated method to calculate local and indoor emissions

The total damage ($D[DALYs]$) can be obtained from:

$$D[DALYs] = DF \times M \quad (18)$$

where
$DF: Damage\ Factor\ [DALYs \cdot kg^{-1}]$
$M: Amount\ of\ chemical\ [kg]$

7.2 Local emissions

At present only air-to-air contamination was evaluated.

7.2.1 Local Fate Factor

Local Fate Factor (LFF) was calculated by replacing:

- Concentration in air at continental scale ($Conc_{air}[mg \cdot m^{-3}]$) with concentration at local scale ($C_{local}[mg \cdot m^{-3}]$).
- $10000\ [kg \cdot d^{-1}]$ with the emission referred to the Functional Unit of the analyzed process.

The area of emission(A_{emit}) was hypothesized.
Therefore *Local Fate Factor* may be obtained from:

- LFF, air→air

$$LFF_{air}\ [(m^2 \cdot anno) \cdot m^{-3}] = \frac{C_{local}}{\frac{E_{air} \times T}{A_{emit}}} \quad (19)$$

$C_{local}: concentration\ in\ air\ at\ local\ scale\ [mg \cdot m^{-3}]$
$E_{air}: emission\ in\ air\ reffered\ to\ Functional\ Unit\ [mg \cdot d^{-1}]$
$T: reference\ period\ [d \cdot yr^{-1}]$
$Aemit: emission\ area\ [m^2]$

7.2.1.1 Gaussian Plume Model

Gaussian Plume Modeling (GPM) was used to calculate local concentration (C_{local}) due to the plume relapse.

The following parameters were defined:

- x: distance downwind from the stack [m];
- y: crosswind distance from the plume centerline [m];
- z: vertical distance from ground level [m];
- H: effective stack height, which is the sum of the height of the stack (Hstack) and plume rise [m];
- Q:source emission rate [g/sec]
- U:average wind speed at stack height [m/sec]
- X (x, y, z, H): concentration in the point of coordinates (x, y, z, H) [g/m^3]
- σ_y, σ_z: standard deviations of concentration distributions in the crosswind and vertical directions, respectively.

Approximated method to calculate local and indoor emissions

The coordinate system used is shown in Figure 7-1:

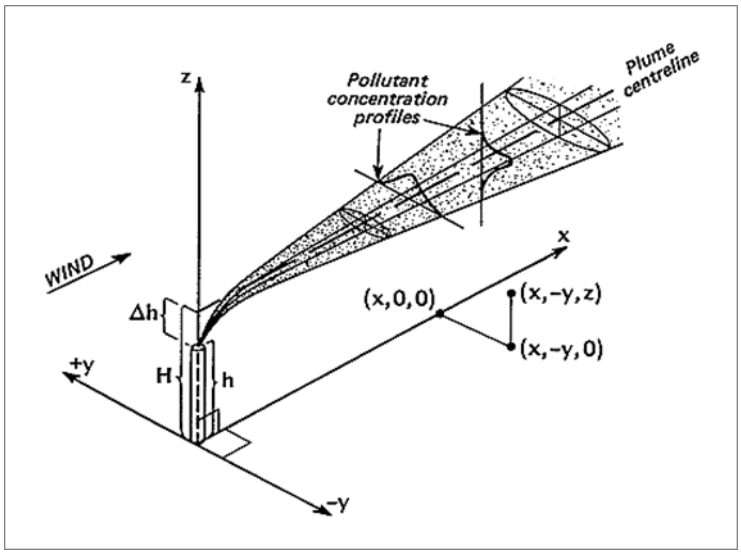

Figure 7-1 Coordinate system used for the Gaussian plume equation (Reproduced from Professors Allen and Durrenberger)

The most general form of the Gaussian dispersion equation is:

(20)

$$X(x,y,z,H) = \frac{Q}{2\pi U\sigma_y\sigma_z} \cdot \exp\left[-\frac{y^2}{2\sigma_y^2}\right] \cdot \left\{\exp\left[-\frac{(z-H)^2}{2\sigma_z^2}\right] + \exp\left[-\frac{(z+H)^2}{2\sigma_z^2}\right]\right\}$$

For ground level concentrations (z=0) the simplified equation becomes the following:

(21)

$$X(x,y,0,H) = \frac{Q}{\pi U\sigma_y\sigma_z} \cdot \exp\left[-\frac{1}{2}\left(\frac{y}{\sigma_y}\right)^2\right] \cdot \exp\left[-\frac{1}{2}\left(\frac{H}{\sigma_z}\right)^2\right]$$

The ground level concentration X [μg/m^3] at the point (x, y) may be written as:

(22)

$$X(x,y,0,H) = \frac{Q \cdot 10^6}{\pi U\sigma_y\sigma_z} \cdot \exp\left[-\frac{1}{2}\left(\frac{y}{\sigma_y}\right)^2\right] \cdot \exp\left[-\frac{1}{2}\left(\frac{H}{\sigma_z}\right)^2\right]$$

7.2.1.1.1 Assumptions

The assumptions deriving from steady-state conditions (constant source emission strength) were the following:

- Dispersion (diffusion) was negligible in the downwind direction (x).
- The horizontal meteorological conditions were homogeneous over the space being modelled. For each hour of the model:
  a. average wind speed was used.
  b. Wind direction was constant.
  c. Temperature was constant.
  d. Atmospheric stability class was constant.
  e. Mixing height was constant.
- No wind shear in the horizontal or vertical directions.
- In the absence of historical data on the plume this was assumed infinite (each hour being modelled was independent from the previous one).
- The pollutans were non-reactive gases or areosol that remained suspended in the air following the turbolent movement of the atmosphere.
- The plume was reflected at the surface with no deposition or reaction with the surface.
- The dispersion in the crosswind (y direction) and vertical direction (z direction) took the form of Gaussian distributions around the plume centerline, as shown in Figure 7-2:

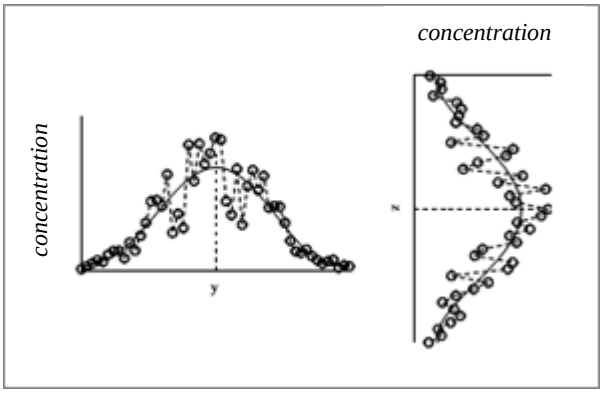

Figure 7-2 Gaussian distributions along the *y* and *z* planes (Reproduced from Professors Allen and Durrenberger)

7.2.1.1.2 Parameters

- *Atmospheric stability*

One of the elements considered by the model was atmospheric stability, which is divided into six different descriptive classes, each of which denoted by a letter as shown below:

- A: extremely unstable.
- B: moderately unstable.
- C: slightly unstable.
- D: neutral conditions. The neutral class (D) is assumed for all overcast conditions during day and night, where night is defined as the period from one hour before sunset to one hour after sunrise.
- E: slightly stable
- F: moderately stable

- *Diffusion coefficients*

The standard deviation of the distribution of the plume concentration relative to the horizontal plane (σ_y) and that relative to the vertical plane (σ_z) are also called dispersion coefficients or diffusion coefficients and their values vary according to: height from the surface, surface roughness, reference period, wind speed and distance from the source of the emission in the direction of the wind. These values are also based on the atmospheric stability class. Schemes for determining the diffusion coefficients have been developed by many researches. Turner developed the most widely accepted approach based on work by Pasquill, Gifford and Turner (Figure 7-3).

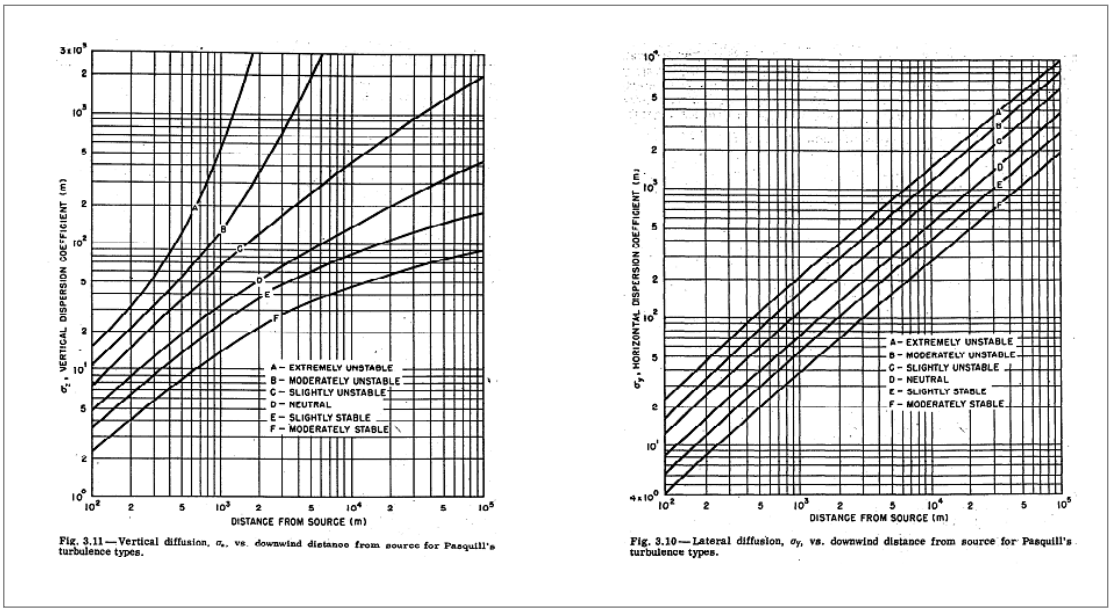

Fig. 3.11—Vertical diffusion, σ_z, vs. downwind distance from source for Pasquill's turbulence types.

Fig. 3.10—Lateral diffusion, σ_y, vs. downwind distance from source for Pasquill's turbulence types.

Figure 7-3 Vertical diffusion coefficients on the left (σz), and lateral diffusion coefficients on the right (σy), as a function of the distance from the source in the direction of the wind and of the atmospheric stability class (Reproduced from Professors Allen and Durrenberger)

The best approach to approximate these curves was that proposed by Caraway, which defines the dispersion coefficients through the equations:

(23)

$$\sigma_y = c \cdot x^d$$
$$\sigma_z = a \cdot x^b$$

where
x: $downwind\ distance\ from\ the\ stack\ [m]$
a, b, c, d: $coefficients$

The values a, b, c, and d are shown in Table 7-1 and Table 7-2.

Atmosferic stability class	Distance along the plane x [m]			
	x < 10.000		x > 10.000	
	c	d	c	d
A = 1	0.495	0.873	0.606	0.851
B = 2	0.310	0.897	0.523	0.840
C = 3	0.197	0.908	0.285	0.867
DD = 4	0.122	0.916	0.193	0.865
DN = 5	0.122	0.916	0.193	0.865
E = 6	0.0934	0.912	0.141	0.868
F = 7	0.0625	0.911	0.080	0.884

Table 7-1 Parameters to calculate σ_y

Atmosferic stability class	Distance along the plane x [m]					
	100 < x ≤ 500		500 < x ≤ 5000		x > 5000	
	a	b	*a*	b	*a*	b
A = 1	0.0383	1.281	0.0002539	2.089	0.0002539	2.089
B = 2	0.1393	0.9467	0.04936	1.114	0.04936	1.114
C = 3	0.1120	0.9100	0.1014	0.926	0.1154	0.9109
DD = 4	0.0856	0.8650	0.2591	0.6869	0.7368	0.5642
DN = 5	0.0818	0.8155	0.2527	0.6341	1.297	0.4421
E = 6	0.1094	0.7657	0.2452	0.6358	0.9204	0.4805
F = 7	0.05645	0.8050	0.1930	0.6072	1.505	0.3662

Table 7-2 Parameters to calculate σ_z

➢ *Point of maximum concentration*

The maximum concentration downwind occoured along the plume centerline. For points located on the plume centerline, equation (21) reduced to equation (24):

(24)

$$X = \frac{Q \cdot 10^6}{\pi U \sigma_y \sigma_z} \cdot \exp\left[-\frac{1}{2}\left(\frac{H}{\sigma_z}\right)^2\right]$$

The values of σ_y and σ_z in equation (24) were replaced with Caraway equation (23). Then this equation differentiated with respect to x, was set to zero and the equation solved for x.
This provided the distance to the maximum concentration as shown in equation (25):

(25)

$$x_{max} = \left[\frac{b \cdot H^2}{a^2(d+b)}\right]^{\frac{1}{2b}}$$

The maximum concentration at a given set of conditions may be determined by using the value in equation (25) (x_{max}) in the previous equation (24).

➢ *Wind speed*

In the lower layers of the atmosphere, wind speed normally increased with height. Most National Weather Services wind speed measurements were taken at the height of 10 meters above the surface and were listed as "ground level" wind speed. The wind speed at stack height had the greatest effect on the plume. Wind speed may be adjusted to stack height with the following equation:

(26)

$$U_z = U_0(Z/Z_0)^p$$

where

U_z: $wind\ speed\ at\ height\ z\ [m \cdot s^{-1}]$

U_0: $wind\ speed\ at\ anemometer\ height\ [m \cdot s^{-1}]$

Z: $desidered\ height\ [m]$

Z_0: $anemometer\ height\ (usually\ 10\ m)\ [m]$

p: $defined\ parameter\ as\ a\ function\ of\ atmosferic\ stability\ class$

For p values see Table 7-3

Atmosferic stability class	Rural exponent (p)	Urban exponent (p)
A	0.07	0.15
B	0.07	0.15
C	0.10	0.20
D	0.15	0.30
E	0.35	0.30
F	0.55	0.30

Table 7-3 p parameters used to calculate wind speed

Context types considered were the following:

- rural context: relative to a ground with low surface roughness and high stacks.
- Urban context: relative to a ground with high surface roughness and emissions at low altitude.

In order to determine the crosswind concentration at the distance y from the centerline, the centerline concentration was multiplied by:

(27)

$$k_y = exp\left[-\frac{1}{2}\left(\frac{y}{\sigma_y}\right)^2\right]$$

where

σ_y: *value at crosswind distance y*

➢ *Plume rise*

In many situations, the final height of a plume from a stack is higher than the stack from which it was released. This increase in plume height is called plume rise. The most comprehensive and widely accepted approach for determining the increase of the plume is that developed by Briggs. The approach was developed based on theoretical relationships and empirical data derived from measurements of plume rise.

The Briggs equations are shown in the following Table 7-4:

	Stable atmosfere	**Neutral/unstable atmosfere**
Buoyancy dominated plume	$\Delta h(x) = 1.6\,\frac{F^{1/3}\,x^{2/3}}{U}$ or $\Delta h_{max} = 2.6\,(F/U\,s)^{1/3}$ where $s = 0.02g/T_A$ for stability class E $s = 0.035g/T_A$ for stability class F	$\Delta h(x) = 1.6\,\frac{F^{1/3}\,x^{2/3}}{U}$ per $x < 3.5\,x^*$ or $\Delta h_{max} = 1.6\,\frac{F^{1/3}\,(3.5x^*)^{2/3}}{U}$ per $x > 3.5\,x^*$ dove $x^* = 14\,F^{5/8}$ se $F < 55$ $x^* = 34\,F^{2/5}$ se $F > 55$
Momentum dominated plume	$\Delta h_{max} = 1.5\,\frac{(VR)^{2/3}\,s^{-1/6}}{U^{1/3}}$ where s is previously defined	$\Delta h(x) = 3.78\left(\frac{V^2}{U(V+3U)}\right)^{2/3}\left(\frac{xR^2}{2}\right)^{1/3}$ or $\Delta h_{max} = 3VD/U$

Table 7-4 Briggs equations

The F parameter used in the Briggs equations is calculated by the following equation:

(28)

$$F = \frac{gVR^2(T - T_A)}{T}$$

where
$T: source\ temperature\ [°K]$
$T_A: ambient\ temperature\ [°K]$
$V: stack\ exit\ velocity\ [m \cdot s^{-1}]$
$R: stack\ radius\ [m]$
$D: stack\ diameter\ [m]$
$x: downwind\ distance\ [m]$
$U: wind\ speed\ at\ physical\ source\ height\ [m \cdot s^{-1}]$
$g: acceleration\ due\ to\ gravity\ [m \cdot s^{-2}]: g = 9.8\ m \cdot s^{2}$
$\Delta h: plume\ rise\ [m]$
$\Delta h_{max}: final\ plume\ rise\ [m]$

The neutral/unstable plume rise equations were used for atmospheric stability classes from A to D. For atmospheric stability classes E and F the stable plume rise equations are used. Stack diameter, stack exit velocity, stack exit temperature, and ambient temperature indicate whether the upward motion of the plume is dominated by momentum or by thermal buoyancy. There are four different situations for plume rise:

- stable atmosphere with buoyancy dominated plume;
- stable atmosphere with momentum dominated plume;
- neutral/unstable atmosphere with buoyancy dominated plume;
- neutral/unstable atmosphere with momentum dominated plume.

In each case, except for a stable atmosphere with a momentum dominated plume, plume rise is calculated as a function of downwind distance from the sources until the final plume rise.
For each stack, both momentum and buoyancy dominated final plume rise should be calculated. Then the higher of the two is used for further calculations.
The effective stack height (Heff) is the sum of the stack height (Hstack) and the plume rise (Δh).

7.2.1.2 Implementation in SimaPro calculation code

In order to simplify the calculation of local concentration, a process was created in the SimaPro calculation code, where the *Gaussian Plume Modeling* (GPM) equations were implemented.
We chose the atmospheric stability class that produced max local concentration in order to simulate the worst scenario.

Approximated method to calculate local and indoor emissions

INPUT PARAMETERS		
Name	**Value**	**Comment**
ASC	1	Atmospheric stability classes (ASC)) A: extremely unstable (1) B: moderately unstable (2) C: slightly unstable (3) D: neutral conditions DDay (4) DNight (5) E: slightly ustable (6) F: moderately stable (7) We chose the atmospheric stability class that produce max local concentration.
Z_0	10	Anemometer height (usually 10 meters) [m]
U_0	2	wind speed at anemometer height [m/s]
Hstack	Hstack	Height of the stack [m]
Dstack	Dstack	Diameter of the stack [m]
Vstack	Vstack	Stack exit velocity [m/sec]
Tstack	Tstack	Source temperature [°C]
TstackK	TstackK	Source temperature [°K]
TambK	TambK	Ambient temperature [°K] We used the same value of USEtox (285°K)
g	9,8	Acceleration due to gravity [m/s2]
mass_received	Received mass	Total received mass [kg]

Approximated method to calculate local and indoor emissions

CALCULATED PARAMETERS		
Name	**Expression**	**Comment**
Q	Mass_received*1E3/(24*3600)	Source emission rate [g/sec]
Z	Hstack	Height of the stack [m]
pr	Iff (ASC=1; 0,15; Iff (ASC=2; 0,15;Iff(ASC=3; 0,20; Iff(ASC=4; 0,30; Iff (ASC=5; 0,30; Iff (ASC=6; 0,30; 0,30))))))	Rural exponent (p) used to calculate wind speed at effective stack height (Hstack).
pu	Iff (ASC=1; 0,15; Iff (ASC=2; 0,15;Iff(ASC=3; 0,20; Iff(ASC=4; 0,30; Iff (ASC=5; 0,30; Iff (ASC=6; 0,30; 0,30))))))	Urban exponent (p) used to calculate wind speed at effective stack height (Hstack).
a	Iff (x<500; a1; Iff (x<5000; a2; a3))	Table [7.2]
a_1	Iff (ASC=1; 0,0383; Iff (ASC=2; 0,1393;Iff(ASC=3; 0,1120; Iff (ASC=4; 0,0856; Iff(ASC=5; 0,0818; Iff (ASC=6; 0,1094; 0,05645))))))	Table [7.2]
a_2	Iff (ASC=1; 0,0002539; Iff (ASC=2; 0,04936; Iff (ASC=3; 0,1014; Iff (ASC=4; 0,2591; Iff (ASC=5; 0,2527; Iff (ASC=6; 0,2452; 0,1930))))))	Table [7.2]
a_3	Iff (ASC=1; 0,0002539; Iff (ASC=2; 0,04936; Iff (ASC=3; 0,1154; Iff (ASC=4; 0,7368; Iff (ASC=5; 1,297; Iff (ASC=6; 0,9204; 1,505))))))	Table [7.2]
b	Iff (x<500; b1; Iff (x<5000; b2; b3))	Table [7.2]
b_1	Iff (ASC=1; 1,281; Iff (ASC=2; 0,9467; Iff (ASC=3; 0,91; Iff (ASC=4; 0,865; Iff (ASC=5; 0,8155; Iff(ASC=6; 0,7657; 0,805))))))	Table [7.2]
b_2	Iff (ASC=1; 2,089; Iff (ASC=2; 1,114;Iff (ASC=3; 0,926; Iff (ASC=4; 0,6869; Iff (ASC=5; 0,6341; Iff (ASC=6; 0,6358; 0,6072))))))	Table [7.2]
b_3	Iff (ASC=1; 2,089; Iff (ASC=2; 1,114;Iff (ASC=3; 0,9109; Iff (ASC=4; 0,5642; Iff (ASC=5; 0,4421; Iff (ASC=6; 0,4805; 0,3662))))))	Table [7.2]
c	Iff (x<10000; c1; c2)	Table [7.2]
c_1	Iff (ASC=1; 0,495; Iff (ASC=2; 0,31; Iff (ASC=3; 0,197; Iff (ASC=4; 0,122; Iff (ASC=5; 0,122; Iff (ASC=6; 0,0934; 0,0625))))))	Table [7.2]
c_2	Iff (ASC=1; 0,606; Iff (ASC=2; 0,523; Iff (ASC=3; 0,285; Iff (ASC=4; 0,193; Iff (ASC=5; 0,193; Iff (ASC=6; 0,141; 0,08))))))	Table [7.2]
d	Iff (x<10000; d1; d2)	Table [7.2]
d_1	Iff (ASC=1; 0,873; Iff (ASC=2; 0,897; Iff (ASC=3; 0,908; Iff (ASC=4; 0,916; Iff (ASC=5; 0,916; Iff (ASC=6; 0,912; 0,911))))))	Table [7.2]
d_2	Iff (ASC=1; 0,851; Iff (ASC=2; 0,84; Iff (ASC=3; 0,867; Iff (ASC=4; 0,865; Iff (ASC=5; 0,865; Iff (ASC=6; 0,868; 0,884))))))	Table [7.2]

Approximated method to calculate local and indoor emissions

CALCULATED PARAMETERS		
Name	**Expression**	**Comment**
F	(g*Vstack*(Dstack/2)^2*(TstackK-TambK))/TstackK	Parameter used in the Briggs equations
Uzru	U_0*(Z/Z_0)^pr	Wind speed at height Z in rural area [m/s]
Uzu	U_0*(Z/Z_0)^pu	Wind speed at height Z in urban area [m/s]
xfactor	34*F^(2/5)	x* (Briggs equations) x*=14 F^(5/8) se F < 55 x*=34 F^(2/5) se F > 55
x	3,5*xfactor	Downwind distance [m]
Dhmaxneutunstbuoyancyru	1,6*F^(1/3)*(x)^(2/3)*(Uzru)^-1	Plume rise neutral/unstable atmosphere with buoyancy dominated plume, rural area [m] For atmospheric stability classes (ASC) A through D
Dhmaxneutunstmomru	3*Vstack*Dstack/Uzru	Plume rise neutral/unstable atmosphere with momentum dominated plume, rural area [m] For atmospheric stability classes (ASC) A through D
s_1	0,002*g/TambK	Parameters "s" used to calculate: -plume rise stable atmosphere with buoyancy dominated plume, rural/urban area [m]; -plume rise stable atmosphere with momentum dominated plume, rural/urban area [m]. Atmospheric stability classes E
s_2	0,035*g/TambK	Parameters "s" used to calculate: -plume rise stable atmosphere with buoyancy dominated plume, rural/urban area [m]; -plume rise stable atmosphere with momentum dominated plume, rural/urban area [m]. Atmospheric stability classes F
DhmaxstabbuoyancyruE	2,6*(F/(Uzru)*s1)^1/3	Plume rise stable atmosphere with buoyancy dominated plume, rural area [m]-->atmospheric stability classes E
DhmaxstabbuoyancyruF	2,6*(F/(Uzru)*s2)^1/3	Plume rise stable atmosphere with buoyancy dominated plume, rural area [m]-->atmospheric stability classes F
DhmaxstabmomruE	1,5*((Vstack*Dstack/2)^2/3)*((Uzru)^-1/3)*(s1^-1/6)	Plume rise stable atmosphere with momentum dominated plume, rural area [m]-->atmospheric stability classes E

CALCULATED PARAMETERS		
Name	**Expression**	**Comment**
DhmaxstabmomruF	1,5*((Vstack*Dstack/2)^2/3)*((Uzru)^-1/3)*(s2^-1/6)	Plume rise stable atmosphere with momentum dominated plume, rural area [m]-->atmospheric stability classes F
Dhmaxbuoyancyru	Iff (ASC=1;Dhmaxneutunstbuoyancyru; Iff(ASC=2; Dhmaxneutunstbuoyancyru;Iff (ASC=3; Dhmaxneutunstbuoyancyru; Iff (ASC=4; Dhmaxneutunstbuoyancyru; Iff (ASC=5; Dhmaxneutunstbuoyancyru; iff (ASC=6;DhmaxstabbuoyancyruE;DhmaxstabbuoyancyruF))))))	Max plume rise with buoyancy dominated plume, rural area [m]
Dhmaxmomru	Iff (ASC=1;Dhmaxneutunstmomru; Iff(ASC=2; Dhmaxneutunstmomru;Iff (ASC=3; Dhmaxneutunstmomru; Iff (ASC=4; Dhmaxneutunstmomru; Iff(ASC=5; Dhmaxneutunstmomru; iff (ASC=6;DhmaxstabmomruE;DhmaxstabmomruF))))))	Max plume rise with momentum dominated plume, rural area [m]
Dhmaxru	Max (Dhmaxbuoyancyru; Dhmaxmomru)	Max plume rise with buoyancy and momentum dominated plume, rural area [m]
Zeffru	Hstack+Dhmaxru	Effective stack height rural area (Heffru) [m]. It's the sum of the height of the stack (Hstack) and plume rise [m].
DhmaxstabbuoyancyuE	2,6*(F/(Uzu)*s_1)^1/3	Plume rise stable atmosphere with buoyancy dominated plume, urban area [m]-->atmospheric stability classes E
DhmaxstabbuoyancyuF	2,6*(F/(Uzu)*s_2)^1/3	Plume rise stable atmosphere with buoyancy dominated plume, urban area [m]-->atmospheric stability classes F
DhmaxstabmomuE	1,5*((Vstack*Dstack/2)^2/3)*((Uzu)^-1/3)*(s_1^-1/6)	Plume rise stable atmosphere with momentum dominated plume, urban area [m]-->atmospheric stability classes E
DhmaxstabmomuF	1,5*((Vstack*Dstack/2)^2/3)*((Uzu)^-1/3)*(s_2^-1/6)	Plume rise stable atmosphere with momentum dominated plume, urban area [m]-->atmospheric stability classes F
Dhmaxbuoyancyu	Iff (ASC=1;Dhmaxneutunstbuoyancyu; Iff (ASC=2; Dhmaxneutunstbuoyancyu;Iff (ASC=3; Dhmaxneutunstbuoyancyu; Iff (ASC=4; Dhmaxneutunstbuoyancyu; Iff(ASC=5; Dhmaxneutunstbuoyancyu; Iff (ASC=6;DhmaxstabbuoyancyuE;DhmaxstabbuoyancruF))))))	Max plume rise with buoyancy dominated plume, urban area [m]
Dhmaxmomu	Iff (ASC=1;Dhmaxneutunstmomu; Iff (ASC=2; Dhmaxneutunstmomu;Iff (ASC=3; Dhmaxneutunstmomu; Iff (ASC=4; Dhmaxneutunstmomu; Iff (ASC=5; Dhmaxneutunstmomu; iff (ASC=6;DhmaxstabmomuE;DhmaxstabmomuF))))))	Max plume rise with momentum dominated plume, urban area [m]

Approximated method to calculate local and indoor emissions

CALCULATED PARAMETERS		
Name	**Expression**	**Comment**
Dhmaxu	Max (Dhmaxbuoyancyu; Dhmaxmomu)	Max plume rise with buoyancy and momentum dominated plume, urban area [m]
Zeffu	Hstack+Dhmaxu	Effective stack height rural area (Heffu) [m]. It's the sum of the height of the stack (Hstack) and plume rise [m].
Ueffru	U_0*(Zeffru/Z_0)^pr	Wind speed at effective height Z in rural area [m/s]
Ueffu	U_0*(Zeffru/Z_0)^pu	Wind speed at effective height Z in urban area [m/s]
Ky	exp(-1/2*(y/sy)^2)	Factor used to determine the crosswind concentration at distance y from the centerline. Equation [26]
sy	c*x^d	Standard deviation of the distribution of the plume concentration relative to the vertical plane also called dispersion diffusion coefficients [m].
sz	a*x^b	Standard deviation of the distribution of the plume concentration relative to the horizontal plane also called dispersion coefficient [m].
X_{1max}	(b_1*Hstack^2/(a_1^2*(d_1+b_1)))^(1/(2*b_1))	[m] Equation [25]
X_{2max}	(b_2*Hstack^2/(a_2^2*(d_1+b_2)))^(1/(2*b_2))	[m] Equation [25]
X_{3max}	(b_3*Hstack^2/(a_3^2*(d_1+b_3)))^(1/(2*b_3))	[m] Equation [25]
X_{4max}	(b_3*Hstack^2/(a_3^2*(d_2+b_3)))^(1/(2*b_3))	[m] Equation [25]
concxmaxdownwindru	Q*1E6/(pi*Ueffru*sz*sy)*Exp(-Zeffru^2/(2*sz^2))	Downwind concentration rural area [microgr/m^3]
concxmaxdownwindu	Q*1E6/(pi*Ueffu*sz*sy)*Exp(-Zeffu^2/(2*sz^2))	Downwind concentration urban area [microgr/m^3]
concxmaxdownwindmedru	concxmaxdownwindru/2	Average downwind concentration rural area [microgr/m^3]
concxmaxdownwindmedu	concxmaxdownwindu/2	Average downwind concentration urban area [microgr/m^3]
concxmaxdownwindmedru_kg	concxmaxdownwindru*1E-9/2	Average downwind concentration rural area [kg/m^3]
concxmaxdownwindmedu_kg	concxmaxdownwindu*1E-9/2	Average downwind concentration urban area [kg/m^3]

Table 7-5 Input parameters and calculated parameters in SimaPro calculation code used to calculate concentration at local scale

7.2.2 Local Effect Factor

In the developed model it was hypothesized that the risk unit and the lifetime remain the same as those adopted in the continental diffusion calculation. Thus, in this first phase of implementation, it was assumed that the risk unit was independent from the area of diffusion of the emissions.
Continental population density was substituted by local population density (PD_{local}).
Therefore

(29)

$$Local\ Effect\ Factor\left[\frac{cases\cdot\mu gr^{-1}\cdot m^3}{yr\cdot m^2}\right]=\frac{UR}{70}\times PD_{local}$$

where
UR: $risk\ unit\ [cases\cdot\mu gr^{-1}\cdot m^3]$
LT: $time\ of\ average\ life\ of\ an\ individual\ [70\ yr](correction\ factor\ for\ UR\ according\ EcoIndicator99)$
PD_{local}: $local\ population\ density\ [person\cdot m^2]$

(30)

$$LIF\left[\frac{cases}{kg_{emission}}\right]=LEF\times 10^9\times LFF$$

where
LEF: $Effect\ Factor\ at\ local\ scale\ [cases\cdot\mu gr^{-1}\cdot m^3\cdot yr^{-1}\cdot m^{-2}]$
LFF: $Local\ Fate\ Factor\ [(m^2\cdot anno)\cdot m^{-3}]$
10^9: $conversion\ factor\ [\mu gr\cdot kg^{-1}]$

7.2.3 Local Damage-level characterization factor

The following equation (31) was uset to scale Damage-level characterization factor from continental to local.

(31)

$$Local\ Damage-level\ characterization\ factor\ \left[\frac{DALYs}{kg_{emission}}\right]=DF_{EI99}\times\frac{LFF}{FF_{EI99}}\times\frac{PD_{local}}{PD_{EI99}}$$

Where:
LFF is *Local Fate Factor*, FF_{EI99} and PD_{EI99} values were obtained from Annex report *Eco-indicator 99* (Goedkoop and Spriensma, 2001) for substances having a *Carcinogens* (Annex report Table 4.1 pp 19-21), *Respiratory Inorganics* (Annex report Table 4.2 pg 28) and *Respiratory Organics* (Table 4.3) effects. For these last two categories, *Eco-indicator 99* method indicated only FF_{cont} values and not PD_{cont} ones. In this case the average of the population density values for all substances comprised in Carcinogens category was considered as value of PD_{cont}.
If the substance was only found in IMPACT 2002+ method and in *Carcinogens* impact category, a search in *Eco-Indicator 99* was performed in order to find a substance that had the closer value of *Damage Factor (DF)* to that of IMPACT 2002+ method and its *Fate Factor (FF)* and Population Density (PD) values were used.
If the substance was found only in IMPACT 2002+ method but in *Non-carcinogens* impact category (impact category not present in *Eco-Indicator 99*), a search in IMPACT 2002+ method was made in order to find a substance that had the closer value of *Damage Factor (DF)* to that of the substance

studied, and that was also present in *Carcinogens* impact category. Then the same theory to the previous point was applied.
The main assumption made is that DALY/cases is independent of population distribution (which in actual fact is not true). Moreover, since the complete formulation of the Damage Factor calculation would include three exposure pathways (air, drinking water and food) (section 7.1.3), with this formulation the approximate assumption was made that the three Local Icident Factors $\left(LIF_{air-air},\ LIF_{air-drinking\ water},\ LIF_{air-food}\right)$ are equal to $LIF_{air-air}$ was made.

7.3 Indoor emissions

7.3.1 Indoor emissions amount

It was assumed that part of the emissions produced (E_{prod}) remained indoors (E_{ind}) and another part (E_{asp}) passed through the filter placed before leaving the chimney.
The daily emission ($\mu gr \cdot d^{-1}$), upstream of the aspiration filter, was equal to:

$$E_{asp} \times \left(1 - e_{filtro}\right) = E_{tot,atm} \rightarrow E_{asp} = \frac{E_{tot,atm}}{1 - e_{filtro}} \quad (32)$$

$$E_{ind} = E_{prod} \times f_{ind} \quad (33)$$

$$E_{prod} = E_{ind} + E_{asp} = E_{prod} \times f_{ind} + E_{asp} \rightarrow E_{prod} = \frac{E_{asp}}{1 - f_{ind}} \quad (34)$$

Therefore indoor emission ($\mu gr \cdot d^{-1}$) was equal to:

$$E_{ind} = \frac{E_{asp}}{1 - f_{ind}} \cdot f_{ind} \quad (35)$$

where
E_{prod}: $total\ amount\ of\ emissions\ that\ are\ produced$ [$\mu gr \cdot d^{-1}$]
E_{asp}: $amount\ of\ emissions\ that\ passed\ through\ the\ filter\ before\ leaving\ the\ chiminery$ [$\mu gr \cdot d^{-1}$]
e_{filtro}: $filter\ efficiency$ [−](99%)
$E_{tot,atm}$: $amount\ of\ emissions\ that\ were\ relaesed\ in\ the\ atmosfere$ [$\mu gr \cdot d^{-1}$]
E_{ind}: $amount\ of\ indoor\ emissions$ [$\mu gr \cdot d^{-1}$]
f_{ind}: $fraction\ of\ indoor\ emissions$ [–]

7.3.2 Average indoor concentration

The average indoor concentration ($\bar{C}_{ind}[\mu gr \cdot m^{-3}]$) may be obtained from:

(36)

$$\bar{C}_{ind} = \frac{\frac{E_{ind}}{V_{p,work}}}{2}$$

where
E_{ind}: $amount\ of\ indoor\ emissions\ [\mu gr]$
$V_{p,work}$: $Workplace\ volume[-]$

7.3.3 Indoor Fate Factor

Indoor Fate Factor (IFF) may be obtained from:

(37)

$$IFF_{air}\ [(m^2 \cdot anno) \cdot m^{-3}] = \frac{\bar{C}_{ind}}{\frac{E_{ind} \times T}{A_{emit,indoor}}}$$

where
C_{ind}: $average\ indoor\ concentration\ in\ air\ [mg \cdot m^{-3}]$
E_{ind}: $emission\ in\ air\ reffered\ to\ Functional\ Unit\ [mg \cdot d^{-1}]$
T: $reference\ period\ [d \cdot yr^{-1}]$
$Aemit$: $emission\ area\ [m^2]$

7.3.4 Indoor Effect Factor

Indoor Effect Factor (IEF) may be obtained from:

(38)

$$Indoor\ Effect\ Factor\left[\frac{cases \cdot \mu gr^{-1} \cdot m^3}{yr \cdot m^2}\right] = \frac{UR}{70} \times PD_{indoor}$$

where
UR: $risk\ unit\ [cases \cdot \mu gr^{-1} \cdot m^3]$
LT: $time\ of\ average\ life\ of\ an\ individual\ [70\ yr](correction\ factor\ for\ UR\ according\ EcoIndicator99)$
PD_{indoor}: $indoor\ population\ density\ [person \cdot m^2]$

(39)

$$IIF\left[\frac{cases}{kg_{emission}}\right] = IEF \times 10^9 \times IFF$$

where
IEF: $Effect\ Factor\ at\ indoor\ scale\ [cases \cdot \mu gr^{-1} \cdot m^3 \cdot yr^{-1} \cdot m^{-2}]$
IFF: $Indoor\ Fate\ Factor\ [(m^2 \cdot anno) \cdot m^{-3}]$
10^9: $conversion\ factor\ [\mu gr \cdot kg^{-1}]$

Approximated method to calculate local and indoor emissions

7.3.5 Indoor Damage-level characterization factor

In order to move from continental scale to indoor one, the same formula used to calculate *Local Damage – level characterization factor* was used as reported hereafter:

$$Indoor\ Damage - level\ characterization\ factor\ \left[\frac{DALYs}{kg_{emission}}\right] = DF_{EI99} \times \frac{IFF}{FF_{EI99}} \times \frac{PD_{indoor}}{PD_{EI99}} \quad (40)$$

7.3.6 Total Damage

Total damage related to a chemical local and indoor emission may be obtained from:

$$D_{loc} = DF_{loc} \cdot E_{tot} \quad (41)$$

$$D_{ind} = DF_{ind} \cdot E_{tot} \quad (42)$$

where
D_{loc}: $total\ damage\ at\ local\ scale\ [DALYs]$
D_{ind}: $total\ damage\ at\ indoor\ scale\ [DALYs]$
DF_{loc}: $Local\ Damage - level\ characterization\ factor\ \left[DALYs \cdot kg_{emission}{}^{-1}\right]$
DF_{ind}: $Indoor\ Damage - level\ characterization\ factor\ \left[DALYs \cdot kg_{emission}{}^{-1}\right]$
E_{tot}: $total\ amount\ of\ chemical\ (emission)[kg]$

7.4 Remarcks

In this first phase only the air-air uptake was considered, since we considered that incidences due to air-drinking water and air-food uptakes were equal to air-air incidence. This is a very important approximation. Therefore a further implementation phase that takes these elements into consideration should be designed.

Furthermore, it seems that the local air dispersion model is completely independent of the physico-chemical properties of the pollutant. Therefore, specific inputs from other sources need to be used for background concentrations. It is important to understand how to combine the dispersion model with a model that takes into account the physical and chemical properties of the pollutant.

This is why an in depth study of the USEtox model was started to be carried out, as described in the following Chapter 8. In particular the equations on which USEtox Environmental Fate is based were accurately revised.

It would be important to consult all updated Eco-indicator 99 data needed to calculate the Damage Factor associated with local and indoor emissions for *Carcinogens*, *Respiratory Inorganics* and *Respiratory Organics* impact categories, using this approximated method. In particular, they would include: Fate Factor, Unit Risk factor, Population Density and Damage Factor for substances considered in *Carcinogens*, *Respiratory inorganics* and *Respiratory Organics* impact categories by the Eco-indicator 99 method.

It would also important to understand if the same data (Fate Factor, Unit Risk factor, Population Density and Damage Factor) are available for all substances considered by IMPACT 2002+ method (in *Carcinogens*, *Non-Carcinogens*, *Respiratory Inorganics*, *Respiratory Organics* impact categories), since this is the method in which LCA Working Group is implementing the calculated indoor and local damage factors, by adopting the approximated method previously described.

Chapter 8
Review of the USEtox method (Environmental Fate)

8 USETOX METHOD

USEtox is a consensus model developed within the Life Cycle Initiative led by the United Nations Environmental Program and the Society of Environmental Toxicology and Chemistry (UNEP - SETAC).

8.1 General framework

USEtox calculated characterization factors of contaminants for human toxicity and freshwater ecotoxicity. Assessing the toxicological effects of a contaminant emitted into the environment implied a cause-effect chain that links emissions to impacts through three calculation steps:

1. calculation of Fate Factor (FF);
2. calculation of Exposure Factor (EX);
3. calculation of Effect Factor (EF).

The characterization factor (CF) that is required for the calculation of impact score for either human or ecological impacts is generally defined as a combination of these three factors:

(43)

$$\overline{\boldsymbol{CF}} = \overline{\boldsymbol{FF}} \times \overline{\boldsymbol{EX}} \times \overline{\boldsymbol{EF}}$$

Fate Factor (FF) $[day]$ was the same for human toxicity and freshwater ecotoxicity.
For human toxicity assessment, the Exposure Factor (XF) expressed in $[day^{-1}]$, was calculated by an exposure model. This model described the effective human intake of a contaminant from a specific environmental medium (air, water, soil) through inhalation and ingestion. For freshwater ecotoxicity assessment, the Exposure Factor (XF) was dimensioneless and applied only to freshwater compartment. It expresses the fraction of the chemical within the freshwater compartment that is dissolved in water.
The modelling regarding the effect factors used the outcomes of the previous steps. The human Effect Factor (EF) $[cases/kg_{intake}]$ evaluated the change in lifetime disease probability due to the change of lifetime intake of a chemical. Effect factors were reported separately for carcinogenic and non-carcinogenic effects, as well as data for effects after inhalation and oral exposure. A set of three human health characterization factors could be reported, namely "*carcinogenic*", "*non-carcinogenic*" and "*total*", of which the latter was the sum of "*carcinogenic*" and "*non-carcinogenic*" effects. The ecotoxicological EF evaluated the change in the Potentially Affected Fraction (PAF) of species due to change in concentration ($\mathrm{PAF \cdot m^3 \cdot kg^{-1}}$).
Characterization factor for human toxicity impacts at midpoint level (human toxicity potential) was expressed in $[comparative\ toxic\ units\ (CTU_h)/kg_{emitted}]$, providing the estimated increase in

morbidity in the total human population per unit mass of an emitted contaminant. Due to a lack of more precise insights into this issue, an equal weighting between cancer and not cancer it was assumed.

(44)

$$[comparative\ toxic\ units\ (CTU_h)/kg_{emitted}] = [disease\ cases/kg_{emitted}]$$

Characterization factor for aquatic ecotoxicity impacts at midpoint level (ecotoxicity potential) was expressed in $[comparative\ toxic\ units\ (CTU_e)/kg_{emitted}]$, and provides an estimate of the potentially affected fraction of species (PAF) integrated over time and volume per unit mass of a chemical emitted.

(45)

$$[\boldsymbol{comparative\ toxic\ units\ (CTU_e)/kg_{emitted}}] = [\boldsymbol{PAF \cdot m^3 \cdot day/kg_{emitted}}]$$

These USEtox characterization factors were not normalized to a reference substance.
In order to determine the endpoint effects expressed as disability adjusted life years $(DALY)$ for human health impacts, it was necessary to determine the magnitude of the DALY related to a chemical emission. This involved the application of a weighting factor or damage factor to the disease cases that accounted for years of life lost and years of disabled life associated with that disease. For cancer effects, the relationship for 1 case = 11.5 DALY applied, while for non-cancer effects, the relationship for 1 case = 2.7 DALY applied (Huijbregts et al. 2005).
Determining the endpoint effects expressed as potentially disappeared fraction of species (PDF) for ecotoxicological impacts involved translation of the Potentially Affected Fraction (PAF) into PDF related to a chemical emission. Jolliet et al. 2003 proposed that PDF = 0.5 PAF.

8.2 USEtox - Environmental Fate - Compartments

8.2.1 Air compartment

In USEtox, air was treated as a homogeneous compartment.
Air compartment consisted of three sub-compartments:

1. gas phase;
2. areosol phase;
3. rain water phase.

8.2.1.1 Volume

The volume of the air compartment in the urban, continental and global scales $(V_{air[S]})$ might be obtained from:

(46)

$$\boldsymbol{V_{air[S]} = A_{[S]} \cdot h_{air[S]}} \quad \boldsymbol{[m^3]}$$

where
$A_{[S]} = urban, continental\ and\ global\ system\ area\ [m^2]$
$h_{air[S]} = mixed\ height\ of\ the\ urban, continental\ and\ global\ air\ [m]$

8.2.1.2 Calculation of total concentration of chemical

Total concentration of chemical in the air compartment in the urban, continental and global scales $(C_{tot,air[S]})$ might be obtained from:

(47)

$$\boldsymbol{C_{tot,air[S]} = C_{gas,air[S]} + C_{areosol,air[S]} + C_{rain\ water,air[S]}} \quad \boldsymbol{[kg \cdot m^{-3}]}$$

with
$C_{gas,air[S]}: total\ concentration\ in\ urban, continental\ and\ global\ gas\ phase\ [kg \cdot m^{-3}]$
$C_{areosol,air[S]}: total\ concentration\ in\ urban, continental\ and\ global\ areosol\ phase\ [kg \cdot m^{-3}]$
$C_{rain\ water,air[S]}: total\ concentration\ in\ urban, continental\ and\ global\ rain\ water\ phase\ [kg \cdot m^{-3}]$

8.2.1.3 Mass fraction of the organic chemical in the gas phase

The mass fraction of the organic chemical in the gas phase of air compartment in the urban, continental and global scales $(\boldsymbol{fr\_m_{gas,air\ [S]}})$ might be obtained from:

(48)

$$\boldsymbol{fr\_m_{gas,air\ [S]} = \frac{1}{1 + \left(\frac{K_{ow,app,pH7}}{K_{aw\ [S]} \cdot fr\_m_{cldw}}\right) \times fr\_V_{water,air\ [S]}}} \quad [-]$$

where
$K_{ow,app,pH7}: apparent\ \ octanol/water\ \ partition\ coefficient\ at\ neutral\ pH\ \ [-]$
$K_{aw}: dimensionless\ urban, continental\ and\ global\ \ air/water\ partition\ coefficient\ of\ \ original\ species\ [-]$
$fr\_m_{cldw}: mass\ fraction\ original\ species\ in\ cloud\ water\ [-]$
$fr\_V_{water,air\ [S]}: volume\ fraction\ water\ in\ the\ urban, continental\ and\ global\ air\ [-]$

8.2.1.4 Mass of original species in the cloud water

The mass fraction of original species in the cloud water (fr_m_{cldw}) might be obtained from:

a. if $\boldsymbol{pKa_{loss} < pKa_{gain}}$

(49)

$$\boldsymbol{fr\_m_{cldw}} = \frac{\mathbf{1}}{\mathbf{1} + \mathbf{10}^{(\boldsymbol{pKa_{loss}} - \boldsymbol{pH_{cloud}})} + \mathbf{10}^{(\boldsymbol{pH_{cloud}} - \boldsymbol{pKa_{gain}})}} \; [-]$$

b. If $\boldsymbol{pKa_{loss} \geq pKa_{gain}}$

(50)

$$\boldsymbol{fr\_m_{cldw}} = \frac{\mathbf{1}}{\mathbf{1} + \mathbf{10}^{(\boldsymbol{pKa_{gain}} - \boldsymbol{pH_{cloud}})} + \mathbf{10}^{(\boldsymbol{pH_{cloud}} - \boldsymbol{pKa_{loss}})}} \; [-]$$

where

pH_{cloud}: $pH\ cloud\ water$ [–]
pKa_{loss}: $equilibrium\ constant\ proton\ loss\ from\ conjugated\ acid\ of\ parent\ compound$ [–]
pKa_{gain}: $equilibrium\ constant\ proton\ loss\ from\ parent\ compound$ [–]

Demonstration of equation (49)

$pKa_{loss} = -\log Ka_{loss}$
$pKa_{gain} = -\log Ka_{gain}$

We suppose that:

$pKa_{loss} < pKa_{gain} \rightarrow -\log Ka_{loss} < -\log Ka_{gain} \rightarrow\ Ka_{loss} > Ka_{gain}$

It was supposed chemical was a diprotic acid, HA^-

(51)

$$\mathbf{H_2A} \rightleftarrows\ \mathbf{HA^-} + \mathbf{H^+} \rightleftarrows\ \mathbf{A^{2-}} + \mathbf{2H^+}$$

The first constant of dissociation is Ka_{loss} (equilibrium constant proton loss from parent compound (H_2A)), the second Ka_{gain} (equilibrium constant proton loss from conjugated acid of parent compound (H_2A)).

(52)

$$\boldsymbol{fr_{HA^-}} = \frac{[\mathbf{HA^-}]}{[\mathbf{A^{2-}}] + [\mathbf{HA^-}] + [\mathbf{H_2A}]}$$

By dividing the numerator and the denominator by $[\mathbf{HA^-}]$:

(53)

$$fr\_HA^- = \frac{[HA^-]}{[HA^-] + [A^{2-}] + [H_2A]} = \frac{1}{1 + \frac{[H_2A]}{[HA^-]} + \frac{[A^{2-}]}{[HA^-]}}$$

$$\frac{[A^{2-}]}{[HA^{-}]} = 10^{(pH-pKa_{gain})} \quad (54)$$

$$\frac{[H_2A]}{[HA^{-}]} = \frac{1}{10^{(pH-pKa_{loss})}} = 10^{(pKa_{loss}-pH)} \quad (55)$$

Then substituting terms (54) and (55) in equation (53):

$$fr\_HA^{-} = \frac{1}{1 + 10^{(pKa_{loss}-pH)} + 10^{(pH-pKa_{gain})}} \quad (56)$$

where $pH = pH_{cloud}$

Demonstration of equation (50)

It was supposed that:

$pKa_{loss} = pKa_{gain}$

or

$pKa_{loss} > pKa_{gain} \rightarrow -\log Ka_{loss} > -\log Ka_{gain} \rightarrow Ka_{loss} < Ka_{gain}$

It was supposed chemical is a diprotic acid, HA^{-}

$$H_2A \rightleftarrows HA^{-} + H^{+} \rightleftarrows A^{2-} + 2H^{+} \quad (57)$$

$$fr\_HA^{-} = 1 - \frac{1}{1 + 10^{(pKa_{loss}-pH)} + 10^{(pH-pKa_{gain})}} \quad (58)$$

$$fr\_HA^{-} = \frac{\cancel{1} + 10^{(pKa_{loss}-pH)} + 10^{(pH-pKa_{gain})} - \cancel{1}}{1 + 10^{(pKa_{loss}-pH)} + 10^{(pH-pKa_{gain})}} \quad (59)$$

By dividing the numerator and the denominator by $10^{(pKa_{loss}-pH)} + 10^{(pH-pKa_{gain})}$:

$$fr\_HA^{-} = \frac{1}{\frac{1}{10^{(pKa_{loss}-pH)} + 10^{(pH-pKa_{gain})}} + 1} \quad (60)$$

$$fr\_HA^{-} = \frac{1}{\frac{1}{10^{(pKa_{loss}-pH)} + 10^{(pH-pKa_{gain})}} + 1} \quad (61)$$

(62)

$$fr\_HA^- = \frac{1}{1 + 10^{(pKa_{gain} - pH)} + 10^{(pH - pKa_{loss})}}$$

where $pH = pH_{cloud}$

Equation (55) could be demonstrated.
All state functions may be expressed via chemical potential:

(63)

$$\mu_j = \left(\frac{\partial G}{\partial n_j}\right)_{T,P,n_{i \neq j}}$$

with
μ_j: *chemical potential of species j*
j: *species considered*
n_j: *number of moles of the species j*
n_i: *number of initial moles of the species j*
T: *temperature*
P: *pressur*

Chemical potential indicated how Gibbs free energy changes as a function of the added moles.
For each reaction

(64)

$$dG = \sum \mu_j \cdot n_j$$

In a chemical equilibrium:

(65)

$$dG = 0 = \sum \mu_j \cdot n_j$$

Therefore for the following reaction:

(66)

$$\mathrm{H_2A} \rightleftarrows \mathrm{HA^-} + \mathrm{H^+}$$

(67)

$$dG = (\mu_{H^+} \cdot n_{H^+}) + (\mu_{HA^-} \cdot n_{HA^-}) - (\mu_{H_2A} \cdot n_{H_2A})$$

(68)

$$\frac{d(dG)}{dn_j} = (\mu_{H^+}) + (\mu_{HA^-}) - (\mu_{H_2A})$$

$$dG = VdP - SdT \quad (69)$$

If T is constant,

$$dT = 0 \quad (70)$$

Then

$$dG = VdP \quad (71)$$

In the case of a gaseous species, according to the following ideal gas law:

$$PV = nRT \quad (72)$$

$$V = \frac{nRT}{P} \quad (73)$$

Thus

$$dG = \frac{nRT}{P}dP = \frac{RT}{P}dP \text{ (if n is constant)} \quad (74)$$

$$\Delta G = RT \cdot \int_{P_0}^{P_{finale}} \frac{dP}{P} = RT \ln\left(\frac{P_o}{P_{finale}}\right) \quad (75)$$

$P_o = 1\ atmosfere$

Therefore

$$\Delta G = RT \cdot \left(\ln P_{finale} - \ln 1\right) = RT \cdot \left(\ln P_{finale}\right) \quad (76)$$

$$\Delta\mu = RT \cdot \left(\ln P_{finale}\right) \quad (77)$$

$$\mu = \mu_0 + RT \cdot \left(\ln P_{finale}\right) \quad (78)$$

In chemical thermodynamics, activity (a) was a measure of the "effective concentration" of a species in a mixture.

It was given by the following equation where γ was activity coefficient and $[A]$ was the molar concentrationof the generic A species.

$$a = \gamma[A] \quad (79)$$

For an diluted solution, activity was equal to concentration.

$$a = [A] \quad (80)$$

$$\mu = \mu_0 + RT \cdot (\ln a) \quad (81)$$

Therefore

$$\mu_{H_2A} = \mu^0_{H_2A} + RT \ln\left(\gamma_{H_2A} \cdot [H_2A]\right) \quad (82)$$

$$\mu_{HA^-} = \mu^0_{HA^-} + RT \ln(\gamma_{HA^-} \cdot [HA^-]) \quad (83)$$

$$\mu_{H^+} = \mu^0_{H^+} + RT \ln(\gamma_{H^+} \cdot [H^+]) \quad (84)$$

$$\frac{dG}{dn} = \Delta_r G = (\mu_{H^+}) + (\mu_{HA^-}) - \left(\mu_{H_2A}\right) \quad (85)$$

$$\frac{dG}{dn} = \Delta_r G = \left(\mu^0_{H^+} + \mu^0_{HA^-} - \mu^0_{H_2A}\right) + RT \ln\left(\frac{\left((\gamma_{HA^-} \cdot [HA^-]) \cdot (\gamma_{H^+} \cdot [H^+])\right)}{\left(\gamma_{H_2A} \cdot [H_2A]\right)}\right) \quad (86)$$

$$\left(\mu^0_{H^+} + \mu^0_{HA^-} - \mu^0_{H_2A}\right) = \Delta_r G^0 \quad (87)$$

$$Ka = (\gamma_{H^+} \cdot [H^+]) \cdot \frac{[HA^-]}{[H_2A]} \cdot \frac{\gamma_{HA^-}}{\gamma_{H_2A}} \quad (88)$$

$$\gamma_{HA^-} \cong \gamma_{H_2A} \cong \gamma_{H^+} \cong 1 \quad (89)$$

(90)

$$Ka = ([H^+]) \cdot \frac{[HA^-]}{[H_2A]}$$

(91)

$$\log Ka = \log([H^+]) + \log\left(\frac{[HA^-]}{[H_2A]}\right)$$

(92)

$$\log\left(\frac{[HA^-]}{[H_2A]}\right) = \log Ka - \log([H^+]) = -pKa + pH$$

(93)

$$\frac{[HA^-]}{[H_2A]} = 10^{(pH-pKa)}$$

Therefore

(94)

$$\left(\frac{[HA^-]}{[H_2A]}\right)^{-1} = \frac{1}{10^{(pH-pKa)}}$$

Therefore

(95)

$$\frac{[H_2A]}{[HA^-]} = 10^{(pKa-pH)}$$

8.2.1.5 Mass fraction of the inorganic chemical in the gas phase

Inorganic chemicals are non-volatile, therefore the mass fraction of chemical in the urban, continental and global gas phase $(fr\_m_{gas,air[S]})$ was zero:

(96)

$$fr\_m_{gas,air[S]} = 0 \quad [-]$$

8.2.1.6 Air flows between different scales

As depicted in Figure 8-1, there were the following airflows between the different scales:

1. air flows from the urban scale to the continental scale;
2. air flow from the continental to the urban and global scale and back from the global to the continental scale;
3. air flow from indoor module to urban and continental scale.

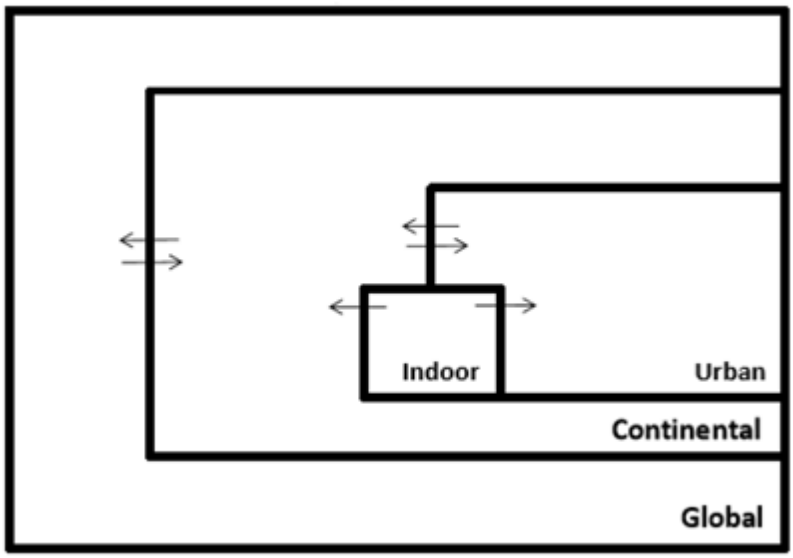

Figure 8-1 Airflow between the scales and compartments (Reproduced from USEtox 2.0 Documentation)

Each air flow was characterized by transfer rate constant (k) $[h^{-1}]$.
It was the reciprocal of residence time τ (Mackay 2001):

$$k = \frac{1}{\tau} \quad (97)$$

According to Mackay 2001, total k rate $[k_{total}]$ for the compartment characterized by "n" air flows, might be obtained from:

$$k_{total} = k_1 + k_2 + \cdots k_n \quad (98)$$

Transfer rate of urban air to continental air $\left[k_{air[U\rightarrow C]}\ [d^{-1}]\right]$ might be obtained from:

$$k_{air[U\rightarrow C]} = \frac{1}{\tau_{air[U]}} \quad (99)$$

where

$\tau_{air[U]} = residence\ time\ of\ the\ air\ in\ urban\ air\ compartment\ [day]$

Transfer rate of continental air to urban air $\left[k_{air[C\to U]}\ [d^{-1}]\right]$might be obtained from:

(100)

$$k_{air[C\to U]} = \frac{\frac{V_{air[U]}}{\tau_{air[U]}}}{V_{air[C]}} \quad [d^{-1}]$$

where
$k_{air[C\to U]} = transfer\ rate\ of\ continental\ air\ to\ urban\ air\ [d^{-1}]$
$V_{air[U]} = volume\ of\ the\ urban\ air\ [m^3]$
$\tau_{air[U]} = residence\ time\ of\ the\ air\ in\ urban\ air\ compartment\ [day]$
$V_{air[C]} = volume\ of\ the\ continental\ air\ [m^3]$

Demonstration equation (100)
Generally, flow (Q) was equal to:

(101)

$$Q = kV\ [m^3 \cdot day^{-1}]$$

with
$Q: flow\ [m^3 \cdot day^{-1}]$
$k: transfer\ rate\ of\ compartment\ under\ study\ [d^{-1}]$
$V: volume\ of\ compartment\ under\ study\ [m^3]$

For mass balance, air flow transferred in the unit of time $[day]$ from continental air compartment to urban air compartment will be equal to air flow transferred in the unit of time $[day]$ from urban air compartment to continental air compartment.

(102)

$$k_{air[U\to C]} \times V_{air[U]} = \frac{V_{air[U]}}{\tau_{air[U]}} = k_{air[C\to U]} \times V_{air[C]} \to k_{air[C\to U]} = \frac{\frac{V_{air[U]}}{\tau_{air[U]}}}{V_{air[C]}} \quad [d^{-1}]$$

Transfer rate of continental air to global air $k_{air[C\to G]}\ [d^{-1}]$ might be obtained from:

(103)

$$k_{air[C\to G]} = \frac{1}{\tau_{air[C]}} - k_{air[C\to U]} \quad [d^{-1}]$$

where
$k_{air[C\to G]} = transfer\ rate\ of\ continental\ air\ to\ global\ air\ [d^{-1}]$
$\tau_{air[C]} = residence\ time\ of\ air\ in\ continental\ air\ compartment\ [d]$
$k_{air[C\to U]} = transfer\ rate\ of\ continental\ air\ to\ urban\ air\ [d^{-1}]$

Demonstration of equation (103)

According to equation (98):

$$k_{air[C]} = k_{air\,[C\rightarrow U]} + k_{air\,[C\rightarrow G]} \quad (104)$$

Therefore

$$k_{air\,[C\rightarrow G]} = k_{air[C]} - k_{air\,[C\rightarrow U]} \quad (105)$$

$$k_{air[C]} = \frac{1}{\tau_{air[C]}} \quad (106)$$

Thus by substituting equation (106) in equation (105):

$$k_{air\,[C\rightarrow G]} = \frac{1}{\tau_{air[C]}} - k_{air\,[C\rightarrow U]} \quad (107)$$

Transfer rate of global air to continental air $\left[k_{air[G\rightarrow C]}\ [d^{-1}]\right]$ might be obtained from:

$$\boldsymbol{k_{air\,[G\rightarrow C]} = \frac{\frac{V_{air[C]}}{\tau_{air[C]}} - \frac{V_{air[U]}}{\tau_{air[U]}}}{V_{air[G]}}\ [d^{-1}]} \quad (108)$$

where

$V_{air[C]} = volume\ of\ the\ continental\ air\ [m^3]$

$V_{air[U]} = volume\ of\ the\ urban\ air\ [m^3]$

$V_{air[G]} = volume\ of\ the\ global\ air\ [m^3]$

$\tau_{air[C]} = residence\ time\ of\ the\ air\ in\ continental\ air\ compartment\ [d]$

$\tau_{air[U]} = residence\ time\ of\ the\ air\ in\ urban\ air\ compartment\ [d]$

Demonstration of equation (108)

For mass balance, air flow transferred in the unit of time $[day]$ from continental air compartment to global air compartment will be equal to air flow in the continental air compartment except air flow transferred in the unit of time $[day]$ from continental scale to urban scale.

Therefore

$$V_{air[C]} \times k_{air\,[C\rightarrow G]} = V_{air[C]} \times k_{air[C]} - V_{air[C]} \times k_{air\,[C\rightarrow U]} = V_{air[G]} \times k_{air\,[G\rightarrow C]} \quad (109)$$

For equation (102)

(110)

$$k_{air[C\rightarrow U]} \times V_{air[C]} = \frac{V_{air[U]}}{\tau_{air[U]}}$$

According to Mackay (2001):

(111)

$$k_{air[C]} = \frac{1}{\tau_{air\,[C]}}$$

Therefore substituting equation (110) and (111) in the equation (109):

(112)

$$V_{air[G]} \times k_{air\,[G\rightarrow C]} = V_{air[C]} \times \frac{1}{\tau_{air\,[C]}} - \frac{V_{air[U]}}{\tau_{air[U]}} \rightarrow k_{air\,[G\rightarrow C]} = \frac{\frac{V_{air[C]}}{\tau_{air[C]}} - \frac{V_{air[U]}}{\tau_{air[U]}}}{V_{air[G]}}$$

The process of exchange of air flows between different scales was based on advection processes such as wind transport. The advection process could remove a substance from the modelled system due to the wind transport. The advection process was characterized by a transfer rate $\left[k_{adv}\,[day^{-1}]\right]$.

(113)

$$\tau_{air[S]} = \frac{1}{k_{adv[S]}}$$

with
$\tau_{air[S]} = residence\ time\ in\ urban, continental\ and\ global\ air\ [s^{-1}]$

For urban and continental scales:

(114)

$$\tau_{air[S]} = cf_{\tau,air[S]} \times \frac{1}{k_{adv[S]}} = cf_{\tau,air[S]} \times \left(\frac{\left(\frac{\sqrt{A_{[S]}}}{u_{[S]}}\right)}{(3600 \times 24)} \right)$$

with
$cf_{\tau,air[S]} = correction\ factor\ of\ urban, continental\ and\ global\ air\ residence\ time\ [-]$
$u_{[S]} = urban\ and\ continental\ wind\ speed\ [m \cdot s^{-1}]$
$A_{[S]} = urban\ and\ continental\ [m^2]$
$(3600 \times 24) = conversion\ factor\ [s \cdot d^{-1}]$

"$cf_{\tau,air[S]}$" rappresented the correction factor to account for the fact that: (i) a pollutant could be emitted anywhere in the i^{th} urban area and not only along the up-wind periphery, and (ii) the air that left the i^{th} urban area could return with some of the pollutant (i.e., a back-and-forth movement of air) (Humbert S, 2011).

Demonstration of equation (114)

(115)

$$k_{adv[S]} = \frac{Q}{V_{air[S]}} = \frac{u_{[S]} \times dA_{[S]}}{A_{[S]} \times h_{air[S]}} = \frac{u_{[S]} \times \sqrt{A_{[S]}} \times \int_0^{h_{air[S]}} dh_{air[S]}}{A_{[S]} \times h_{air[S]}}$$

where

$Q = flow\ [m^3 \cdot s^{-1}]$

$V_{air[S]} = volume\ of\ the\ urban\ and\ continental\ air\ [m^3]$

$A_{[S]} = urban\ and\ continental\ [m^2]$

$h_{air[S]} = mixed\ height\ of\ urban\ and\ continental\ [m]$

$u_{[S]} = urban\ and\ continental\ wind\ speed\ [m \cdot s^{-1}]$

By substituting the term (115) in the equation (114), the following equations might be obtained:

(116)

$$\tau_{air[S]} = cf_{\tau,air[S]} \times \left(\frac{\left(\frac{A_{[S]} \times h_{air[S]}}{u_{[S]} \times \sqrt{A_{[S]}} \times \int_0^{h_{air[S]}} dh_{air[S]}} \right)}{(3600 \times 24)} \right) = cf_{\tau,air[S]} \times \left(\frac{\left(\frac{A_{[S]} \times h_{air[S]}}{u_{[S]} \times \sqrt{A_{[S]}} \times h_{air[S]}} \right)}{(3600 \times 24)} \right)$$

$$= cf_{\tau,air[S]} \times \left(\frac{\left(\frac{\sqrt{A_{[S]}}}{u_{[S]}} \right)}{(3600 \times 24)} \right)$$

8.2.2 Water compartment

Only at the continental and global scale two water compartments were present, namely ***freshwater compartment*** and ***sea water compartment.***
The water compartments were treated as homogeneus boxes, consisting of a suspended matter phase, a dissolved (colloidal) organic carbon (DOC) phase and a biota phase. The fate of chemicals was influenced by presence of suspended matter, *DOC* and biota in a very similar way to that of aerosols and rain water in the atmosphere. These phases bound the chemical, thus inhibiting it from taking part in mass transfer and degradation processes occurring in the water phase. Suspended matter acted as a physical carrier of the chemical across the sediment-water interface.

8.2.2.1 Volume of fresh and sea water

The volume of freshwater and sea water compartments in the continental and global scales might be obtained from:

(117)

$$V_{w[S]} = fr\_A_{w[S]} \cdot A_{[S]} \cdot h_{w[S]}$$

where
$V_{w[S]} = volume\ of\ the\ continental\ and\ global\ fresh\ and\ sea\ water\ [m^3]$
$fr\_A_{w[S]} = area\ fraction\ of\ continental\ and\ global\ fresh\ and\ sea\ water\ [-]$
$A_{[S]} = continental\ and\ global\ system\ area\ [m^2]$
$h_{w[S]} = mixed\ depth\ of\ the\ continental\ and\ global\ fresh\ and\ sea\ water\ [m]$

(118)

$$A_{[S]} = A_{land[S]} + A_{w[S]}$$

where

(119)

$$A_{land[S]} = A_{land,nsl[S]} + A_{land,asl[S]} = A_{land[S]} \cdot fr\_A_{land,nsl[S]} + A_{land[S]} \cdot fr\_A_{land,asl[S]}$$

(120)

$$A_{w[S]} = A_{land,fw[S]} + A_{land,sea[S]} = A_{land[S]} \cdot fr\_A_{land,fw[S]} + A_{land[S]} \cdot fr\_A_{land,sw[S]}$$

where
$A_{land[S]} = area\ of\ continental\ and\ global\ land\ [m^2]$
$A_{land,nsl[S]} = area\ of\ continental\ and\ global\ natural\ soil\ [m^2]$
$A_{land,asl[S]} = area\ of\ continental\ and\ global\ agricoltural\ soil\ [m^2]$
$A_{w[S]} = area\ of\ continental\ and\ global\ water\ [m^2]$
$A_{land,fw[S]} = area\ of\ continental\ and\ global\ fresh\ water\ [m^2]$
$A_{land,sw[S]} = area\ of\ continental\ and\ global\ sea\ water\ [m^2]$
$fr\_A_{land,nsl[S]} = fraction\ of\ continental\ and\ global\ natural\ soil\ [-]$
$fr\_A_{land,asl[S]} = fraction\ of\ continental\ and\ global\ agricoltural\ soil\ [-]$
$fr\_A_{land,fw[S]} = fraction\ of\ continental\ and\ global\ fresh\ water\ [-]$
$fr\_A_{land,sw[S]} = fraction\ of\ continental\ and\ global\ sea\ water\ [-]$

The area fraction of freshwater $\left[fr\_A_{fw[S]}\right]$ might be obtained from:

$$fr\_A_{fw[S]} = \frac{A_{land[S]} \cdot fr\_A_{land,fw[S]}}{A_{[S]}} \quad (121)$$

The area fraction of natural soil $\left[fr\_A_{nsl[S]}\right]$ might be obtained from:

$$fr\_A_{nsl[S]} = \frac{A_{land[S]} \cdot fr\_A_{land,nsl[S]}}{A_{[S]}} \quad (122)$$

The area fraction of agricoltural soil $\left[fr\_A_{asl[S]}\right]$ might be obtained from:

$$fr\_A_{asl[S]} = \frac{A_{land[S]} \cdot fr\_A_{land,asl[S]}}{A_{[S]}} \quad (123)$$

where

$A_{land[S]} = area\ of\ continental\ and\ global\ area\ [m^2]$
$fr\_A_{fw[S]} = area\ fraction\ of\ continental\ and\ global\ fresh\ water\ [-]$
$fr\_A_{nsl[S]} = area\ fraction\ of\ continental\ and\ global\ natural\ soil\ [-]$
$fr\_A_{asl[S]} = area\ fraction\ of\ continental\ and\ global\ agricoltural\ soil\ [-]$
$A_{[S]} = continental\ and\ global\ system\ area\ [m^2]$

The area fraction of sea water $\left[fr\_A_{sw[S]}\right]$ might be obtained from:

$$fr\_A_{sw[S]} = 1 - fr\_A_{fw[S]} - fr\_A_{nsl[S]} - fr\_A_{asl[S]} \quad (124)$$

where

$fr\_A_{fw[S]} = area\ fraction\ of\ continental\ and\ global\ fresh\ water\ [-]$
$fr\_A_{nsl[S]} = area\ fraction\ of\ continental\ and\ global\ natural\ soil\ [-]$
$fr\_A_{asl[S]} = area\ fraction\ of\ continental\ and\ global\ agricoltural\ soil\ [-]$

Demonstration of equation (124)

$$fr\_A_{sw[S]} = \frac{A_{sea[S]}}{A_{[S]}} = \frac{A_{[S]} - A_{land[S]}}{A_{[S]}} = 1 - \frac{A_{land[S]}}{A_{[S]}} \quad (125)$$

$$= 1 - \frac{A_{land[S]} \cdot fr\_A_{land,fw[S]}}{A_{[S]}} - \frac{A_{land[S]} \cdot fr\_A_{land,nsl[S]}}{A_{[S]}} - \frac{A_{land[S]} \cdot fr\_A_{land,asl[S]}}{A_{[S]}}$$

From equations (121), (122) and (123):

$$\frac{A_{land[S]} \cdot fr\_A_{land,fw[S]}}{A_{[S]}} = fr\_A_{fw[S]}$$

$$\frac{A_{land[S]} \cdot fr\_A_{land,nsl[S]}}{A_{[S]}} = fr\_A_{nsl[S]}$$

$$\frac{A_{land[S]} \cdot fr\_A_{land,asl[S]}}{A_{[S]}} = fr\_A_{asl[S]}$$

Substituting terms in equation (125):

$$fr\_A_{sw[S]} = 1 - fr\_A_{fw[S]} - fr\_A_{nsl[S]} - fr\_A_{asl[S]} \quad (126)$$

8.2.2.2 Mass fraction of the chemical dissolved in fresh water and sea water

The fraction of chemical dissolved in continental and global fresh and sea water $[fr\_m_{diss,w[S]}]$ might be obtained from:

$$fr\_m_{diss,w[S]} = \frac{1}{1 \times \left(1 + K_{susp|w,w[S]} \times \frac{C_{susp,w[S]}}{1000} + K_{DOC|w,w[S]} \times \frac{C_{DOC,w[S]}}{1000} + BCF_{fish,w[S]} \times \frac{C_{bio,w[S]}}{1000}\right)} \quad (127)$$

where

$fr\_m_{diss,w[S]}$: $fraction\ of\ the\ chemical\ dissolved\ in\ continental\ and\ global\ fresh\ and\ sea\ water$ $[-]$

$K_{susp|w,w[S]}$: $suspended\ solids/water\ \ partition\ coefficient\ in\ continental\ and\ global\ fresh\ and\ sea\ water$ $[L/kg]$

$C_{susp,w[S]}$: $concentration\ of\ suspended\ matter\ in\ continental\ and\ global\ fresh\ and\ sea\ water$ $[kg/m^3]$

$K_{DOC|w,w[S]}$: $dissolved\ organic\ carbon/water\ \ partition\ coefficient\ in\ continental\ and\ global\ fresh\ and\ sea\ water$ $[L/kg]$

$C_{DOC,w[S]}$: $concentration\ of\ dissolved\ organic\ carbon\ in\ continental\ and\ global\ fresh\ and\ sea\ water$ $[kg/m^3]$

$BCF_{fish,w[S]}$: $bioconcentration\ factor\ for\ continental\ and\ global\ fresh\ and\ sea\ water$ $[L/kg]$

$C_{bio,w[S]}$: $concentration\ of\ biota\ in\ continental\ and\ global\ fresh\ and\ sea\ water$ $[kg/m^3]$

Demonstration of equation (127)

$$fr\_m_{diss,w[S]} = \frac{m_{diss,w\,[S]}}{m_{tot\,[S]}} = \frac{m_{diss,w\,[S]}}{m_{diss,w\,[S]} + m_{susp,w\,[S]} + m_{DOC,w\,[S]} + m_{bio,w\,[S]}} \quad (128)$$

$$= \frac{m_{diss,w\,[S]}}{m_{diss,w\,[S]} \times \left(1 + \frac{m_{susp,w\,[S]}}{m_{diss,w\,[S]}} + \frac{m_{DOC,w\,[S]}}{m_{diss,w\,[S]}} + \frac{m_{bio,w\,[S]}}{m_{diss,w\,[S]}}\right)}$$

By dividing the numerator and the denominator by $m_{diss,w\,[S]}$:

(129)

$$fr\_m_{diss,w[S]} = \frac{1}{1 \times \left(1 + \frac{m_{susp,w\,[S]}}{m_{diss,w\,[S]}} + \frac{m_{DOC,w\,[S]}}{m_{diss,w\,[S]}} + \frac{m_{bio,w\,[S]}}{m_{diss,w\,[S]}}\right)}$$

(130)

$$m_{diss,w\,[S]} = C_{diss,w[S]} \times V_{w[S]}$$

(131)

$$m_{susp,w\,[S]} = C_{susp,w[S]} \times M_{susp,w[S]}$$

(132)

$$m_{DOC,w\,[S]} = C_{doc,w[S]} \times M_{DOC,w[S]}$$

(133)

$$m_{bio,w\,[S]} = C_{bio,w[S]} \times M_{bio,w[S]}$$

with

$m_{diss,w\,[S]}$: $mass\ of\ chemical\ dissolved\ in\ continental\ and\ global\ fresh\ and\ sea\ water\ [mg]$
$C_{diss,w[S]}$: $concentration\ of\ the\ chemical\ dissolved\ in\ continental\ and\ global\ fresh\ and\ sea\ water\ [mg/L]$
$V_{w[S]}$: $volume\ of\ continental\ and\ global\ fresh\ and\ sea\ water\ [m^3]$
$m_{susp,w\,[S]}$: $mass\ of\ chemical\ in\ suspended\ matter\ in\ continental\ and\ global\ fresh\ and\ sea\ water\ [mg]$
$C_{susp,w[S]}$: $cocentration\ of\ the\ chemical\ in\ suspended\ matter\ in\ continental\ and\ global\ fresh\ and\ sea\ water\ [mg/kg]$
$M_{susp,w[S]}$: $mass\ of\ suspended\ matter\ in\ continental\ and\ global\ fresh\ and\ sea\ water\ [kg]$
$m_{DOC,w\,[S]}$: $mass\ of\ dissolved\ organic\ carbon\ in\ continental\ and\ global\ fresh\ and\ sea\ water\ [mg]$
$C_{DOC,w[S]}$: $chemical\ cocentration\ in\ dissolved\ organic\ carbon\ in\ continental\ and\ global\ fresh\ and\ sea\ water\ [mg/kg]$
$M_{DOC,w[S]}$: $mass\ of\ dissolved\ organic\ carbon\ in\ continental\ and\ global\ fresh\ and\ sea\ water\ [kg]$
$m_{bio,w\,[S]}$: $mass\ of\ biota\ in\ continental\ and\ global\ fresh\ and\ sea\ water\ [mg]$
$C_{bio,w[S]}$: $cocentration\ of\ the\ chemical\ in\ biota\ in\ continental\ and\ global\ fresh\ and\ sea\ water\ [mg/kg]$
$M_{bio,w[S]}$: $mass\ of\ biota\ in\ continental\ and\ global\ fresh\ and\ sea\ water\ [kg]$

By subtituting (130), (131), (132) and (133) in equation (129):

(134)

$$fr\_m_{diss,w[S]} = \frac{1}{1 \times \left(1 + \frac{C_{susp,w[S]} \times M_{susp,w[S]}}{C_{diss,w[S]} \times V_{w[S]}} + \frac{C_{DOC,w[S]} \times M_{DOC,w[S]}}{C_{diss,w[S]} \times V_{w[S]}} + \frac{C_{bio,w[S]} \times M_{bio,w[S]}}{C_{diss,w[S]} \times V_{w[S]}}\right)}$$

$$= \frac{1}{1 \times \left(1 + \frac{C_{susp,w[S]}}{C_{diss,w[S]}} \times \frac{M_{susp,w[S]}}{V_{w[S]} \times 1000} + \frac{C_{DOC,w[S]}}{C_{diss,w[S]}} \times \frac{M_{DOC,w[S]}}{V_{w[S]} \times 1000} + \frac{C_{bio,w[S]}}{C_{diss,w[S]}} \times \frac{M_{bio,w[S]}}{V_{w[S]} \times 1000}\right)}$$

$$= \frac{1}{1 \times \left(1 + K_{susp|w,w[S]} \times \frac{C_{susp,w[S]}}{1000} + K_{DOC|w,w[S]} \times \frac{C_{DOC,w[S]}}{1000} + BCF_{fish,w[S]} \times \frac{C_{bio,w[S]}}{1000}\right)}$$

8.2.2.3 Mass of original species in the water

The mass fraction of original species in water (fr_m_w) might be obtained from:

a. if $\boldsymbol{pKa_{loss} < pKa_{gain}}$

(135)

$$\boldsymbol{fr\_m_w = \frac{1}{1 + 10^{(pKa_{loss} - pH_w)} + 10^{(pH_w - pKa_{gain})}}} \; [-]$$

b. If $\boldsymbol{pKa_{loss} \geq pKa_{gain}}$

(136)

$$\boldsymbol{fr\_m_w = \frac{1}{1 + 10^{(pKa_{gain} - pH_w)} + 10^{(pH_w - pKa_{loss})}}} \; [-]$$

where

pH_w: $pH\ fresh\ and\ sea\ water$ [-]

pKa_{loss}: $equilibrium\ constant\ proton\ loss\ from\ conjugated\ acid\ of\ parent\ compound$ [−]

pKa_{gain}: $equilibrium\ constant\ proton\ loss\ from\ parent\ compound$ [−]

For demonstration see equations (49) and (50).

8.2.2.4 Water flows between different scales

The freshwater compartment exchanged water flows with sea compartment at the continental and global scale. Freshwater at continental scale exchanged water flow with fresh water at global scale. There was also water flow from global freshwater compartment to continental fresh water.

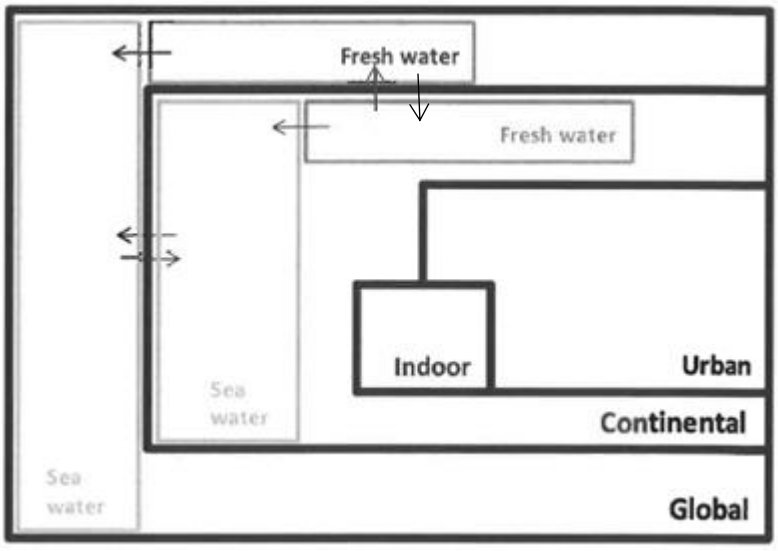

Figure 8-2 Water flows between compartments at different scales (Reproduced from USEtox 2.0 Documentation)

8.2.2.4.1 Water flows between fresh water and sea water compartment at different scales

The transfer rate from continental and global fresh water to continental and global sea water $\left[k_{fw\rightarrow sw[S]}\right]$ was equal to:

(137)

$$\left[k_{fw\rightarrow sw[S]}\right] = \frac{Q_{des,fw\rightarrow sw[S]}}{V_{fw[S]}} \cdot (3600 \cdot 24) \quad [day^{-1}]$$

where

$Q_{des,fw\rightarrow sw[S]}$: $flow\ from\ continental\ and\ global\ fresh\ water\ to\ continental\ and\ global\ sea\ water$ $[m^3 \cdot s^{-1}]$
$V_{w[S]}$: $volume\ of\ continental\ and\ global\ fresh\ water$ $[m^3]$
$(3600 \cdot 24)$: $conversion\ factor$ $[s \cdot day^{-1}]$

At the continental scale there was a water flow from continental freshwater to continental sea water. At the continental scale, the water input $\left(I_{fw[C]}[m^3 \cdot s^{-1}]\right)$ in the freshwater compartment was due to:

1. rain input $\left(Q_{rain,air\rightarrow fw[C]}\ [m^3 \cdot s^{-1}]\right)$;
2. runoff from continental natural soil $\left(Q_{runoff,water,nsl[C]}\ [m^3 \cdot s^{-1}]\right)$;
3. runoff from continental agricoltural soil $\left(Q_{runoff,water,asl[C]}\ [m^3 \cdot s^{-1}]\right)$.

Therefore,

(138)

$$I_{fw[C]} = \left(Q_{rain,air\rightarrow fw[C]} + Q_{runoff,water,nsl[C]} + Q_{runoff,water,asl[C]}\right)\ [m^3 \cdot s^{-1}]$$

The freshwater compartment at the continental scale exchanged water flow with freshwater compartment at the global scale and sea water compartment at the continental scale. The discharged fraction of continental freshwater to global scale was equal to $\left(fr\_M_{disc,fw[C\rightarrow G]}\ [-]\right)$. Therefore the flow from continental fresh water to continental sea water $\left(Q_{des,fw\rightarrow sw[C]}\ [m^3 \cdot s^{-1}]\right)$ might be obtained to:

(139)

$$Q_{des,fw\rightarrow sw[C]} = I_{fw[C]} \times \left(1 - fr\_M_{disc,fw[C\rightarrow G]}\right)\ [m^3 \cdot s^{-1}]$$

The **rain input** into fresh water and sea water at continental and global scale might be obtained from:

(140)

$$Q_{rain,air\rightarrow w[S]} = v_{rain[S]} \times fr\_A_{w[S]} \times A_{[S]}\ [m^3 \cdot s^{-1}]$$

with

$v_{rain[S]}$: $annual\ average\ precipitation\ on\ continental\ and\ global\ scale$ $[m \cdot s^{-1}]$
$fr\_A_{w[S]}$: $area\ fraction\ of\ continental\ and\ global\ fresh\ water\ and\ sea\ water$ $[-]$
$A_{[S]}$: $continental\ and\ global\ system\ area$ $[m^2]$

The volume fraction of water **runoff** from continental and global natural and agricultural soil $\left(fr\_V_{rain,runoff,sl[S]}\ [-]\right)$ was a part of total water input volume on the continental and global natural

and agricultural soil. The total water input volume on the soil $\left(V_{inpu,sl[S]}\ [m^3]\right)$ might be obtained by:

$$V_{input,sl[S]} = V_{runoff,water,sl[S]} + V_{infiltrating,water,sl[S]} \quad (141)$$

where:

$V_{runoff,water,sl[S]}$: $volume\ of\ water\ runoff\ at\ continental\ and\ global\ natural\ and\ agricultural\ soil\ [m^3]$

$V_{infiltr.,water,sl[S]}$: $volume\ of\ water\ infiltrating\ at\ continental\ and\ global\ natural\ and\ agricultural\ soil\ [m^3]$

Therefore

$$fr\_V_{rain,runoff,sl\,[S]} = \frac{V_{runoff,water,sl[S]}}{V_{runoff,water,sl[S]} + V_{infiltrating,water,sl[S]}} \quad (142)$$

The water runoff from continental and global natural and agricultural soil might be obtained from:

$$Q_{runoff,water,sl\,[S]} = fr\_A_{sl\,[S]} \times fr\_V_{rain,runoff,sl\,[S]} \times v_{rain[S]} \times A_{[S]} \quad (143)$$

where

$Q_{runoff,water,sl\,[S]}$: $water\ runoff\ from\ continental\ and\ global\ natural\ and\ agricultural\ soil\ [m^3 \cdot s^{-1}]$

$fr\_A_{sl\,[S]}$: $area\ fraction\ of\ continental\ and\ global\ natural\ and\ agricultural\ soil\ [-]$

$fr\_V_{rain,runoff,sl\,[S]}$: $volume\ fraction\ of\ water\ runoff\ from\ continental\ and\ global\ natural\ and\ agricultural\ soil\ [-]$

$v_{rain[S]}$: $annual\ average\ precipitation\ on\ continental\ and\ global\ scale\ [m \cdot s^{-1}]$

$A_{[S]}$: $continental\ and\ global\ system\ area\ [m^2]$

For the flow from continental sea water to global sea water:

$$\left[k_{adv,sw[C\to G]}\right] = \frac{Q_{adv,sw[C\to G]}}{V_{sw[S]}} \cdot (3600 \cdot 24) \quad [day^{-1}] \quad (144)$$

where

$Q_{adv,sw[C\to G]}$: $flow\ of\ continental\ and\ global\ sea\ water\ to\ the\ global\ ocean\ [m^3 \cdot s^{-1}]$

$V_{sw[S]}$: $volume\ of\ continental\ and\ global\ sea\ water\ [m^3]$

$(3600 \cdot 24)$: $conversion\ factor\ [s \cdot day^{-1}]$

The flow of continental sea water to the global sea water might be obtained from:

$$Q_{adv,sw[C\to G]} - Q_{adv,sw[G\to C]} = Q_{rain,air\to sw[C]} + Q_{des,fw\to sw[C]} \quad (145)$$

$$Q_{adv,sw[C\to G]} = Q_{rain,air\to sw[C]} + Q_{des,fw\to sw[C]} + Q_{adv,sw[G\to C]} \quad (146)$$

where

$Q_{adv,sw[C\to G]}$: $flow\ of\ continental\ sea\ water\ to\ the\ global\ ocean\ [m^3 \cdot s^{-1}]$

$Q_{rain,air\to sw[C]}$: $rain\ input\ into\ continental\ sea\ water\ [m^3 \cdot s^{-1}]$

$Q_{des,fw\to sw[C]}$: $flow\ of\ continental\ fresh\ water\ to\ sea\ water\ [m^3 \cdot s^{-1}]$

$Q_{adv,sw[G\to C]}$: $flow\ of\ global\ sea\ water\ to\ continental\ sea\ water\ [m^3 \cdot s^{-1}]$

The fresh water compartment at global scale exchanged water flow with global sea water.
The flow of global fresh water to global sea water might be obtained from:

(147)

$$Q_{des,fw\rightarrow sw[G]} = I_{fw[G]} \times \left(1 - fr\_M_{disc,fw[G\rightarrow C]}\right)$$

where
$Q_{des,fw\rightarrow sw[G]}$: $flow\ of\ global\ fresh\ water\ to\ global\ sea\ water$ $[m^3 \cdot s^{-1}]$
$I_{fw[G]}$: $rain\ input\ into\ global\ fresh\ water$ $[m^3 \cdot s^{-1}]$
$fr\_M_{disc,fw[G\rightarrow C]}$: $discharged\ fraction\ \ global\ fresh\ water\ to\ continental\ sea\ water$ [–]

At global scale, as continental scale, the water input $\left(I_{fw[G]}[m^3 \cdot s^{-1}]\right)$ in the freshwater compartment was due to:

1. rain input $\left(Q_{rain,air\rightarrow fw[G]}\ [m^3 \cdot s^{-1}]\right)$;
2. runoff from continental natural soil $\left(Q_{runoff,water,nsl[G]}\ [m^3 \cdot s^{-1}]\right)$;
3. runoff from continental agricoltural soil $\left(Q_{runoff,water,asl[G]}\ [m^3 \cdot s^{-1}]\right)$.

Therefore,

(148)

$$I_{fw[G]} = \left(Q_{rain,air\rightarrow fw[G]} + Q_{runoff,water,nsl[G]} + Q_{runoff,water,asl[G]}\right)$$

For the flow from global sea water to continental sea water:

(149)

$$\left[k_{adv,sw[G\rightarrow C]}\right] = \frac{Q_{adv,sw[G\rightarrow C]}}{V_{sw[G]}} \cdot (3600 \cdot 24) \quad [day^{-1}]$$

where
$Q_{adv,sw[G\rightarrow C]}$: $flow\ of\ continental\ sea\ water\ to\ the\ global\ ocean$ $[m^3 \cdot s^{-1}]$
$V_{sw[G]}$: $volume\ of\ global\ sea\ water$ $[m^3]$
$(3600 \cdot 24)$: $conversion\ factor$ $[s \cdot day^{-1}]$

The flow of global sea water to the continental sea water $\left(Q_{adv,sw[G\rightarrow C]}\right)$ might be obtained from:

(150)

$$Q_{adv,sw[G\rightarrow C]} = \frac{V_{sw[C]}}{\tau_{sw[C]}} - Q_{des,fw\rightarrow sw[C]} \quad [m^3 \cdot s^{-1}]$$

$V_{sw[G]}$: $volume\ of\ global\ sea\ water$ $[m^3]$
$\tau_{sw[C]}$: $residence\ time\ of\ continental\ sea\ water$ $[s]$
$Q_{des,fw\rightarrow sw[C]}$: $flow\ of\ continental\ fresh\ water\ to\ continental\ sea\ water$ $[m^3 \cdot s^{-1}]$

8.2.3 Suspended matter compartment

Suspended matter is treated as the dissolved fraction of the water compartment.
The suspended matter in continental natural and agricultural soil can be "imported" to the continental fresh water by erosion. The suspended matter in continental fresh water can be "imported" to the continental costal sea water. The suspended matter in global fresh water can be "imported" to the global costal sea water. The suspended matter in continental coastal sea water can be "imported" and "exported" to and from the global costal sea water.

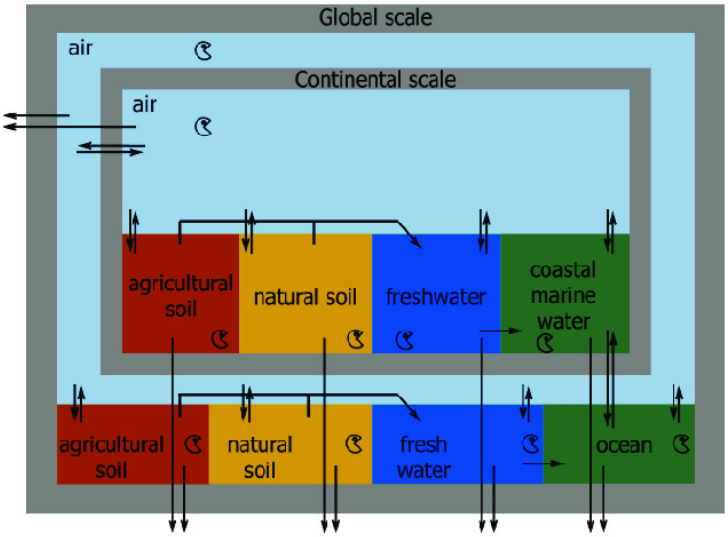

Figure 8-3 Compartments used in USEtox model at continental and global scale (Reproduced from USEtox 2.0 Documentation)

8.2.3.1 Velocity of suspended particles in the water

According to Hollander & Van Meent (2004), the velocity of suspended particles in the water was:

(151)

$$v_{sed,susp,w[S]} = \frac{2{,}5}{(3600 \cdot 24)} \quad [m \cdot s^{-1}]$$

where

2,5: $settling\ velocity\ suspended\ particles\ of\ the\ continental\ and\ global\ fresh\ and\ sea\ water\ [m \cdot d^{-1}]$

$(3600 \cdot 24)$: $conversion\ factor\ [m \cdot s^{-1}]$

8.2.3.2 Net sediment accumulation rate in continental and global freshwater

(152)

$$v_{sed,acc,fw[S]} = \frac{\left(v_{nsl[S]} \times fr\_A_{nsl[S]} \times fr\_V_{solid,nsl[S]} + v_{asl[S]} \times fr\_A_{asl[S]} \times fr\_V_{solid,asl[S]}\right) \times A_{[S]} \times \rho_{sd,sl} + J_{susp,fw[S]} - C_{susp,fw[S]} \times \left(Q_{des,fw \to sw[S]}\right)}{\frac{fr\_V_{solid,sd[S]} \times \rho_{sd,sl}}{A_{[S]} \times fr\_A_{fw[S]}}}$$

where

$v_{sed,acc,fw[S]}$: $net\ sediment\ accumulation\ rate\ in\ continental\ and\ global\ freshwater\ [m \cdot s^{-1}]$

$v_{nls[S]}$: $erosion\ of\ continental\ and\ global\ natural\ soil\ [m \cdot s^{-1}]$

$C_{susp,fw[S]}$: $concentration\ of\ suspended\ matter\ in\ continental\ and\ global\ freshwater\ [kg \cdot m^{-3}]$

$fr\_A_{nsl[S]}$: $area\ fraction\ of\ continental\ and\ global\ natural\ soil$ $[-]$
$fr\_V_{solid,nsl[S]}$: $volume\ fraction\ of\ solids\ in\ continental\ and\ global\ natural\ soil$ $[-]$
$v_{als[S]}$: $erosion\ of\ continental\ and\ global\ agricultural\ soil$ $[m \cdot s^{-1}]$
$fr\_A_{asl[S]}$: $area\ fraction\ of\ continental\ and\ global\ agricultural\ soil$ $[-]$
$fr\_V_{solid,asl[S]}$: $volume\ fraction\ of\ solids\ in\ continental\ and\ global\ agricultural\ soil$ $[-]$
$A_{[S]}$: $continental\ and\ global\ system\ area$ $[m^2]$
$\rho_{sd,sl}$: $mineral\ density\ of\ sediment\ and\ soil$ $[kg \cdot m^{-3}]$
$J_{susp,fw[S]}$: $autochtonous\ production\ of\ suspended\ matter\ in\ continental\ and\ global\ freshwater$ $[kg \cdot s^{-1}]$
$C_{susp,fw[S]}$: $concentration\ of\ suspended\ matter\ in\ continental\ and\ global\ freshwater$ $[kg \cdot m^{-3}]$
$Q_{des,fw\rightarrow sw[S]}$: $flow\ of\ continental\ and\ global\ freshwater\ to\ continental\ and\ global\ sea\ water$ $[m^3 \cdot s^{-1}]$
$fr\_V_{solid,sd[S]}$: $volume\ fraction\ of\ solids\ in\ continental\ and\ global\ sediment$ $[-]$
$fr\_A_{fw[S]}$: $area\ fraction\ of\ continental\ and\ global\ freshwater$ $[-]$

By analyzing the formula (152), it can be rewritten as follows:

(153)

$$v_{sed,acc,fw[S]} \times A_{[S]} \times fr\_A_{fw[S]} \times fr\_V_{solid,sd[S]} \times \rho_{sd,sl} = \left(v_{nsl[S]} \times fr\_A_{nsl[S]} \times fr\_V_{solid,nsl[S]} + v_{asl[S]} \times fr\_A_{asl[S]} \times fr\_V_{solid,asl[S]}\right) \times A_{[S]} \times \rho_{sd,sl} + J_{susp,fw[S]} - C_{susp,fw[S]} \times \left(Q_{des,fw\rightarrow sw[S]}\right)$$

Suspended matter acted as a physical carrier of the chemical across the sediment-water interface. The flow of suspended matter accumulated in sediment at continental and global scale across the sediment-freshwater interface was equal to:

(154)

$$Q_{sed[S]} = v_{sed,acc,fw[S]} \times A_{[S]} \times fr\_A_{fw[S]} \ \ [m^3 \cdot s^{-1}]$$

It was necessary to consider the volume fraction of the entire volume corresponding to the solids in sediment. Therefore, by multiplying the flow by the volume fraction of solids in continental and global sediment and by multiplying the density of sediment (expressed in $[kg \cdot m^{-3}]$), the amount of solids that was accumulated in sediment at continental and global scale could be obtained, according the following term:

(155)

$$v_{sed,acc,fw[S]} \times A_{[S]} \times fr\_A_{fw[S]} \times fr\_V_{solid,sd[S]} \times \rho_{sd,sl} \ \ [kg \cdot s^{-1}]$$

For mass balance at continental scale (Figure 8-3) you might write:

(156)

$$A = B + C - D$$

with

$A = v_{sed,acc,fw[S]} \times A_{[S]} \times fr\_A_{fw[S]} \times fr\_V_{solid,sd[S]} \times \rho_{sd,sl} \quad [kg \cdot s^{-1}]$
$B = \left(v_{nsl[S]} \times fr\_A_{nsl[S]} \times fr\_V_{solid,nsl[S]} + v_{asl[S]} \times fr\_A_{asl[S]} \times fr\_V_{solid,asl[S]}\right) \times A_{[S]} \times \rho_{sd,sl} \quad [kg \cdot s^{-1}]$
$C = J_{susp,fw[S]} = \quad [kg \cdot s^{-1}]$
$D = C_{susp,fw[S]} \times \left(Q_{des,fw\rightarrow sw[S]}\right) \quad [kg \cdot s^{-1}]$

The term "B" was the flow of suspended matter imported by erosion to freshwater from natural soil and agricultural soil at continental and global scale multiplied by the volume fraction of solids in continental and global natural and agricultural soil, and multiplied by density of sediment in continental and global natural and agricultural soil (expressed in $[kg \cdot m^3]$). The term "C" as indicated above was the autochtonous production of suspended matter in continental and global freshwater $[kg \cdot s^{-1}]$. The term "D" represented the amount of suspended matter that was exported from continental and global freshwater to continental and global seawater.

By eplacing A, B, C, and D terms and by dividing both terms by $\left(fr\_V_{solid,sd[S]} \times \rho_{sd,sl}\right)$ it was possible to obtained net sediment accumulation rate in continental and global freshwater (152).

8.2.3.3 Net sediment accumulation rate in continental and global sea water

Similarly, for the sea water at continental and global scale, the following equation (157) and (158) might be written:

$$v_{sed,acc,sw[C]} = \frac{C_{susp,fw[C]} \times \left(Q_{des,fw\rightarrow sw[C]}\right) + C_{susp,sw[G]} \times \left(Q_{adv,sw[G\rightarrow C]}\right) + J_{susp,sw[C]} - C_{susp,sw[C]} \times \left(Q_{adv,sw[C\rightarrow G]}\right)}{\frac{fr\_V_{solid,sd[C]} \times \rho_{sd,sl}}{A_{[C]} \times fr\_A_{sw[C]}}} \quad (157)$$

where

$v_{sed,acc,sw[C]}$: $net\ sediment\ accumulation\ rate\ in\ continental\ sea\ water\ [m \cdot s^{-1}]$

$C_{susp,fw[C]}$: $concentration\ of\ suspended\ matter\ in\ continental\ freshwater\ [kg \cdot m^{-3}]$

$Q_{des,fw\rightarrow sw[C]}$: $flow\ of\ continental\ freshwater\ to\ continental\ sea\ water\ [m^3 \cdot s^{-1}]$

$C_{susp,sw[G]}$: $concentration\ of\ suspended\ matter\ in\ global\ sea\ water\ [kg \cdot m^{-3}]$

$Q_{adv,sw[G\rightarrow C]}$: $flow\ of\ global\ sea\ water\ to\ continental\ scale\ [m^3 \cdot s^{-1}]$

$J_{susp,sw[C]}$: $autochtonous\ production\ of\ suspended\ matter\ in\ continental\ sea\ water\ [kg \cdot s^{-1}]$

$C_{susp,sw[G]}$: $concentration\ of\ suspended\ matter\ in\ continental\ sea\ water\ [kg \cdot m^{-3}]$

$Q_{adv,sw[C\rightarrow G]}$: $flow\ of\ continental\ sea\ water\ to\ the\ global\ ocean\ [m^3 \cdot s^{-1}]$

$fr\_V_{solid,sd[C]}$: $volume\ fraction\ of\ solids\ in\ continental\ sediment [-]$

$\rho_{sd,sl}$: $mineral\ density\ of\ sediment\ and\ soil\ [kg \cdot m^{-3}]$

$A_{[C]}$: $continental\ and\ global\ system\ area\ [m^2]$

$fr\_A_{sw[C]}$: $area\ fraction\ of\ continental\ sea\ water\ [-]$

$$v_{sed,acc,sw[G]} = \frac{C_{susp,fw[G]} \times \left(Q_{des,fw\rightarrow sw[G]}\right) + C_{susp,sw[C]} \times \left(Q_{adv,sw[C\rightarrow G]}\right) + J_{susp,fw[G]} - C_{susp,sw[G]} \times \left(Q_{adv,sw[G\rightarrow C]}\right)}{\frac{fr\_V_{solid,sd[G]} \times \rho_{sd,sl}}{A_{[G]} \times fr\_A_{fw[G]}}} \quad (158)$$

where

$v_{sed,acc,sw[G]}$: $net\ sediment\ accumulation\ rate\ in\ global\ sea\ water\ [m \cdot s^{-1}]$

$C_{susp,fw[G]}$: $concentration\ suspended\ matter\ in\ global\ freshwater\ [kg \cdot m^{-3}]$

$Q_{des,fw\rightarrow sw[G]}$: $flow\ of\ global\ freshwater\ to\ global\ sea\ water\ [m^3 \cdot s^{-1}]$

$C_{susp,sw[C]}$: $concentration\ suspended\ matter\ in\ continental\ sea\ water\ [kg \cdot m^{-3}]$

$Q_{adv,sw[C\rightarrow G]}$: $flow\ of\ continental\ sea\ water\ to\ global\ scale\ [m^3 \cdot s^{-1}]$

$J_{susp,sw[G]}$: $autochtonous\ production\ of\ suspended\ matter\ in\ global\ sea\ water\ [kg \cdot s^{-1}]$
$C_{susp,sw[G]}$: $concentration\ of\ suspended\ matter\ in\ global\ sea\ water\ [kg \cdot m^{-3}]$
$Q_{adv,sw[C\rightarrow G]}$: $flow\ of\ global\ sea\ water\ to\ the\ continental\ scale\ [m^3 \cdot s^{-1}]$
$fr\_V_{solid,sd[G]}$: $volume\ fraction\ of\ solids\ in\ global\ sediment [-]$
$\rho_{sd,sl}$: $mineral\ density\ of\ sediment\ and\ soil\ [kg \cdot m^{-3}]$
$A_{[G]}$: $global\ system\ area\ [m^2]$
$fr\_A_{sw[G]}$: $area\ fraction\ of\ global\ sea\ water\ [-]$

8.2.3.4 Net gross sediment rate from the water to the sediment compartment

The gross sediment rate from the water to the sediment compartment might be obtained from:
If

$$v_{sed,susp,w[S]} \cdot \frac{C_{susp,w[S]}}{\rho_{sd}} - v_{sed,acc,w[S]} > 0 \quad (159)$$

$v_{sed,susp,w[S]} \cdot \frac{C_{susp,w[S]}}{\rho_{sd}} > v_{sed,acc,w[S]}$, then (160)

$$v_{sed,w[S]} = v_{sed,susp,w[S]} \cdot \frac{C_{susp,w[S]}}{\rho_{sd}}, \text{ else} \quad (161)$$

$$v_{sed,w[S]} = v_{sed,acc,w[S]} \quad (162)$$

where
$v_{sed,susp,w[S]}$: $velocity\ of\ the\ suspended\ particles\ of\ the\ continental\ and\ global\ fresh\ and\ sea\ water\ [m \cdot s^{-1}]$
$C_{susp,w[S]}$: $concentration\ of\ suspended\ matter\ in\ continental\ and\ global\ fresh\ and\ sea\ water\ [kg \cdot m^{-3}]$
ρ_{sd}: $bulk\ density\ of\ continental\ and\ global\ sediment\ [kg \cdot m^{-3}]$
$v_{sed,acc,w[S]}$: $net\ sediment\ accumulation\ rate\ in\ continental\ and\ global\ fresh\ and\ sea\ water\ [m \cdot s^{-1}]$
$v_{sed,w[S]}$: $gross\ sedimentation\ rate\ from\ continental\ and\ global\ fresh\ and\ sea\ water\ [m \cdot s^{-1}]$

8.2.4 Sediment compartment

The sediment phase was treated as a homogeneous phase consisting of a water and a solid sub-phases. Equilibrium is assumed between the pore water and solid sub-phases of the sediment phase. Chemicals were transported between water and sediment via direct adsorption/desorption and by sedimentation/resuspension. Top layer of the sediment was considered to be well-mixed. If the sedimentation of particles from the water column was greater than the resuspension, this top layer was continuously being refreshed. The older sediment layer, and the chemicals that were associated with the sediment, got buried under the freshly deposited material.

8.2.4.1 Volume of freshwater and sea water sediment

The volume of continental and global fresh and sea water sediment $[m^3]$ might be obtained from:

$$V_{wsd[S]} = A_{[S]} \cdot fr\_A_{w[S]} \cdot h_{wsd[S]}$$

with

$A_{[S]}$: $continental\ and\ global\ system\ area$ $[m^2]$

$fr\_A_{w[S]}$: $area\ fraction\ of\ continental\ and\ global\ fresh\ and\ sea\ water$ $[-]$

$h_{wsd[S]}$: $mixed\ depth\ continental\ and\ global\ fresh\ and\ sea\ water\ sediment$ $[m]$

8.2.4.2 Mass of original species in sediment

The mass fraction of original species in water (fr_m_{wsd}) might be obtained from:

c. if $\boldsymbol{pKa_{loss} < pKa_{gain}}$

(163)

$$\boldsymbol{fr\_m_{wsd} = \frac{1}{1 + 10^{(pKa_{loss} - pH_w)} + 10^{(pH_w - pKa_{gain})}}}\ [-]$$

d. If $\boldsymbol{pKa_{loss} \geq pKa_{gain}}$

(164)

$$\boldsymbol{fr\_m_{wsd} = \frac{1}{1 + 10^{(pKa_{gain} - pH_w)} + 10^{(pH_w - pKa_{loss})}}}\ [-]$$

where

pH_w: $pH\ fresh\ and\ sea\ water$ [-]

pKa_{loss}: $equilibrium\ constant\ proton\ loss\ from\ conjugated\ acid\ of\ parent\ compound$ $[-]$

pKa_{gain}: $equilibrium\ constant\ proton\ loss\ from\ parent\ compound$ $[-]$

For demonstration see equations (49) and (50).

8.2.4.3 Volume fraction solids in the sediments

In USEtox for the volume fraction water in continental and global sediments $(fr\_V_{water,sd[S]}\ [-])$ default value of 0.2 was used. The volume fraction solids $(fr\_V_{solid,sd[S]}\ [-])$ in the sediment might be obtained from:

(165)

$$fr\_V_{solid,sd[S]} = 1 - fr\_V_{water,sd[S]}$$

8.2.4.4 Bulk density

The bulk density $[\rho_{sd}]$ of sediment might be obtained from:

$$\rho_{sd} = fr\_V_{water,sd[S]} \cdot \rho_w + fr\_V_{solid,sd[S]} \cdot \rho_{sd,sl} \quad (166)$$

where

$fr\_V_{water,sd[S]} = volume\ fraction\ water\ in\ continental\ and\ global\ sediment$ [–]

$\rho_w = density\ of\ water\ [kg \cdot m^{-3}]$

$fr\_V_{solid,sd[S]} = volume\ fraction\ solid\ in\ continental\ and\ global\ sediment$ [–]

$\rho_{sd,sl} = mineral\ density\ of\ sediment\ and\ soil\ [kg \cdot m^{-3}]$

8.2.4.5 Burial rate

The burial rate in continental and global fresh and sea water sediment $\left[v_{burial,wsd[S]}\right]$ might be obtained from:

$$v_{burial,wsd[S]} = v_{sed,acc,w[S]}\ [m \cdot s^{-1}] \quad (167)$$

where

$v_{sed,acc,w[S]}$: $net\ sediment\ accumulation\ rate\ in\ continental\ and\ global\ fresh\ and\ sea\ water\ [m \cdot s^{-1}]$

8.2.5 Soil compartment

Among all environmental compartments, soil was the most stationary one and, as a result, the most spatially inhomogeneous. There are many different soil types as well as differences in soil use. Unfortunately, the fate of chemicals was largely determined by the characteristics that vary significantly (i.e. porosity, water content and organic matter content). The key factor determining whether soil might be loaded directly with a chemical was the soil use. One soil compartment might not be sufficient to reflect the role of "soil" in the multimedia fate of chemicals. USEtox considered two different type of soil both in contintinental-global scale and at the urban scale:

1. "natural soil" and "agricultural soil" at continental and global scale;
2. "paved" and "non-paved" at the urban scale.

In USEtox soil compartment is treated as a homogeneous compartment constisting of three subphase:

1. gas subphase;
2. water subphase;
3. solid subphase.

The concentration in soil was obtained summing the concentration in each of all three subphases. All soil subphase were assumed to be in equilibrium during all times.

8.2.5.1 Volume of soil compartment

The volume of continental and global "natural"and "agricultural" soil $\left(V_{sl[S]}\right)$ might be obtained from:

$$V_{sl[S]} = A_{[S]} \cdot fr\_A_{sl[S]} \cdot h_{sl[S]} \quad (168)$$

with

$A_{[S]}$: $continental\ and\ global\ system\ area\ [m^2]$

$fr\_A_{sl[S]}$: $area\ fraction\ of\ continental\ and\ global\ natural\ and\ agricultural\ soil\ [-]$

$h_{sl[S]}$: $depth\ continental\ and\ global\ natural\ and\ agricultural\ soil\ [m]$

For the area fraction of continental and global "natural" and "agricultural" soil see equations (122) and (123) in which global area land $(A_{land[G]})$ in the equation (122) and (123) might be obtained from:

(169)

$$A_{land[G]} = A_{land[G]} - A_{land[C]}$$

8.2.5.2 Bulk density of the soil

The bulk density of the soil (ρ_{sl} $[kg \cdot m^{-3}]$) might be calculated from:

(170)

$$\rho_{sl} = fr\_V_{gas,sl[C]} \cdot \rho_{air} + fr\_V_{water,sl[C]} \cdot \rho_w + fr\_V_{solid,sl[C]} \cdot \rho_{sd}$$

with

$fr\_V_{gas,sl[C]}$: $volume\ fraction\ of\ gas\ in\ continental\ and\ global\ natural\ and\ agricultural\ soil$ [–]
$fr\_V_{water,sl[C]}$: $volume\ fraction\ of\ water\ in\ continental\ and\ global\ natural\ and\ agricultural\ soil$ [–]
$fr\_V_{solid,sl[C]}$: $volume\ fraction\ of\ solid\ in\ continental\ and\ global\ natural\ and\ agricultural\ soil$ [–]
ρ_{air}: $density\ of\ air$ $[kg \cdot m^{-3}]$
ρ_w: $density\ of\ water$ $[kg \cdot m^{-3}]$
ρ_{sd}: $density\ of\ sediment\ and\ soil$ $[kg \cdot m^{-3}]$

In USEtox, for the volume fraction gas in continental and global "natural" and "agrcultural" soil $(fr\_V_{gas,sl[S]}$ [–]$)$, the default value of 0.2 was used. The same value was used for the volume fraction of water in continental and global "natural" and "agrcultural" soil $(fr\_V_{water,sl[S]}$ [–]$)$. The volume fraction of solid at continental and global scale $(fr\_V_{solid,sl[S]}$ [–]$)$ might be calculated from:

(171)

$$fr\_V_{solid,sl[S]} = 1 - fr\_V_{gas,sl[S]} - fr\_V_{water,sl[S]}$$

8.2.5.3 Mass fraction of chemical in solid subphase of soil

The mass fraction of the chemical in solid subphase of "natural" and "agricultural" soil at continental scale may be obtained from:

(172)

$$fr\_m_{solid,sl[S]} = \frac{fr\_V_{solid,sl[S]}}{fr\_V_{solid,sl[S]} + \frac{K_{aw[S]}}{K_{solid,sl|w,sl[S]} \cdot \frac{\rho_{sd,sl[C]}}{1000}} \cdot fr\_V_{gas,sl[C]} + \frac{fr\_V_{water,sl[S]}}{K_{solid,sl|w,sl[S]} \cdot \frac{\rho_{sd,sl\,[S]}}{1000}}}$$

with

$fr\_V_{solid,sl[S]}$: $volume\ fraction\ of\ solids\ in\ continental\ and\ global\ natural\ and\ agricultural\ soil$ [–]
$fr\_V_{water,sl[S]}$: $volume\ fraction\ of\ water\ in\ continental\ and\ global\ natural\ and\ agricultural\ soil$ [–]
$fr\_V_{gas,sl[S]}$: $volume\ fraction\ of\ gas\ in\ continental\ and\ global\ natural\ and\ agricultural\ soil$ [–]
$K_{solid,sl|w,sl[S]}$: $solid/water\ patition\ coefficient\ of\ continental\ and\ global\ natural\ and\ agricoltural\ soil$ $[L \cdot kg^{-1}]$
$K_{aw[S]}$: $air/water\ patition\ coefficient\ of\ continental\ and\ global\ natural\ and\ agricoltural\ soil$ [–]
$\rho_{sd,sl}$: $mineral\ density\ of\ sediment\ and\ soil$ $[kg \cdot m^{-3}]$
1000: $conversion\ factor$ $[dm^3 \cdot m^{-3}]$

Demonstration of equation (172)

$$fr\_m_{solid,sl[S]} = \frac{m_{solid,sl[S]}}{m_{solid,sl[S]} + m_{water,sl[S]} + m_{gas,sl[S]}} \quad (173)$$

with

$m_{solid,sl[S]}$: $mass\ of\ chemical\ in\ the\ solid\ subphase\ of\ natural\ and\ agric.soil\ at\ continental\ and\ global\ scale\ [kg]$

$m_{water,sl[S]}$: $mass\ of\ chemical\ in\ the\ water\ subphase\ of\ natural\ and\ agric.soil\ at\ continental\ and\ global\ scale\ [kg]$

$m_{gas,sl[S]}$: $mass\ of\ chemical\ in\ the\ gas\ subphase\ of\ natural\ and\ agric.soil\ at\ continental\ and\ global\ scale\ [kg]$

$$m_{solid,sl[S]} = C_{solid,sl[S]} \times V_{solid,sl[S]} \quad (174)$$

$$m_{water,sl[S]} = C_{water,sl[S]} \times V_{water,sl[S]} \quad (175)$$

$$m_{gas,sl[S]} = C_{gas,sl[S]} \times V_{gas,sl[S]} \quad (176)$$

with

$C_{solid,sl[S]}$: $concentration\ of\ chemical\ in\ solid\ subphase\ of\ soil\ at\ continental\ and\ global\ scale\ [kg \cdot m^{-3}]$

$C_{water,sl[S]}$: $concentration\ of\ chemical\ in\ water\ phase\ of\ soil\ at\ continental\ and\ global\ scale\ [kg \cdot m^{-3}]$

$C_{gas,sl[S]}$: $concentration\ of\ chemical\ in\ gas\ subphase\ of\ soil\ at\ continental\ and\ global\ scale\ [kg \cdot m^{-3}]$

$V_{solid,sl[C]}$: $volume\ of\ solid\ subphase\ of\ continental\ and\ global\ natural\ and\ agricultural\ soil\ [m^3]$

$V_{water,sl[C]}$: $volume\ of\ water\ subphase\ of\ continental\ and\ global\ natural\ and\ agricultural\ soil\ [m^3]$

$V_{gas,sl[C]}$: $volume\ of\ gas\ subphase\ of\ continental\ and\ global\ natural\ and\ agricultural\ soil\ [m^3]$

By subtituting (174), (175), (176) in (173) the following equation (177) was obtained:

$$fr\_m_{solid,sl[C]} = \frac{C_{solid,sl[C]} \cdot V_{solid,sl[S]}}{C_{solid,sl[S]} \cdot V_{solid,sl[C]} + C_{water,sl[S]} \cdot V_{water,sl[S]} + C_{gas,sl[C]} \cdot V_{gas,sl[S]}} \quad (177)$$

By dividing the numerator and the denominator by the total volume of soil at continental and global scale $[V_{soil[S]}]$:

$$fr\_m_{solid,sl[S]} = \frac{C_{solid,sl[S]} \cdot \frac{V_{solid,sl[S]}}{V_{soil[S]}}}{C_{solid,sl[S]} \cdot \frac{V_{solid,sl[S]}}{V_{soil[S]}} + C_{water,sl[S]} \cdot \frac{V_{water,sl[S]}}{V_{soil[S]}} + C_{gas,sl[S]} \cdot \frac{V_{gas,sl[S]}}{V_{soil[S]}}} \quad (178)$$

$$\frac{V_{i,sl[S]}}{V_{soil[S]}} = fr\_m_{i,s[S]} \quad (179)$$

where

$fr\_V_{i,s[S]}$: $volume\ fraction\ of\ chemical\ in\ the\ phase$ "i"$of\ the\ soil\ at\ continental\ and\ global\ scale$ [−]

$i = soil, water, gas$

Therefore:

(180)

$$fr\_m_{solid,sl\,[S]} = \frac{C_{solid,sl[S]} \cdot fr\_V_{solid,sl[S]}}{C_{solid,sl[S]} \cdot fr\_V_{solid,sl[S]} + C_{water,sl[S]} \cdot fr\_V_{water,sl[S]} + C_{gas,sl[S]} \cdot fr\_V_{gas,sl[S]}}$$

By dividing the numerator and the denominator by $C_{solid,sl[S]}$

(181)

$$fr\_m_{solid,s[S]} = \frac{fr\_V_{solid,sl[S]}}{fr\_V_{solid,sl[S]} + \frac{C_{water,sl[S]}}{C_{solid,sl[S]}} \cdot fr\_V_{water,sl[S]} + \frac{C_{gas,sl[S]}}{C_{solid,sl[S]}} \cdot fr\_V_{gas,sl[S]}}$$

(182)

$$\frac{C_{water,sl[S]}}{C_{solid,sl[S]}} = \frac{1}{\frac{C_{solid,sl[S]}}{C_{water,sl[S]}}} = \frac{1}{K_{solid,sl|w,sl[S]}}$$

(183)

$$\frac{C_{gas,sl[S]}}{C_{solid,sl[S]}} = \frac{\frac{C_{gas,sl[S]}}{C_{water,sl[S]}}}{\frac{C_{solid,sl[S]}}{C_{water,sl[S]}}} = \frac{K_{aw[S]}}{K_{solid,sl|w,sl[S]}}$$

By subtituting (182), (183) in (181) the following equation (184) was obtained:

(184)

$$fr\_m_{solid,s[S]} = \frac{fr\_V_{solid,sl[S]}}{fr\_V_{solid,sl[S]} + \frac{K_{aw[S]}}{K_{solid,sl|w,sl[S]} \cdot \frac{\rho_{sd,sl[S]}}{1000}} \cdot fr\_V_{gas,sl[S]} + \frac{fr\_V_{water,sl[S]}}{K_{solid,sl|w,sl[C]} \cdot \frac{\rho_{sd,sl[S]}}{1000}}}$$

The partition coefficient $K_{solid,sl|w,sl[S]}$ was expressed in $[L \cdot kg^{-1}]$, thus it was s necessary to be multiplied by the mineral density of sediment and soil $\left(\rho_{sd,sl[S]}\ [kg \cdot m^{-3}]\right)$.

8.2.5.4 Mass fraction of chemical in water subphase of soil

The mass fraction of the chemical in water subphase of "natural" and "agricultural" soil at continental scale might be obtained from:

(185)

$$fr\_m_{water,sl[S]} = \frac{fr\_V_{water,sl[S]}}{fr\_V_{solid,sl[S]} \cdot \left(K_{solid,sl|w,sl[C]} \cdot \frac{\rho_{sd,sl[S]}}{1000}\right) + fr\_V_{water,sl[S]} + K_{aw[C]} \cdot fr\_V_{gas,sl[S]}}$$

with

$fr\_V_{solid,sl[S]}$: $volume\ fraction\ of\ solids\ in\ continental\ and\ global\ natural\ and\ agricultural\ soil$ [–]
$fr\_V_{water,sl[S]}$: $volume\ fraction\ of\ water\ in\ continental\ and\ global\ natural\ and\ agricultural\ soil$ [–]
$fr\_V_{gas,sl[S]}$: $volume\ fraction\ of\ gas\ in\ continental\ and\ global\ natural\ and\ agricultural\ soil$ [–]
$K_{solid,sl|w,sl[S]}$: $solid/water\ patition\ coefficient\ of\ continental\ and\ global\ natural\ and\ agricoltural\ soil$ $[L \cdot kg^{-1}]$
$K_{aw[S]}$: $air/water\ patition\ coefficient\ of\ continental\ and\ global\ natural\ and\ agricoltural\ soil$ [–]
$\rho_{sd,sl}$: $mineral\ density\ of\ sediment\ and\ soil$ $[kg \cdot m^{-3}]$
1000: $conversion\ factor$ $[dm^3 \cdot m^{-3}]$

Demonstration of equation (185)

(186)

$$fr\_m_{water,sl[C]} = \frac{m_{water,sl[C]}}{m_{solid,sl[C]} + m_{water,sl[C]} + m_{gas,sl[C]}}$$

with

$m_{solid,sl[S]}$: $mass\ of\ chemical\ in\ the\ solid\ subphase\ of\ natural\ and\ agric.soil\ at\ continental\ and\ global\ scale$ $[kg]$
$m_{water,sl[S]}$: $mass\ of\ chemical\ in\ the\ water\ subphase\ of\ natural\ and\ agric.soil\ at\ continental\ and\ global\ scale$ $[kg]$
$m_{gas,sl[S]}$: $mass\ of\ chemical\ in\ the\ gas\ subphase\ of\ natural\ and\ agric.soil\ at\ continental\ and\ global\ scale$ $[kg]$

(187)

$$m_{solid,sl[S]} = C_{solid,sl[S]} \times V_{solid,sl[S]}$$

(188)

$$m_{water,sl[S]} = C_{water,sl[S]} \times V_{water,sl[S]}$$

(189)

$$m_{gas,sl[S]} = C_{gas,sl[S]} \times V_{gas,sl[S]}$$

with

$C_{solid,sl[S]}$: $concentration\ of\ chemical\ in\ solid\ subphase\ of\ soil\ at\ continental\ and\ global\ scale$ $[kg \cdot m^{-3}]$
$C_{water,sl[S]}$: $concentration\ of\ chemical\ in\ water\ subphase\ of\ soil\ at\ continental\ and\ global\ scale$ $[kg \cdot m^{-3}]$
$C_{gas,sl[S]}$: $concentration\ of\ chemical\ in\ gas\ subphase\ of\ soil\ at\ continental\ and\ global\ scale$ $[kg \cdot m^{-3}]$
$V_{solid,sl[C]}$: $volume\ of\ solid\ subphase\ of\ continental\ and\ global\ natural\ and\ agricultural\ soil$ $[m^3]$
$V_{water,sl[C]}$: $volume\ of\ water\ subphase\ of\ continental\ and\ global\ natural\ and\ agricultural\ soil$ $[m^3]$
$V_{gas,sl[C]}$: $volume\ of\ gas\ subphase\ of\ continental\ and\ global\ natural\ and\ agricultural\ soil$ $[m^3]$

By subtituting (187), (188) and (189) in (186), the following equation (190) might be obtained:

(190)

$$fr\_m_{water,sl[S]} = \frac{C_{water,sl[S]} \cdot V_{water,sl[S]}}{C_{solid,sl[S]} \cdot V_{solid,sl[S]} + C_{water,sl[S]} \cdot V_{water,sl[S]} + C_{gas,sl[S]} \cdot V_{gas,sl[S]}}$$

By dividing the numerator and the denominator by the total volume of soil at continental and global scale $[V_{soil[S]}]$:

(191)

$$fr\_m_{water,sl[S]} = \frac{C_{water,sl[S]} \cdot \frac{V_{water,sl[S]}}{V_{soil[S]}}}{C_{solid,sl[S]} \cdot \frac{V_{solid,sl[S]}}{V_{soil[S]}} + C_{water,sl[S]} \cdot \frac{V_{water,sl[S]}}{V_{soil[S]}} + C_{gas,sl[S]} \cdot \frac{V_{gas,sl[S]}}{V_{soil[S]}}}$$

(192)

$$\frac{V_{i,sl[S]}}{V_{soil[S]}} = fr\_m_{i,s[S]}$$

where
$fr\_V_{i,s[S]}$: $volume\ fraction\ of\ chemical\ in\ the\ phase$ "i"$of\ the\ soil\ at\ continental\ and\ global\ scale$ [−]
$i = soil, water, gas$

Therefore:

(193)

$$fr\_m_{water,s[S]} = \frac{C_{water,sl[S]} \cdot fr\_V_{water,sl[S]}}{C_{solid,sl[S]} \cdot fr\_V_{solid,sl[S]} + C_{water,sl[S]} \cdot fr\_V_{water,sl[S]} + C_{gas,sl[S]} \cdot fr\_V_{gas,sl[S]}}$$

By dividing the numerator and the denominator by $C_{water,sl[S]}$

(194)

$$fr\_m_{water,s[C]} = \frac{fr\_V_{water,sl[S]}}{\frac{C_{solid,sl[S]}}{C_{water,sl[S]}} \cdot fr\_V_{solid,sl[S]} + fr\_V_{water,sl[S]} + \frac{C_{gas,sl[S]}}{C_{water,sl[S]}} \cdot fr\_V_{gas,sl[S]}}$$

(195)

$$\frac{C_{solid,sl[S]}}{C_{water,sl[S]}} = K_{solid,sl|w,sl[S]}$$

(196)

$$\frac{C_{gas,sl[S]}}{C_{water,sl[S]}} = K_{aw[S]}$$

By subtituting (195) and (196) in (194), the following equation (197) was obtained:

(197)

$$fr\_m_{water,sl[S]} = \frac{fr\_V_{water,sl[S]}}{fr\_V_{solid,sl[S]} \cdot \left(K_{solid,sl|w,sl[C]} \cdot \frac{\rho_{sd,sl[S]}}{1000}\right) + fr\_V_{water,sl[S]} + K_{aw[C]} \cdot fr\_V_{gas,sl[S]}}$$

The partition coefficient $K_{solid,sl|w,sl[S]}$ was expressed in $[L \cdot kg^{-1}]$, thus it was necessary to multiply it by the mineral density of sediment and soil $(\rho_{sd,sl[S]}\ [kg \cdot m^{-3}])$.

8.2.5.5 Mass of original species in soil

The mass fraction of original species in soil (fr_m_{sl}) might be obtained from:

e. if $\boldsymbol{pKa_{loss} < pKa_{gain}}$

(198)

$$\boldsymbol{fr\_m_{sl} = \frac{1}{1 + 10^{(pKa_{loss} - pH_{sl})} + 10^{(pH_{sl} - pKa_{gain})}}}\ [-]$$

f. If $\boldsymbol{pKa_{loss} \geq pKa_{gain}}$

(199)

$$\boldsymbol{fr\_m_{sl} = \frac{1}{1 + 10^{(pKa_{gain} - pH_{sl})} + 10^{(pH_{sl} - pKa_{loss})}}}\ [-]$$

where
pH_{sl}: *pH natural and agricultural soil* [-]
pKa_{loss}: *equilibrium constant proton loss from conjugated acid of parent compound* [−]
pKa_{gain}: *equilibrium constant proton loss from parent compound* [−]

For demonstration see equations (49) and (50).

8.2.5.6 Mass of original species in pore water of the soil

The mass fraction of original species in pore water of the soil $(fr\_m_{sl,water})$ might be obtained from:

g. if $\boldsymbol{pKa_{loss} < pKa_{gain}}$

(200)

$$\boldsymbol{fr\_m_{sl} = \frac{1}{1 + 10^{(pKa_{loss} - pH_{sl})} + 10^{(pH_{sl} - pKa_{gain})}}}\ [-]$$

h. If $\boldsymbol{pKa_{loss} \geq pKa_{gain}}$

(201)

$$\boldsymbol{fr\_m_{sl} = \frac{1}{1 + 10^{(pKa_{gain} - pH_{sl})} + 10^{(pH_{sl} - pKa_{loss})}}}\ [-]$$

where
pH_{w}: *pH natural and agricultural soil* [-]
pKa_{loss}: *equilibrium constant proton loss from conjugated acid of parent compound* [−]
pKa_{gain}: *equilibrium constant proton loss from parent compound* [−]

For demonstration see equations (49) and (50).

8.2.5.7 Penetration depth

Chemicals tended to migrate down into the soil vertically, whereby processes of diffusion, absorption and degradation control the depth of migration.
The penetration depth in the continental and global natural and agricultural soil may be obtained from:

(202)

$$z = \frac{\left(\sqrt{\left(v_e^2 + \left(4 \times \frac{k}{(3600 \times 24)} \times D_e\right)\right)}\right) + (v_e)}{2\frac{k}{(3600 \times 24)}}$$

where

z: $h_{sl,penetr[S]}$: $penetration\ depth\ in\ continental\ and\ global\ natural\ and\ agricultural\ soil\ [m]$
v_e: $v_{eff,adv,sl[S]}$: $effective\ advective\ transport\ in\ continental\ and\ global\ natural\ and\ agricultural\ soil\ [m \cdot s^{-1}]$
D_e: $D_{eff,sl[S]}$: $effective\ diffusion\ coefficient\ in\ continental\ and\ global\ natural\ and\ agricultural\ soil\ [m^2 \cdot s^{-1}]$
k: $k_{deg,sl[S]}$: $degradation\ rate\ in\ continental\ natural\ and\ agricultural\ soil [d^{-1}]$
(3600×24): $conversion\ factor [s \cdot d^{-1}]$

Demonstration of equation (202)

At any depth z of a soil layer, there was competition between reaction processes and dispersion/diffusion and advection processes. The ratio of these competing processes is expressed by the Damkoehler number (N_{DA}), which was the ratio of the rate of loss by chemical transformation to the rate of loss by diffusion/dispersion and advection (Cowan et al., 1995) and was defined as:

(203)

$$(N_{DA}) = \frac{Transformation\ loss\ rate}{Advection\ and\ \ diffusion/dispersion\ loss\ rate} = \frac{C \times k \times z}{C \cdot \left(v_e + \frac{D_e}{z}\right)} = \frac{k \times z}{\left(v_e + \frac{D_e}{z}\right)}$$

When the Damkoehler number was 1, rates of transformation losses and diffusion/advection transport were equal. This happened when z was the characteristic depth or the average depth of penetration for chemical molecules moving into a soil layer from its surface (Cowan et al., 1995). When (N_{DA}), was 1, Equation (203) can be rearranged to find the z corresponding to the characteristic penetration depth.

(204)

$$k \cdot z^2 - v_e \cdot z - D_e = 0$$

By dividing by D_e:

(205)

$$\frac{k}{D_e} \cdot z^2 - \frac{v_e}{D_e} \cdot z - 1 = 0$$

By using the quadratic formula to solve Equation (205):

(206)

$$z_1 = \frac{\frac{v_e}{D_e} + \sqrt{\left[\left(\frac{v_e}{D_e}\right)^2 + \frac{4k}{D_e}\right]}}{\frac{2k}{D_e}} \rightarrow \frac{1}{z_1} = \frac{\frac{2k}{D_e}}{\frac{v_e}{D_e} + \sqrt{\left[\left(\frac{v_e}{D_e}\right)^2 + \frac{4k}{D_e}\right]}}$$

(207)

$$\frac{1}{z_1} = \frac{\frac{2k}{D_e}}{\frac{v_e}{D_e} + \sqrt{\left[\left(\frac{v_e}{D_e}\right)^2 + \frac{4k}{D_e}\right]}} \times \frac{\frac{v_e}{D_e} - \sqrt{\left[\left(\frac{v_e}{D_e}\right)^2 + \frac{4k}{D_e}\right]}}{\frac{v_e}{D_e} - \sqrt{\left[\left(\frac{v_e}{D_e}\right)^2 + \frac{4k}{D_e}\right]}} = \frac{\frac{2k}{D_e} \times \left(\frac{v_e}{D_e} - \sqrt{\left[\left(\frac{v_e}{D_e}\right)^2 + \frac{4k}{D_e}\right]}\right)}{\left(\frac{v_e}{D_e}\right)^2 - \left(\frac{v_e}{D_e}\right)^2 - \frac{4k}{D_e}}$$

(208)

$$\frac{1}{z_1} = \frac{\frac{2k}{D_e} \times \left(\frac{v_e}{D_e} - \sqrt{\left[\left(\frac{v_e}{D_e}\right)^2 + \frac{4k}{D_e}\right]}\right)}{-\frac{4k}{D_e}} = \left(-\frac{D_e}{4k}\right) \times \frac{2k}{D_e} \times \left(\frac{v_e}{D_e} - \sqrt{\left[\left(\frac{v_e}{D_e}\right)^2 + \frac{4k}{D_e}\right]}\right)$$

(209)

$$\frac{1}{z_1} = \left(-\frac{1}{2}\right) \times \left(\frac{v_e}{D_e} - \sqrt{\left[\left(\frac{v_e}{D_e}\right)^2 + \frac{4k}{D_e}\right]}\right) = \frac{1}{2} \cdot \sqrt{\left[\left(\frac{v_e}{D_e}\right)^2 + \frac{4k}{D_e}\right]} - \frac{v_e}{2D_e} = \sqrt{\left[\left(\frac{v_e}{2D_e}\right)^2 + \frac{k}{D_e}\right]} - \frac{v_e}{2D_e}$$

(210)

$$z_2 = \frac{\frac{v_e}{D_e} - \sqrt{\left[\left(\frac{v_e}{D_e}\right)^2 + \frac{4k}{D_e}\right]}}{\frac{2k}{D_e}} \rightarrow \frac{1}{z_2} = \frac{\frac{2k}{D_e}}{\frac{v_e}{D_e} - \sqrt{\left[\left(\frac{v_e}{D_e}\right)^2 + \frac{4k}{D_e}\right]}}$$

(211)

$$\frac{1}{z_2} = \frac{\frac{2k}{D_e}}{\frac{v_e}{D_e} - \sqrt{\left[\left(\frac{v_e}{D_e}\right)^2 + \frac{4k}{D_e}\right]}} \times \frac{\frac{v_e}{D_e} + \sqrt{\left[\left(\frac{v_e}{D_e}\right)^2 + \frac{4k}{D_e}\right]}}{\frac{v_e}{D_e} + \sqrt{\left[\left(\frac{v_e}{D_e}\right)^2 + \frac{4k}{D_e}\right]}} = \frac{\frac{2k}{D_e} \times \left(\frac{v_e}{D_e} - \sqrt{\left[\left(\frac{v_e}{D_e}\right)^2 + \frac{4k}{D_e}\right]}\right)}{\left(\frac{v_e}{D_e}\right)^2 - \left(\frac{v_e}{D_e}\right)^2 - \frac{4k}{D_e}}$$

(212)

$$\frac{1}{z_2} = \frac{\frac{2k}{D_e} \times \left(\frac{v_e}{D_e} + \sqrt{\left[\left(\frac{v_e}{D_e}\right)^2 + \frac{4k}{D_e}\right]}\right)}{-\frac{4k}{D_e}} = \left(-\frac{D_e}{4k}\right) \times \frac{2k}{D_e} \times \left(\frac{v_e}{D_e} + \sqrt{\left[\left(\frac{v_e}{D_e}\right)^2 + \frac{4k}{D_e}\right]}\right)$$

(213)

$$\frac{1}{z_2} = \left(-\frac{1}{2}\right) \times \left(\frac{v_e}{D_e} + \sqrt{\left[\left(\frac{v_e}{D_e}\right)^2 + \frac{4k}{D_e}\right]}\right) = -\frac{1}{2} \cdot \sqrt{\left[\left(\frac{v_e}{D_e}\right)^2 + \frac{4k}{D_e}\right]} - \frac{v_e}{2D_e} = \sqrt{\left[\left(\frac{v_e}{2D_e}\right)^2 + \frac{k}{D_e}\right]} - \frac{v_e}{2D_e}$$

Therefore:

(214)

$$\frac{1}{z_1} = \frac{1}{z_2} = \frac{1}{z} = \sqrt{\left(\left(\frac{v_e}{2D_e}\right)^2 + \frac{k}{D_e}\right)} - \frac{v_e}{2D_e}$$

Thus, the penetration depth in the soil at continental and global scale was equal:

(215)

$$\frac{1}{z} = \sqrt{\left(\left(\frac{v_e}{2D_e}\right)^2 + \frac{k}{D_e}\right)} - \frac{v_e}{2D_e}$$

(216)

$$z = \frac{1}{\sqrt{\left(\left(\frac{v_e}{2D_e}\right)^2 + \frac{k}{D_e}\right)} - \frac{v_e}{2D_e}}$$

(217)

$$z = \frac{1}{\left(\sqrt{\left(\left(\frac{v_e}{2D_e}\right)^2 + \frac{k}{D_e}\right)} - \frac{v_e}{2D_e}\right)} \times \frac{\left(\sqrt{\left(\left(\frac{v_e}{2D_e}\right)^2 + \frac{k}{D_e}\right)} + \frac{v_e}{2D_e}\right)}{\left(\sqrt{\left(\left(\frac{v_e}{2D_e}\right)^2 + \frac{k}{D_e}\right)} + \frac{v_e}{2D_e}\right)}$$

(218)

$$z = \frac{\sqrt{\left(\left(\frac{v_e}{2D_e}\right)^2 + \frac{k}{D_e}\right)} + \frac{v_e}{2D_e}}{\left(\left(\frac{v_e}{2D_e}\right)^2 + \frac{k}{D_e}\right) - \frac{v_e^2}{4D_e^2}} = \frac{\sqrt{\left(\left(\frac{v_e}{2D_e}\right)^2 + \frac{k}{D_e}\right)} + \frac{v_e}{2D_e}}{\frac{v_e^2}{4D_e^2} + \frac{k}{D_e} - \frac{v_e^2}{4D_e^2}} = \frac{\sqrt{\left(\left(\frac{v_e}{2D_e}\right)^2 + \frac{k}{D_e}\right)} + \frac{v_e}{2D_e}}{\frac{k}{D_e}}$$

(219)

$$z = \frac{D_e \times \left(\sqrt{\left(\left(\frac{v_e}{2D_e}\right)^2 + \frac{k}{D_e}\right)} + \frac{v_e}{2D_e}\right)}{k} = \frac{\left(\sqrt{\left(\frac{v_e^2}{4D_e^2} \times D_e^2 + \frac{k}{D_e} \times D_e^2\right)}\right) + \left(\frac{v_e}{2D_e} \times D_e\right)}{k}$$

(220)

$$z = \frac{\left(\sqrt{\left(\frac{v_e^2 + (4 \times k \times D_e)}{4}\right)}\right) + \left(\frac{v_e}{2}\right)}{k} = \frac{\left(\sqrt{\left(v_e^2 + (4 \times k \times D_e)\right)}\right) + (v_e)}{2k}$$

k must be expressed in $[s^{-1}]$, thus the following equation (221) was obtained:

(221)

$$z = \frac{\left(\sqrt{\left(v_e^2 + \left(4 \times \frac{k}{(3600 \times 24)} \times D_e\right)\right)}\right) + (v_e)}{2\frac{k}{(3600 \times 24)}}$$

8.2.5.8 Effective advective transport in soil

The effective advective transport in soil $\left(v_{eff,adv,sl[S]}[m \cdot s^{-1}]\right)$ might be obtained from:

(222)

$$v_{eff,adv,sl[S]} = \left(v_{rain[S]} \cdot fr\_V_{rain,inf,sl[S]}\right) \times \left(\frac{fr\_m_{water,sl[S]}}{fr\_V_{water,sl[S]}}\right) + v_{adv,solid,sl[S]} \times \left(\frac{fr\_m_{solid,sl[S]}}{fr\_V_{solid,sl[S]}}\right)$$

where

$v_{rain[S]}$: *continental and global annual average precipitation* $[m \cdot s^{-1}]$
$fr\_V_{rain,inf,sl[S]}$: *volume fraction of precipitation infiltrating into continental and global natural and agricultural soil* [−]
$fr\_V_{water,sl[S]}$: *volume fraction of water subphase in continental and global natural and agricultural soil* [−]
$fr\_m_{water,sl[S]}$: *fraction of chemical in water subphase of continental and global natural and agricultural soil* [−]
$v_{adv,solid,sl[S]}$: *solid subphase advection velocity in continental and global natural and agricultural soil* $[m \cdot s^{-1}]$
$fr\_V_{solid,sl[S]}$: *volume fraction of solid subphase in continental and global natural and agricultural soil* [−]
$fr\_m_{solid,sl[S]}$: *fraction of chemical in solid subphase of continental and global natural and agricultural soil* [−]

In USEtox $v_{rain[S]}$ was equal to $700\, mm \cdot yr^{-1}$ both for continental and global "natural" and "agrcultural" soil. In USEtox, for gas volume fraction in continental and global "natural" and "agrcultural" soil $\left(fr\_V_{gas,sl[S]}\ [-]\right)$, the default value of 0.2 was used. The same value was used for the volume fraction of water in continental and global "natural" and "agrcultural" soil $\left(fr\_V_{water,sl[S]}\ [-]\right)$. Volume fraction of solid at continental and global scale $\left(fr\_V_{solid,sl[S]}\ [-]\right)$ was described in equation (171).
The mass fractions of chemical in solid and water subphase of soil were described in equations (172) and (185).
$v_{adv,solid,sl[S]}$ was equal to $0.0002\ m \cdot yr^{-1}$ (Den Hollander & Van de Meent 2004). It was conversed to $m \cdot s^{-1}$ through conversion factor $(3600 \cdot 24 \cdot 365)\ s \cdot yr^{-1}$:

(223)

$$v_{adv,solid,sl[S]} = \frac{0.0002}{3600 \cdot 24 \cdot 365}$$

Demonstration of equation (222)

Equation (222) might be rewritten as:

$$v_{eff,adv,sl[S]} = \left(v_{rain[S]} \cdot fr\_V_{rain,inf,sl[S]}\right) \times \left(\frac{C_{water,sl[S]}}{C_{soil\ [S]}}\right) + v_{adv,solid,sl[S]} \times \left(\frac{C_{solid,sl[S]}}{C_{soil\ [S]}}\right) \quad (224)$$

$$C_{water,sl[S]} = \frac{m_{water,sl[S]}}{V_{water,sl[S]}} \quad (225)$$

$$C_{solid,sl[S]} = \frac{m_{solid,sl[S]}}{V_{solid,sl[S]}} \quad (226)$$

$$C_{soil[S]} = \frac{m_{soil[S]}}{V_{soil[S]}} \quad (227)$$

$C_{water,sl[S]}$: $concentration\ of\ chemical\ in\ water\ subphase\ of\ soil\ at\ continental\ and\ global\ scale\ [kg \cdot m^{-3}]$
$m_{water,sl[S]}$: $mass\ of\ chemical\ in\ water\ subphase\ of\ natural\ and\ agric.soil\ at\ continental\ and\ global\ scale\ [kg]$
$V_{water,sl[C]}$: $volume\ of\ water\ subphase\ of\ continental\ and\ global\ natural\ and\ agricultural\ soil\ [m^3]$
$C_{solid,sl[S]}$: $concentration\ of\ chemical\ in\ solid\ subphase\ of\ soil\ at\ continental\ and\ global\ scale\ [kg \cdot m^{-3}]$
$m_{solid,sl[S]}$: $mass\ of\ chemical\ in\ the\ solid\ subphase\ of\ natural\ and\ agric.soil\ at\ continental\ and\ global\ scale\ [kg]$
$V_{water,sl[C]}$: $volume\ of\ solid\ subphase\ of\ continental\ and\ global\ natural\ and\ agricultural\ soil\ [m^3]$
$m_{soil\ [S]}$: $mass\ of\ chemical\ in\ the\ natural\ and\ agricultural\ soil\ at\ continental\ and\ global\ scale\ [kg]$
$C_{soil\ [S]}$: $concentration\ of\ chemical\ in\ the\ natural\ and\ agric.soil\ at\ continental\ and\ global\ scale\ [kg \cdot m^{-3}]$
$V_{soil\ [C]}$: $volume\ of\ continental\ and\ global\ natural\ and\ agricultural\ soil\ [m^3]$

$$\frac{C_{water,sl[S]}}{C_{soil\ [S]}} = \frac{\frac{m_{water,sl[S]}}{V_{water,sl[S]}}}{\frac{m_{soil[S]}}{V_{soil[S]}}} = \frac{m_{water,sl[S]}}{V_{water,sl[S]}} \times \frac{V_{soil[S]}}{m_{soil[S]}} = \frac{m_{water,sl[S]}}{m_{soil[S]}} \times \frac{V_{soil[S]}}{V_{water,sl[S]}} \quad (228)$$

$$\frac{m_{water,sl[S]}}{m_{soil[S]}} = fr\_m_{water,sl[S]} \quad (229)$$

$$\frac{V_{soil[S]}}{V_{water,sl[S]}} = \frac{1}{fr\_V_{water,sl[S]}} \quad (230)$$

Therefore,

(231)

$$\frac{C_{water,sl[S]}}{C_{soil\ [S]}} = \frac{\frac{m_{water,sl[S]}}{V_{water,sl[S]}}}{\frac{m_{soil[S]}}{V_{soil[S]}}} = \frac{fr\_m_{water,sl[S]}}{fr\_V_{water,sl[S]}}$$

(232)

$$\frac{C_{solid,sl[S]}}{C_{soil\ [S]}} = \frac{\frac{m_{solid,sl[S]}}{V_{solid,sl[S]}}}{\frac{m_{soil[S]}}{V_{soil[S]}}} = \frac{m_{solid,sl[S]}}{V_{solid,sl[S]}} \times \frac{V_{soil[S]}}{m_{soil[S]}} = \frac{m_{solid,sl[S]}}{m_{soil[S]}} \times \frac{V_{soil[S]}}{V_{solid,sl[S]}}$$

(233)

$$\frac{m_{solid,sl[S]}}{m_{soil[S]}} = fr\_m_{solid,sl[S]}$$

(234)

$$\frac{V_{soil[S]}}{V_{solid,sl[S]}} = \frac{1}{fr\_V_{solid,sl[S]}}$$

Therefore,

(235)

$$\frac{C_{solid,sl[S]}}{C_{soil\ [S]}} = \frac{\frac{m_{solid,sl[S]}}{V_{solid,sl[S]}}}{\frac{m_{soil[S]}}{V_{soil[S]}}} = \frac{fr\_m_{solid,sl[S]}}{fr\_V_{solid,sl[S]}}$$

By subtituting (231) and (235) in (224), the following equation (236) might be obtained:

(236)

$$v_{eff,adv,sl[S]} = \left(v_{rain[S]} \cdot fr\_V_{rain,inf,sl[S]}\right) \times \left(\frac{fr\_m_{water,sl[S]}}{fr\_V_{water,sl[S]}}\right) + v_{adv,solid,sl[S]} \times \left(\frac{fr\_m_{solid,sl[S]}}{fr\_V_{solid,sl[S]}}\right)$$

8.2.5.9 Effective diffusion coefficient in soil

Effective diffusion in soil at continental and global scale $\left(D_{eff,sl[S]}\ [m^2 \cdot s^{-1}]\right)$ involved pore gas and pore water subphase. Diffusion in solid subphase was negligible. For solid subphase a turbation coefficient was considered.

(237)

$$D_{eff,sl[S]} = D_{gas} \times \left(fr\_V_{gas,sl[S]}\right)^{1.5} \times \left(\frac{fr\_m_{gas,sl[S]}}{fr\_V_{gas,sl[S]}}\right) + D_{water} \times \left(fr\_V_{water,sl[S]}\right)^{1.5} \times \left(\frac{fr\_m_{water,sl[S]}}{fr\_V_{water,sl[S]}}\right) + D_{solid,sl[S]} \times \left(\frac{fr\_m_{solid,sl[S]}}{fr\_V_{solid,sl[S]}}\right)$$

with

D_{gas}: $gas\ phase\ diffusion\ coefficient$ $[m^2 \cdot s^{-1}]$
$fr\_V_{gas,sl[S]}$: $volume\ fraction\ of\ gas\ subphase\ of\ continental\ and\ global\ natural\ and\ agricultural\ soil$ $[-]$
$fr\_m_{gas,sl[S]}$: $fraction\ of\ chemical\ in\ gas\ subphase\ of\ continental\ and\ global\ natural\ and\ agricultural\ soil$ $[-]$
D_{water}: $water\ phase\ diffusion\ coefficient$ $[m^2 \cdot s^{-1}]$
$fr\_V_{water,sl[S]}$: $volume\ fraction\ of\ water\ subphase\ continental\ and\ global\ natural\ and\ agricultural\ soil$ $[-]$
$fr\_m_{water,sl[S]}$: $fraction\ of\ chemical\ in\ water\ subphase\ of\ continental\ and\ global\ natural\ and\ agricultural\ soil$ $[-]$
$D_{solid,sl[S]}$: $solid\ subphase\ turbation\ coefficient\ of\ continental\ and\ global\ natural\ and\ agricultural\ soil$ $[m^2 \cdot s^{-1}]$
$fr\_V_{solid,sl[S]}$: $volume\ fraction\ of\ solid\ subphase\ in\ continental\ and\ global\ natural\ and\ agricultural\ soil$ $[-]$
$fr_{m_{solid,sl[S]}}$: $fraction\ of\ chemical\ in\ solid\ subphase\ in\ continental\ and\ global\ natural\ and\ agricultural\ soil$ $[-]$
1.5: $experimental\ coefficient$ $[-]$

In USEtox, for the volume fraction of gas in continental and global "natural" and "agricultural" soil $(fr\_V_{gas,sl[S]}\ [-])$, the default value of 0.2 was used. The same value was used for the volume fraction of water in continental and global "natural" and "agrcultural" soil $(fr\_V_{water,sl[S]}\ [-])$. Volume fraction of solid at continental and global scale $(fr\_V_{solid,sl[S]}\ [-])$ was described in equation (171). The mass fractions of chemical in solid and water in soil are described in equations (172) and (185) respectively.

Demonstration of equation (237)

The equation for the effective diffusion coefficient of organic chemicals in soil was based on SimpleBox (e.g. equation 111 in Brandes et al. 1996), where the exponents are empirically derived as further described e.g. in Chapter 7.6 of Mackay (2001) or Liu & Nie (2001).
Equation (237) might be rewritten as:

$$D_{eff,sl[S]} = D_{gas} \times \left(fr\_V_{gas,sl[S]}\right)^{1.5} \times \left(\frac{C_{gas,sl[S]}}{C_{soil\ [S]}}\right) + D_{water} \times \left(fr\_V_{water,sl[S]}\right)^{1.5} \times \left(\frac{C_{water,sl[S]}}{C_{soil\ [S]}}\right) + D_{solid,sl[S]} \times \left(\frac{C_{solid,sl[S]}}{C_{soil\ [S]}}\right) \quad (238)$$

$$C_{gas,sl[S]} = \frac{m_{gas,sl[S]}}{V_{gas,sl[S]}} \quad (239)$$

$$C_{water,sl[S]} = \frac{m_{water,sl[S]}}{V_{water,sl[S]}} \quad (240)$$

$$C_{solid,sl[S]} = \frac{m_{solid,sl[S]}}{V_{solid,sl[S]}} \quad (241)$$

(242)

$$C_{soil[S]} = \frac{m_{soil[S]}}{V_{soil[S]}}$$

$C_{gas,sl[S]}$: $concentration\ of\ chemical\ in\ gas\ subphase\ of\ soil\ at\ continental\ and\ global\ scale\ [kg \cdot m^{-3}]$
$m_{gas,sl[S]}$: $mass\ of\ chemical\ in\ gas\ subphase\ of\ natural\ and\ agric.soil\ at\ continental\ and\ global\ scale\ [kg]$
$V_{water,sl[C]}$: $volume\ of\ gas\ subphase\ of\ continental\ and\ global\ natural\ and\ agricultural\ soil\ [m^3]$
$C_{water,sl[S]}$: $concentration\ of\ chemical\ in\ water\ subphase\ of\ soil\ at\ continental\ and\ global\ scale\ [kg \cdot m^{-3}]$
$m_{water,sl[S]}$: $mass\ of\ chemical\ in\ water\ subphase\ of\ natural\ and\ agric.soil\ at\ continental\ and\ global\ scale\ [kg]$
$V_{water,sl[C]}$: $volume\ of\ water\ subphase\ of\ continental\ and\ global\ natural\ and\ agricultural\ soil\ [m^3]$
$C_{solid,sl[S]}$: $concentration\ of\ chemical\ in\ solid\ subphase\ of\ soil\ at\ continental\ and\ global\ scale\ [kg \cdot m^{-3}]$
$m_{solid,sl[S]}$: $mass\ of\ chemical\ in\ the\ solid\ subphase\ of\ natural\ and\ agric.soil\ at\ continental\ and\ global\ scale\ [kg]$
$V_{water,sl[C]}$: $volume\ of\ solid\ subphase\ of\ continental\ and\ global\ natural\ and\ agricultural\ soil\ [m^3]$
$m_{soil\ [S]}$: $mass\ of\ chemical\ in\ the\ natural\ and\ agricultural\ soil\ at\ continental\ and\ global\ scale\ [kg]$
$C_{soil\ [S]}$: $concentration\ of\ chemical\ in\ the\ natural\ and\ agric.soil\ at\ continental\ and\ global\ scale\ [kg \cdot m^{-3}]$
$V_{soil\ [C]}$: $volume\ of\ continental\ and\ global\ natural\ and\ agricultural\ soil\ [m^3]$

(243)

$$\frac{C_{gas,sl[S]}}{C_{soil\ [S]}} = \frac{\frac{m_{gas,sl[S]}}{V_{gas,sl[S]}}}{\frac{m_{soil[S]}}{V_{soil[S]}}} = \frac{m_{gas,sl[S]}}{V_{gas,sl[S]}} \times \frac{V_{soil[S]}}{m_{soil[S]}} = \frac{m_{gas,sl[S]}}{m_{soil[S]}} \times \frac{V_{soil[S]}}{V_{gas,sl[S]}}$$

(244)

$$\frac{m_{gas,sl[S]}}{m_{soil[S]}} = fr\_m_{gas,sl[S]}$$

(245)

$$\frac{V_{soil[S]}}{V_{gas,sl[S]}} = \frac{1}{fr\_V_{gas,sl[S]}}$$

(246)

$$\frac{C_{gas,sl[S]}}{C_{soil\ [S]}} = \frac{fr\_m_{gas,sl[S]}}{fr\_V_{gas,sl[S]}}$$

(247)

$$\frac{C_{water,sl[S]}}{C_{soil\ [S]}} = \frac{\frac{m_{water,sl[S]}}{V_{water,sl[S]}}}{\frac{m_{soil[S]}}{V_{soil[S]}}} = \frac{m_{water,sl[S]}}{V_{water,sl[S]}} \times \frac{V_{soil[S]}}{m_{soil[S]}} = \frac{m_{water,sl[S]}}{m_{soil[S]}} \times \frac{V_{soil[S]}}{V_{water,sl[S]}}$$

(248)

$$\frac{m_{water,sl[S]}}{m_{soil[S]}} = fr\_m_{water,sl[S]}$$

(249)

$$\frac{V_{soil[S]}}{V_{water,sl[S]}} = \frac{1}{fr\_V_{water,sl[S]}}$$

(250)

$$\frac{C_{water,sl[S]}}{C_{soil\ [S]}} = \frac{fr\_m_{water,sl[S]}}{fr\_V_{water,sl[S]}}$$

(251)

$$\frac{C_{solid,sl[S]}}{C_{soil\ [S]}} = \frac{\frac{m_{solid,sl[S]}}{V_{solid,sl[S]}}}{\frac{m_{soil[S]}}{V_{soil[S]}}} = \frac{m_{solid,sl[S]}}{V_{solid,sl[S]}} \times \frac{V_{soil[S]}}{m_{soil[S]}} = \frac{m_{solid,sl[S]}}{m_{soil[S]}} \times \frac{V_{soil[S]}}{V_{solid,sl[S]}}$$

(252)

$$\frac{m_{solid,sl[S]}}{m_{soil[S]}} = fr\_m_{solid,sl[S]}$$

(253)

$$\frac{V_{soil[S]}}{V_{solid,sl[S]}} = \frac{1}{fr\_V_{solid,sl[S]}}$$

(254)

$$\frac{C_{solid,sl[S]}}{C_{soil\ [S]}} = \frac{fr\_m_{solid,sl[S]}}{fr\_V_{solid,sl[S]}}$$

By subtituting (246), (250) and (254) in (238), the following equation (255) might be obtained:

(255)

$$D_{eff,sl[S]} = D_{gas} \times \left(fr\_V_{gas,sl[S]}\right)^{1.5} \times \left(\frac{fr\_m_{gas,sl[S]}}{fr\_V_{gas,sl[S]}}\right) + D_{water} \times \left(fr\_V_{water,sl[S]}\right)^{1.5} \times \left(\frac{fr\_m_{water,sl[S]}}{fr\_V_{water,sl[S]}}\right) + D_{solid,sl[S]} \times \left(\frac{fr\_m_{solid,sl[S]}}{fr\_V_{solid,sl[S]}}\right)$$

8.2.5.10 Diffusion coefficients

A technique to calculate diffusion coefficients involved adjusting the known diffusivities for one chemical to values approximated for chemicals of related structure, thus assuming that molecular velocities and thus molecular diffusivities roughly varied inversely with the square root of molecular mass (Schwarzenbach et al. 1993). This readily available parameter could be used in order to adjust the known diffusivity of a reference substance to the unknown diffusivity of the ith substance according to the following equation:

(256)

$$\frac{D_{i,a}}{D_{ref,a}} = \left(\frac{MW_i}{MW_{ref}}\right)^{-\frac{1}{2}}$$

where

$D_{i,a}$: $diffusion\ coefficient\ of\ chemical\ "i"$ $[m^2 \cdot s^{-1}]$
$D_{ref,a}$: $diffusion\ coefficient\ of\ reference\ chemical$ $[m^2 \cdot s^{-1}]$
MW_i: $molar\ weight\ of\ chemical\ "i"$ $[gr \cdot mol^{-1}]$
MW_i: $molar\ weight\ of\ reference\ chemical$ $[gr \cdot mol^{-1}]$

The **gas phase** diffusion coefficient $\left(D_{gas}[m^2 \cdot s^{-1}]\right)$ might be obtained from:

(257)

$$D_{gas} = 0.0000257 \cdot \frac{\sqrt{18}}{\sqrt{MW \cdot 1000}}$$

where

D_{gas}: $gas\ phase\ diffusion\ coefficient$ $[m^2 \cdot s^{-1}]$
0.0000257: $gas\ phase\ diffusion\ coefficient\ of\ water$ $[m^2 \cdot s^{-1}]$
18: $molar\ weight\ of\ water$ $[gr \cdot mol^{-1}]$
MW: $molar\ weight\ of\ chemical$ $[kg \cdot mol^{-1}]$
1000: $conversion\ factor$ $[gr \cdot kg^{-1}]$

The **water phase** diffusion coefficient ($D_{water}[m^2 \cdot s^{-1}]$) might be obtained from:

(258)

$$D_{water} = 0.00000002 \cdot \frac{\sqrt{32}}{\sqrt{MW \cdot 1000}}$$

where

D_{water}: $water\ phase\ diffusion\ coefficient$ $[m^2 \cdot s^{-1}]$
0.00000002: $water\ phase\ diffusion\ coefficient\ of\ oxygen\ gas$ $[m^2 \cdot s^{-1}]$
32: $molar\ weight\ of\ oxygen\ gas$ $[gr \cdot mol^{-1}]$
MW: $molar\ weight\ of\ chemical$ $[kg \cdot mol^{-1}]$
1000: $conversion\ factor$ $[gr \cdot kg^{-1}]$

8.2.5.11 Solid phase turbation

The solid phase turbation coefficient $\left(D_{solid,sl[S]}[m^2 \cdot s^{-1}]\right)$ was by default equal to 0.0000005 $m^2 \cdot d^{-1}$ (McLachlan et al. (2002)) and it was converted to $m^2 \cdot s^{-1}$ as follows:

(259)

$$D_{solid,sl[S]} = \frac{0.0000005}{3600 \cdot 24}$$

with

$D_{solid,sl[S]}$: *solid phase turbation coefficient in continental and global "natural"and "agricultural" soil* $[m^2 \cdot s^{-1}]$

0.0000005: *solid phase turbation coefficient in continental and global* natural*and* agricultural*soil* $[m^2 \cdot s^{-1}]$

$3600 \cdot 24$: *conversion factor* $[s \cdot d^{-1}]$

8.3 Transformation processes

8.3.1 Air

The removal from the air is caused by two different processes:

1. degradation in the air;
2. escape of the substance from the air to the stratosphere.

For air compartment in urban, continental and global scale, the total rate constant $[k_{tot,air\,[S]}]$ was equal to:

(260)

$$k_{tot,air\,[S]} = k_{deg,air\,[S]} + k_{adv,air\rightarrow strat[S]} \quad [d^{-1}] \quad \text{(Mackay 6.3.3)}$$

8.3.1.1 Degradation in air

Degradation in the atmosphere is assumed to take place in the gas phase only.
The transfer from air in urban, continental and global scale $[k_{deg,air\,[S]}]$ by degradation can be obtained from:

(261)

$$k_{deg,air\,[S]} = fr\_m_{gas,air[S]} \times k_{deg,air\,25°C} \cdot (3600 \cdot 24) \quad [d^{-1}]$$

where

$k_{deg,air\,[S]}$: $degradation\ in\ urban, continental\ and\ global\ air$ $[d^{-1}]$
$fr\_m_{gas,air[S]}$: $fraction\ of\ chemical\ in\ gas\ phase\ of\ urban, continental\ and\ global\ air$ [–]
$k_{deg,air25°C}$: $gas\ phase\ degradation\ rate\ constant\ at\ 25°C, in\ air$ $[s^{-1}]$
$(3600 \cdot 24)$: $conversion\ factor$ $[s \cdot d^{-1}]$

Degradation in air is dependent on temperature.
Degradation rate constants at the other temperatures are derived from the standard $KDeg_{a[S]}$, by applying:

a. correction for the fraction of the substance in the gas phase. By default, this was done by using the Junge-Pankow equation;
b. correction for differences in OH-radical concentration;
c. correction for differences in temperature.

The factor of temperature correction $[TempFactor_{a[S]}]$ might be obtained from:

(262)

$$TempFactor_{a[S]} = e^{\frac{Ea_{OHrad} \times (Temp_{[S]} - 298)}{8.314 \times (298)^2}} \quad [-]$$

where

Ea_{OHrad}: $activation\ energy\ for\ OH\ radical\ reaction$ $[6000\ J \cdot mol^{-1}]$
$Temp_{[S]}$: $considered\ temperature\ in\ urban, continental, global\ scale$ $[K]$
8.314: $gas\ constant$ $[Pa \cdot m^3 \cdot mol^{-1}K^{-1}]$
298: $temperature$ $[K]$

For organic chemicals, in order to derive the degradation rate in air, the k_{OH} (the hydroxyl radical rate costant $[cm^3 \cdot (molecules\ sec)]$) was multiplied with the $[OH]$ (the hydroxyl radical concentration $[cm^3 \cdot (molecules\ or\ radicals)]$). For k_{OH}, experimental values were available in

EPI Suite™. If experimental data is not available, the estimation methods for k_{OH} were based on structure-activity relationship (SAR) using "fragments costants".
For inorganic chemicals, the degradation rate in air was set at $1 \cdot 10^{-20} \cdot s^{-1}$, thus indicating that no degradation of inorganic in the environment occurred.

8.3.1.2 Escape of the substance from the air

The transfer from air by escape to the stratosphere can be obtained from:

(263)

$$k_{adv,air \rightarrow strat[S]} = \frac{\ln(2)}{60 \cdot 365} \quad [d^{-1}]$$

with

$k_{adv,air \rightarrow strat[S]}$: $escape\ from\ urban, continental\ and\ global\ air\ to\ stratophere\ [d^{-1}]$
60: $half\ life\ in\ air\ [yr]$
360: $conversion\ factor\ [d \cdot yr^{-1}]$

Demonstration of equation (263)

By defining a kinetic reaction of the first order for the following generic reaction:

$$A \rightarrow X$$

(264)

$$v = -\frac{d[A]}{dt} = \frac{dX}{dt} = k \cdot [A]$$

"v" was the velocity with which "A" ws consumed when "X" was produced. "k" was named kinetic constant.

(265)

$$-\frac{d[A]}{dt} = k \cdot [A]$$

(266)

$$-\frac{d[A]}{[A]} = k \cdot dt$$

(267)

$$\frac{d[A]}{[A]} = -k \cdot dt$$

We integrated both terms between $t_1 = t$ and $t_0 = t = 0$
At $t_1 = t$, $[A] = [A]$
At $t_0 = t = 0$, $[A] = [A_0]$

(268)

$$\int_{[A_0]}^{[A]} \frac{d[A]}{[A]} = -k \int_0^t dt$$

$$ln([A]) - ln([A_0]) = -k(t - 0) \quad (269)$$

$$ln\left(\frac{[A]}{[A_0]}\right) = -kt \quad (270)$$

The half-life time of $[A_0]$ was equal to $t_{1/2}$:

$$t_{1/2} \rightarrow [A] = \frac{1}{2} \cdot [A_0] \quad (271)$$

Thus at time $t = t_{1/2}$:

$$ln\left(\frac{[A_0]}{2[A_0]}\right) = -kt_{1/2} \quad (272)$$

$$ln(2)^{-1} = -kt_{1/2} \quad (273)$$

$$-ln(2) = -kt_{1/2} \quad (274)$$

$$ln(2) = kt_{1/2} \quad (275)$$

Thus

$$k = \frac{ln(2)}{t_{1/2}} \quad (276)$$

In the air $t_{1/2} = 60\ [yr]$

Therefore the following equation (277) was obtained:

$$k = \frac{ln(2)}{60 \cdot 365}\ [d^{-1}] \quad (277)$$

8.3.2 Water

8.3.2.1 Degradation in water

The transfer from water by degradation at continental and global scale might be obtained from:

$$k_{deg,w\,[S]} = k_{deg,w\,25°C} \cdot (3600 \cdot 24)\ \ [d^{-1}] \quad (278)$$

with

$k_{deg,w\,[S]}$: *degradation in continental and global fresh and sea water* $[d^{-1}]$

$k_{deg,w\,25°C}$: *bulk degradation rate constant at* $25°C$, *in water* $[s^{-1}]$

$(3600 \cdot 24)$: *conversion factor* $[s \cdot d^{-1}]$

For organic chemicals, degradation rate in water was extrapolated from biodegradation rate using division factor of "1". Specifically, Biowin3 model was used to estimate biodegradation half lifes in EPI Suite™. Biodegradation half lifes was correlated to default biodegradation rates as reported in Table 3-1. Biodegradation half lifes were used to match default biodegradation rate and then to calculate degradation rate in water. For inorganic chemicals degradation rate in water was set at $1 \cdot 10^{-20} \cdot s^{-1}$, thus indicating that no degradation of inorganic in the environment occurred.

Biowin3 Output	Assigned half-life (days)	Rate constant (1/s)
Hours	0.17	4.7×10^{-5}
Hours to Days	1.25	6.4×10^{-6}
Days	2.33	3.4×10^{-6}
Days to Weeks	8.67	9.3×10^{-7}
Weeks	15	5.3×10^{-7}
Weeks to Months	37.5	2.1×10^{-7}
Months	60	1.3×10^{-7}
Recalcitrant	180	4.5×10^{-8}

Table 8-1 Relation between Biowin3 output and default biodegradation half-lives and biodegradation rate constants (Reproduced from USEtox 2.0 Documentation)

8.3.3 Sediment

8.3.3.1 Degradation in sediment

The transfer from sediment in continental and global scale $[k_{deg,sd\,[S]}]$ might be obtained from:

$$k_{deg,sd\,[S]} = k_{deg,sd\,25°C} \cdot (3600 \cdot 24) \quad [d^{-1}] \tag{279}$$

where

$k_{deg,sd\,[S]}$: *degradation in continental and global fresh and sea water sediment* $[d^{-1}]$

$k_{deg,w\,25°C}$: *bulk degradation rate constant at* $25°C$, *in sediment* $[s^{-1}]$

$(3600 \cdot 24)$: *conversion factor* $[s \cdot d^{-1}]$

For organic chemicals, degradation rate in sediment was extrapolated from biodegradation rate using division factor of "1". Specifically, Biowin3 model was used to estimate biodegradation half lifes in EPI Suite™. Biodegradation half lifes were correlated to default biodegradation rate in Table 3-1. Biodegradation half lifes were used to match default biodegradation rate and then to calculate degradation rate in water. For inorganic chemicals degradation rate in sediment was set at $1 \cdot 10^{-20} \cdot s^{-1}$, indicating that no degradation of inorganic in the environment occurred.

8.3.4 Soil

8.3.4.1 Degradation in soil

The transfer from natural and agricultural soil in continental and global scale might be obtained from:

$$k_{deg,sl\,[S]} = k_{deg,sl\,25°C} \cdot (3600 \cdot 24) \quad [d^{-1}] \qquad (280)$$

where

$k_{deg,sl\,[S]}$: $degradation\ in\ continental\ and\ global\ natural\ and\ agricultural\ soil\ [d^{-1}]$

$k_{deg,sl\,25°C}$: $bulk\ degradation\ rate\ constant\ at\ 25°C, in\ natural\ and\ agricultural\ soil\ [s^{-1}]$

$(3600 \cdot 24)$: $conversion\ factor\ [s \cdot d^{-1}]$

For organic chemicals, degradation rate in natural and agricultural soil was extrapolated from biodegradation rate using division factor of "1". Specifically, Biowin3 model was used to estimate biodegradation half lifes in EPI Suite™. Biodegradation half lifes was correlated to default biodegradation rate in Table 3-1. Biodegradation half lifes were used to match default biodegradation rate and then to calculate degradation rate in water. For inorganic chemicals degradation rate in natural and agricultural soil was set at $1 \cdot 10^{-20} \cdot s^{-1}$, thus indicating that no degradation of inorganic in the environment occurred.

8.4 Intermedia partition processes

Intermedia equilibrium constants (air-water; aerosol-water; sediment-water; soil-water) or partition coefficients were required in order to estimate intermedia mass transfer coefficients. The coefficients represented concentration ratios in the considered phase. The plot of the concentration data was often linear at low concentrations (Mackay 2001 5.4.1); therefore, with two immiscible phases "phase 1" and "phase 2" the following equation (291) might be written:

(281)

$$\frac{C_2}{C_1} = K_{21}$$

where

K_{21}: $partition\ coefficient$ $[-]$
C_2: $concentration\ of\ chemical\ in\ the\ phase$ "2" $[kg \cdot m^{-3}]$
C_2: $concentration\ of\ chemical\ in\ the\ phase$ "1" $[kg \cdot m^{-3}]$

The slope of the line is K_{21}.

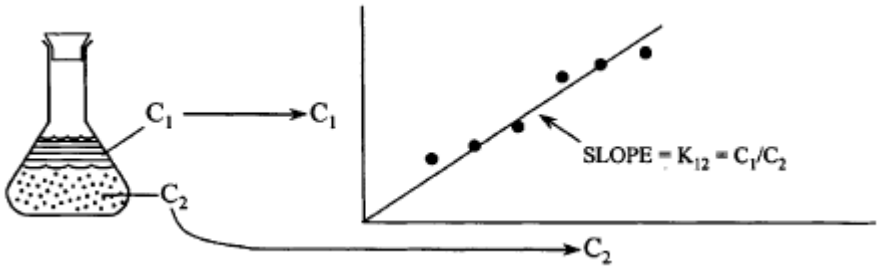

Figure 8-4 Experimental determination of Partition Coefficient (Reproduced from Mackay 2001)

Since

(282)

$$C_2 = f_2 \cdot Z_2$$

(283)

$$C_1 = f_1 \cdot Z_1$$

with

C_2: $concentration\ in\ the\ phase$ "2" $[kg \cdot m^{-3}]$
C_1: $concentration\ in\ the\ phase$ "1" $[kg \cdot m^{-3}]$
f_2: $fugacity\ in\ the\ phase$ "2" $[Pa]$
f_1: $fugacity\ in\ the\ phase$ "1" $[Pa]$
Z_2: $fugacity\ capacity\ in\ the\ phase$ "2" $[moli \cdot Pa^{-1} \cdot m^{-3}]$
Z_1: $fugacity\ capacity\ in\ the\ phase$ "1" $[moli \cdot Pa^{-1} \cdot m^{-3}]$

(284)

$$\frac{C_2}{C_1} = K_{21} = \frac{Z_2 \cdot f_2}{Z_1 \cdot f_1}$$

Fugacity (f) measures the tendency of molecules to escape from an environmental compartment, thus the tendency to move and redistribute to achieve balance (Mackay 2001).

Intermedia partition processes

The fugacity capacity (Z) represented the tendency of the unit of volume of the environmental compartment to retain the chemical compound, or, in other words the maximum concentration potentially retained by the volume unit of the compartment at the unit pressure (Mackay 2001). According to these definitions, fugacity could be considered a chemical property, while fugacity capacity represented a property of both the chemical and the environmental compartment in which chemical is find. At the equilibrium

(285)

$$f_2 = f_1 = f$$

Therefore:

(286)

$$\frac{C_2}{C_1} = K_{21} = \frac{Z_2 \cdot f_2}{Z_1 \cdot f_1} = \frac{Z_2 \cdot f}{Z_1 \cdot f} = \frac{Z_2}{Z_1}$$

Partition coefficients were available from experimental data or field measurements. More often, however, these information were not available. In these cases, the estimation methods described below could be used. It should be noted that, in general, the applicability of these estimation methods was limited to those classes of (organic) chemicals for which the relationships were derived. Extrapolation beyond these limits might lead to errors of orders of magnitude.

8.4.1 Air-Water

For air compartment

(287)

$$Z_{air} = \frac{1}{R \cdot 298} \quad [Pa^{-1} \cdot m^{-3} \cdot moli]$$

with
$R = 8.314$: $gas\ constant$ $[Pa \cdot m^3 \cdot mol^{-1}K^{-1}]$
298: $temperature$ $[K]$

For water

(288)

$$Z_{water} = \frac{1}{KH_{25°C}} \quad [Pa^{-1} \cdot m^{-3} \cdot moli]$$

with
$KH_{25°C}$: $costant\ di\ Henry\ at\ 25°C$ $[Pa \cdot m^3 \cdot moli^{-1}]$

It follows that dimensionless air/water partition coefficient is equal to:

(289)

$$K_{aw} = \frac{C_{air}}{C_{water}} = \frac{Z_{air}}{Z_{water}} = \frac{KH_{25°C}}{R \cdot 298} \quad [-]$$

Generally, $KH_{25°C}$ is defined for a given substance in EPI Suite™. If Henry's constant is not defined, it may be derived from quantitative structure-activity relationship (QSAR). The estimation may be obtained with the temperature dependent ratio of vapor pressure and the water solubility.

Intermedia partition processes

For $P_{vap,25°C} > 100000$:

(290)

$$K_{aw} = \frac{\frac{100000}{S_{w,25°C}}}{8.31 \cdot 298} \quad [-]$$

with

$P_{vap,25°C}$: $vapor\ pressure\ at\ 25°C\ [Pa]$

100000: $maximum\ vapor\ pressure\ of\ original\ species\ at\ 25°C\ [Pa]$

$S_{w,25°C}$: $water\ solubility\ of\ original\ species\ at\ 25°C\ [moli \cdot m^{-3}]$

$R = 8.314$: $gas\ constant\ [Pa \cdot m^3 \cdot moli^{-1}K^{-1}]$

298: $temperature\ [K]$

For $P_{vap,25°C} < 100000$:

(291)

$$K_{aw} = \frac{\frac{P_{vap,25°C}}{S_{w,25°C}}}{8.31 \cdot 298} \quad [-]$$

with

$P_{vap,25°C}$: $vapor\ pressure\ at\ 25°C\ [Pa]$

100000: $maximum\ vapor\ pressure\ of\ original\ species\ at\ 25°C\ [Pa]$

$S_{w,25°C}$: $water\ solubility\ of\ original\ species\ at\ 25°C\ [moli \cdot m^{-3}]$

$R = 8.314$: $gas\ constant\ [Pa \cdot m^3 \cdot moli^{-1}K^{-1}]$

298: $temperature\ [K]$

The urban, continental and global scale temperatures are equal to 285 K in USEtox.
In the estimation method for the air/water partition coefficient T is 298 K. So, for the scale specific air/water partition coefficient calculation it was necessary to apply a correction in order to account for differences in temperature.

8.5 Intermedia transfer processes

The constant for mean removal rate from continental and global air might be obtained from:

(292)

$$1/k_{mean,air[S]} = \left(\left(\frac{1}{k_{tot,dry,air[S]}} \right) \times \frac{t_{dry\,[S]}}{t_{dry\,[S]}+t_{wet\,[S]}} + \left(\frac{1}{k_{tot,wet,air[S]}} \right) \times \frac{t_{wet\,[S]}}{t_{dry\,[S]}+t_{wet\,[S]}} - \left(\frac{\left(\frac{1}{k_{tot,wet,air[S]}} + \frac{1}{k_{tot,dry,air[S]}} \right)^2}{t_{dry\,[S]}+t_{wet\,[S]}} \right) \times \left(1 - e^{-k_{dry\,tot,air[S]} \cdot t_{dry}[S]}\right) \times \frac{\left(1-e^{-k_{wet\,tot,air[S]} \cdot t_{wet}[S]}\right)}{\left(1-e^{-\left(k_{dry\,tot,air[S]} \cdot t_{dry}[S] + k_{wet\,tot,air[S]} \cdot t_{wet}[S]\right)}\right)} \right)$$

Demonstration of equation (292)

According to the intermittent model of Jolliet et al. (2005), the deposition process might be described by the following two equations:

(293)

$$\frac{dM_{dry}(t)}{dt} = S - k_{dry\,tot} \cdot M_{dry}(t)$$

(294)

$$\frac{dM_{wet}(t)}{dt} = S - k_{wet\,tot} \cdot M_{wet}(t)$$

At $t = 0$

(295)

$$M_{dry}(t=0) = M_{wet}^{min} = M_{wet} \cdot \left(t_{dry} + t_{wet}\right)$$

(296)

$$M_{wet}\left(t = t_{dry}\right) = M_{dry}^{max} = M_{dry} \cdot \left(t_{dry}\right)$$

By solving equation (293) and (294), the following equation (297) was obtained:

(297)

$$M_{dry}(t) = \frac{S}{k_{dry\,tot}} - \left(\frac{S}{k_{dry\,tot}} - M_{wet}^{min} \right) \cdot e^{-k_{dry\,tot} \cdot t}$$

(298)

$$M_{wet}(t) = \frac{S}{k_{wet\,tot}} - \left(\frac{S}{k_{wet\,tot}} - M_{dry}^{max} \right) \cdot e^{-k_{wet\,tot} \cdot \left(t - t_{dry}\right)}$$

where

(299)

$$M_{dry}^{max} = \frac{S}{k_{wet\ tot}} + \left(\frac{S}{k_{dry\ tot}} - \frac{S}{k_{wet\ tot}}\right) \times \frac{\left(1 - e^{-k_{dry\ tot} \cdot t_{dry}}\right)}{\left(1 - e^{-\left(k_{dry\ tot} \cdot t_{dry} + k_{wet\ tot} \cdot t_{wet}\right)}\right)}$$

(300)

$$M_{wet}^{min} = \frac{S}{k_{dry\ tot}} + \left(\frac{S}{k_{wet\ tot}} - \frac{S}{k_{dry\ tot}}\right) \times \frac{\left(1 - e^{-k_{wet\ tot} \cdot t_{wet}}\right)}{\left(1 - e^{-\left(k_{dry\ tot} \cdot t_{dry} + k_{wet\ tot} \cdot t_{wet}\right)}\right)}$$

Demonstration of equation (297)

(301)

$$\frac{dM_{dry}(t)}{dt} = S - k_{dry\ tot} \cdot M_{dry}(t) = \left(M_{dry}(t)\right)' + k_{dry\ tot} \cdot M_{dry}(t) = S$$

where $M_{dry}(t) = t$

This is a differential equation of first degree having the following solution:

(302)

$$M_{dry}(t) = e^{-A(t)} \cdot \left[C_1 + \int \left(g(t) \cdot e^{A(t)}\right) \cdot dt\right]$$

(303)

$$A(t) = \int \left(a_0(t)\right) \cdot dt = \int \left(k_{dry\ tot}\right) \cdot dt = k_{dry\ tot} \cdot t$$

(304)

$$g(t) = S$$

Therefore

(305)

$$M_{dry}(t) = e^{-k_{dry\ tot} \cdot t} \cdot \left[C_1 + \int \left(S \cdot e^{k_{dry\ tot} \cdot t}\right) \cdot dt\right]$$

(306)

$$\int \left(S \cdot e^{k_{dry\ tot} \cdot t}\right) \cdot dt = S \cdot \int \left(e^{k_{dry\ tot} \cdot t}\right) \cdot dt = \frac{S}{k_{dry\ tot}} \cdot \left(e^{k_{dry\ tot} \cdot t}\right)$$

Thus

(307)

$$M_{dry}(t) = e^{-k_{dry\ tot} \cdot t} \cdot \left[C_1 + \frac{S}{k_{dry\ tot}} \cdot \left(e^{k_{dry\ tot} \cdot t}\right)\right]$$

If $t = 0$

(308)

$$M_{dry}(t) = M_{wet}^{min} = \left[C_1 + \frac{S}{k_{dry\,tot}}\right] \rightarrow C_1 = M_{wet}^{min} - \frac{S}{k_{dry\,tot}}$$

Therefore, by substituting C_1 it could be obtained the following equation (309):

(309)

$$M_{dry}(t) = e^{-k_{dry\,tot}\cdot t} \cdot \left[\left(M_{wet}^{min} - \frac{S}{k_{dry\,tot}}\right) + \frac{S}{k_{dry\,tot}} \cdot \left(e^{k_{dry\,tot}\cdot t}\right)\right]$$
$$= e^{-k_{dry\,tot}\cdot t} \cdot M_{wet}^{min} - e^{-k_{dry\,tot}\cdot t} \cdot \frac{S}{k_{dry\,tot}} + \frac{S}{k_{dry\,tot}} = \frac{S}{k_{dry\,tot}} - \left(\frac{S}{k_{dry\,tot}} - M_{wet}^{min}\right) \cdot e^{-k_{dry\,tot}\cdot t}$$

Demonstration of equation (298)

(310)

$$\frac{dM_{wet}(t)}{dt} = S - k_{wet\,tot} \cdot M_{wet}(t) = \left(M_{wet}(t)\right)' + k_{wet\,tot} \cdot M_{wet}(t) = S$$

where $M_{wet}(t) = t$
This is a differential equation of first degree having the following solution:

(311)

$$M_{wet}(t) = e^{-A(t)} \cdot \left[C_1 + \int \left(g(t) \cdot e^{A(t)}\right) \cdot dt\right]$$

where

(312)

$$A(t) = \int \left(a_0(t)\right) \cdot dt = \int (k_{wet\,tot}) \cdot dt = k_{wet\,tot} \cdot t$$

(313)

$$g(t) = S$$

Therefore:

(314)

$$M_{wet}(t) = e^{-k_{wet\,tot}\cdot t} \cdot \left[C_1 + \int (S \cdot e^{k_{wet\,tot}\cdot t}) \cdot dt\right]$$

(315)

$$\int (S \cdot e^{k_{wet\,tot}\cdot t}) \cdot dt = S \cdot \int (e^{k_{wet\,tot}\cdot t}) \cdot dt = \frac{S}{k_{wet\,tot}} \cdot (e^{k_{wet\,tot}\cdot t})$$

Thus,

(316)

$$M_{wet}(t) = e^{-k_{wet\,tot}\cdot t}\cdot\left[C_1 + \frac{S}{k_{wet\,tot}}\cdot\left(e^{k_{wet\,tot}\cdot t}\right)\right]$$

If $t = t_{dry}$

(317)

$$M_{wet}\left(t_{dry}\right) = M_{dry}^{max} = e^{-k_{wet\,tot}\cdot t_{dry}}\cdot\left[C_1 + \frac{S}{k_{wet\,tot}}\cdot e^{k_{wet\,tot}\cdot t_{dry}}\right]$$

(318)

$$e^{-k_{wet\,tot}\cdot t_{dry}}\cdot C_1 = M_{dry}^{max} - \frac{S}{k_{wet\,tot}} \rightarrow C_1 = M_{dry}^{max}\cdot e^{k_{wet\,tot}\cdot t_{dry}} - \frac{S}{k_{wet\,tot}}\cdot e^{k_{wet\,tot}\cdot t_{dry}}$$

Therefore, by substituting C_1 the following equation could be written:

(319)

$$M_{wet}(t) = e^{-k_{wet\,tot}\cdot t}\cdot\left[M_{dry}^{max}\cdot e^{k_{wet\,tot}\cdot t_{dry}} - \frac{S}{k_{wet\,tot}}\cdot e^{k_{wet\,tot}\cdot t_{dry}} + \frac{S}{k_{wet\,tot}}\cdot\left(e^{k_{wet\,tot}\cdot t}\right)\right]$$

$$= M_{dry}^{max}\cdot e^{k_{wet\,tot}\cdot(t_{dry}-t)} - \frac{S}{k_{wet\,tot}}\cdot e^{k_{wet\,tot}\cdot(t_{dry}-t)} + \frac{S}{k_{wet\,tot}}$$
$$= \frac{S}{k_{wet\,tot}} - \left(\frac{S}{k_{wet\,tot}} - M_{dry}^{max}\right)\cdot e^{k_{wet\,tot}\cdot(t_{dry}-t)}$$
$$= \frac{S}{k_{wet\,tot}} - \left(\frac{S}{k_{wet\,tot}} - M_{dry}^{max}\right)\cdot e^{-k_{wet\,tot}\cdot(t-t_{dry})}$$

In order to determine M_{dry}^{max}, equation (309) solved for $\left(t = t_{dry}\right)$ was substituted in equation (296):

(320)

$$M_{dry}^{max} = M_{dry}\cdot\left(t_{dry}\right) = \frac{S}{k_{dry\,tot}} - \left(\frac{S}{k_{dry\,tot}} - M_{wet}^{min}\right)\cdot e^{-k_{dry\,tot}\cdot t_{dry}}$$

(321)

$$M_{wet}^{min} = M_{wet}\cdot\left(t_{dry} + t_{wet}\right) = \frac{S}{k_{wet\,tot}} - \left(\frac{S}{k_{wet\,tot}} - M_{dry}^{max}\right)\cdot e^{-k_{wet\,tot}\cdot(t_{wet})}$$

By introducing (321) in (320):

(322)

$$M_{dry}^{max} = M_{dry} \cdot \left(t_{dry}\right)$$
$$= \frac{S}{k_{dry\,tot}} - \left(\frac{S}{k_{dry\,tot}} - \left[\frac{S}{k_{wet\,tot}} - \left(\frac{S}{k_{wet\,tot}} - M_{dry}^{max}\right) \cdot e^{-k_{wet\,tot} \cdot (t_{wet})}\right]\right) \cdot e^{-k_{dry\,tot} \cdot t_{dry}}$$
$$= \frac{S}{k_{dry\,tot}} - \frac{S}{k_{dry\,tot}} \cdot e^{-k_{dry\,tot} \cdot t_{dry}} + \frac{S}{k_{wet\,tot}} \cdot e^{-k_{dry\,tot} \cdot t_{dry}} - \frac{S}{k_{wet\,tot}}$$
$$\cdot e^{-\left(k_{wet\,tot} \cdot t_{wet} + k_{dry\,tot} \cdot t_{dry}\right)} + M_{dry}^{max} \cdot e^{-\left(k_{wet\,tot} \cdot t_{wet} + k_{dry\,tot} \cdot t_{dry}\right)}$$

By adding and subtracting the quantity $\left(\frac{S}{k_{wet\,tot}}\right)$

(323)

$$M_{dry}^{max} \cdot \left(1 - e^{-\left(k_{wet\,tot} \cdot t_{wet} + k_{dry\,tot} \cdot t_{dry}\right)}\right)$$
$$= \frac{S}{k_{dry\,tot}} - \frac{S}{k_{dry\,tot}} \cdot e^{-k_{dry\,tot} \cdot t_{dry}} + \frac{S}{k_{wet\,tot}} \cdot e^{-k_{dry\,tot} \cdot t_{dry}} - \frac{S}{k_{wet\,tot}} \cdot$$
$$\cdot e^{-\left(k_{wet\,tot} \cdot t_{wet} + k_{dry\,tot} \cdot t_{dry}\right)} + \frac{S}{k_{wet\,tot}} - \frac{S}{k_{wet\,tot}}$$

(324)

$$M_{dry}^{max} \cdot \left(1 - e^{-\left(k_{wet\,tot} \cdot t_{wet} + k_{dry\,tot} \cdot t_{dry}\right)}\right)$$
$$= \left(\frac{S}{k_{dry\,tot}} - \frac{S}{k_{wet\,tot}}\right) - \left(\frac{S}{k_{dry\,tot}} - \frac{S}{k_{wet\,tot}}\right) \cdot e^{-k_{dry\,tot} \cdot t_{dry}} + \frac{S}{k_{wet\,tot}}$$
$$\cdot \left(1 - e^{-\left(k_{wet\,tot} \cdot t_{wet} + k_{dry\,tot} \cdot t_{dry}\right)}\right)$$

(325)

$$\boldsymbol{M_{dry}^{max} = \frac{S}{k_{wet\,tot}} + \left(\frac{S}{k_{dry\,tot}} - \frac{S}{k_{wet\,tot}}\right) \cdot \frac{\left(1 - e^{-k_{dry\,tot} \cdot t_{dry}}\right)}{\left(1 - e^{-\left(k_{wet\,tot} \cdot t_{wet} + k_{dry\,tot} \cdot t_{dry}\right)}\right)}}$$

In order to determine M_{wet}^{min}, we substitute equation (325) in the following equation (321):

(326)

$$M_{wet}^{min} = M_{wet} \cdot \left(t_{dry} + t_{wet}\right) = \frac{S}{k_{wet\,tot}} - \left(\frac{S}{k_{wet\,tot}} - M_{dry}^{max}\right) \cdot e^{-k_{wet\,tot} \cdot (t_{wet})}$$

By introducing (325) in (321):

(327)

$$M_{wet}^{min} = M_{wet} \cdot \left(t_{dry} + t_{wet}\right)$$
$$= \frac{S}{k_{wet\,tot}} - \left(\frac{S}{k_{wet\,tot}} - \left(\frac{S}{k_{wet\,tot}} + \left(\frac{S}{k_{dry\,tot}} - \frac{S}{k_{wet\,tot}}\right) \cdot \frac{\left(1 - e^{-k_{dry\,tot} \cdot t_{dry}}\right)}{\left(1 - e^{-\left(k_{wet\,tot} \cdot t_{wet} + k_{dry\,tot} \cdot t_{dry}\right)}\right)}\right)\right)$$
$$\cdot e^{-k_{wet\,tot} \cdot (t_{wet})}$$

(328)

$$M_{wet}^{min} = \frac{S}{k_{wet\,tot}} - \frac{S}{k_{wet\,tot}} \cdot e^{-k_{wet\,tot} \cdot (t_{wet})} + \frac{S}{k_{wet\,tot}} \cdot e^{-k_{wet\,tot} \cdot (t_{wet})} + \left(\frac{S}{k_{dry\,tot}} - \frac{S}{k_{wet\,tot}}\right) \cdot \frac{\left(1 - e^{-k_{dry\,tot} \cdot t_{dry}}\right)}{\left(1 - e^{-\left(k_{wet\,tot} \cdot t_{wet} + k_{dry\,tot} \cdot t_{dry}\right)}\right)} \cdot e^{-k_{wet\,tot} \cdot (t_{wet})}$$

(329)

$$M_{wet}^{min} \times \left(1 - e^{-\left(k_{wet\,tot} \cdot t_{wet} + k_{dry\,tot} \cdot t_{dry}\right)}\right) = \frac{S}{k_{wet\,tot}} \cdot \left(1 - e^{-\left(k_{wet\,tot} \cdot t_{wet} + k_{dry\,tot} \cdot t_{dry}\right)}\right) + \left(\frac{S}{k_{dry\,tot}} - \frac{S}{k_{wet\,tot}}\right) \cdot e^{-k_{wet\,tot} \cdot (t_{wet})} - \left(\frac{S}{k_{dry\,tot}} - \frac{S}{k_{wet\,tot}}\right) \cdot e^{-\left(k_{wet\,tot} \cdot t_{wet} + k_{dry\,tot} \cdot t_{dry}\right)}$$

(330)

$$M_{wet}^{min} \times \left(1 - e^{-\left(k_{wet\,tot} \cdot t_{wet} + k_{dry\,tot} \cdot t_{dry}\right)}\right) = \frac{S}{k_{wet\,tot}} - \frac{S}{k_{wet\,tot}} \cdot e^{-\left(k_{wet\,tot} \cdot t_{wet} + k_{dry\,tot} \cdot t_{dry}\right)} + \left(\frac{S}{k_{dry\,tot}} - \frac{S}{k_{wet\,tot}}\right) \cdot e^{-k_{wet\,tot} \cdot (t_{wet})} - \frac{S}{k_{dry\,tot}} \cdot e^{-\left(k_{wet\,tot} \cdot t_{wet} + k_{dry\,tot} \cdot t_{dry}\right)} + \frac{S}{k_{wet\,tot}} \cdot e^{-\left(k_{wet\,tot} \cdot t_{wet} + k_{dry\,tot} \cdot t_{dry}\right)}$$

By adding and subtracting the quantity $\left(\frac{S}{k_{dry\,tot}}\right)$:

(331)

$$M_{wet}^{min} \times \left(1 - e^{-\left(k_{wet\,tot} \cdot t_{wet} + k_{dry\,tot} \cdot t_{dry}\right)}\right) = \frac{S}{k_{wet\,tot}} + \left(\frac{S}{k_{dry\,tot}} - \frac{S}{k_{wet\,tot}}\right) \cdot e^{-k_{wet\,tot} \cdot (t_{wet})} - \frac{S}{k_{dry\,tot}} \cdot e^{-\left(k_{wet\,tot} \cdot t_{wet} + k_{dry\,tot} \cdot t_{dry}\right)} - \frac{S}{k_{dry\,tot}} + \frac{S}{k_{dry\,tot}}$$

Thus,

(332)

$$M_{wet}^{min} \times \left(1 - e^{-\left(k_{wet\,tot} \cdot t_{wet} + k_{dry\,tot} \cdot t_{dry}\right)}\right) = \left(\frac{S}{k_{wet\,tot}} - \frac{S}{k_{dry\,tot}}\right) \cdot \left(1 - e^{-k_{wet\,tot} \cdot (t_{wet})}\right) + \frac{S}{k_{dry\,tot}} \cdot \left(1 - e^{-\left(k_{wet\,tot} \cdot t_{wet} + k_{dry\,tot} \cdot t_{dry}\right)}\right)$$

(333)

$$\boldsymbol{M_{wet}^{min} = \left(\frac{S}{k_{wet\,tot}} - \frac{S}{k_{dry\,tot}}\right) \cdot \frac{\left(1 - e^{-k_{wet\,tot} \cdot (t_{wet})}\right)}{\left(1 - e^{-\left(k_{wet\,tot} \cdot t_{wet} + k_{dry\,tot} \cdot t_{dry}\right)}\right)} + \frac{S}{k_{dry\,tot}}}$$

Average Mass in air

The average resulting mass in air ($\bar{M}\ in\ kg$) or the total equivqlent decay rate $\overline{k_{tot}}$ were defined as:

(334)

$$\bar{M} = \frac{1}{t_{dry} + t_{wet}} \left[\int_0^{t_{dry}} M_{dry}(t)\, dt + \int_{t_{dry}}^{t_{dry}+t_{wet}} M_{wet}(t)\, dt \right] = \frac{S}{\overline{k_{tot}}}$$

(335)

$$\int_0^{t_{dry}} M_{dry}(t)\, dt = \int_0^{t_{dry}} \frac{S}{k_{dry\ tot}} dt - \int_0^{t_{dry}} \left(\frac{S}{k_{dry\ tot}} - M_{wet}^{min} \right) \cdot e^{-k_{dry\ tot} \cdot t}\, dt$$

(336)

$$\int_0^{t_{dry}} M_{dry}(t)\, dt = \frac{S}{k_{dry\ tot}} \cdot t_{dry} + \left(\frac{S}{k_{dry\ tot}} - M_{wet}^{min} \right) \cdot \left(\frac{\left(1 - e^{-k_{dry\ tot} \cdot t_{dry}}\right)}{-k_{dry\ tot}} \right)$$

Substituting M_{wet}^{min} by equation (300):

(337)

$$\int_0^{t_{dry}} M_{dry}(t)\, dt = \frac{S}{k_{dry\ tot}} \cdot t_{dry} + \left(\frac{S}{k_{dry\ tot}} - M_{wet}^{min} \right) \cdot \left(\frac{\left(1 - e^{-k_{dry\ tot} \cdot t_{dry}}\right)}{-k_{dry\ tot}} \right)$$

$$\left(\frac{S}{k_{dry\ tot}} - M_{wet}^{min} \right)$$
$$= \left(\frac{S}{k_{dry\ tot}} - \frac{S}{k_{dry\ tot}} - \left(\frac{S}{k_{dry\ tot}} - \frac{S}{k_{wet\ tot}} \right) \cdot \frac{\left(1 - e^{-k_{wet\ tot} \cdot (t_{wet})}\right)}{\left(1 - e^{-\left(k_{wet\ tot} \cdot t_{wet} + k_{dry\ tot} \cdot t_{dry}\right)}\right)} \right)$$

Therefore

(338)

$$\int_0^{t_{dry}} M_{dry}(t)\, dt$$
$$= \frac{S}{k_{dry\ tot}} \cdot t_{dry} + \left(\frac{S}{k_{wet\ tot}} - \frac{S}{k_{dry\ tot}} \right) \cdot \frac{\left(1 - e^{-k_{wet\ tot} \cdot (t_{wet})}\right)\left(1 - e^{-k_{dry\ tot} \cdot t_{dry}}\right)}{\left(1 - e^{-\left(k_{wet\ tot} \cdot t_{wet} + k_{dry\ tot} \cdot t_{dry}\right)}\right) \cdot \left(-k_{dry\ tot}\right)}$$

Similarly,

(339)

$$\int_{t_{dry}}^{t_{dry}+t_{wet}} M_{wet}(t)\,dt = \frac{S}{k_{wet\,tot}} \cdot t_{wet} + \left(\frac{S}{k_{wet\,tot}} - M_{dry}^{max}\right) \cdot \left(\frac{\left(1 - e^{-k_{wet\,tot} \cdot t_{wet}}\right)}{-k_{wet\,tot}}\right)$$

By substituting in equation (334) it was possible to obtained $\bar{M}$ and consequently $1/k_{mean,air[S]}$

(340)

$$\bar{M} = \frac{1}{t_{dry} + t_{wet}} \left[\frac{S}{k_{drytot}} \times t_{dry} + \frac{S}{k_{wet\,tot}} \cdot t_{wet} + \left(\frac{S}{k_{wet\,tot}} - \frac{S}{k_{dry\,tot}}\right) \cdot \frac{\left(1 - e^{-k_{wet\,tot} \cdot (t_{wet})}\right)\left(1 - e^{-k_{dry\,tot} \cdot t_{dry}}\right)}{\left(1 - e^{-\left(k_{wet\,tot} \cdot t_{wet} + k_{dry\,tot} \cdot t_{dry}\right)}\right)} \times \left(\frac{1}{k_{wet\,tot}} - \frac{1}{k_{dry\,tot}}\right) \right]$$

(341)

$$\bar{M} = S \times \left[\frac{1}{k_{drytot}} \times \frac{t_{dry}}{t_{dry} + t_{wet}} + \frac{1}{k_{wet\,tot}} \times \frac{t_{wet}}{t_{dry} + t_{wet}} - \varepsilon \right]$$

where

$$\varepsilon = \frac{\left(\frac{1}{k_{wet\,tot}} - \frac{1}{k_{dry\,tot}}\right)^2}{t_{dry} + t_{wet}} \times \frac{\left(1 - e^{-k_{wet\,tot} \cdot (t_{wet})}\right)\left(1 - e^{-k_{dry\,tot} \cdot t_{dry}}\right)}{\left(1 - e^{-\left(k_{wet\,tot} \cdot t_{wet} + k_{dry\,tot} \cdot t_{dry}\right)}\right)}$$

9 CONCLUSIONS

This study confirmed that proteins extracted from BSF prepupae can be employed to obtain bioplastic films, which are promising as bio-compostable plastics. The added value of these films is that they are generated by waste processing and reduction in volume by insects, increasing their positive effect in a circular economy perspective. The addition of glycerol as plasticizer showed a high potential, due to favorable mechanical properties (also after aging tests) if the protein content is near 12 wt%, even after aging tests. However, tensile stress at break must be increased using other additives, in order to obtain values closer to those of other bioplastics available by employing other additives.

The breeding of Black Soldier Flies larvae on chicken manure (C), zeolitic tuff (Ca-chabazite) (B), soil improver obtained from pruning shears of urban green (SL) and water (A), was optimized in order to maximize the number and weight of prepupae. The optimal conditions (climate, light, diet) for breeding adults were identified as well, in order to maximize egg production. All experiments performed at 27 and 33°C showed that:

- it is recommended to remove the soil improver and avoid the higher temperature (33°C), due to higher larvae mortality;
- it is also recommended to exclude micronized Ca-chabazite because of a 3-4 day of delay in the development of prepupae.

Four different mixtures were identified where chicken manure ranged from 34.5 to 45.0%, Ca-chabazite (larger particle size) from 5.0 to 7.2%, and water from 50.0 to 58.3%. These four mixtures gave a percentage of prepupae of 72-97%, with mortality between 20-25%, average weight of 60-100 mg, and a percentage of emerged adults of 94-100%. Considering percentage of prepupae (PP) as the response variable, the optimum corresponds to mixture A (58.3%), followed by C (34.5%) and B (7.20%); considering average weight of prepupae (AW) as response variable the optimum corresponds to mixture A (50%), followed by C (45%) and B (5%). If both parameters were concurrently considered (U), the optimal mixture is A (55.5%), followed by C (38.9%) and B (5.6%) while if both parameters are considered (U), with an increased importance for percentage of prepupae (D) the optimal mixture is A (56.7%), followed by C (36.9%) and B (6.4%).

The best egg production per day was observed by using a UV-green-blue combination of LEDs associated to a water diet.

For population density, tests were carried out varying density up to 20,000 adults per cubic meter. No negative effects were observed on the number of eggs laid, therefore density was not a relevant parameter.

The evaluation of olfactory impact on the composts obtained by breeding the larvae on the different mixtures showed a significant reduction of bad smells thanks to the action of the larvae. In particular, for these tests, four different substrates without black soldier flies were compared with the same substrates digested by black soldier flies, showing a reduction in the olfactory impact.

Among the different procedures tested in the laboratory in order to extract lipid, protein and chitin fractions from BSF prepupae, the most promising one for the final application of the present study,

was the chemical extraction protocol, since it was not necessary for the extracted proteins to be intact. Although it was characterized by a lower proteins yield with respect to the chemical extraction protocol 2, it allowed both obtaining a better degree of chitin purity, and avoiding the use of another organic solvent (ethanol) in addition to petroleum ether.

Life Cycle Assessment (LCA) was applied by using the SimaPro 8.3 software and the IMPACT 2002+ evaluation method. The results showed that the total damage associated to 1 g of bioplastic production process was equal to 4.157E-3 Pt. Furthermore, the main environmental impact was due to energy consumption (44.20%), in particular, due to the energy consumption of the aspiration system (93.06%), because of the incubation phases under the aspiration hoods. Indeed, bioplastic production required incubation steps under the aspiration hood whose duration was very high. This consumption should be reduced in order to minimize environmental impact, even if this process step was essential to dryf the materials. This high environmental impact was probably due to the fact that the laboratory-scale production process was assessed, and not yet an industrial one. Therefore, hopefully these results will contribute to the eco-design of an industrial-scale production of these innovative bioplastics in order to minimize their environmental burdens.

The analysis of results showed that two other important sources of potential environmental impact were work equipment and the materials (proteins).
Life Cycle Assessment of the "Extraction of lipid, protein, chitin fraction" process showed that the total damage at end-point level was due for 59.91% to the "BSF Breeding" process. From the analysis at end point level of the "BSF Breeding" process, it emerged that the total damage was due for 87.08% to the "Bioconversion unit" process, in particular the damage was attributable to the amount of energy necessary to ensure temperature and humidity conditions for optimal bioconversion process.

Critical analysis of the approximated method employed to calculate local and indoor emissions showed that it was highly desiderable a further implementation phase able to consider also incidences due to air-drinking water and air-food uptakes. In this first phase these two oral uptakes were considered equal to air-air incidence. This is a very important approximation.
Furthermore, it seemed that the local air dispersion model was completely independent of the physico-chemical properties of the pollutant. Therefore, for background concentrations, specific inputs from other sources need to be used for. It is important to understand how to combine the dispersion model with a model that takes into account the physical and chemical properties of the pollutant. Thus, an in depth study of the USEtox model was carried out, in order to understand and demonstrate the equations on which USEtox Environmental Fate is based.

Bibliography

Intoduction

De Boer H.C., Van Krimpen M.M., Blonk, H. & Tyszler, M., *Replacement of Soybean Meal in Compound Feed by European Protein Sources e Effects on Carbon Footprint*. (University and Research Centre) Livestock Research, Wageningen,Wageningen UR, Livestock Research Report 819, 2014.

Diener S., Zurbrügg C. & Tockner K., *Conversion of organic material by black soldier fly larvae: establishing optimal feeding rates*. Waste Management & Research, Volume 27 (6), 2009, pp. 603–610, https://doi.org/10.1177/0734242X09103838

Durrenberger A, Gaussian Plume Modeling, Chemical Engineering 357

Goedkoop M, Spriensma R, *The Eco-Indicator 99-A damage oriented method for Life Cycle Impact Assessment* , Methodology Annex, PRé-product ecology consultants, 22 June 2001-Third edition

Oonincx, D.G. & De Boer, I.J., *Environmental impact of the production of mealworms as a protein source for humans: a life cycle assessment*. PLoS One, Volume 7 (12): e51145, https://doi.org/10.1371/journal.pone.0051145

Salomone R., Saija G., Mondello G., Giannetto A., Fasulo S. & Savastano D., *Environmental impact of food waste bioconversion by insects: Application of Life Cycle Assessment to process using Hermetia illucens*. "Journal of Cleaner Production", Volume 140 Part. 2, January 2017, pp. 890 - 905, https://doi.org/10.1016/j.jclepro.2016.06.154

Van Huis, A. et al., 2013. *Edible Insects e Future Prospects for Food and Feed Security*, FAO Forestry, Paper 171, http://www.fao.org/docrep/018/i3253e/i3253e00.htm

Van Zanten H. H. E., Mollenhorst H., Oonincx Dennis G A B, *From environmental nuisance to environmental opportunity: Housefly larvae convert waste to livestock feed*, Journal of Cleaner Production, Volume 102 (1), September 2015, pp 362-369, https://doi.org/10.1016/j.jclepro.2015.04.106

Chapter 1

Bradley S.W., Sheppard D.C., 1984, *House fly oviposition inhibition by larvae of Hermetia illucens, the black soldier fly, Journal of Chemical Ecology*, Volume 10, Issue 6, pp 853 - 859, https://doi.org/10.1007/BF00987968

Caruso D., Devic E., Subamia I., Talamond P. and Baras E., *Technical handbook of domestication and production of Diptera black soldier fly (BSF), Hermetia illucens, Stratiomyidae, Bogor (IDN)* ; Marseille : IPB Press; IRD, 2014, p. 141

Chippindale A.K., Leroi A.M., Kim S.B., Rose M.R., 1993, *Phenotypic plasticity and selection in Drosophila life-history evolution. I. Nutrition and the cost of reproduction*, Journal Evolutionary Biology, March 1993, Volume 6, Issue 2, pp 171 - 193, https://doi.org/10.1046/j.1420-9101.1993.6020171.x

Bibliography

Choi, Y.C., Choi, J.Y., Kim, J.G., Kim, M.S., Kim, W.T., Park, K.H., Bae, S.W., Jeong, G.S., *Potential usage of food waste as a natural fertilizer after digestion by Hermetia illucens (Diptera: stratiomyidae)*, International journal of industrial entomology, January 2009, Volume 19, Issue 1, pp 171 - 174

Cickova H., Newton G.L., Lacy R.C., Kozánek M., 2015, *The use of fly larvae for organic waste treatment*, Waste Management, Volume 35, January 2015, pp 68-80, https://doi.org/10.1016/j.wasman.2014.09.026

Devic, E., and Maquart, P.-O., *Dirhinus giffardii (Hymenoptera: Chalcididae), parasitoid affecting Black Soldier Fly production systems in West Africa*, Entomology, April 2015, Volume 3, https://doi.org/10.4081/entomologia.2015.284

Diclaro J.W. and Kaufman P.E., *Black soldier fly Hermetia illucens Linnaeus (Insecta: Diptera: Stratiomyidae)*, EENY-461, Featured Creatures from the Entomology and Nematology Department, Florida Cooperative Extension Service, Institute of Food and Agricultural Sciences, University of Florida, June 2009

Diener, S., Zurbrügg, C., Tockner, K., *Bioaccumulation of heavy metals in the black soldier fly, Hermetia illucens and effects on its life cycle*, Journal of Insects as Food and Feed, July 2015, Volume 1, Issue 4, pp 261 - 270, https://doi.org/10.3920/JIFF2015.0030

Diener, S., Studt Solano, N.M., Roa Gutiérrez, F. et al., *Biological treatment of municipal organic waste using black soldier fly larvae*, Waste Biomass Valorization, November 2011, Volume 2, Issue 4, pp 357 - 363, https://doi.org/10.1007/s12649-011-9079-1

Diener, S., Zurbrügg, C., Tockner, K., 2009, *Conversion of organic material by black soldier fly larvae: establishing optimal feeding rates*. Waste Management & Research, June 2009, Volume 27, Issue 6, pp 603 - 610. https://doi.org/10.1177/0734242X09103838

Erickson, M.C., Islam, M., Sheppard, C., Liao, J., Doyle, M.P., *Reduction of Escherichia coli O157: H7 and Salmonella enterica serovar enteritidis in chicken manure by larvae of the black soldier fly*, Journal of Food Protection, April 2004, Volume 67, Issue 4, pp 685 - 690, https://doi.org/10.4315/0362-028X-67.4.685

Furman D.P., Young R.D., Catts P.E., 1959, *Hermetia illucens (Linnaeus) as a factor in the natural control of Musca domestica Linnaeus*, Journal of Economic Entomology, Volume 52, Issue 5, pp 917 - 921, https://doi.org/10.1093/jee/52.5.917

Gabler, F., Vinneras, B., *Using Black Soldier Fly for Waste Recycling and Effective Salmonella Spp. Reduction*. Theses. Swedish University of Agricultural Sciences, Swedish , Accessed date: 31 July 2019.

Green T.R., Popa R., 2012, *Enhanced ammonia content in compost leachate processed by black soldier fly larvae*. Appl. Biochemistry and Biotechnology, March 2012, Volume 166, Issue 6, pp 1381 – 1387, https://doi.org/10.1007/s12010-011-9530-6

Gujarathi G.R., Pejaver M.K., 2013, *Occurrence of black soldier fly, Hermetia illucens (Diptera: stratiomyidae) in biocompost*. Res. J. Recent Sci., Volume 2, Issue (4), Pages 65-66, April, 2 (2013)

Hale O.M., 1973, *Dried Hermetia illucens larvae (Diptera: stratiomyidae) as a feed additive for poultry*, Journal of the Georgia Entomological Society, 8, 16-20.

Bibliography

Hall DC, Gerhardt RR. 2002, *Flies (Diptera)*, Mullen G, Durden L. (editors). Medical and Veterinary Entomology, Academic Press. San Diego, California, https://trove.nla.gov.au/version/30949372

Holmes L.A., Vanlaerhoven S.L., Tomberlin J.K., 2012, *Relative humidity effects on the life history of Hermetia illucens (Diptera: stratiomyidae)*, Environmental Entomology, Volume 41, Issue 4, 1 August 2012, Pages 971-978, https://doi.org/10.1603/EN12054

Jeffery K. Tomberlin and D. Craig Sheppard (2002), *Factors Influencing Mating and Oviposition of Black Soldier Flies (Diptera: Stratiomyidae) in a Colony*. Journal of Entomological Science: October 2002, Vol. 37, No. 4, pp. 345-352, https://doi.org/10.18474/0749-8004-37.4.345

Jeon H., Park S., Choi J., Jeong G., Lee S.B., Choi Y. and Lee S.J., 2011, *The intestinal bacterial community in the food waste-reducing larvae of Hermetia illucens*, Current Microbiology, Volume 62, Issue 5, pp 1390 - 1399, https://doi.org/10.1007/s00284-011-9874-8

Lalander, C.H., Fidjeland, J., Diener, S., Eriksson, S., Vinneras, B., 2015, *High waste-tobiomass conversion and efficient Salmonella spp. reduction using black soldier fly for waste recycling*, Agronomy for Sustainable Development, January 2015, Volume 35, Issue 1, pp 261-271, https://doi.org/10.1007/s13593-014-0235-4

Leclercq, M., 1997. *Á propos de Hermetia illucens (Linnaeus, 1758) ("soldier fly") (Diptera Stratiomyidae: Hermetiinae)*, Bull. Ann. Soc. R. Belge Entomol. 133, 275 – 282

Leek A., *The future of insect bioconversion products in poultry feeds*. A Nuffield Farming Scholarships Trust Report, 2017

Leong S.Y., Kutty S.R.M., Malakahmad A. and Tan C.K., *Feasibility study of biodiesel production using lipids of Hermetia illucens larva fed with organic waste*, Waste Management, January 2016, Volume 47, Part A, pp 84 - 90, https://doi.org/10.1016/j.wasman.2015.03.030

Li, Q., Zheng, L., Qiu, N., Cai, H., Tomberlin, J.K., Yu, Z., *Bioconversion of dairy manure by black soldier fly (Diptera: stratiomyidae) for biodiesel and sugar production*, Waste Management, June 2011, Volume 31, Issue 6, pp 1316 - 1320, https://doi.org/10.1016/j.wasman.2011.01.005

Manzano-Agugliaro F., Sanchez-Muros M., Barroso F., Martínez-Sánchez A., Rojo S. and Pérez-Bañón C., *Insects for biodiesel production*, Renewable and Sustainable Energy Reviews, August 2012, Volume 16, Issue 6, pp 3744 - 3753, https://doi.org/10.1016/j.rser.2012.03.017

Maryanski, M., Kramarz, P., Laskowski, R., Niklinska, M., *Decreased energetic reserves, morphological changes and accumulation of metals in carabid beetles (Poecilus cupreus L.) exposed to zinc-or cadmium contaminated food*, April 2002, Ecotoxicology, Volume 11, Issue 2, pp 127 - 139, https://doi.org/10.1023/A:1014425113481

McCallan E., 1974, *Hermetia illucens (L.) (Dipt., Stratiomyidae), a cosmopolitan American species long established in Australia and New Zealand*, Entomologist's Monthly Magazine 109, 232-234

Myers H.M., Tomberlin J.K. Lambert B.D. and Kattes D., 2008, *Development of black soldier fly (Diptera: Stratiomyidae) larvae fed dairy manure*, Environmental Entomology, Volume 37, Issue 1, February 2008, pp 11 - 15, https://doi.org/10.1093/ee/37.1.11

Bibliography

Olivier, P.A., 2009, *Utilizing lower life forms for the bioconversion of putrescent waste and how this could dramatically reduce carbon emissions*. Available at: http://tinyurl.com/gub7bfy

Ortel, J., *Accumulation of Cd and Pb in successive stages of Galleria mellonella and metal transfer to the pupal parasitoid Pimpla turionellae*, October 1995, Entomologia Experimentalis et Applicata, Volume 77, Issue 1, pp 89 - 97, https://doi.org/10.1111/j.1570-7458.1995.tb01989.x.

Rozkosny, R., 1983. *A biosystematic study of the european stratiomyidae (Diptera), Clitellariinae, Hermetiinae, pachygasterinae and bibliography*. Ser. Entomol. 2 (21), 401.

Schremmer, F., 1986. *The polymetabol development of the soldier fly larva Hermetia illucens- A contribution to the Metamorphosis of the Stratiomyidae*. Ann. Nathist. Mus. Wien Ser. B fürBot. Zool.

Sheppard D.C., Tomberlin J.K., Joyce J.A., Kiser B.C., Sumner S.M., 2002, *Rearing methods for the black soldier fly (Diptera: stratiomyidae)*, Journal of Medical Entomology, Volume 39, Issue 4, 1 July 2002, Pages 695 - 698, https://doi.org/10.1603/0022-2585-39.4.695

SMITH, R. & PRYOR, R. 2013, *Mapping Exercise Report with regard to current Legislation &Regulation: Europe and Africa & China*, PROteINSECT - Work Package 5: Pro-Insect Platform - Deliverable 5.1

Stamer A., Erschliessung alternativer Proteinquellen zum Fischmehl für Forellenfuttermittel, Verband für ökologischen Landbau e.V., Fachabteilung Aquakultur, Gräfelfing, 2005

St-Hilaire, S., Cranfill, K., McGuire, M.A., Mosley, E.E., Tomberlin, J.K., Newton, L., Sealey, W., Sheppard, C., Irving, S., *Fish offal recycling by the black soldier fly produces a foodstuff high in omega-3 fatty acids*, Journal of World Aquaculture Society, Volume 38, Issue 2, pp 309 - 313, https://doi.org/10.1111/j.1749-7345.2007.00101.x

Üstüner T., Hasbenli A. & Rozkošný (2003). *First record of Hermetia illucens (Linnaeus, 1758) (Diptera, Stratiomyidae) from the Near East*. Studia Dipterologica 10(1): 181–185, Halle, (Saale).

Van Itterbeeck, J., Sivongxay, N., Praxaysombath, B., and Van Huis, A., *Indigenous knowledge of the edible weaver ant Oecophylla smaragdina Fabricius Hymenoptera: Formicidae from the Vientiane Plain, Lao PDR*. Ethnobiology Letters, April 2012, Volume 5, https://doi.org/10.14237/ebl.5.2014.125

Zheng L., Hou Y., Li W., Yang S., Li Q., Yu Z., *Biodiesel production from rice straw and restaurant waste employing black soldier fly assisted by microbes*, Energy, November 2012, Volume 47, Issue 1, https://doi.org/10.1016/j.energy.2012.09.006

Chapter 2

Banks I.J., *To Assess the Impact of Black Soldier Fly (Hermetia illucens) Larvae on Faecal Reduction in Pit Latrines*, "PhD thesis", London School of Hygiene & Tropical Medicine, 2014 https://doi.org/10.17037/PUBS.01917781

Cheng Jack Y.K., Chiu Sam L.H., Lo Irene M.C., *Effects of moisture content of food waste on residue separation, larval growth and larval survival in black soldier fly bioconversion*, "Waste Management", Vol. 67, September 2017, pp 315 - 323, https://doi.org/10.1016/j.wasman.2017.05.046

Diener S., Zurbrügg C., Gutiérrez F. Roa, Nguyen D. Hong, Morel A., Koottatep T., Tockner K., *Black soldier fly larvae for organic waste treatment - prospects and constraints*, "Proceedings of the Waste Safe 2011 - 2nd International Conference on Solid Waste Management in the Developing Countries", February 2011, Khulna, Bangladesh

Fatchurochim S., Geden C.J., Axtell R.C., *Filth fly (Diptera) oviposition and larval development in poultry manure of various moisture levels*, "Journal of Entomological Science", , Vol. 24, no. 2, April 1989, pp. 224 - 231, https://doi.org/10.18474/0749-8004-24.2.224

Montgomery D. C., "*Design and Analysis of Experiments*", Wiley, New York 2012.

Chapter 3

Anzani C., Prandi B., Tedeschi T., Baldinelli C., Sorlini G., Wierenga P. A., Dossena A., Sforza S., *Degradation of collagen increases nitrogen solubilisation during enzymatic hydrolysis of fleshing meat*, "Waste and Biomass Valorization", pp 1-7, https://doi.org/10.1007/s12649-017-9866-4

Bajaj M., Winter J. & Gallert C., *Effect of deproteination and deacetylation conditions on viscosity of chitin and chitosan extracted from Crangon crangon shrimp waste*, "Biochemical Engineering Journal", Vol. 56, (1-2), September 2011, pp 51- 62, https://doi.org/10.1016/j.bej.2011.05.006

Bußler S., Rumpold Birgit A., Jander E., Rawel H.M., & Schlüter O.K., *Recovery and techno-functionality of flours and proteins from two edible insect species: Mealworm (Tenebrio molitor) and black soldier fly (Hermetia illucens) larvae*, "Heliyon", Vol. 2 (12), December 2016, https://doi.org/10.1016/j.heliyon.2016.e00218

Del Valle F.R., Mena M.H., & Bourges H., *An investigation into insect protein*, "Journal of Food Processing and Preservation", Vol. 6 (2), June 1982, pp 99 - 110, https://doi.org/10.1111/j.1745-4549.1982.tb00645.x

Flannery, M. B., Stott, A. W., Briggs, D. E. G., & Evershed, R. P., *Chitin in the fossil record: Identification and quantification of D-glucosamine*, "Organic Geochemistry", Volume 32, pp 745 - 754

Gortari M.C., & Hours R.A., *Biotechnological processes for chitin recovery out of crustacean waste: A mini-review*, "Electronic Journal of Biotechnology", Vol. 16, No 3, May 2013, http://dx.doi.org/10.2225/vol16-issue3-fulltext-10

Hall F.G., Jones O.G., O'Haire, M.E., & Liceaga, A.M., *Functional properties of tropical banded cricket (Gryllodes sigillatus) protein hydrolysates*, "Food Chemistry", Vol. 224, June 2017, pp 414 - 422, https://doi.org/10.1016/j.foodchem.2016.11.138

Kristinsson HG, Rasco B.A., *Fish protein hydrolysates: production, biochemical, and functional properties. Critical Reviews*, "Food Science and Nutrition", January 2000, Volume 40 (1), pp. 43-81, https://doi.org/10.1080/10408690091189266

Osborne T.B., *The proteins of the wheat kernel*, Washington, DC: Carnegie Inst, 1907

Pillai C.K.S., Willi P., & Chandra P.S., *Chitin and chitosan polymers: Chemistry, solubility and fiber formation*, "Progress in Polymer Science", Vol. 34 (7), July 2009, pp 641 - 678,

https://doi.org/10.1016/j.progpolymsci.2009.04.001

Ramos-Bueno, González-Fernández, Sánchez-Muros-Lozano, García-Barroso, & Guil-Guerrero, *Fatty acid profiles and cholesterol content of seven insect species assessed by several extraction systems*, " European Food Research and Technology", Volume 242 (9), February 2016, pp 1471 – 1477, https://doi.org/10.1007/s00217-016-2647-7

Schwass D.E. & Finley J.W., *Heat and alkaline damage to proteins: Racemization and lysinoalanine formation*, "Journal of Agricultural and Food Chemistry",Vol. 32, no.6, pp 1377 – 1382

Schwert, G.W. (1956). *Recovery of Native Bovine Serum Albumin after Precipitation with Trichloroacetic Acid and Solution in Organic Solvents*, " Journal of the American Chemical Society", Vol. 79 (1), January 1957, pp 139 - 141, https://doi.org/10.1021/ja01558a035

Sheppard, D. C., Tomberlin, J. K., Joyce, J. A., Kiser, B. C., & Sumner, S. M., *Rearing methods for the black soldier fly (Diptera: Stratiomyidae)*, "Journal of Medical Entomology", Volume 39 (4), July 2002 pp 695 – 698, https://doi.org/10.1603/0022-2585-39.4.695

Sheppard, D. C., Newton G.L., Thompson S.A. & Savege S., *A value added manure management system using the black soldier fly*, Bioresource Technology, Volume 50 (3), 1994, pp 275-279, https://doi.org/10.1016/0960-8524(94)90102-3

Sivaraman T, Kumar T.K.S., Jayaraman G. and Yu C., *The mechanism of 2,2,2-trichloroacetic acid-induced protein precipitation*, "Journal of Protein Chemistry", Vol. 16 (4), May 1997, pp 291 - 297, https://doi.org/10.1023/A:1026357009886

Synowiecki J., & Al-Khateeb N.A.A.Q., *The recovery of protein hydrolysate during enzymatic isolation of chitin from shrimp Crangon crangon processing discards*, "Food Chemistry", Vol. 68 (2), pp 147 - 152, February 2000, https://doi.org/10.1016/S0308-8146(99)00165-X

Spellman D., McEvoy E., O'Cuinn G., & Fitsgerald R. J., *Proteinase and exopeptidase hydrolysis of whey protein: Comparison of the TNBS, OPA and pH stat methods for quantification of degree of hydrolysis*, "International Dairy Journal", Volume 13 (6), pp 447 - 453, 2003 https://doi.org/10.1016/S0958-6946(03)00053-0

Tkachuk, *Nitrogen-to-protein conversion factors for cereals and oilseed meals*, "Cereal Chemistry", Volume 46, 419 – 424

Tzompa-Sosa D.A., Yi L., van Valenberg H.J.F.,van Boekel,M.A.J.S.,& Lakemond C. M. M., *Insect lipid profile: Aqueous versus organic solvent-based extraction methods*, "Food Research International", Volume 62, August 2014, pp 1087 – 1094, https://doi.org/10.1016/j.foodres.2014.05.052

Yi L., Lakemond C.M.M, Sagis L.M.C., Eisner-Schadler V., van Huis A., van Boekel M.A.J.S., *Extraction and characterisation of protein fractions from five insect species*, in "Food Chemistry", Vol. 141 (4), pp 3341-3348, https://doi.org/10.1016/j.foodchem.2013.05.115

Zhang H., Yuna S., Songa L., Zhanga Y. & Zhaob Y., *The preparation and characterization of chitin and chitosan underlarge-scale submerged fermentation level using shrimp by-products as substrate*, "International Journal of Biological Macromolecules", Vol. 96, March 2017, pp 334 – 339, https://doi.org/10.1016/j.ijbiomac.2016.12.017

Chapter 4

Awadhiya A., Kumar D., Vivek V., *Crosslinking of agarose bioplastic using citric acid* "Carbohydrate Polymers", Volume 151, October 2016, pp 60 – 67, https://doi.org/10.1016/j.carbpol.2016.05.040

Bharti S. N., Swetha G. S., *Need for Bioplastics and Role of Biopolymer PHB: A Short Review*, "Journal of Petroleum & Environmental Biotechnology", Volume 7 (2), January 2016

Chen P., Zhang L., *New Evidences of Glass Transitions and Microstructures of Soy Protein Plasticized with Glycerol*, "Macromolecular Bioscience", Volume 5 (3), March 2005, pp 237-245, https://doi.org/10.1002/mabi.200400179

Félix M., Romero A., Guerrero A., *Development of albumen/soy biobased plastic materials processed by injection molding* "Journal of Food Engineering" Volume 125, March 2014, pp 7-16. https://doi.org/10.1016/j.jfoodeng.2013.10.018

Ganglani M., Carr S. H., Torkelson J. M., *Influence of cure via network structure on mechanical properties of a free-radical polymerizing thermoset*, "Polymer", Volume 43 (9), April 2002, pp 2747-2760, https://doi.org/10.1016/S0032-3861(01)00805-9

Gontard N. , Guilbert S. and Cuq J.L., *Edible wheat gluten films: influence of the main process variables on the film properties using response surface methodology*, "Journal of Food Science", Volume 57 (1), January 1992, pp 190 - 195, https://doi.org/10.1111/j.1365-2621.1992.tb05453.x

Hazarika D., Karak N., ACS Sustainable Chemistry & Engineering, August 2015, 3, pp 2458 - 2468, https://doi.org/10.1021/acssuschemeng.5b00494

Jiang L., Zhang J., "Applied Plastics Engineering Handbook: Processing, Materials, and Applications", Vol. 1 (Ed: M. Kutz), Elsevier, London, England, March 2016, p. 127.

Martelli M., Moore S., Silva Paes S., Gandolfo C., Laurindo J. B., *Influence of plasticizers on water sorption isotherms and water vapor permeability of chicken feather keratin films*, "LWT- Food Science and Technology", Volume 39 (3), April 2006, pp 292 – 301

Niaounakis M., "*Biopolymers: Applications and Trends*", Elsevier, Oxford, England 2015.

Ramakrishnan N., Sharma S., Gupta A., Alashwal B. Y., *Keratin based bioplastic film from chicken feathers and its characterization*, "International Journal of Biological Macromolecules", Volume 111, May 2018, pp 352-358

Robertson N. L. M., Nychka J. A., Alemaskin K., Wolodko J. D. J., "Journal of Applied Polymer Science" 2013, 130, 969.

Woods K., Selling G. W., *Melt Reaction of Zein with Glyoxal to Improve Tensile Strength and Reduce Solubility*, "Journal of Applied Polymer Science" May 2008, 109, 2375, https://doi.org/10.1002/app.28334

Xu H., Shen L., Xu L., Yang Y., *Low-temperature crosslinking of proteins using non-toxic citric acid in neutral aqueous medium: Mechanism and kinetic study*, "Industrial Crops Products", Volume 74, November 2015, pp 234 - 240, https://doi.org/10.1016/j.indcrop.2015.05.010

https://www.plasticseurope.org/application/files/5715/1717/4180/Plastics_the_facts_2017_FINAL_for_website_one_page.pdf (accessed: May 2018)

www.ibaw.org (accessed: May 2018)

Chapter 5

ISO 14040. (2006). *Environmental management - life cycle assessment - principles and framework.* International Standards Organization, a.

ISO 14044. (2006). *Environmental management - life cycle assessment - principles and framework.* International Standards Organization, b.

Chapter 6

Bare J. C., Hofstetter P., Pennington D. W., & de Haes H. A. U., Midpoints versus endpoints: The sacrifices and benefits "The International Journal of Life Cycle Assessment", Volume 5 (6), November 2000, pp 319-326, https://doi.org/10.1007/BF02978665

Ecoinvent Centre, *Ecoinvent Data v 3.1*. Available at. https://www.ecoinvent.org/ ecoinvent Association, Zürich. Retrieved from http://www.ecoinvent.ch., 2014.

Goedkoop M, Spriensma R, *The Eco-Indicator 99-A damage oriented method for Life Cycle Impact Assessment*, Methodology Annex, PRé-product ecology consultants, 22 June 2001-Third edition

Hackstein H.P., Joannes H.P & Stumm C., *Methane production in terrestrial arthropods*, Proceedings of the National Academy of Sciences of the United States of America, Volume 91 (12), June 1994, pp 5441-5445, https://doi.org/10.1073/pnas.91.12.5441

Hischier R., Hellweg S., Capello C., Primas A., *Establishing Life Cycle Inventories of Chemicals Based on Differing Data Availability*, "The International Journal of Life Cycle Assessment", Volume 10 (1), January 2005, pp 59-67, https://doi.org/10.1065/lca2004.10.181.7

Jolliet O., Margni, M., Charles R., Humbert S., Payet J., Rebitzer G., Rosenbaum R., *IMPACT2002+: A new life cycle impact assessment methodology*, "The International Journal of Life Cycle Assessment", Volume 8, November 2003, pp 324-330, https://doi.org/10.1007/BF02978505

Potting J. and Hauschild M., *Background for spatial differentiation in life cycle impact assessment - The EDIP 2003 methodology*, Report, Danish Environmental Protection Agency, Copenhagen, 2003

SimaPro 8.5.2.2.; PRé Consultants B.V.: Amersfoort, The Netherlands, 2018

Chapter 7

Durrenberger A, *Gaussian Plume Modeling,* Chemical Engineering 357

Goedkoop M, Spriensma R, *The Eco-Indicator 99-A damage oriented method for Life Cycle Impact Assessment", Methodology Annex,* PRé-product ecology consultants, 22 June 2001-Third edition

Goedkoop M, Spriensma R, *De Eco-Indicator 95, Final Report,* NOH Report 9523, PRé consultants, Amersfoort (NL), July 1995-ISBN 90-72130-77-4

Guineé J. et al., LCA Impact Assessment of Toxic Releases, Product Policy Report 1996/21, Ministry of Environment (VROM), The Hague.

Hofstetter P., *Perspectives in Life Cycle Impact Assessment; A Structured Approach to combine Models of the Technosphere, Ecosphere and Valuesphere,* Kluwers Academic Publishers, 1998

Humbert S. et al., *IMPACT 2002+: User Guide - Draft for version Q2.21,* 2012

Chapter 8

Brandes LJ, den Hollander HA, van de Meent D 1996: *SimpleBox 2.0: A nested multimedia fate model for evaluating the environmental fate of chemicals,* National Institute for Public Health and the Environment (RIVM), Bilthoven, The Netherlands

Briggs GG, Bromilow RH, Evans AA (1982): *Relationships between lipophilicity and root uptake and translocation of non-ionised chemicals by barley*, Pesticide Science 13: 495-504

Hollander A, Hessel L, de Voogt P, van de Meent D (2004): *Implementation of Depth-dependent Soil Concentrations in Multimedia Mass Balance Models*, SAR and QSAR in Environmental Research 15: 457-468

Huijbregts MAJ, Rombouts LJA, Ragas AMJ, van de Meent D (2005): *Human-toxicological effect and damage factors of carcinogenic and noncarcinogenic chemicals for life cycle impact assessment*, Integrated Environmental Assessment and Management 1: 181-244

Jolliet O, Margni MD, Charles R, Humbert S, Payet J, Rebitzer G, Rosenbaum RK (2003): *IMPACT 2002+: A new life cycle impact assessment methodology,* The International Journal of Life Cycle Assessment 8: 324-330

Mackay D, Fraser A (2000): *Bioaccumulation of persistent organic chemicals: Mechanisms and models*, Environmental Pollution 110: 375-391

Mackay D (2001): *Multimedia Environmental Models: The Fugacity Approach, Second Edition*, Toxicology and Environmental Health Series. CRC Press, Chelsea, Michigan, 272 pp

Rosenbaum RK, Margni MD, Jolliet O (2007): *A flexible matrix algebra framework for the multimedia multipathway modeling of emission to impacts,* Environment International 33: 624-634

Bibliography

Schwarzenbach R.P, Gschwend Philip M., and Imboden Dieter M., Environmental Organic Chemistry, 2nd Edition

Cowan C.E., Mackay D., Feijtel T.C.J., van de Meent D., Di Guardo A., Davies J., and Mackay N. (1995) The multi-media fate model: A vital tool for predicting the fate of chemicals. Proceedings of a workshop organized by the Society of Environmental Toxicology and Chemistry (SETAC), STEAC Press, Pensacola, FL, pp.78

McLachlan M.S., Czub G., Wania F., (2002) The Influence of Vertical Sorbed Phase Transport on the Fate of Organic Chemicals in Surface Soils Environ. Sci. Technol. 2002, 36, 22, 4860-4867 https://doi.org/10.1021/es025662y

Liu J.-G., Nie Y.-F. (2001). Fractal scaling of effective diffusion coefficient of solute in porous media. J. Environ. Sci. 13, 170–172. www.jesc.ac.cn/jesc_En/ch/reader/create_pdf.aspx?file_no=20010208&year_id=2001&quarter_id=2&falg=1

List of tables

List of figures